Report No. CCEER 14-04

NONLINEAR EVALUATION OF THE PROPOSED SEISMIC DESIGN PROCEDURE FOR STEEL BRIDGES WITH DUCTILE END CROSS FRAMES

Eric V. Monzon
Ahmad M. Itani
Michael A. Grubb

Center for Civil Engineering Earthquake Research
University of Nevada, Reno

July 2014

Abstract

Neither the AASHTO LRFD Bridge Design Specifications nor the AASHTO Guide Specification for LRFD Seismic Bridge Design provides a design procedure to achieve the desired seismic performance of essentially elastic substructure and ductile superstructure. This Type 2 design strategy in the Guide Specifications limits the inelastic activity to the superstructure of steel plate girder bridges. Due to the lack of these specifications, bridge engineers have been reluctant of using this strategy which will only limit the damage to the support cross frames in steel plate girder bridges. This controlled damage will keep the substructure essentially elastic and thus limit its repair after a major earthquake.

This report presents a proposed 'force-based' design procedure that will achieve an essentially elastic substructure and ductile superstructure. The reinforced concrete (R/C) substructure flexural resistance is designed for the combined effect of seismic forces similar to conventional seismic design with a force reduction factor equal to 1.5. Meanwhile, the shear resistance and the confinement requirements of the substructure are determined in a way similar to the seismic design of conventional bridges. To achieve a ductile superstructure, the horizontal resistance of the support cross frames is based on the lesser of the pier nominal shear resistance and the elastic seismic cross forces obtained from the response spectrum analysis, divided by a proposed response modification factor for ductile cross frames equal to 4. This will ensure that support cross frames will act as a 'fuse' and will not subject the substructure to forces that may cause nonlinear response in that direction. To achieve a ductile response of support cross frames, the diagonal members, which are expected to undergo inelastic response, are detailed to have limits on width-to-thickness and slenderness ratios. The other cross frame components and the shear resistance of the substructure are then checked for a fully yielded and strain hardened support cross frame.

Three bridges were selected to illustrate the proposed design procedure for Type 2 design strategy. The substructure of these bridges included single-column pier, two-column pier, and wall piers. Examples showing the design of these bridges using conventional Type 1 design strategy with Critical and other Operational Categories are also shown. Thus, a total of eight bridge design examples are shown in this report. The proposed design strategy for Type 2 design showed an increase in the size of the substructure when compared to 'Other' bridge operational category. However, it showed a decrease in the size of the substructure when compared to 'Critical' bridge operational category. The seismic performance was evaluated through nonlinear response history analysis using fourteen ground motions representing the design and maximum considered earthquakes. The nonlinear seismic evaluation showed the Type 2 design strategy has indeed achieved an essentially elastic substructure and ductile superstructure as intended to. It also showed that bridges with stiff substructure designed according to Type 1 strategy have an inelastic activity in the superstructure. This will subject the connections and bearings to seismic forces that they are not designed for, which may result in undesirable seismic performance. Thus utilizing Type 2 design strategy for bridges with stiff substructure, i.e. pier wall, will offer great advantages by limiting the lateral seismic forces and having a 'fuse' to dissipate the input energy. This will reduce the seismic forces on the bearings and thus will lower the foundation cost.

Acknowledgement

The work in this report was funded by American Iron and Steel Institute, AISI, contract CC-3070. Mr. Dan Snyder was contract manager of which the authors sincerely appreciate his support and collaboration. The authors appreciate the comments by a task group funded by AASHTO to support HSCOBS Technical Committee on Seismic Design. The chair of this group is Dr. Lee Marsh. The authors wish to thank the following individuals for their help and suggestions: Mr. Richard Pratt, Prof. Ian Buckle, Dr. Elmer Marx, Dr. John Kulicki, Dr. Lian Duan, Mr. Greg Perfetti, Mr. Keith Fulton, and Dr. Gichuru Muchane.

Disclaimer

The materials set fourth here in are for general information only. They are not a substitute for competent professional assistance. The opinions expressed in this report are those of the authors and do not necessarily represents the views of the University of Nevada, Reno, the American Iron and Steel Institute and the individuals who kindly provided the authors information and comments.

Table of Contents

List of Tables

List of Figures

Chapter 1 Introduction

1.1 Background

A ductile superstructure with an essentially elastic substructure may be used as an alternative to conventional seismic design strategy of an elastic superstructure and a ductile substructure. The ductile superstructure elements must be specially designed and detailed to undergo large cyclic deformation without premature failure. The inelastic activity in these elements will dissipate seismic energy and will limit the seismic forces transferred to the substructure. In this design strategy, special cross-frames are provided at pier supports. The substructure in this case is designed to be essentially elastic in the longitudinal and transverse directions of the bridge. Ideally, ductile superstructures have shown the most effectiveness when used with stiff substructures. Flexible substructures will attract smaller seismic forces and, thus, the pier cross-frames will be subjected to low seismic forces (Alfawakhiri and Bruneau, 2001; Bahrami et al., 2010).

The special ductile pier cross-frames are designed with a response reduction factor, *R*, equal to 4.0. Thus, the diagonal members of these cross frames will undergo nonlinear response and will limit the seismic forces in that direction. Experimental investigations were conducted on diagonal members and subassemblies to determine nonlinear response of single angles that will be able to withstand large cyclic deformations without premature failure. These experiments also provided the physical data of the overstrength factor for these diagonal members and their failure mode (Carden et al., 2006). Nonlinear response history analyses conducted on 3D bridge models confirmed the seismic response of the proposed seismic design procedure.

1.2 Proposed AASHTO LRFD Bridge Design Specifications on Type 2 Design Strategy

The following are the proposed language for Type 2 Design Strategy that may be included in the AASHTO LRFD Bridge Design Specifications. The proposed language is 'force-based' in line with these specifications.

6.16.4.5–Ductile Superstructures

6.16.4.5.1–General

For a ductile superstructure, special support cross-frames, designed as specified in Article 6.16.4.5.2, shall be provided at all supports. The substructure shall be designed to be essentially elastic as specified in Article 4.6.2.8.2.

The seismic design forces for the diagonal members of the special support cross-frames shall be taken as the unreduced elastic seismic forces divided by a response modification factor, *R*, which shall be taken equal to 4.0.

The superstructure drift, Δ, determined as the ratio of the relative lateral displacement of the girder top and bottom flanges to the total depth of the steel girder, shall

C6.16.4.5.1

A ductile superstructure with an essentially elastic substructure may be used as an alternative to an elastic superstructure in combination with a ductile substructure. Ductile superstructures must be specially designed and detailed to dissipate seismic energy. In ductile superstructures, special support cross-frames are to be provided at all supports and must be detailed and designed to undergo significant inelastic activity and dissipate the seismic input energy without premature failure or strength degradation in order to limit the seismic forces on the substructure. The substructure in

not exceed 4%. The drift shall be determined from the results of an elastic analysis.

this case is designed to be essentially elastic as specified in Article 4.6.2.8.2 and described in Article C6.16.4.1. This strategy has been analytically and experimentally validated using subassembly and shake table experiments on steel I-girder bridges with no skew or horizontal curvature.

Ideally ductile superstructures have shown the most effectiveness when utilized in conjunction with stiff substructures. Flexible substructures will attract smaller seismic forces, and thus, the special support cross-frames will also be subjected to smaller seismic forces and will be less effective (Alfawakhiri and Bruneau, 2001). Bridge dynamic analyses conducted according to the provisions of Article 4.7.4 can provide insight on the effectiveness of special support cross-frames (Alfawakhiri and Bruneau, 2001; Bahrami et al., 2010; and Itani et al., 2013).

The *R* factor of 4.0 specified for the design of the special support cross-frame diagonal members in a ductile superstructure is the result of nonlinear time history analyses conducted on 3D bridge models (Bahrami et al., 2010 and Itani et al., 2013). For these nonlinear analyses, the deck and steel plate girders were modeled with shell elements, while the cross-frames, cap beams and columns were modeled with nonlinear frame elements.

The drift, Δ, of the superstructure is to be determined from an elastic structural analysis without the use of an *R* value.

6.16.4.5.2–Special Support Cross-Frames

Special support cross-frames shall consist of top and bottom chords and diagonal members. The diagonal members shall be configured either in an X-type or an inverted V-type configuration. Only single angles or double angles with welded end connections shall be permitted for use as members of special support cross-frames.

In an X-type configuration, diagonal members shall be connected where the members cross by welds. The welded connection at that point shall have a nominal resistance equal to at least 0.25 times the tensile resistance of the diagonal member, P_t, determined as specified in Article 6.16.4.5.2c.

In both configurations, the top chord shall be designed for an axial force taken as the horizontal component of the tensile resistance of the diagonal member, P_t, determined as specified in Article 6.16.4.5.2c.

In an inverted V-type configuration, the top chord and the concrete deck at the location where the diagonals intersect shall be designed to resist a vertical force, V_t, taken equal to:

C6.16.4.5.2

Concentric support cross-frames are those in which the centerlines of members intersect at a point to form a truss system that resists lateral loads. Concentric configurations that are permitted for special support cross-frames in ductile superstructures are X-type and inverted V-type configurations. The use of tension-only bracing in any configuration is not permitted. V-type configurations and solid diaphragms are also not permitted. Members other than single-angle or double-angle members are not currently permitted, as other types of members have not yet been sufficiently studied for potential use in special support cross-frames (AISC, 2010b and Bahrami et al., 2010).

The required resistance of the welded connection at the point where diagonal members cross in X-type configurations is intended to permit the unbraced length for determining the compressive buckling resistance of the member to be taken as half of the full length (Goel and El-Tayem, 1986; Itani and Goel, 1991; Carden et al., 2005a and 2005b, and Bahrami et al., 2010).

Inverted V-type configurations exhibit a special problem that sets them apart from X-type configurations.

$$V_t = \left|\left(P_t - \left|0.3P_{nc}\right|\right)\right| \sin\theta \qquad \text{(6.16.4.5.2-1)}$$

where:

θ = angle of inclination of the diagonal member with respect to the horizontal (degrees)

P_{nc} = nominal compressive resistance of the diagonal member determined as specified in Article 6.16.4.5.2c (kip)

P_t = tensile resistance of the diagonal member determined as specified in Article 6.16.4.5.2c (kip)

Members of special support cross-frames in either configuration shall satisfy the applicable requirements specified in Articles 6.16.4.5.2a through 6.16.4.5.2e. The welded end connections of the special support cross-frame members shall satisfy the requirements specified in Article 6.16.4.5.3.

Under lateral displacement after the compression diagonal buckles, the top chord of the cross-frame and the concrete deck will be subjected to a vertical unbalanced force. This force will continue to increase until the tension diagonal starts to yield. This unbalanced force is equal to the vertical component of the difference between the tensile resistance of the diagonal member and the absolute value of $0.3P_{nc}$. $0.3P_{nc}$ is taken as the nominal post-buckling compressive resistance of the member (Carden et al., 2006a). A similar overstrength factor is applied in the design of the welded end connections for special support cross-frame members in Article 6.16.4.5.3, and in determining the transverse seismic force on the piers/bents for the design of the essentially elastic substructure in Article 4.6.2.8.2.

During a moderate to severe earthquake, special support cross-frames and their end connections are expected to undergo significant inelastic cyclic deformations into the post-buckling range. As a result, reversed cyclic rotations occur at plastic hinges in much the same way as they do in beams. During severe earthquakes, special support cross-frames are expected to undergo 10 to 20 times the yield deformation. In order to survive such large cyclic deformations without premature failure, the elements of special support cross-frames and their connections must be properly designed (Zahrai and Bruneau, 1999a and 1999b; Zahrai and Bruneau, 1998; Carden et al., 2006, and Bahrami et al., 2010).

The requirements for the seismic design of special support cross-frames are based on the seismic requirements for Special Concentric Braced Frames (SCBFs) given in AISC (2010b). These requirements are mainly based on sections and member lengths that are more suitable for building construction. However, Carden et al. (2006) and Bahrami et al. (2010) tested more typical sections and member lengths utilized in bridge construction and verified that the AISC seismic provisions for SCBFs can be used for the seismic design of special support cross-frames. These studies, in addition to other analytical and experimental investigations conducted by numerous researchers, have identified three key parameters that affect the ductility of cross-frame members:

- Width-to-thickness ratio;
- Slenderness ratio; and
- End conditions.

During earthquake motions, the cross-frame member will be subjected to cyclic inelastic deformations. The plot of the axial force versus the axial deformation of the inelastic member is often termed a hysteresis loop. The characterization of these loops is highly dependent on

the aforementioned parameters. Satisfaction of the requirements related to these parameters specified in Articles 6.16.4.5.2a through 6.16.4.5.2e will help to ensure that the diagonal members of special support cross-frames can undergo large inelastic cyclic deformations without premature fracture and strength degradation when subjected to the design seismic forces.

6.16.4.5.2a–Width-to-Thickness Ratio

Diagonal members of special support cross-frames shall satisfy the following ratio:

$$\frac{b}{t} \le 0.3\sqrt{\frac{E}{F_y}} \qquad \text{(6.16.4.5.2a-1)}$$

where:

b = full width of the outstanding leg of the angle (in.)

t = thickness of the outstanding leg of the angle (in.)

C6.16.4.5.2a

Traditionally, diagonal cross-frame members have shown little or no ductility during a seismic event after overall member buckling, which produces plastic hinges at the mid-point of the member and at its two ends. At a plastic hinge, local buckling can cause large strains, leading to fracture at small deformations. It has been found that diagonal cross-frame members with ultra-compact elements are capable of achieving significantly more ductility by forestalling local buckling (Astaneh-Asl et al., 1985, Goel and El-Tayem, 1986). Therefore, width-to-thickness ratios of outstanding legs of special support cross-frame diagonal members are set herein to not exceed the requirements for ultra-compact elements taken from AISC (2010b) in order to minimize the detrimental effect of local buckling and subsequent fracture during repeated inelastic cycles.

6.16.4.5.2b–Slenderness Ratio

Diagonal members of special support cross-frames shall satisfy the following ratio:

$$\frac{K\ell}{r} \le 4.0\sqrt{\frac{E}{F_y}} \qquad \text{(6.16.4.5.2b-1)}$$

where:

K = effective length factor in the plane of buckling determined as specified in Article 4.6.2.5

ℓ = unbraced length (in.). For members in an X-type configuration, ℓ shall be taken as one-half the length of the diagonal member.

r = radius of gyration about the axis normal to the plane of buckling (in.)

C6.16.4.5.2b

The hysteresis loops for special support cross-frames with diagonal members having different slenderness ratios vary significantly. The area enclosed by these loops is a measure of that component's energy dissipation capacity. Loop areas are greater for a stocky member than for a slender member; hence, the slenderness ratio of diagonal members in special support cross-frames is limited accordingly herein to the requirement for stocky members in SCBFs given in AISC (2010b).

6.16.4.5.2c– Tensile and Nominal Compressive Resistance

The tensile resistance, P_r, of diagonal members of

C6.16.4.5.2c

The diagonal members of special support cross-

special support cross-frames shall be taken as:

$$P_t = 1.2 R_y P_{ny} \qquad (6.16.4.5.2c\text{-}1)$$

where:

P_{ny} = nominal tensile resistance for yielding in the gross section of the diagonal member determined as specified in Article 6.8.2 (kip)

R_y = ratio of the expected yield strength to the specified minimum yield strength of the diagonal member determined as specified in Article 6.16.2

The nominal compressive resistance, P_{nc}, of diagonal members of special support cross-frames shall be taken as:

$$P_{nc} = P_n \qquad (6.16.4.5.2c\text{-}3)$$

where:

P_n = nominal compressive resistance of the diagonal member determined as specified in Article 6.9.4.1 using an expected yield strength, $R_y F_y$ (kip)

frames are designed and detailed to act as "fuses" during seismic events to dissipate the input energy. These members will experience large cyclic deformations beyond their expected yield and compressive resistances. The limitations on the width-to-thickness and slenderness ratios specified in the preceding articles will allow the diagonals of the special support cross-frames to go through significant yielding and strain hardening prior to fracture. The tensile resistance of diagonal members of special support cross-frames, P_t, is to be determined using an expected yield strength, $R_y F_y$ (AISC, 2010b). The resulting resistance is then multiplied by a factor of 1.2 in Eq. 6.16.4.5.2c-1. This factor is the upper bound of the ratio of P_t to the expected nominal tensile resistance, $R_y P_{ny}$, of the diagonal members as determined experimentally by Carden et al. (2006).

The nominal compressive resistance of diagonal members of special support cross-frames, P_{nc}, is also to be determined using an expected yield strength, $R_y F_y$, according to Eq. 6.16.4.5.2c-3.

6.16.4.5.2d–Lateral Resistance

The lateral resistance, V_{lat}, of a special support cross-frame in a single bay between two girders shall be taken as the sum of the horizontal components of the tensile resistance and the nominal post-buckling compressive resistance of the diagonal members, or:

$$V_{lat} = \left(P_t + 0.3\left|P_{nc}\right|\right)\cos\theta \qquad (6.16.4.5.2d\text{-}1)$$

where:

θ = angle of inclination of the diagonal member with respect to the horizontal (degrees)

P_{nc} = nominal compressive resistance of the diagonal member determined as specified in Article 6.16.4.5.2c (kip)

P_t = tensile resistance of the diagonal member determined as specified in Article 6.16.4.5.2c (kip)

C6.16.4.5.2d

During seismic events, special support cross-frames are expected to undergo large cyclic deformations. The tension diagonal will yield and strain harden while the compression diagonal will buckle. The dissipated energy from this system depends on the ability of the tension diagonal to undergo large deformations without premature fracture. Furthermore, the compression diagonal should also be able to withstand large deformations without fracture due to local and global buckling. Hence, the lateral resistance of a special support cross-frame in a single bay is to be taken equal to the sum of the horizontal components of the tensile resistance and the nominal post-buckling compressive resistance of the diagonal members. Carden et al. (2006a) showed experimentally that for angle sections satisfying the limiting width-to-thickness and slenderness ratios specified in Articles 6.16.4.5.2a and 6.16.4.5.2b, respectively, the nominal post-buckling compressive resistance of a diagonal member may be taken equal to 0.3 times P_{nc}.

6.16.4.5.2e–Double-Angle Compression Members

Double angles used as diagonal compression members in special support cross-frames shall be interconnected by welded stitches. The spacing of the stitches shall be such that the slenderness ratio, ℓ/r, of the individual angle elements between the stitches does not exceed 0.4 times the governing slenderness ratio of the member. Where buckling of the member about its critical buckling axis does not cause shear in the stitches, the spacing of the stitches shall be such that the slenderness ratio, ℓ/r, of the individual angle elements between the stitches does not exceed 0.75 times the governing slenderness ratio of the member. The sum of the nominal shear resistances of the stitches shall not be less than the nominal tensile resistance of each individual angle element.

The spacing of the stitches shall be uniform. No less than two stitches shall be used per member.

C6.16.4.5.2e

More stringent spacing and resistance requirements are specified for stitches in double-angle diagonal members used in special support cross-frames than for conventional built-up members subject to compression (Aslani and Goel, 1991). These requirements are indented to restrict individual element buckling between the stitch points and consequent premature fracture of these members during a seismic event.

6.16.4.5.3–End Connections of Special Support Cross-Frame Members

End connections of special support cross-frame members shall be welded to a gusset plate. The gusset plate may be bolted or welded to the bearing stiffener. The gusset plate and gusset plate connection shall be designed to resist a vertical design shear acting in combination with a moment taken equal to the vertical design shear times the horizontal distance from the working point of the connection to the centroid of the bolt group or weld configuration. The vertical gusset-plate design shear, V_g, shall be taken as:

$$V_g = P_t \sin\theta \qquad (6.16.4.5.3\text{-}1)$$

where:

θ = angle of inclination of the diagonal member with respect to the horizontal (degrees)

P_t = tensile resistance of the diagonal member determined as specified in Article 6.16.4.5.2c (kip)

The axial resistance of the end connections of special support cross-frame diagonal members subject to tension or compression, P_d, shall not be taken less than:

$$P_d = P_t \qquad (6.16.4.5.3\text{-}2)$$

where:

P_t = tensile resistance of the diagonal member determined as specified in Article 6.16.4.5.2c (kip)

The axial resistance of the end connections of special support cross-frame top chord members subject to tension or compression, P_{tc}, shall not be taken less than:

$$P_{tc} = P_t \cos\theta \qquad (6.16.4.5.3\text{-}3)$$

where:

θ = angle of inclination of the diagonal member with respect to the horizontal (degrees)

C.6.16.4.5.3

Due to the size of the gusset plate and its attachment to the bearing stiffener in typical support cross-frames, the diagonal members tend to buckle in the plane of the gusset (Astaneh-Asl et al., 1985; Carden et al., 2004, Bahrami et al., 2010). During a seismic event, plastic hinges in special support cross-frames are expected at the ends of the diagonal members next to the gusset plate locations. It has been found experimentally (Itani et al., 2004; Carden et al., 2004, Bahrami et al., 2010) that bolted end connections of special support cross-frame diagonal members may suffer premature fracture at bolt-hole locations if the ratio of net to gross area, A_n/A_g, of the member at the connection is less than 0.85. Therefore, the use of welded end connections is conservatively required for special support cross-frame members in order to ensure ductile behavior during a seismic event.

The welded end connections of the diagonal members of special support cross-frames are to be designed for the tensile resistance, P_t, of the special support cross-frame diagonal member.

The specified axial resistance of the end connections of special support cross-frame members ensures that the connections are protected by capacity design; that is, it ensures that the member is the weaker link.

The following are the proposed specifications on the affected sections in AASHTO LRFD Bridge Design Specifications.

Item #1

In Section 6, add Article 6.16.4.5 as shown in Attachment A. **(All remaining items below are contingent on passage of Item #1.)**

Item #2

Revise the 3rd paragraph of Article 4.6.2.8.2 as follows:

The analysis and design of ~~end~~ diaphragms and cross-frames at supports shall consider the effect of the bearing constraints~~horizontal supports at an appropriate number of bearings~~. Slenderness and connection requirements of bracing members that are part of the lateral force resisting system shall ~~comply with~~ satisfy the applicable provisions specified for main member design along with any additional applicable provisions specified in Article 6.16.

Item #3

In Article 4.6.2.8.2, revise the 4th paragraph as follows:

~~Members of diaphragms and cross frames identified by the Designer as part of the load path carrying seismic forces from the superstructure to the bearings shall be designed and detailed to remain elastic, based on the applicable gross area criteria, under all design earthquakes, regardless of the type of bearings used. The applicable provisions for the design of main members shall apply~~.

For a ductile superstructure with an essentially elastic substructure designed according to the provisions of Article 6.16.4.5.1, the piers/bents shall be designed according to Article 3.10.9 and using the response modification factors of table 3.10.7.1-1 of critical bridges. The lateral resistance of the substructure shall be check to the lateral force, F, specified in Article 6.16.4.1

Item #4

In Article C4.6.2.8.2, revise the last two sentences as follows:

In ~~the strategy taken herein~~ the most common seismic design strategy, it is assumed that ductile plastic hinging in

the substructure is the primary source of energy dissipation. For rolled or fabricated composite straight steel I-girder bridges with limited skews utilizing cross-frames at supports, an a~~A~~lternative design strategy~~ies~~ may be considered ~~if approved by the Owner~~ as specified in Article 6.16.4.5, in which the diagonal members of all support cross-frames are permitted to undergo controlled inelastic activity thereby dissipating the input seismic energy and limiting the seismic forces on the substructure.

Item #5

In Article C4.6.2.8.3, delete the last sentence in the 2nd paragraph as follows:

~~Although studies of cyclic load behavior of bracing systems have shown that with adequate details, bracing systems can allow for ductile behavior, these design provisions require elastic behavior in end diaphragms (Astaneh-Asl and Goel, 1984; Astaneh-Asl et al., 1985; Haroun and Sheperd, 1986; Goel and El-Tayem, 1986).~~

Item #6

In Article C4.6.2.8.3, delete the 3rd paragraph as follows:

~~Because the end diaphragm is required to remain elastic as part of the identified load path, stressing of intermediate cross-frames need not be considered.~~

Item #7

Add the following definitions to Article 6.2:

Ductile Superstructure−A rolled or fabricated straight steel I-girder bridge superstructure with limited skews and a composite reinforced concrete deck designed and detailed to dissipate seismic energy through the provision of special support cross-frames at all supports.

Special Support Cross-Frame−Support cross-frames in a ductile superstructure designed and detailed to undergo

significant inelastic activity and dissipate the input energy without premature failure or strength degradation during a seismic event.

Perform any necessary modifications to the Notation in Article 6.3.

Item #8

Add the following paragraph to the end of Article 6.9.3:

Single-angle or double-angle diagonal members in special support cross-frames of ductile superstructures for seismic design shall satisfy the slenderness requirement specified in Article 6.16.4.5.2b.

Item #9

Add the following paragraph to the end of Article 6.9.4.2.1:

Outstanding legs of single-angle or double-angle diagonal members in special support cross-frames of ductile superstructures for seismic design shall satisfy the limiting width-to-thickness ratio specified in Article 6.16.4.5.2a.

Item #10

Revise the 1st sentence of Article C6.16.1 as follows:

These specifications are based on the recent work published by Itani et al. (2010), NCHRP (2002, 2006), MCEER/ATC (2003), Caltrans (2006), AASHTO's *Guide Specifications for LRFD Seismic Bridge Design* (~~2009~~2011) and AISC (~~2005 and 2005b~~2010 and 2010b).

Revise the last sentence in the 6th paragraph of Article C6.16.1 as follows:

The designer may find information on this topic in AASHTO's *Guide Specifications for LRFD Seismic Bridge Design* (~~2009~~2011) and MCEER/ATC (2003) to complement information available elsewhere in the literature.

In Article C6.16.2, change the reference to ″(AISC, 2005b)″ to ″(AISC, 2010b)″.

Item #11

Replace the first two paragraphs of Article 6.16.4.1 with the following:

Components of slab-on-steel girder bridges located in Seismic Zones 3 or 4, defined as specified in Article 3.10.6, shall be designed using one of the three types of response strategies specified in this Article. One of the three types of response strategies should be considered for bridges located in Seismic Zone 2:

- *Type 1*—Design an elastic superstructure with a ductile substructure according to the provisions of Article 6.16.4.4.
- *Type 2*—Design a ductile superstructure with an essentially elastic substructure according to the provisions of Article 6.16.4.5.1.
- *Type 3*—Design an elastic superstructure and substructure with a fusing mechanism at the interface between the superstructure and substructure according to the provisions of Article 6.16.4.4.

Structures designed using Strategy Type 2 shall be limited to straight steel I-girder bridges with a composite reinforced concrete deck slab whose supports are normal or skewed not more than 10° from normal.

The deck and shear connectors on bridges located in Seismic Zones 3 or 4 shall also satisfy the provisions of Articles 6.16.4.2 and 6.16.4.3, respectively. If Strategy Type 2 is invoked for bridges in Seismic Zone 2, the provisions of Articles 6.16.4.2 and 6.16.4.3 shall also be invoked for decks and shear connectors. If Strategy Types 1 or 3 are invoked for bridges in Seismic Zone 2, the provisions of Articles 6.16.4.2 and 6.16.4.3 should be considered.

Item #12

Add the following paragraph after the first paragraph of Article C6.16.4.1:

Previous earthquakes have demonstrated that inelastic activity at support cross-frames in some steel I-girder bridge superstructures has reduced the seismic demand on the substructure (Roberts, 1992; Astaneh-Asl and Donikian, 1995). This phenomenon has been investigated both analytically and experimentally by several researchers (Astaneh-Asl and Donikian, 1995; Itani and Reno, 1995; Itani and Rimal, 1996; Zahrai and Bruneau, 1998, 1999a and 1999b; Carden et al., 2005a and 2005b; Bahrami et al., 2010). Based on these investigations, it was concluded that the provision of a ductile superstructure, in which the diagonal members of all support cross-frames are permitted to undergo controlled inelastic activity, dissipates the input seismic energy limiting the seismic forces on the substructure; thereby providing an acceptable alternative strategy for the seismic design of rolled or fabricated composite straight steel I-girder bridges with limited skews and a composite reinforced concrete deck utilizing cross-frames at supports. The substructure is to be designed as essentially elastic as specified in Article 4.6.2.8.2; that is, the reinforced concrete piers/bents are to be capacity protected in the transverse direction for the maximum expected transverse seismic force. In the longitudinal direction, the piers/bents are to be designed for the unreduced axial forces and moments from the longitudinal elastic seismic analysis, with the moments divided by the response modification factor equal to 1.5. All abutments are to be designed to remain elastic. The strategy of designing a ductile superstructure in combination with an essentially elastic substructure has not yet been implemented in practice as of this writing (2013). This strategy is not mandatory, but is instead provided herein as an acceptable and effective alternative strategy to consider for the seismic design of such bridges located in Seismic Zones 2, 3 or 4.

Item #13

Replace the last bullet item in Article 6.16.4.1 with the following two bullet items:

- For structures in Seismic Zones 2, 3 or 4, designed using Strategy Type 2, the total lateral resistance of the special support cross-frames at the support under consideration determined as follows:

$$F = nV_{lat} \qquad (6.16.4.2\text{-}2)$$

where:

n = total number of bays in the cross-section

V_{lat} = lateral resistance of a special support cross-frame in a single bay determined from Eq. 6.16.4.5.2d-1 (kip)

- For structures in Seismic Zones 2, 3 or 4 designed using Strategy Type 3, the expected lateral resistance of the fusing mechanism multiplied by the applicable overstrength factor.

Item #14

Revise the second sentence of the last paragraph of Article C6.16.4.2 as follows:

In lieu of experimental test data, the overstrength ratio for shear key resistance may be obtained from the *Guide Specifications for LRFD Seismic Bridge Design* (~~2009~~2011).

Item #15

Add the following at the end of the second paragraph of Article 6.16.4.3:

In the case of a ductile superstructure, either no shear connectors, or at most one shear connector per row, shall be provided on the girders at the supports.

Item #16

Add the following at the beginning of the third paragraph of Article 6.16.4.3:

Shear connectors on support cross-frames or diaphragms shall be placed within the center two-thirds of the top chord of the cross-frame or top flange of the diaphragm.

Item #17

Add the following to the end of the second paragraph of Article C6.16.4.3:

Improved cyclic behavior can be achieved by instead placing the shear connectors along the central two-thirds of the top chord of the support cross-frames. It was shown experimentally that this detail minimizes the axial forces on the shear connectors thus improving their cyclic response.

Item #18

Add the following paragraph after the second paragraph of Article C6.16.4.3:

In order to reduce the moment transfer at the steel girder-deck joint in a ductile superstructure, it is recommended that either no shear connectors, or at most one shear connector per row, be provided on the steel girder at the supports. Thus, in the case of a ductile superstructure, all or most of the shear connectors should be placed on the top chord of the special support cross-frames within the specified region.

Item #19

Revise the second paragraph of Article 6.16.4.4 as follows:

The lateral force, *F*, for the design of the support cross-frame members or support diaphragms shall be determined as specified in Article 6.16.4.2 for structures designed using Strategy Types 1 or ~~2~~3, as applicable.

Item #20

Perform the following modifications to the Reference List in Article 6.17:

Replace the current ″AISC(2005b)″ reference listing with the following:

AISC, 2010b, *Seismic Provisions for Structural Steel Buildings*, ANSI/AISC 341-10, American Institute of Steel Construction, Chicago, IL.

Revise the current reference listing given below as follows:

Carden, L.P., F. Garcia-Alverez, A.M. Itani, and I.G. Buckle. 2006a. "Cyclic Behavior of Single Angles for Ductile End Cross-Frames," *Engineering Journal*. American Institute of Steel Construction, Chicago, IL, 2nd Qtr., pp. 111-125.

Item #21

In Article 14.6.5.3, revise the last sentence in the 3rd paragraph as follows:

However, forces may be reduced in situations where the ~~end diaphragms~~support cross-frames in the

superstructure have been specifically designed and detailed for inelastic action, in accordance with ~~generally accepted~~ the provisions for ductile ~~end diaphragms~~ superstructures specified in Article 6.16.4.5.

BACKGROUND:

The proposed ductile superstructure seismic design strategy (Strategy Type 2) may only be utilized as an alternative for straight steel I-girder bridges with limited skews and a composite reinforced concrete deck to allow controlled inelastic response at all support cross-frames. These cross-frames are designed and detailed to undergo large cyclic deformations without premature failure during large seismic events. The special support cross-frames are expected to yield and dissipate the earthquake input energy and provide a yield mechanism in the superstructure under transverse seismic loading. The substructure is to be designed as essentially elastic; that is, the reinforced concrete piers/bents are designed with an R factor for critical bridges. In addition, the substructure is checked for the maximum expected transverse seismic force in the end cross frames to ensure it is a capacity protected element.

ANTICIPATED EFFECT ON BRIDGES:

The anticipated benefit of utilizing the Type 2 seismic design strategy for select straight steel I-girder bridges is limiting the damage to support cross-frames while keeping the reinforced concrete bents/piers essentially elastic and the abutments elastic during large seismic events. It is anticipated that after design level earthquakes, the bridge will be able to be reopened to traffic soon after replacing the cross-frames at the support locations.

1.3 Seismic Design Examples

Three sets of seismic design examples were developed to illustrate the use of ductile end cross-frames (DECF) in steel I-girder bridges and compare the design results to the conventional seismic design. Sets I and II have three design examples: (1) bridge under Other category designed based on Type 1 design strategy, (2) bridge under Critical category designed based on Type 1 design strategy, and (3) bridge designed based on Type 2 category. Set III bridges, which are bridges with wall piers, have two examples: (1) bridge under Other category designed based on Type 1 strategy and (2) bridge designed based on Type 2 category. Thus, a total of eight design examples are presented in this report. Thus, a total of six design examples are presented in this report. Table 1-1 provides the description of these examples.

Table 1-1 Design examples

Set	Pier Type	Bridge Category	Superstructure	Designation
I	Single-column	Other	Elastic	Ex. I-1a
		Critical	Elastic	Ex. I-1b
		---	Inelastic	Ex. I-2
II	Two-column	Other	Elastic	Ex. II-1a
		Critical	Elastic	Ex. II-1b
		---	Inelastic	Ex. II-2
III	Wall	Other	Elastic	Ex. III-1
		---	Inelastic	Ex. III-2

1.3.1 Set I Bridges

Set I bridges are straight, three-span, steel I-girder bridges with single-column piers. The spans are continuous over the piers with span lengths of 105 ft, 152.5 ft, and 105 ft for a total length of 362.5 ft, as shown in Figure 1-1a. The superstructure cross-section is assumed to be uniform throughout the bridge length. It consists of three I-girders spaced 11.25 ft with overhang length of 3.75 ft, for a total width of 30 ft. The superstructure cross-section at supports is shown in Figure 1-1b. As can be seen in Figure 1-1b, the top chord is connected to the deck through shear connectors. The girder top flange is connected to the deck with one shear connector only to minimize the framing action between the reinforced concrete (R/C) deck and steel girders. Thus, the deck transverse seismic forces are primarily transferred to the bearings through the cross-frames. The total weight of the superstructure is 1,624 kips.

The piers are comprised of a tapered drop cap and a single R/C column. The column diameters are different for Ex. I-1 and I-2, as discussed in each respective chapter. However, the column clear height is 20 ft in both examples. The depth and width of pier cap are also different in each example. The connection between the cap and the steel girders is assumed to be pin connection.

The abutments are seat type with a 2.0-in. joint gap for thermal deformations. The backfill soil will be engaged after the bridge seismic longitudinal displacement exceeds 2.0 in. The abutments are unrestrained in the transverse direction.

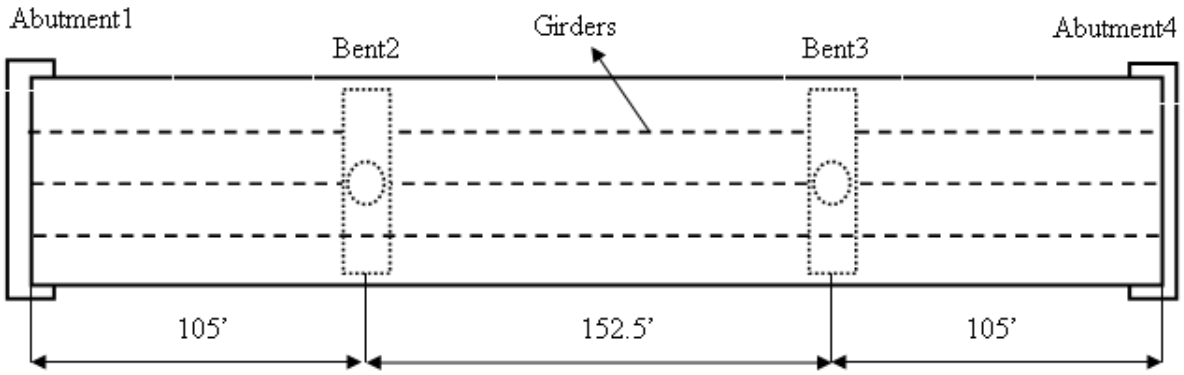

(a) Plan view

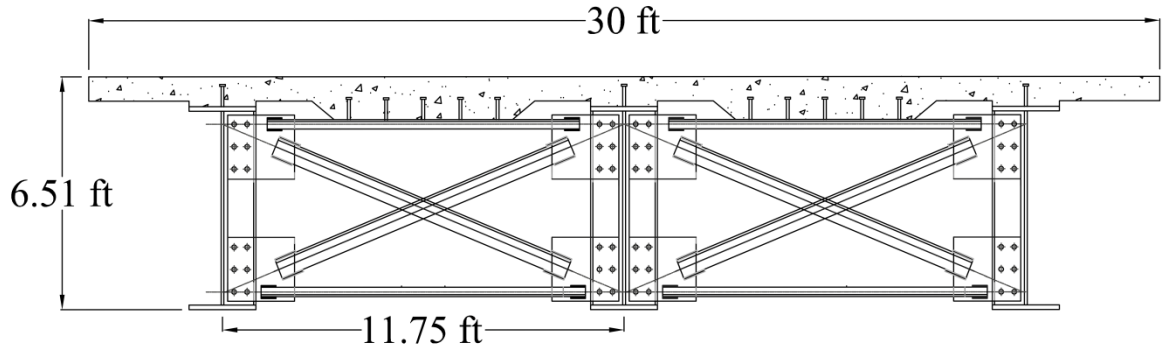

(b) Cross-section at supports

Figure 1-1 Plan view and cross-section of Set I bridges

1.3.2 Set II Bridges

Set II bridges are straight, three-span, steel I-girder bridges with two-column piers. The spans are continuous over the piers with span lengths of 110 ft, 150 ft, and 110 ft for a total length of 370 ft, as shown in Figure 1-2a. The superstructure cross-section is assumed to be uniform throughout the bridge length. It consists of six I-girders spaced 11 ft with overhang length of 5 ft, for a total width of 65 ft. The superstructure cross-section at supports is shown in Figure 1-2b. As can be seen in Figure 1-1b, the top chord is connected to the deck through shear connectors. The girder top flange is connected to the deck with one shear connector similar to Set I bridges. The total weight of the superstructure is 3,428 kips.

The piers are drop cap with two R/C columns. The column diameters are different for Ex. II-1 and II-2, as discussed in each respective chapter. However, the column clear height is 20 ft in both examples. The depth and width of pier cap are also different in each example. The connection between the cap and the steel girders is pin connection.

The abutments are seat type with a 2.0-in. joint gap for thermal deformations. The backfill soil will be engaged after the bridge seismic longitudinal displacement exceeds 2.0 in. The abutments are unrestrained in the transverse direction.

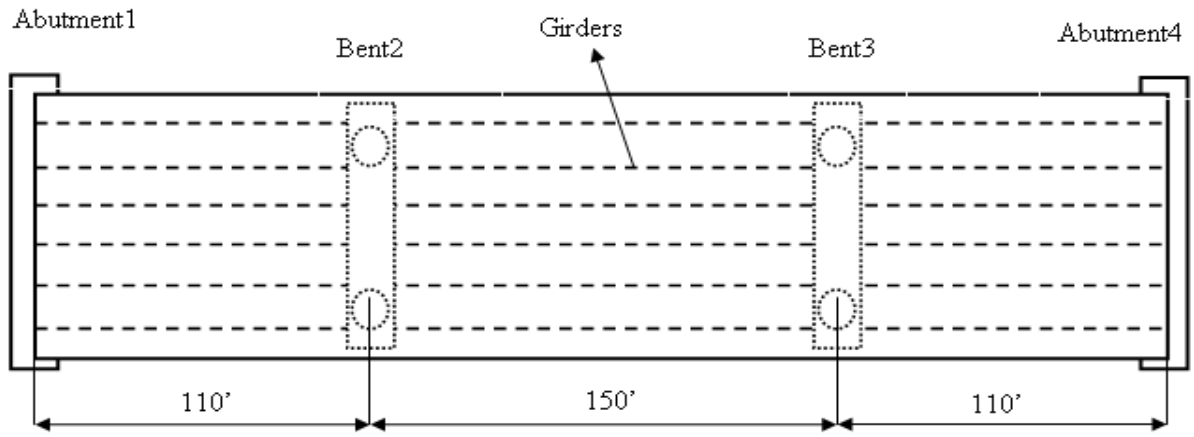

(a) Plan view

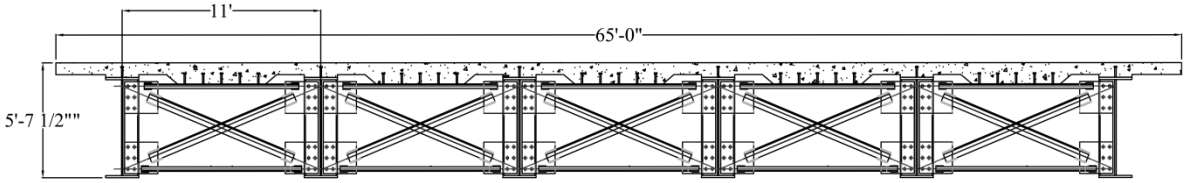

(b) Cross-section at supports

Figure 1-2 Plan view and cross-section of Set IIs and III bridges

1.3.3 Set III Bridges

Set III bridges are straight, three-span, steel I-girder bridges similar to Set II bridge superstructure except the substructure is wall piers. The wall pier dimensions are the same in both Ex. III-1 and III-2. The total height of wall is 25 ft. At the base of wall, the width is 40 ft and the thickness is 3 ft. The connection between the cap and the steel girders is assumed to be pin connection.

The abutments are seat type with a 2.0-in. joint gap for thermal deformations. The backfill soil will be engaged after the bridge seismic longitudinal displacement exceeds 2.0 in. The abutments are unrestrained in the transverse direction.

1.4 Seismic Design Methodology

The seismic design is based on force-based methodology. Elastic multi-mode spectral method of analysis is used to determine the column elastic forces and the design forces are determined by dividing these forces by the response modification factors, R-factor, shown in Table 1-2.

Table 1-2 Response modification factors

Substructure	Operational Category		
	Critical	Essential	Other
Wall-type piers – large dimension	1.5	1.5	2.0
Reinforced concrete pile bents			
• Vertical piles only	1.5	2.0	3.0
• With batter piles	1.5	1.5	2.0
Single columns	1.5	2.0	3.0
Steel or composite steel and concrete pile bents			
• Vertical piles only	1.5	3.5	5.0
• With batter piles	1.5	2.0	3.0
Multiple column bents	1.5	3.5	5.0

The steps for the seismic design of bridges using Type 1 design strategy (conventional) are:

1. Determine the effective moment of inertia of the columns using section analysis.
2. Determine the effective stiffness at the abutments. This stiffness is calculated by estimating the longitudinal displacement. If the contribution of backfill soil is to be ignored, the abutments are free in all horizontal directions.
3. Analyze the bridge for earthquake load in the longitudinal direction. Determine abutment displacement and verify the longitudinal displacement assumed in the previous step. Continue to next step if the displacements are close (i.e. within 5%), otherwise repeat Steps 2 and 3 until there is convergence.
4. Analyze the bridge for earthquake load in the transverse direction.
5. Combine the earthquake forces according to 100%-30% orthogonal combination, and determine the seismic design loads. An appropriate response modification factor, *R*, is used for the column design moments.
6. Design the R/C columns. Compare the column size and its effective moment of inertia to that in Step 1. If they are the same, continue to Step 7. Otherwise, repeat Steps 1 to 6 until there is convergence on the properties of the columns.
7. Determine the pier plastic shear in the longitudinal and transverse directions.

8. Design the support cross-frames such that their horizontal resistance is equal to or larger than the column plastic shear in the transverse direction.

For Type 2 design strategy, the force-based methodology is also used but the R-factor applied to the substructure is equal to 1.5 regardless of substructure type as outlined in Table 1-2 for critical bridges. The proposed steps for the seismic design of bridges using Type 2 design strategy (DECF) are:

1. Determine the effective moment of inertia of the columns using section analysis.
2. Determine the effective stiffness at the abutments. This stiffness is calculated by estimating the longitudinal displacement. If the contribution of backfill soil is to be ignored, the abutments are free in all horizontal directions.
3. Analyze the bridge for earthquake load in the longitudinal direction. Determine abutment displacement and verify the longitudinal displacement assumed in the previous step. Continue to next step if the displacements are close (i.e. within 5%), otherwise repeat Steps 2 and 3 until there is convergence.
4. Analyze the bridge for earthquake load in the transverse direction
5. Combine the earthquake forces according to 100%-30% orthogonal combination, and determine the seismic design loads. A response modification factor, *R*, of 1.5 is used for the column design moments.
6. Design the R/C columns. Compare the column size and its effective moment of inertia to that in Step 1. If they are the same, continue to Step 7. Otherwise, repeat Steps 1 to 6 until there is convergence on the properties of the columns.
7. Determine the pier nominal shear resistance in the longitudinal and transverse directions.
8. Determine the lateral reinforcement based on the plastic hinging of substructure in the longitudinal and transverse directions and minimum required confinement steel.
9. The seismic force for pier cross frames is based the on the lesser of: a) the pier nominal shear resistance and b) the seismic forces obtained from the response spectrum analysis.
10. The design seismic force for pier cross frames is the seismic force of the pier cross frame obtained in step 9 divided by a response modification factor equal to 4.
11. Design and detail the special diagonal member of the pier cross frames.
12. Determine the drift in the superstructure. The drift should be less than 4%. If the drift is more than 4%, then the area of the diagonal members of pier cross-frames should be increased.
13. Determine the expected lateral resistance of the pier cross-frames based on the fully yielded and strain hardened diagonal member. The nominal shear resistance of the substructure should be greater that the cross-frame lateral resistance.

1.5 Presentation of Design Examples

Each design example shown in Table 1-1 is presented as a stand-alone example. Bridge analysis is an iterative process, particularly when the contribution of abutment soil is considered. Design of components such as columns and cross-frames also requires iteration. Only the results of the **last** iteration of both analysis and design are presented. The presentation of each example is divided into the following sections:

- Bridge description
- Computational model – the model used in the elastic and nonlinear analyses are presented.
- Analysis – the forces obtained from the elastic analysis are presented. The earthquake analysis is presented in a two-column, step-by-step format. The left column shows the calculation procedure following to the design methodology. The right column shows the calculations.
- Design of Columns – a two-column, step-by-step format presentation of the design of column.
- Design of Cross-frames – also a two-column, step-by-step format presentation of cross-frame design.
- Cross-frame Properties for Nonlinear Analysis - also a two-column, step-by-step format showing the calculation of expected cross-frame properties for use in nonlinear analysis.
- Performance Assessment – presents the results of nonlinear response history analysis of the designed bridge. Ground motions representing the design and maximum considered earthquakes are used in the analysis (see Section 1.8.1).

The notations referring to specifications are the following

- AASHTO Specifications – AASHTO LRFD Bridge Design Specifications (AASHTO 2012)
- Guide Specifications – AASHTO LRFD Guide Specifications for Seismic Design (AASHTO 2012)
- Caltrans SDC – Seismic Design Criteria Version 1.6 of California Department of Transportation (Caltrans 2010).

1.6 Analytical Model

The computer program SAP2000 (CSI 2012) was used for the seismic analysis. A typical analytical model is shown in Figure 1-4. The global x-, y-, and z-axes correspond to longitudinal, transverse, and vertical directions, respectively.

1.6.1 Material Properties

The specified concrete strength for the deck, column, and pier cap is 4,000 psi. The longitudinal and transverse steel reinforcements are A706 Grade 60. The steel I-girders are composed of A709 Grade 50 plates. The cross-frames are A36 steel angles. These nominal material properties were used in the design calculations.

For nonlinear analysis, the expected material properties were used. The unconfined concrete compressive stress is 5,200 psi. The confined concrete properties were determined according to the final column design based on Mander's model. The expected yield and ultimate stress of A706 reinforcement steel is

68 ksi and 95 ksi, respectively, according to LRFD Seismic Guide Specifications. The expected yield stress (R_yF_y) of A36 steel angles is equal to 54 ksi according to the specifications (AASHTO 2012).

The backfill soil properties were calculated based on the recommended values by Caltrans SDC. The soil passive resistance is:

$$P_p = 5.0A_e\left(\frac{h}{5.5}\right) \quad kips \tag{1-1}$$

where A_e is the effective backwall area in ft^2 and h is the backwall height in ft. The initial soil stiffness is:

$$K_i = 50w\left(\frac{h}{5.5}\right) \quad kip/in \tag{1-2}$$

where w is the backwall width in ft.

1.6.2 Superstructure

The superstructure was modeled as a 3D spine beam with equivalent section properties. In sections where components are composed of nonhomogeneous material, the equivalent section properties are determined by transforming the entire section into an equivalent homogeneous material such that ordinary flexure theory applies. For a steel I-girder superstructure, the cross-section is transformed into either equivalent steel or equivalent concrete. The equations for calculating the section properties shown below are based equivalent steel material (Monzon et al. 2013a). The modular ratio, n, is:

$$n = \frac{E_s}{E_c} \tag{1-3}$$

where E_s is the modulus of elasticity of steel and E_c is the modulus of elasticity of concrete. To account for deck cracking, an effective E_c is used to calculated n. The effective E_c may be assumed to be 50% of the gross E_c (Carden et al., 2005a), unless the degree of cracking in the R/C deck is known and a more accurate estimate for E_c can be deduced. The transformed sections used to determine the equivalent section properties are illustrated in Figure 1-3.

The equivalent area is calculated using the equation

$$A = \sum A_g + A_d = \sum A_g + \frac{b_d t_d}{n} \tag{1-4}$$

where A_g is the area of individual girder, A_d is the area of deck, b_d is the total deck width, and t_d is the thickness of the deck. The contribution of concrete haunch between the girder top flange and deck slab is small and thus neglected.

For section moment of inertia I_x, the deck width is divided by the modular ratio and the equivalent section is as shown in Figure 1-3b. It is the deck width that is modified because it is the dimension parallel to the axis where the moment of inertia is calculated. The thickness is not modified to preserve the strain distribution. Note that the equivalent area is not affected, and Equation (1-4) is still valid. The location of

the neutral axis NA_x measured from the girder bottom flange (assuming all the girder bottom flange is on the same elevation) is given by:

$$\bar{y} = \frac{1}{A}\left[\sum\left(A_g y_g\right) + A_d y_d\right] \tag{1-5}$$

where y_g is the vertical distance to the centroid of individual girder from the soffit and y_d is the vertical distance to the centroid of the deck from the soffit. Then, I_x is calculated using the equation:

$$I_x = \sum\left(I_{gx} + A_g y_{gx}^2\right) + \frac{1}{12}\frac{b_d}{n}t_d^3 + A_d y_{dx}^2 \tag{1-6}$$

where I_{gx} is the individual girder's centroidal moment of inertia about x-axis, y_{gx} is the vertical distance from NA_x to the centroid of the individual girder, and y_{dx} is the vertical distance from NA_x to the centroid of the deck.

For moment of inertia I_y, it is the deck thickness that is divided by n, and the equivalent steel section is as shown Figure 1-3c. The thickness is the dimension that is parallel to the axis where moment of inertia is calculated. The width is not modified to preserve the strain distribution. The area is still the same as that given by Equation (1-4). The location of neutral axis is NA_y measured from the edge of the deck is given by the equation:

$$\bar{x} = \frac{1}{A}\left[\sum\left(A_g x_g\right) + A_d x_d\right] \tag{1-7}$$

where x_g is the horizontal distance to the centroid of individual girder and x_d is the horizontal distance to the centroid of the deck. NA_y is located at the bridge centerline for a uniform girder spacing and uniform deck overhang length. I_y is given the by equation:

$$I_y = \sum\left(I_{gy} + A_g x_{gy}^2\right) + \frac{1}{12}\frac{t_d}{n}b_d^3 + A_d x_{dy}^2 \tag{1-8}$$

where I_{gy} is the individual girder's centroidal moment of inertia about y-axis, x_{gy} is the horizontal distance from NA_y to the centroid of individual girder, and x_{dy} is the horizontal distance from NA_y to the centroid of the deck. For a uniform girder section, spacing, and deck thickness, I_y becomes

$$I_y = \sum\left(I_{gy} + A_g x_{gy}^2\right) + \frac{1}{12}\frac{t_d}{n}b_d^3 \tag{1-9}$$

The torsional constant J is calculated by the applying the thin-walled theory to the transformed section. The deck plays an important role in resisting torsion as it can be considered as top flange of the entire section with the girders acting as the web. The shear flow is similar to that of a channel section, and the transformed section is as shown in Figure 1-3d. The deck, acting as top flange, is continuously connected to the girder web such that thin-walled open section formulas apply (Heins and Kuo 1972). The torsional constant is given by:

$$J = \sum \frac{1}{3}\left(ht_w^3 + b_{bf}t_{bf}^3\right) + \frac{b_d t_d^3}{3m} \tag{1-10}$$

$$m = \frac{G_s}{G_c} \tag{1-11}$$

where h is the is the vertical distance between the center of bottom flange and center of deck as shown in Figure 1-3d, t_w is the web thickness, b_{bf} is the width of the bottom flange, t_{tf} is the thickness of the bottom flange, G_s is the shear modulus of steel, and G_c is the shear modulus of concrete.

The spine beam is located at the center-of-gravity of the superstructure. It is then connected to rigid beam elements using rigid links. These rigid beam elements are located at the center-of-gravity of the deck. They are then connected to the top chords using rigid links, as shown in Figure 1-4b. This modeling is due to the top chords being connected to the deck discussed in Sections 1.3.1 and 1.3.2 and shown in Figure 1-1b and Figure 1-2b. The superstructure vertical and longitudinal forces are transferred to the bearings through the link elements located along the girder lines above the bearings.

The mass from the dead load of superstructure and future wearing surface (see also Section 1.7) were distributed to the nodes along the superstructure elements. The magnitude of mass assigned to each node is proportional to the area tributary to that node.

1.6.3 Cross Frames

For elastic analysis, the cross-frames were modeled using beam elements. The effective axial stiffness of the single angle members is reduced due to end connection eccentricities. In the model, this was achieved by modifying the area of the cross frames. The effective area (A_e) is calculated as follows (AASHTO 2012):

$$A_e = \frac{A_g I}{I + A_g e^2} \tag{1-12}$$

where A_g is the gross area of the member, I is the section moment of inertia, and e is the eccentricity of the connection plate relative to the member centroidal axis. However, the resistance of the member is still calculated using the gross area.

For nonlinear analysis, the cross-frames were modeled using multi-linear plastic link elements. The force-displacement relationship of these link elements is shown in Figure 1-5. This relationship is based on the experiments conducted by Bahrami et al. (2010) and Carden et al. (2005). The expected material properties were used to calculate the yield and buckling load capacities.

1.6.4 Pier Caps and Columns

The pier cap was modeled using beam elements assigned with gross-section properties. In Set I bridges, these elements are non-prismatic sections to account for the tapered cap.

For elastic analysis, the R/C columns were modeled using beam elements with effective section properties. These properties are determined through section analysis. For nonlinear analysis, fiber hinges

were assigned to the expected locations of plastic hinges. The material properties assigned to the elements of these hinges were the expected material properties. Unconfined and confined concrete properties were also used.

The pin connection between the girder and the pier cap was modeled using link elements. The translational degrees of freedom of these elements were assigned with high stiffness. The rotational degrees of freedom were unrestrained (i.e. zero stiffness)

1.6.5 Abutment Backfill Soil

At the abutments, in the longitudinal direction, the joint gap and backfill soil were modeled using a series of gap link element and multi-linear plastic element, respectively. In the transverse direction, the abutments were unrestrained.

For elastic analysis, the nonlinear properties of link elements were not used and were instead assigned with equivalent effective stiffness. This effective stiffness is assigned to the element representing the soil while the gap link element is assigned with high stiffness with no opening. For nonlinear analysis, the gap element is assigned with an opening as specified in Section 1.3.

1.7 Design Loads

Only dead (*DC*), future wearing surface (*DW*), and earthquake (*EQ*) loads were considered in these examples. The *DC* loads were from the weight of the components. For *DW*, a uniformly distributed area load of 35 psf was used on the R/C deck. These loads were distributed to the nodes of the superstructure elements. The magnitude of loads assigned to each node is proportional to its tributary area.

The bridge was assumed to be located in Los Angeles, California with latitude of 34.052 and longitude of -118.244. The peak ground acceleration (*PGA*) is 0.671 g, short-period spectral acceleration (S_s) of 1.584 g, and long-period spectral acceleration (S_1) of 0.534 g. The bridge was assumed to be founded on a Site Class B soil thus all the site factors are equal 1.0. The horizontal response acceleration coefficients at 0.2-second period (S_{DS}) and at 1.0-second period (S_{D1}) are 1.584 g and 0.534 g, respectively. The design spectrum is shown in Figure 1-6.

The load combination used in the design calculations is Extreme Event I. The load factors are 1.25, 1.5, and 1.0 for *DC*, *DW*, and *EQ*, respectively. The orthogonal combination of longitudinal and transverse *EQ* loads was based on the 100%-30% combination prescribed in AASHTO Specifications.

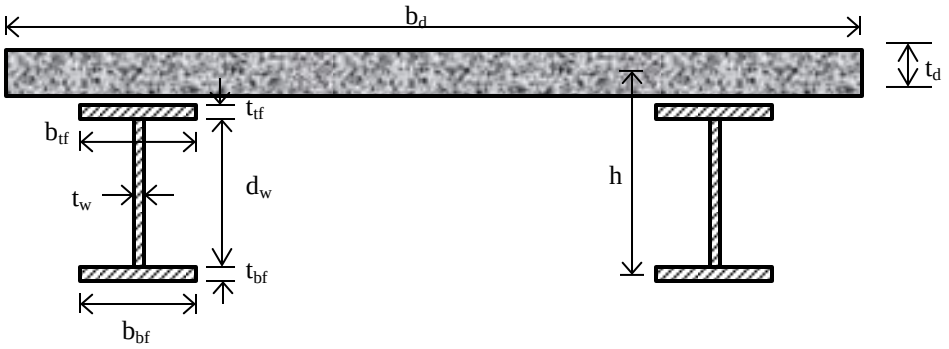

(a) Steel plate girder composite section

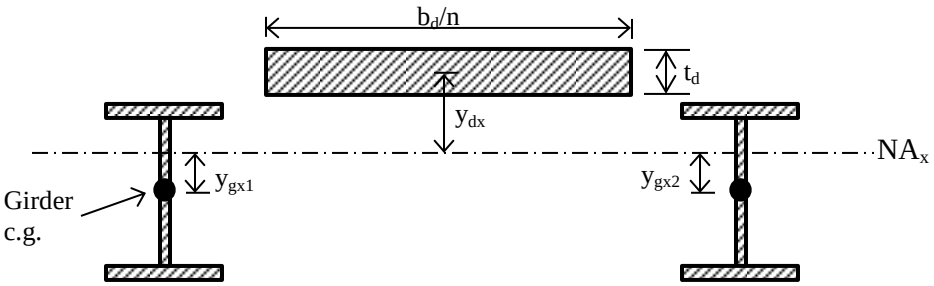

(b) Transformed section for calculation of I_x

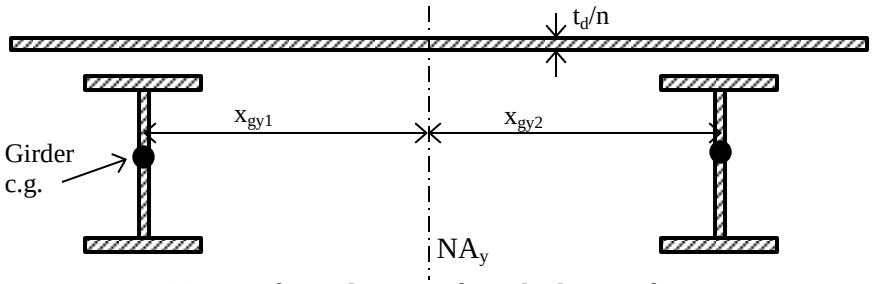

(c) Transformed section for calculation of I_y

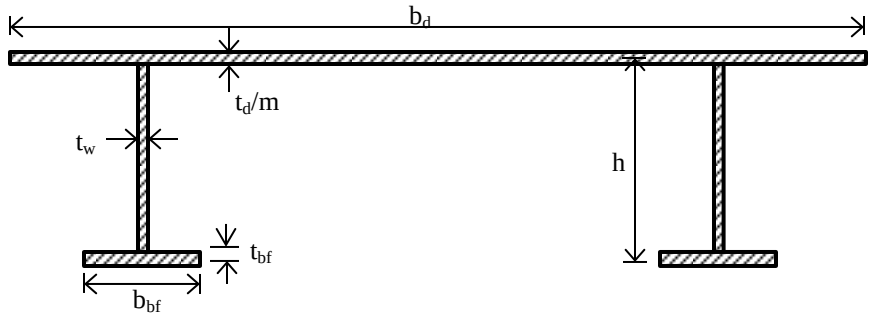

(d) Thin-walled open section for calculation of J

Figure 1-3 Transformed sections used to calculate the equivalent section properties

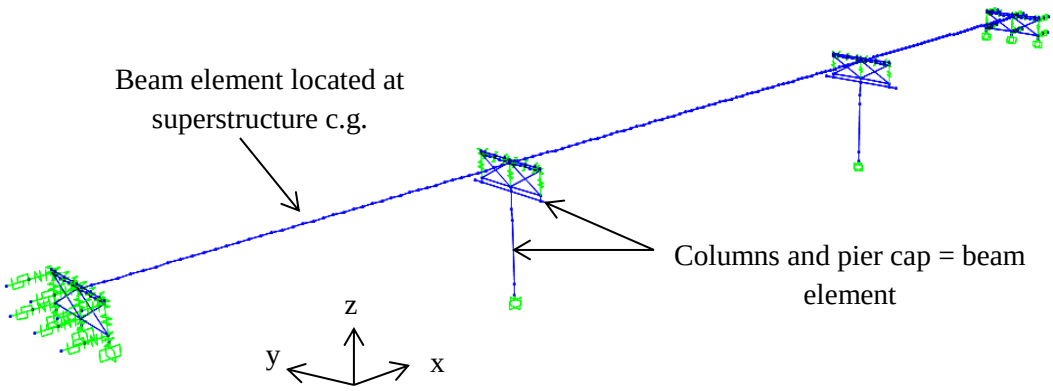

(a) 3D view of model

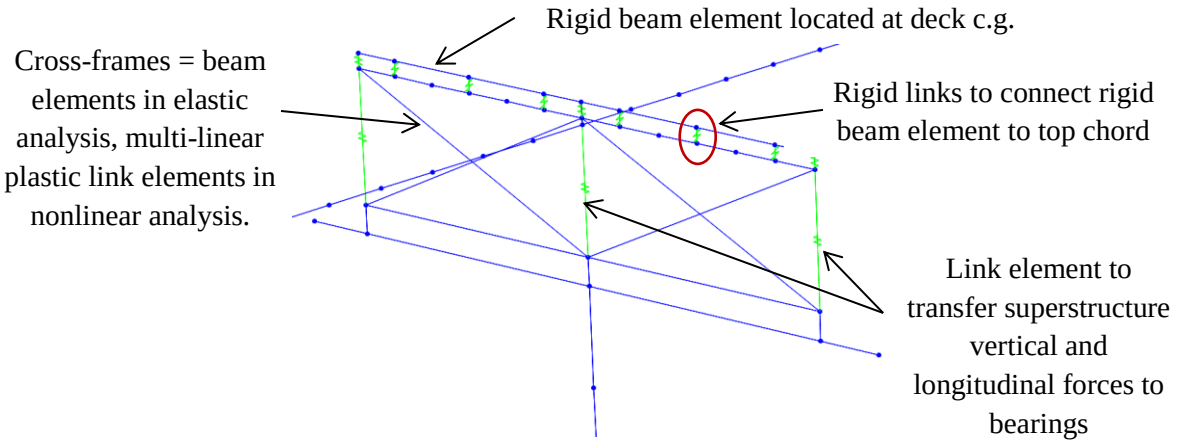

(b) Detail at piers

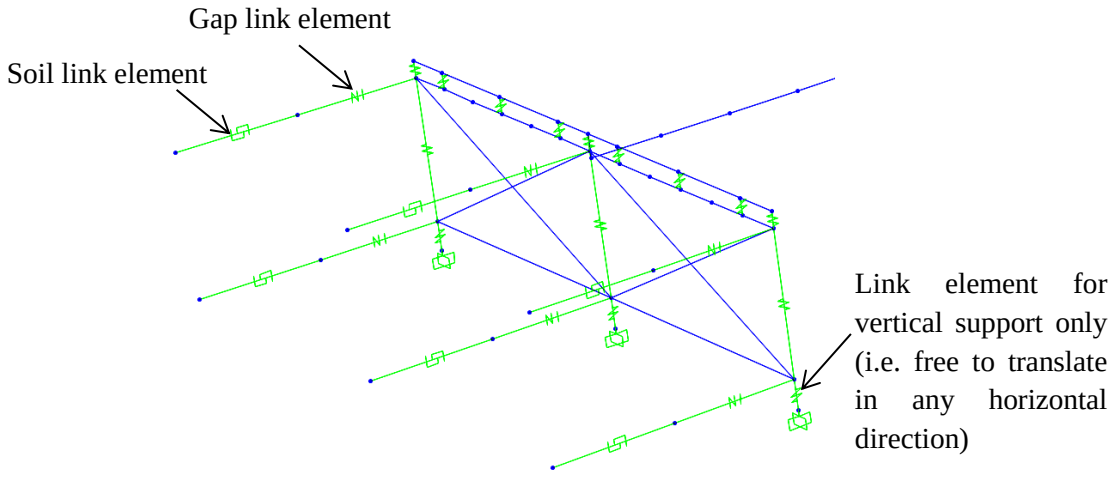

(c) Detail at abutments

Figure 1-4 Details of analytical model

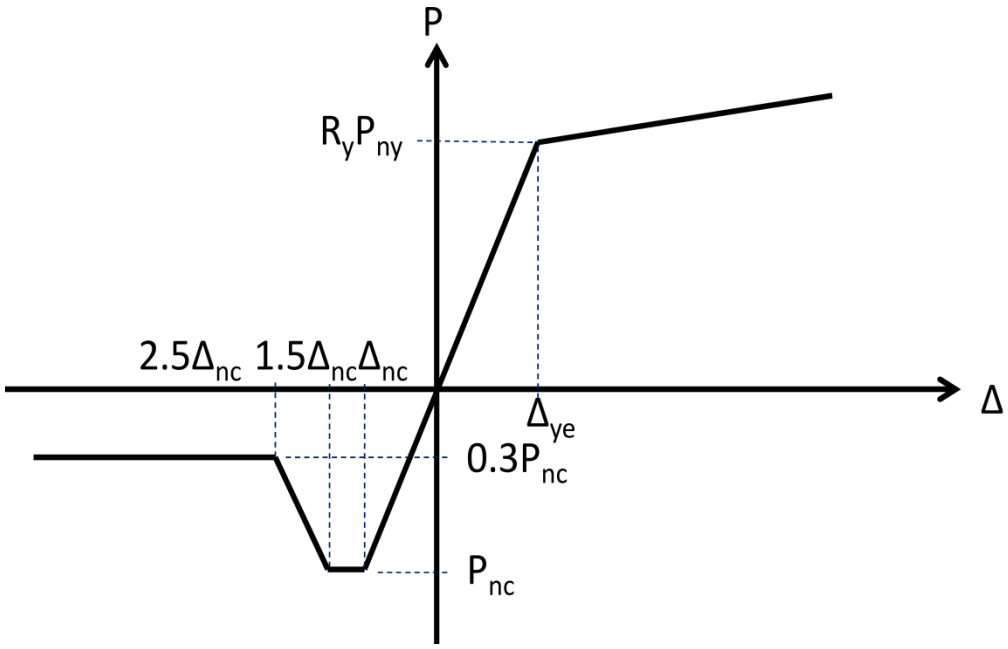

Figure 1-5 Force-displacement relationship of ductile cross-frames used for design evaluation

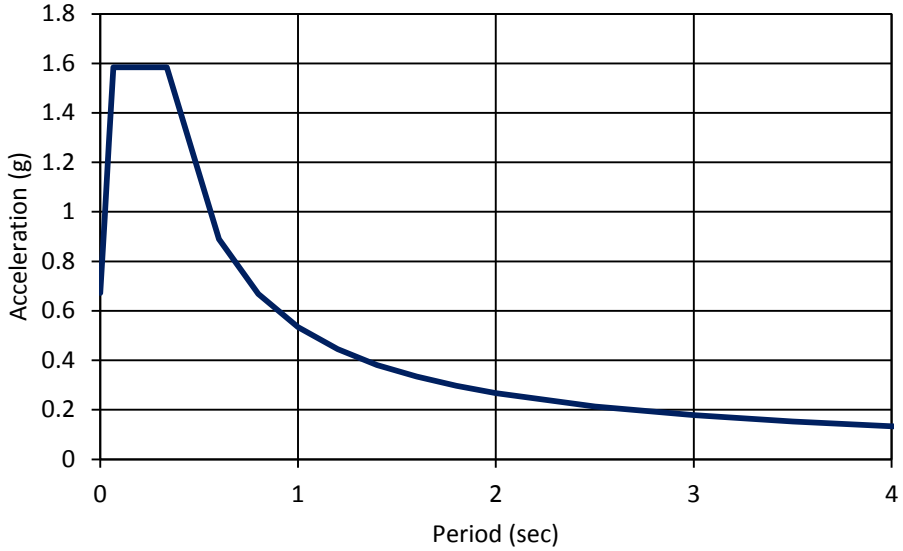

Figure 1-6 Design spectrum

1.8 Seismic Evaluation of Design Examples

The seismic performance of bridges designed according to Type 1 and 2 strategies were evaluated through nonlinear response history analysis.

1.8.1 Ground Motions

The PEER Ground Motion Database (PEER 2013) was used to select historical ground motions that closely match the design spectrum. The ground motions were selected based on the mean squared error (MSE) of the difference between the design spectrum and spectral accelerations of records. The seven ground motions with the lowest MSE were recorded from:

- 1979 Imperial Valley Earthquake at Calexico Fire Station (NGA #162)
- 1983 Coalinga Earthquake at Parkfield – Stone Corral Station (NGA #357)
- 1986 Chalfant Valley Earthquake at Convict Creek station (NGA #551)
- 2003 Big Bear City Earthquake at San Bernardino – Co Service Bldg Station (NGA #2137)
- 1999 Chi-chi Earthquake at CHY039 Station (NGA #2951)
- 1999 Chi-chi Earthquake at CHY088 Station (NGA #2982)
- 1999 Chi-chi Earthquake at TCU075 Station (NGA #3471)

The components of these records were resolved into fault normal (FN) and fault parallel (FP) components. Table 1-3 shows the scale factors applied to each ground motion that minimizes the MSE between the design spectrum and geometric mean of the spectra for these components. Figure 1-7 shows the geometric mean of all spectra from selected records plotted against the design spectrum. The spectra from the FN and FP components of each record, along with their geometric mean spectrum (GM), plotted against the design spectrum are shown in Figure 1-8. The FP components were applied in the longitudinal direction while the FN components were applied in the transverse direction.

These ground motions were also used to analyze the design examples for earthquake levels equivalent to the Maximum Considered Earthquake (MCE). The MCE is defined by *PGA* of 0.873 g, S_s of 2.182 g, and S_1 of 0.733 g. Since the spectral accelerations given in AASHTO Specifications are based on design earthquake, the MCE values were determined from ASCE 7-10 (ASCE 2010). Figure 1-9 shows the MCE spectrum compared against the response spectra of selected ground motions. Figure 1-10 shows the GM of the spectra of the seven records plotted against the MCE spectrum.

Seven analyses were performed for the design earthquake and seven analyses were performed for the MCE earthquake. These analyses are summarized in Table 1-3.

Table 1-3 Summary of nonlinear analyses runs

EQ Level	Designation	Ground Motion NGA #	Ground Motion Component		Scale Factor
			Longitudinal Direction	Transverse Direction	
DE	DE1	162	FP	FN	2.79
	DE2	357	FP	FN	6.14
	DE3	551	FP	FN	10.73
	DE4	2137	FP	FN	49.41
	DE5	2951	FP	FN	9.02
	DE6	2982	FP	FN	7.02
	DE7	3471	FP	FN	8.36
MCE	MCE1	162	FP	FN	3.83
	MCE2	357	FP	FN	8.44
	MCE3	551	FP	FN	14.75
	MCE4	2137	FP	FN	67.91
	MCE5	2951	FP	FN	12.40
	MCE6	2982	FP	FN	9.65
	MCE7	3471	FP	FN	11.50

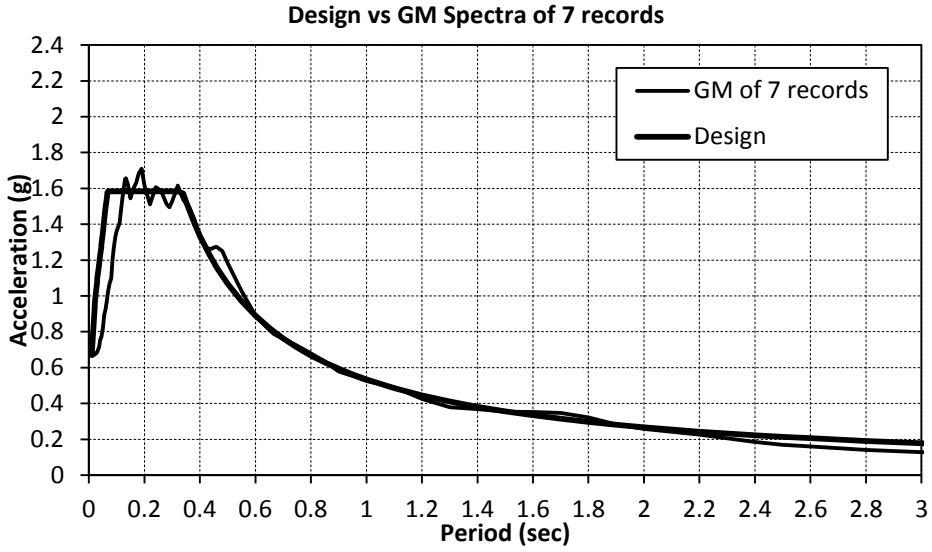

Figure 1-7. Comparison of design spectrum and geometric mean of spectra of selected records

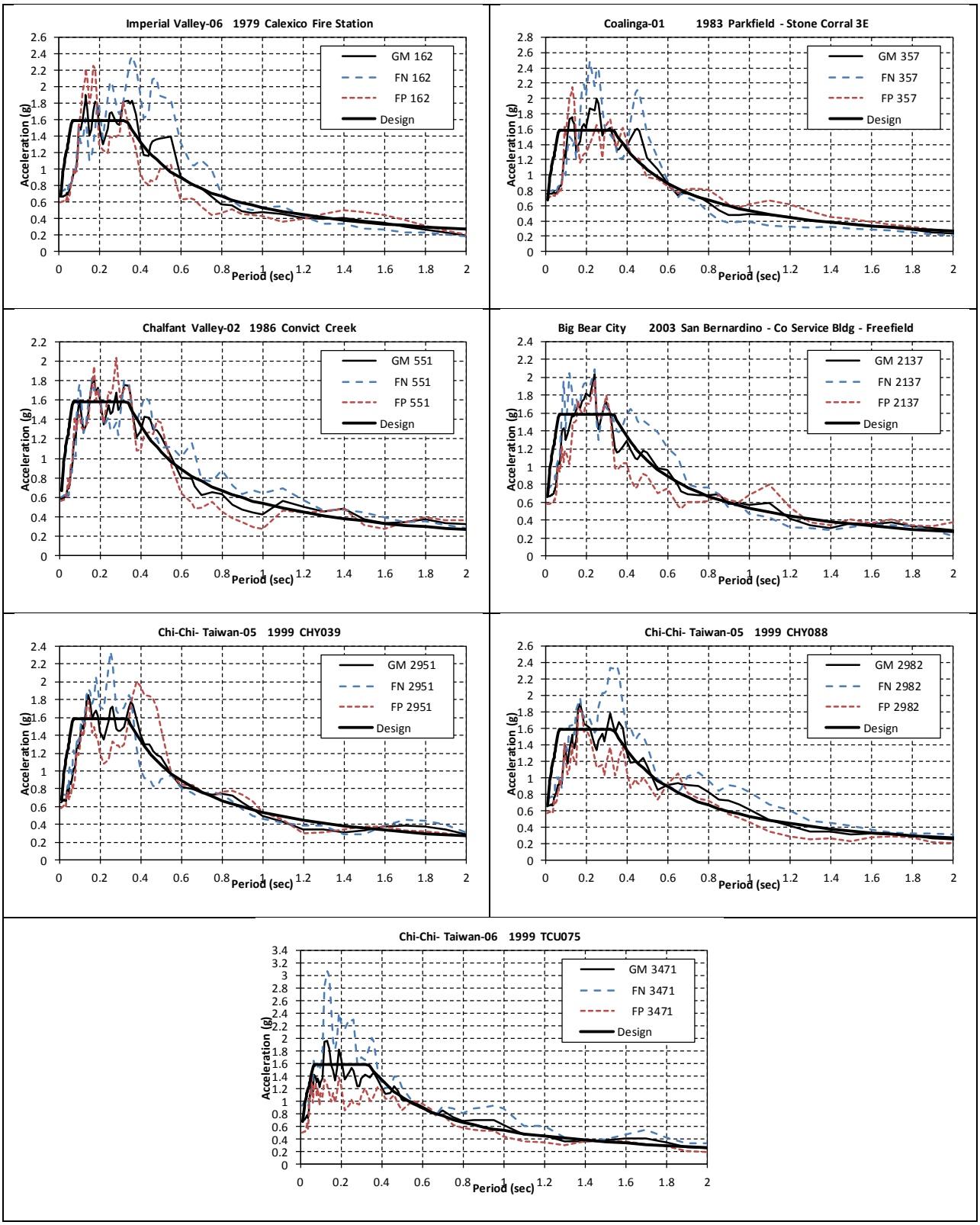

Figure 1-8 Response spectra of selected ground motions compared against design spectrum

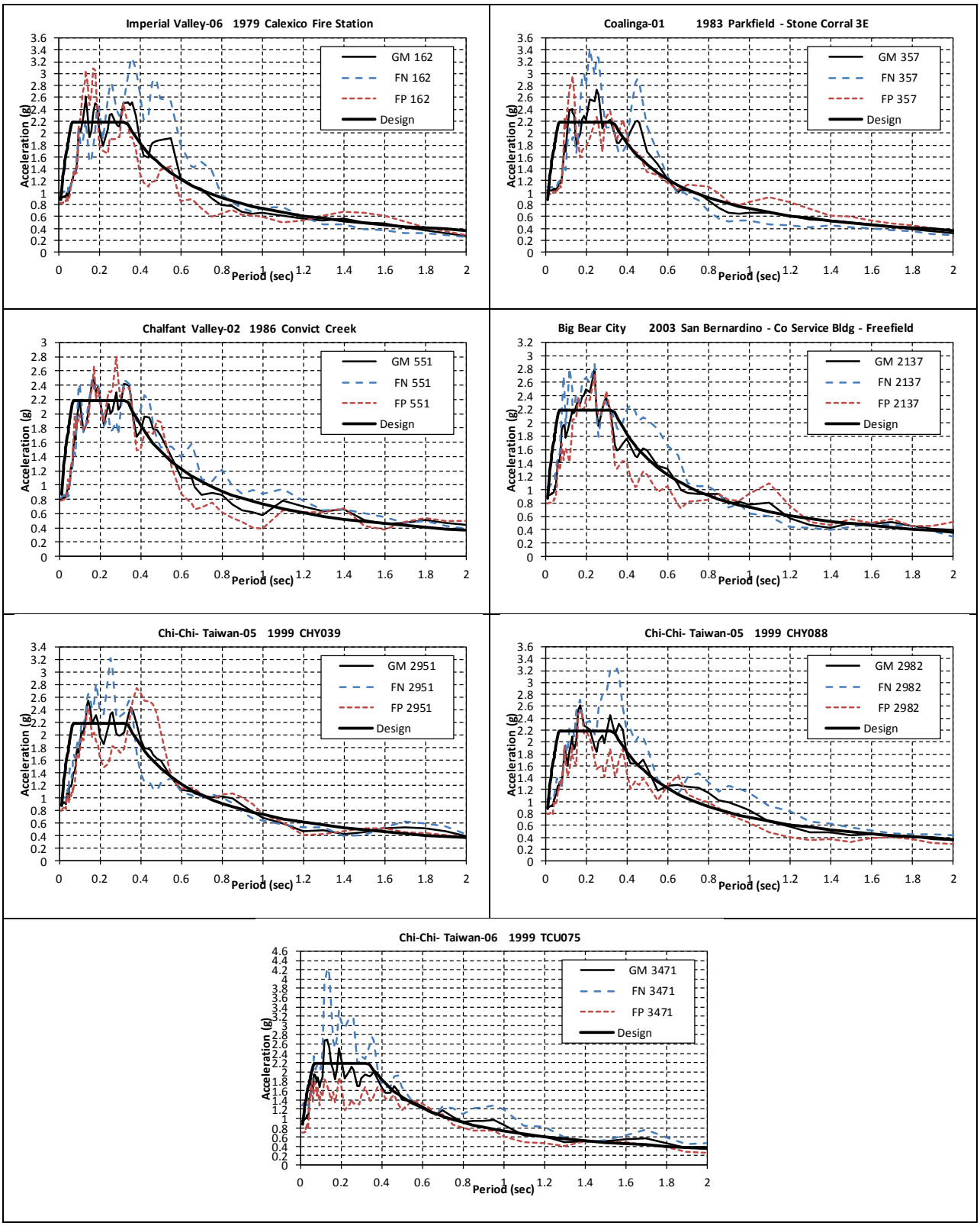

Figure 1-9 Response spectra of selected ground motions compared against MCE

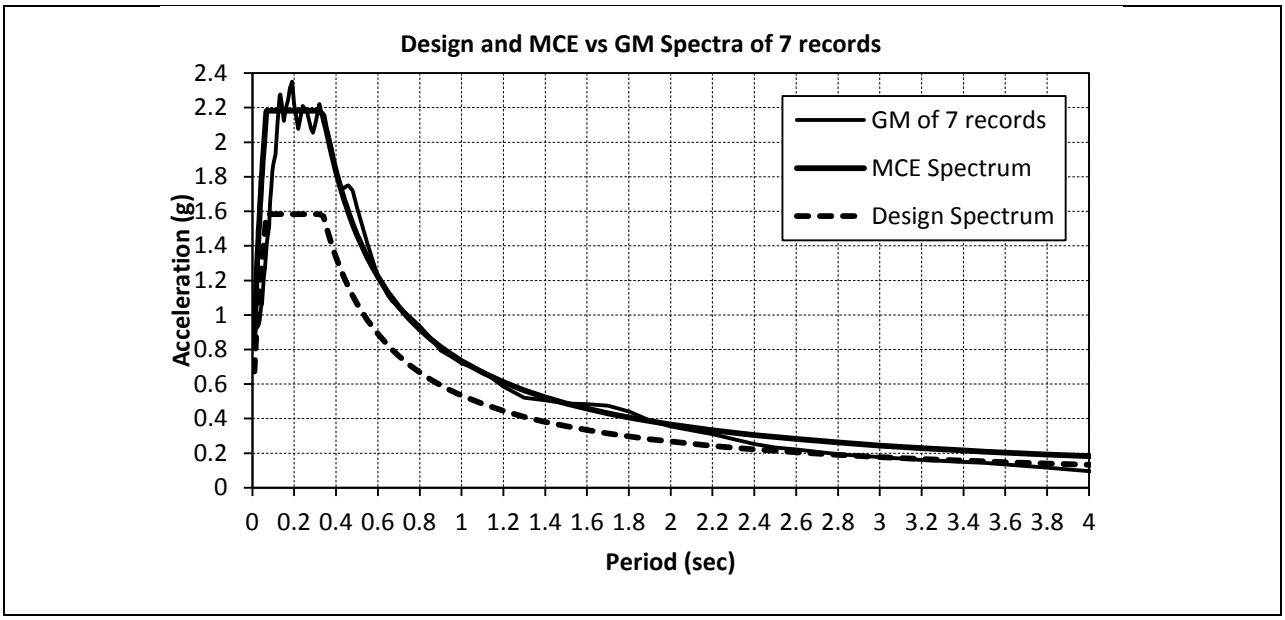

Figure 1-10 Comparison of MCE spectrum and geometric mean of spectra of selected records

1.8.2 Calculation of Column Yield Displacement

The ductility demands shown in the nonlinear evaluation of design examples were calculated by dividing the maximum column displacement by the yield displacement. The maximum column displacement was obtained from nonlinear analysis. The yield displacement was calculated based on the procedure discussed below.

1.8.2.1 Single-Column Pier

1.8.2.1.1 Longitudinal Yield Displacement

The longitudinal shear force that creates moment and lateral reaction at the base of the column is applied to the bearings on top of the pier cap. Since this is at some distance from the top of the column, the moment created by this shear force to the top of column must be considered in calculating the displacement at the top of the column. Figure 1-11 shows the schematic diagram of column displacement and force acting on top of the column. The displacement due to the lateral force *P* and the moment *Pe* is given by the equation:

$$\Delta_1 = \frac{PH^3}{3EI_e} + \frac{PeH^2}{2EI_e} \tag{1-13}$$

P is taken as the yield shear force in the column when calculating yield displacement,

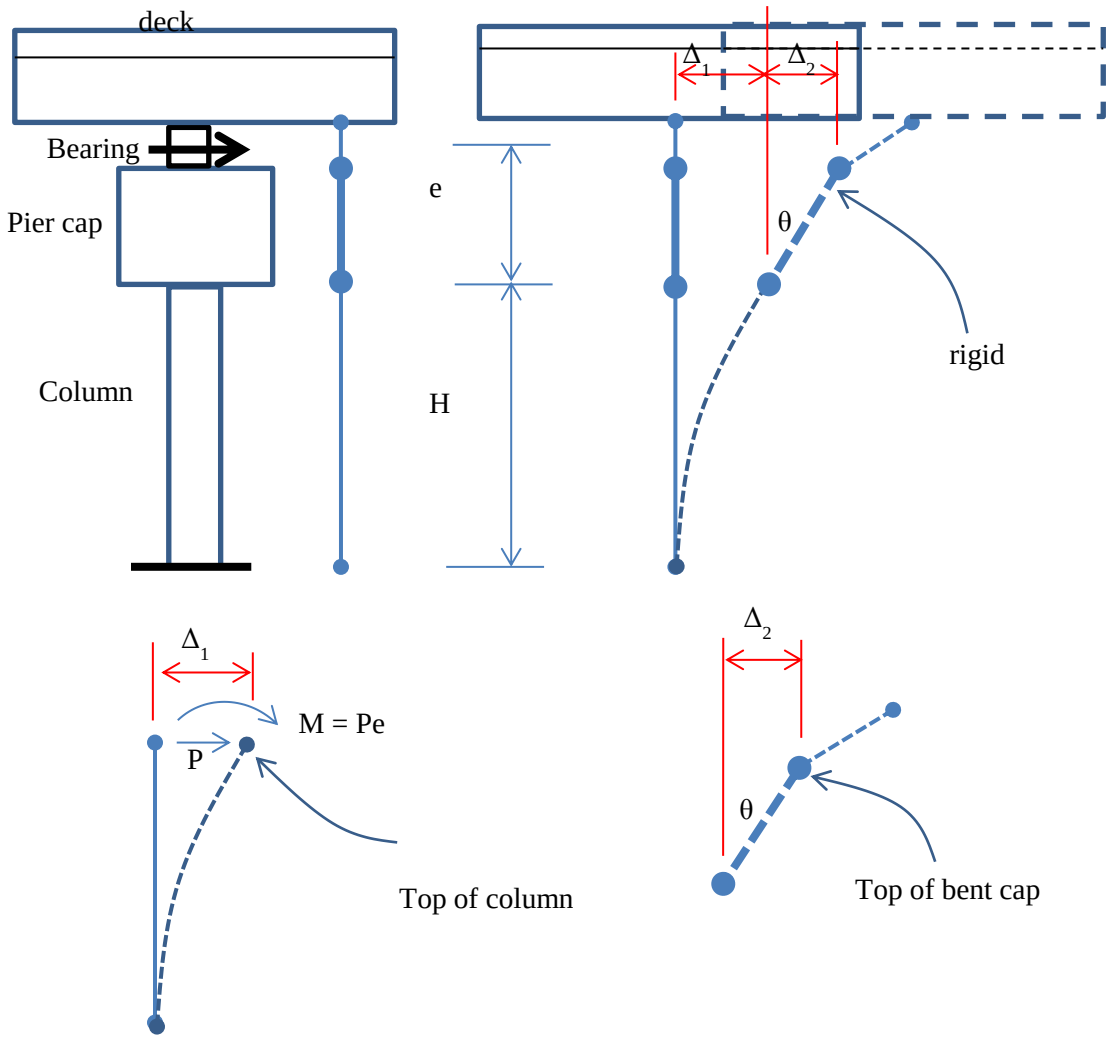

Figure 1-11. Schematic diagram showing the column displacement

1.8.2.1.2 Transverse Direction

Most of the seismic forces are developed in the deck since it comprises more than 80% of the bridge weight. This seismic force creates overturning in the superstructure which results in vertical reactions in the bearings, as illustrated in Figure 1-12. These vertical reactions, in turn, create moment at the top of pier cap. This moment must be added to the moment on top of the column which is created by the shear force in the bearings. These set of forces is illustrated in Figure 1-12. Since the moment created by the bearing forces is equal to the overturning moment created by the deck seismic force, the moment at the top of pier cap is equal to *Ph*. Equation (1-13) is modified to include this moment in the calculation of yield displacement:

$$\Delta_1 = \frac{PH^3}{3EI_e} + \frac{P(e+h)H^2}{2EI_e} \qquad (1\text{-}14)$$

where *e* is the distance from the top of the column to the centerline of the bearing as shown in Figure 1-11, *h* is the distance from the centerline of the bearing to the center of gravity of deck. *P* is taken as the column yield shear force when calculating the yield displacement.

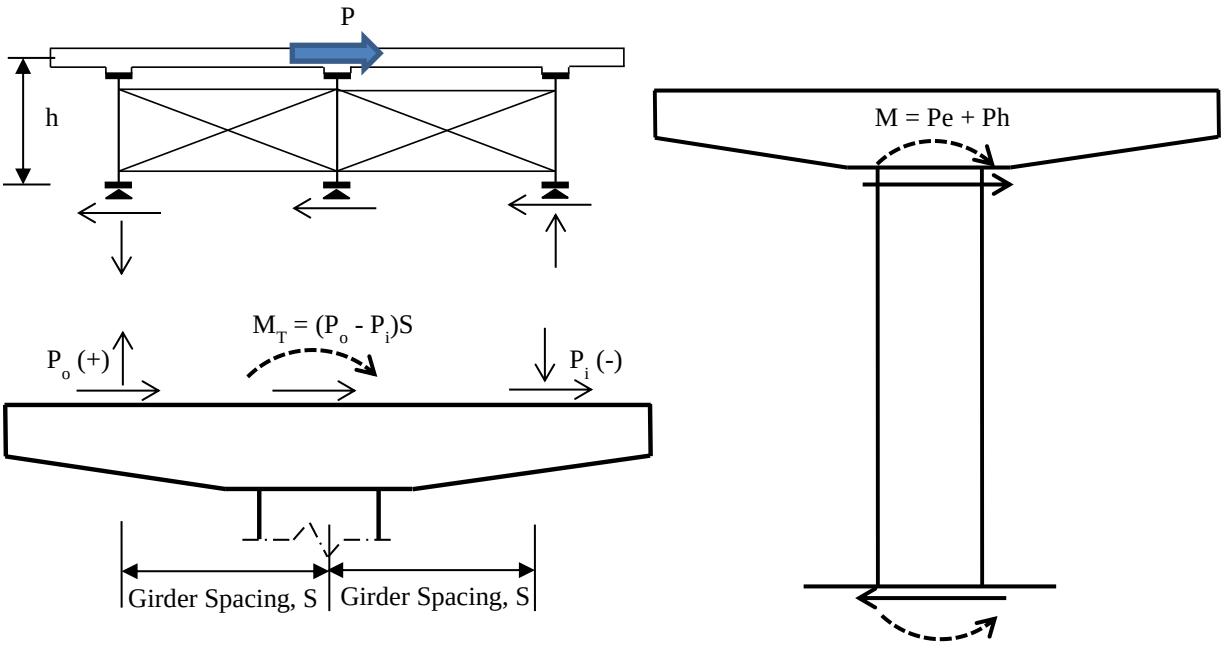

Figure 1-12. Forces in a single-column pier in the transverse direction.

1.8.2.2 Two-Column Pier

Calculation of the yield displacement in the longitudinal direction is similar to that used in single-column pier and given by Equation (1-13). In the transverse direction, the pier cap is assumed as rigid and the displacement at the top of column is calculated using the equation:

$$\Delta_1 = \frac{PH^3}{24EI_e} \tag{1-15}$$

where *H* is the clear height of the column, similar to that shown in Figure 1-11. *P* is taken as the yield shear force when calculating the yield displacement. Note that this force is twice the shear force in each column. This equation is based on double-curvature response in the transverse direction.

1.8.2.3 Wall Pier

The displacement is calculated at the top of the pier. In the longitudinal direction, from the base to top of wall, is essentially a cantilever column. The displacement is given by:

$$\Delta_1 = \frac{PH^3}{3EI_e} \tag{1-16}$$

where H is the height measured from the base of the wall to the top of wall. In the transverse direction, the displacement is negligible as it is the strong direction of pier. The displacement is therefore not evaluated in this direction.

1.8.3 Calculation of Superstructure Drift

The design superstructure drift is calculated using the equation:

$$Drift = \frac{\Delta_{lat}}{d_w} \tag{1-17}$$

where Δ_{lat} is the lateral displacement of the superstructure calculated using Eqn. (1-18) and d_w is the depth of girder web. The superstructure lateral displacement is calculated based on the diagonal member deformation using the equation:

$$\Delta_{lat} = \frac{P_{EQY}L}{EA_e \cos\theta} \tag{1-18}$$

where P_{EQY} is the elastic force in the diagonal member of the cross-frame obtained from response spectrum analysis in the transverse direction, L is the length, E is its modulus of elasticity, A_e is the effective area calculated using Eqn. (1-12), and θ is the angle of inclination measured from the horizontal. Since response spectrum analysis is used in the analysis, the superstructure displacement is not calculated as the difference between the displacement of the node representing the top of the girder and the displacement of the node representing the bottom of the girder. This is because the results obtained from response spectrum analysis are the maximum response after modal combinations. The maximum displacements in the nodes do not necessarily occur at the same time and, thus, may not be used to obtain the relative displacement between the top and the bottom of the girder.

Chapter 2 Bridge with Single-Column Piers Designed using Type 1 Strategy (Example I-1a)

2.1 Bridge Description

The overall geometry of Ex. I-1a is described in Section 1.3.1. From the final design iteration, the reinforced concrete (R/C) column diameter is 4 ft with longitudinal and transverse steel ratios of 1.0%. The pier cap is 5 ft wide, and it is tapered with depth starting from 3 ft-4 in. at the ends to 4 ft at the center. Figure 2-1 shows the elevation of Ex. I-1a at piers. The cross-frames are of X-type pattern with diagonal members made of L8x8x5/8 single angles while the top and bottom chords are 2L4x4x1/2 double angles.

2.2 Computational Model

The computational model is shown in Figure 2-2. The equivalent concrete section properties of superstructure are summarized in Table 2-1. Local axes of the superstructure are shown in Figure 2-1. Deck cracking was accounted for in the calculation of these properties by using 50% of the gross concrete modulus of elasticity (E_c).

For nonlinear response history analysis, the cross-frames were modeled with multi-linear plastic link elements with force-deformation relationship shown in Figure 1-5 to account for inelasticity in case it occurred. Calculation of expected force and deformations are shown in Section 2.6.

Table 2-1 Ex. I-1a superstructure equivalent concrete section properties

Area, A (in^2)	6,028
Moment of inertia about horizontal axis, I_2 (in^4)	4,660,235
Moment of inertia about vertical axis, I_3 (in^4)	69,386,665
Torsional constant, J (in^4)	102,071

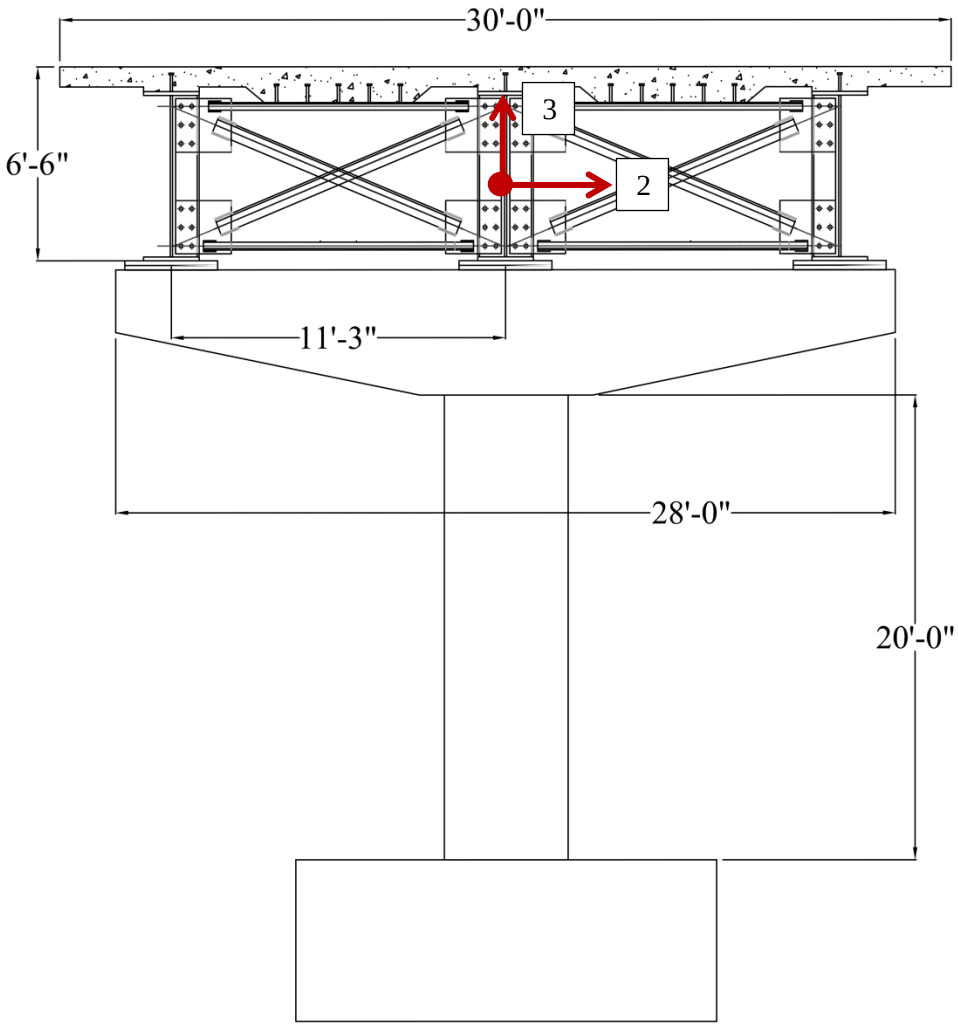

Figure 2-1 Elevation at piers of Ex. I-1a

2.3 Analysis

2.3.1 Gravity Loads – DC and DW

The total *DC* load (i.e. total bridge dead load) is 1,848 kips and the total *DW* load is 378 kips. The reactions at the base of column due to these loads are 763 kips and 152 kips, respectively. These loads were used to calculate the effective section properties of the columns, as illustrated in Section 2.3.2 *Steps 1* and *2*.

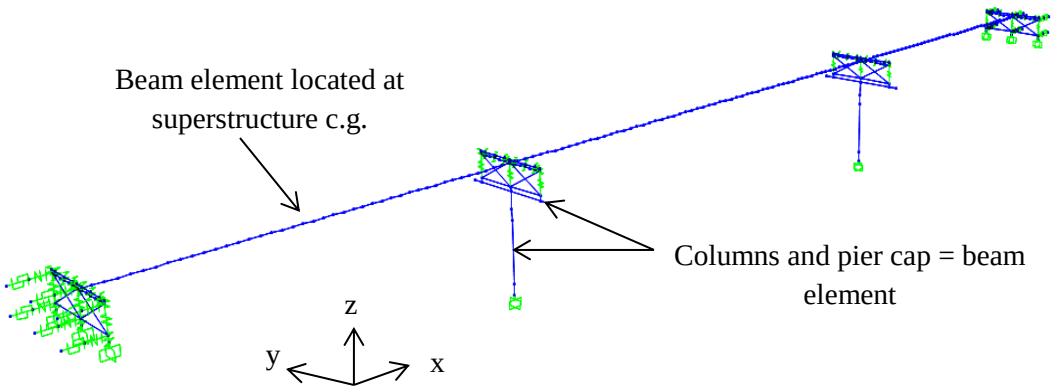

(a) 3D view of model

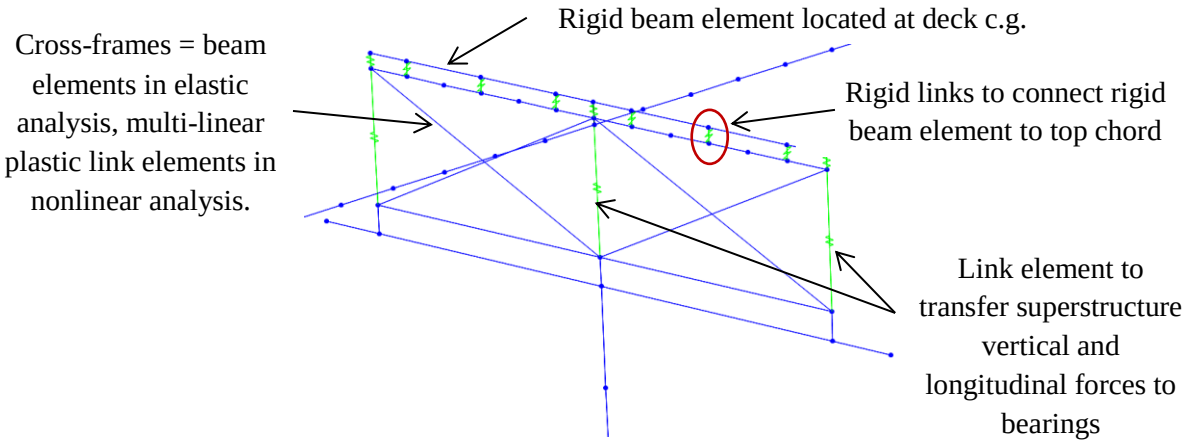

(b) Detail at piers

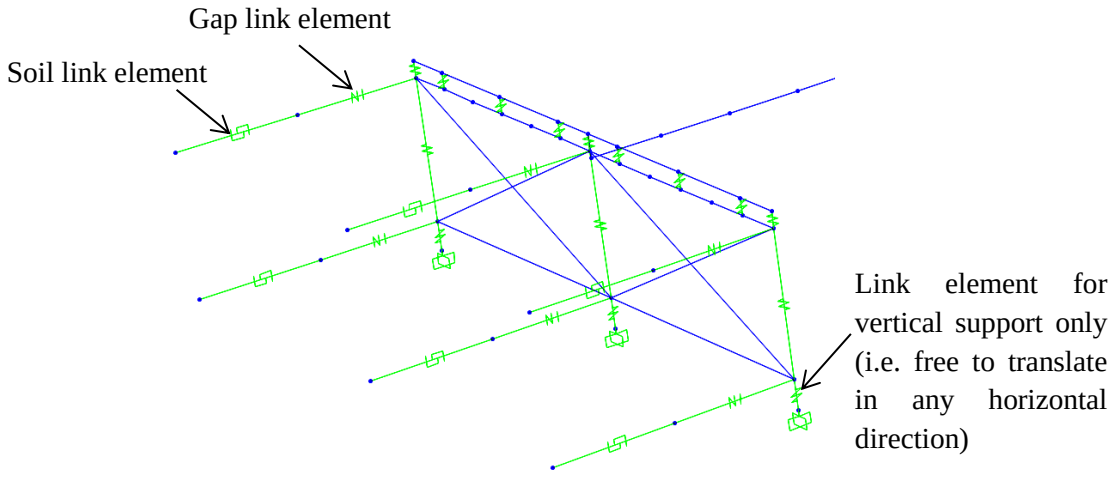

(c) Detail at abutments

Figure 2-2 Analytical model of Ex. I-1a

2.3.2 Earthquake Loads – EQ

Step 1: Calculate column axial loads due to gravity loads, P_{col}. This will be used to determine the effective moment of inertia, I_e, of columns. $$P_{col} = 1.25P_{DC} + 1.5P_{DW}$$		$$P_{col} = 1.25(763) + 1.5(152) = 1{,}182\ kips$$
Step 2: Determine effective moment of inertia, I_e. This is accomplished through section analysis of the column. The required parameters are: column diameter, longitudinal and transverse reinforcements, axial load, and material properties of concrete and steel reinforcement. The calculated I_e is assigned to the beam elements representing the column in the model.		The following are the column properties: D = 4 ft ρ_l = 1% (12 - #11) ρ_s = 1% (#6 @ 4.0 in.) f'_c = 4 ksi f_y = 60 ksi P_{col} = 1,182 kips From section analysis: I_e/I_g = 0.38
Step 3: Estimate soil displacement, Δ_{soil}, and calculate the effective abutment stiffness, K_e. The joint gap is included in the calculation of this stiffness, as shown in the figure below. 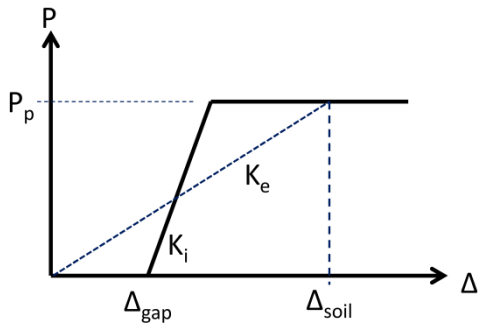 Figure 2-3 Abutment force-displacement The soil passive resistance, P_p, and initial soil stiffness, K_i, are calculated based on the recommended values in Caltrans SDC. $$P_p = 5.0A_e(h/5.5)\ \ (kips)$$ $$K_i = 50w(h/5.5)\ \ (kip/in)$$ where A_e (ft^2) is the effective backwall area, h (ft) is the backwall height, and w is the backwall		Δ_{soil} = 5.01 in. $$P_p = 5.0(6.5x30)(6.5/5.5) = 1{,}152\ kips$$ $$K_i = 50(30)(6.5/5.5) = 1{,}773\ kip/in$$ Check Δ_{soil} against Δ_{gap} + Δ_y to determine if the soil is yielding. $$\Delta_{gap} + \Delta_y = 2 + \frac{1{,}152}{1{,}773} = 2 + 0.65 = 2.65\ in$$ Since this is smaller than Δ_{soil}, the soil is yielding and the effective stiffness is: $$K_e = \frac{1{,}152}{5.01} = 230\ kip/in$$ $$1/2K_e = 115\ kip/in$$

width. Under *EQ* in longitudinal direction, only one abutment is engaged in one direction. To account for this in elastic analyses such as modal and response spectrum analysis, half of K_e is applied to both abutments. This $1/2K_e$ is then distributed to the link elements representing the soil. The gap link elements shown in Figure 2-2c were assigned with high stiffness with no opening during elastic analysis.		Since there are 6 soil springs at each abutment, the effective stiffness assigned to each is: $(1/2K_e)/6 = 19\ kip/in$
Step 4: Perform modal analysis and determine the required number of modes needed for multimode spectral analysis. After the effective stiffnesses of the elements are determined, modal analysis is performed to determine the fundamental vibration periods and the required number of modes needed in the response spectrum analysis. The AASHTO Specifications requires that the total number of modes used should ensure participation of at least 90% of the total bridge mass.		Table 2-2 shows the result of modal analysis. Although only the first 5 modes are shown in this table, a total of 30 modes were used in the response spectrum analysis with total mass participation of 100% in both the longitudinal and transverse directions. The first mode with period of 2.82 sec is in-plane deck rotation; the second with period of 2.23 sec is the transverse translation mode; and the third with period of 0.92 sec is the longitudinal translation mode. The vertical vibration mode is the fourth mode with period of 0.59 sec. Table 2-2 Modal periods and mass participation Mode No | Period Sec | Mass Participation x-dir | Mass Participation y-dir 1 | 2.82 | 0.000 | 0.000 2 | 2.23 | 0.000 | 0.963 3 | 0.92 | 0.983 | 0.000 4 | 0.59 | 0.000 | 0.000 5 | 0.52 | 0.000 | 0.001
Step 5: Perform response spectrum analysis in the longitudinal direction (EQ_x), determine Δ_{soil}, and check against the initial value in *Step 3*. The design spectrum is applied in the longitudinal direction. Multimode spectral analysis is used and the modal responses are combined using the Complete Quadratic Combination (CQC).		From response spectrum analysis, Δ_{soil} = 5.01 in. Therefore, no further iteration is needed.

Step 6: Obtain the column forces due to EQ_x.

These forces will be combined with the forces due to EQ_y to determine the design forces.

Table 2-3 Column forces due to EQ_x

Load	P (kip)	M_x (k-ft)	M_y (k-ft)
EQ_x	19	0	4,507

The seismic base shear of the bridge in the longitudinal direction is 1,285 kips.

Step 7: Perform response spectrum analysis in the transverse direction (EQ_y) and determine the column forces.

Table 2-4 Column forces due to EQ_y

Load	P (kip)	M_x (k-ft)	M_y (k-ft)
EQ_y	0	7,591	0

The seismic base shear of the bridge in the transverse direction is 524 kips.

2.3.3 Design Loads

The 100%-30% combination was used to combine the EQ_x and EQ_y forces. The results are shown in Table 2-5.

Table 2-5 Combination of forces due to EQ_x and EQ_y

Load/Combination	P (kip)	M_x (k-ft)	M_y (k-ft)
EQ_x	19	0	4,507
EQ_y	0	7,591	0
EQ_1: $1.0EQ_x + 0.3EQ_y$	19	2,277	4,507
EQ_2: $0.3EQ_x + 1.0EQ_y$	6	7,591	1,352

The response modification factor, R, is then applied to EQ_1 and EQ_2 column moments. For bridge with single-column piers, R for columns is equal to 3.0. The resulting forces are then combined with DC and DW forces to determine the design forces. The load factors are based on Extreme Event I load combination and the result is shown in Table 2-6.

Table 2-6 Design loads for columns

Load/Combination	P (kip)	M_x (k-ft)	M_y (k-ft)
DC	763	0	0
DW	152	0	0
EQ_1/R	19	759	1,502
EQ_2/R	6	2,530	451
$LC1$: $1.25DC + 1.5DW + 1.0EQ_1/R$	1,201	759	1,502
$LC2$: $1.25DC + 1.5DW + 1.0EQ_2/R$	1,188	2,530	451

2.4 Design of Columns

Step 1: Determine the design axial load and resultant moment from Section 2.3.3.

Table 2-7 Design axial load and resultant moment

Load Combination	P (kip)	M_{res} (kip-ft)
LC1	1,201	1,683
LC2	1,188	2,570

Step 2: Develop the axial force-moment (P-M) interaction curve and check if the design loads are inside the P-M curve.

The AASHTO ϕ factors are used in the interaction curve.

From the final iteration the column properties are:

D = 4 ft
ρ_l = 1% (12 - #11)
ρ_s = 1% (#6 @ 4.0 in.)
f'_c = 4 ksi
f_y = 60 ksi

The design loads are within the boundaries of P-M interaction curve as shown below. Thus, the selected column size and reinforcement are adequate.

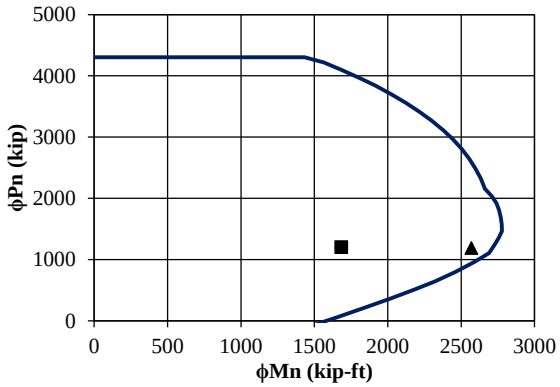

Step 3: Determine the plastic shear resistance, V_p, of the column. This V_p will be used to design the column transverse reinforcement and cross-frames. For single-column piers, V_p is calculated using the equation: $$V_p = \frac{M_p}{H} = \frac{1.3M_n}{H}$$ where M_n is the nominal moment and H is the height from the base of the column to the bearings. M_n is determined from interaction curve based on the axial load, P, in the column. Note that the ϕ factors are included in the values in the interaction curve, thus these values are to be divided by ϕ to get the nominal values. The 1.3 factor is to account for material overstrength.		Using the design axial loads in Table 2-7, determine the nominal moment from interaction curve. • for P = 1,201 kips, M_n = 2,977 kip-ft • for P = 1,188 kips M_n = 2,967 kips. The larger nominal moment is 2,977 kip-ft thus it will be used to calculate V_p. $$V_p = \frac{1.3(2{,}977)}{24.42} = 158\ kips$$
Step 4: Determine the column shear resistance and compare against the plastic shear resistance. The shear resistance can be calculated using the Simplified Procedure described in AASHTO Specifications Art. 5.8.3.4.1. For simplicity and to be conservative, the contribution of concrete to the shear resistance is not included in the calculations. $$V_n = \frac{A_v f_y d_v}{s}$$ where: $A_v = 2A_{sh}$ $d_v = 0.9d_e$ $d_e = \frac{D}{2} + \frac{D_r}{\pi}$ A_{sh} = area of one leg of transverse reinforcement; f_y is the yield stress of transverse reinforcement; s is the spacing of transverse reinforcement; D is the diameter of column; D_r is the diameter of the circle passing through the centers of longitudinal reinforcement.		The transverse reinforcement is #6 rebar spaced at 4.0 in. on center. The longitudinal reinforcement is #11 rebar. The concrete cover is 2.0 in. $A_v = 2(0.44) = 0.88\ in^2$ $D_r = 48 - 2 - 2 - 0.75 - 0.75 - 1.375$ $= 41.125\ in$ $d_e = \frac{48}{2} + \frac{41.125}{\pi} = 37.09\ in$ $d_v = 0.9(37.09) = 33.38\ in$ $V_n = \frac{0.88(60)(33.38)}{4} = 441\ kips$ $\phi V_n = 0.9(441) = 397\ kips$ The demand-resistance ratio is: $\frac{D}{C} = \frac{158}{397} = 0.40\ < 1.0, ok!$

Step 5: Check the transverse reinforcement. The volumetric ratio of transverse reinforcement shall satisfy (AASHTO Specifications Art. 5.10.11.4.1d): $$\rho_s \geq 0.12\frac{f_c'}{f_y}$$ The spacing of transverse reinforcement shall satisfy (AASHTO Specifications Art. 5.10.11.4.1e): $$s \leq \begin{cases} D/4 \\ 4.0 \end{cases}$$		ρ_s = 1% (#6 @ 4.0 in.) f_y = 60 ksi f'_c = 4 ksi $\rho_s = 0.01 \geq 0.12\left(\frac{4}{60}\right) = 0.008 \quad ok!$ $s = 4.0 \leq \begin{cases} 48/4 = 12.0 \\ 4.0 \end{cases} \quad ok!$

2.5 Seismic Design of Cross-Frames

For Type 1 design strategy, the inelasticity is to be limited in the columns. The components along the seismic load path such as cross-frames are designed and detailed to remain elastic.

Step 1: Determine the axial force in each of the cross-frame diagonal members. $$P_{XF} = \frac{V_{XF}}{2N\cos\theta} = \frac{V_p}{2N\cos\theta}$$ where V_p is the column plastic shear, N is the number of panels, and θ is the angle of the diagonal member measured from the horizontal.		V_p = 158 kips N = 2 panels θ = 26 degrees $P_{XF} = \frac{158}{2(2)(\cos 26)} = 44\ kips$
Step 2: Cross-frame member section properties Note that the size of the cross-frames may be governed by slenderness requirements.		Section: *L8x8x5/8* F_y = 36 ksi A_g = 9.61 in^2 r_x = 2.48 in. r_y = 2.48 in. r_z = 1.58 in. L = 149.85 in.

Step 3: Calculate the tensile resistance $\phi P_r = 0.95 F_y A_g$		$\phi P_r = 0.95(36)(9.61) = 328.66\ kips > 44\ kips$
Step 4: Calculate the compressive resistance Under seismic loading, the cross-frames are primary members in the transverse direction as they transmit the deck seismic forces to the bearings. The limiting slenderness ratio for primary members is 120 (AASHTO Specifications Art. 6.9.3). Equal-leg single angle sections will be used as diagonal members. The slenderness ratio is calculated according to AASHTO Specifications Art. 6.9.4.4. ○ If $l/r_x \leq 80$ $\left(\frac{KL}{r}\right)_{eff} = 72 + 0.75\frac{l}{r_x}$ ○ If $l/r_x > 80$ $\left(\frac{KL}{r}\right)_{eff} = 32 + 1.25\frac{l}{r_x}$ where r_x is the radius of gyration about the geometric axis of the angle parallel to the connected leg. The compressive resistance is calculated according to AASHTO Specifications Art. 6.9.2.1, 6.9.4.1.1, and 6.9.4.1.2 $P_e = \frac{\pi^2 E}{\left(\frac{Kl}{r}\right)^2_{eff}} A_g$ $P_o = Q F_y A_g$ The slender element reduction factor, Q, is equal to 1.0 when: $\frac{b}{t} \leq 0.45\sqrt{\frac{E}{F_y}}$		$l/r_x = 149.85/2.48 = 60.42 < 80$ $\left(\frac{KL}{r}\right)_{eff} = 72 + 0.75(60.42) = 117.32 < 120\ ok!$ $P_e = \frac{\pi^2(29{,}000)}{117.32^2}(9.61) = 199.84\ kips$ $\frac{b}{t} = \frac{8}{5/8} = 12.8 \leq 0.45\sqrt{\frac{29{,}000}{36}} = 12.8, Q = 1.0$ $P_o = 1.0(36)(9.61) = 345.96\ kips$ $\frac{P_e}{P_o} = \frac{199.84}{345.96} = 0.58 \geq 0.44$ $\phi P_n = 0.9\left[0.658^{1/0.58}\right](345.96) = 150.86\ kips > 44\ kips, ok!$

○ If $P_e/P_o \geq 0.44$ $$\phi P_n = 0.9\left[0.658^{(P_o/P_e)}\right]P_o$$ ○ If $P_e/P_o < 0.44$ $$\phi P_n = 0.9(0.877P_e)$$ Note that although the calculations shown here is for equal-leg single angle sections for simplicity, unequal leg single angles and double angles may be also used as diagonal members of cross-frames.		The resistance of the selected section, *L8x8x5/8*, is much larger than the demand. However, this section was selected due to limit on slenderness ratio.
Step 5: Calculate the minimum nominal shear resistance of the cross-frames and check against V_p of column. $$V_{XF\_min} = (2P_n)N\cos\theta$$ In this equation, only the nominal compressive resistance, P_n, is used to determine the minimum nominal shear resistance. Note that P_n is smaller than the tensile resistance, P_r, which means buckling would occur first in any of the diagonal members before yielding is reached. Thus, V_{XF} is the minimum nominal shear force before inelasticity starts to occur in the cross-frames. Since this is Type 1 design strategy, V_p should be less than V_{XF}.		$$V_{XF\_min} = 2\left(\frac{150.86}{0.9}\right)2\cos 26 = 603\ kip > V_p = 158\ kips, ok!$$ As can be seen above, the slenderness ratio is the governing parameter in the design of elastic support cross-frames.

2.6 Cross-Frame Properties for Nonlinear Analysis

It is not expected to have inelasticity in the cross-frames using Type I design strategy. However, the expected force and displacement resistance of the cross-frames are calculated for use in the design evaluation in case that inelasticity occurred in the analysis.

Step 1: Calculate the expected tensile yield and displacement resistance. The expected yield resistance is: $$P_{ye} = F_{ye}A_g$$ where F_{ye} is the expected yield stress and is equal to R_yF_y. For A36 steel sections, R_y = 1.5. The effective axial stiffness is: $$K_{XF\_e} = \frac{EA_e}{L}$$ where E is the modulus of elasticity of steel which is 29,000 ksi, A_e is the effective area calculated using Eqn. (1-12), and L is the total length of the diagonal member. The expected yield displacement is then calculated as: $$\Delta_{ye} = \frac{P_{ye}}{K_{XF\_e}}$$		*L8x4x3/4* F_{ye} = 1.5(36) = 54 ksi A_g = 9.61 in^2 I_x = 59.6 in^4 e = 2.21 in. distance from connected leg of angle to its c.g. $P_{ye} = 54(9.61) = 518.94\ kips$ $A_e = \frac{9.61(59.6)}{59.6 + 9.61(2.21)^2} = 5.376\ in^2$ $K_{XF\_e} = \frac{29{,}000(5.376)}{149.85} = 1{,}040.43\ kip/in$ $\Delta_{ye} = \frac{518.94}{1{,}040.43} = 0.50\ in$

Step 2: Calculate the expected compressive resistance and associated displacement. The $(Kl/r)_{eff}$ and P_e is the same as that calculated in Section 2.5 *Step 4*. The expected yield strength is used to calculate P_o. $$P_o = F_{ye}A_g$$ The expected compressive resistance is then calculated as: ○ If $P_e/P_o \geq 0.44$ $$P_{nc} = \left[0.658^{(P_o/P_e)}\right]P_o$$ ○ If $P_e/P_o < 0.44$ $$P_{nc} = 0.877P_e$$ The corresponding displacement is: $$\Delta_{nc} = \frac{P_{nc}}{K_{XF\_e}}$$		$P_o = 54(9.61) = 518.94\ kips$ $\frac{P_e}{P_o} = \frac{199.84}{518.94} = 0.39 < 0.44$ $P_{nc} = 0.877(199.84) = 175.26\ kips$ $\Delta_{nc} = \frac{175.26}{1{,}040.43} = 0.17\ in.$

2.7 Design Summary

The total weight of Ex. I-1a is 1,848 kips. From modal and response spectrum analyses, the periods, forces, and displacements are:

Parameter	Longitudinal Direction	Transverse Direction
Fundamental period, T (sec)	0.92	2.23
Base shear, V_b (kip)	1,285	524
Column displacement demand, Δ_{col} (in)	4.60	8.26
Column shear demand, V_{col} (in)	184	262
Deck displacement demand, Δ_{deck} (in)	4.92	11.58

The column properties are:

Diameter, D	4 ft
Longitudinal reinforcement	12 - #11 (ρ_l = 1%)
Transverse reinforcement	#6 @ 4.0 in. (ρ_s = 1%)
Effective moment of inertia, I_e	$0.38I_g$
Plastic shear resistance, V_p	158 kips

The cross-frame diagonal member section properties are:

Section	L8x8x5/8 (A36)
Area, A	9.61 in^2
Slenderness ratio, KL/r	117.32
Width-thickness ratio, b/t	12.8
Tensile resistance, ϕP_r	329 kips
Compressive resistance, ϕP_n	151 kips
Min. nominal shear resistance, V_{XF_min}	603 kips
Expected tensile resistance, P_{ye}	519 kips
Expected compression resistance, P_{nc}	175 kips

2.8 Nonlinear Evaluation

Example I-1a was analyzed using the ground motions described in Section 1.8.1. The ground motions were scaled to represent the Design (DE) and MCE Earthquake levels. There were seven DE analyses and seven MCE analyses for a total of fourteen analyses. Because of this, only the column force-displacement plots from DE1, DE7, MCE1 and MCE7 are shown in Figure 2-4 and Figure 2-5 to represent the results. However, the column ductility ratios for all runs are shown in Figure 2-6. Nonlinearity was not observed in the support cross-frames.

The yield displacements were calculated according to Section 1.8.2. Since the expected material properties were used in the nonlinear analyses, the yield displacements were also calculated using these properties. The yield displacements are 2.02 in. and 2.15 in. in the longitudinal and transverse directions, respectively.

In the longitudinal direction, the average ductility ratios were 1.5 from DE runs and 1.9 from MCE runs. In the transverse direction, the respective ductility ratios were 2.4 and 3.1. The soil resistance at the abutment reduced the column ductility demand in the longitudinal direction resulting in essentially elastic response in this direction. The ductility demand in the longitudinal direction is also lower compared to that in transverse direction because the minor component of the ground motions is applied in this direction. The ductility demand in the transverse direction clearly indicates yielding of the column, and the demand in this direction is higher because only the column resists the seismic forces and because the major component of the ground motions is applied in this direction.

The negative stiffness observed in the hysteresis plots was not due to instability in the structure or computational error in the analysis. Rather, it is attributed to the coupled biaxial response of the column. This phenomenon was observed when the response is elastic and depends on the frequency content of the input motion and period of the structure (Monzon et al. 2013b).

In the transverse direction, the average column base shear forces were 125 kips from DE runs and 135 kips from MCE runs. These forces are about the same because of column yielding. The respective average of total bearing forces in the transverse direction were 126 kips and 128 kips. Thus, for this bridge, the inertia force in the pier cap was small. The average of resultant shear forces at the base of the column were 149 kips from DE runs and 159 kips from MCE runs. From Section 2.7, the plastic shear resistance of the column is 158 kips.

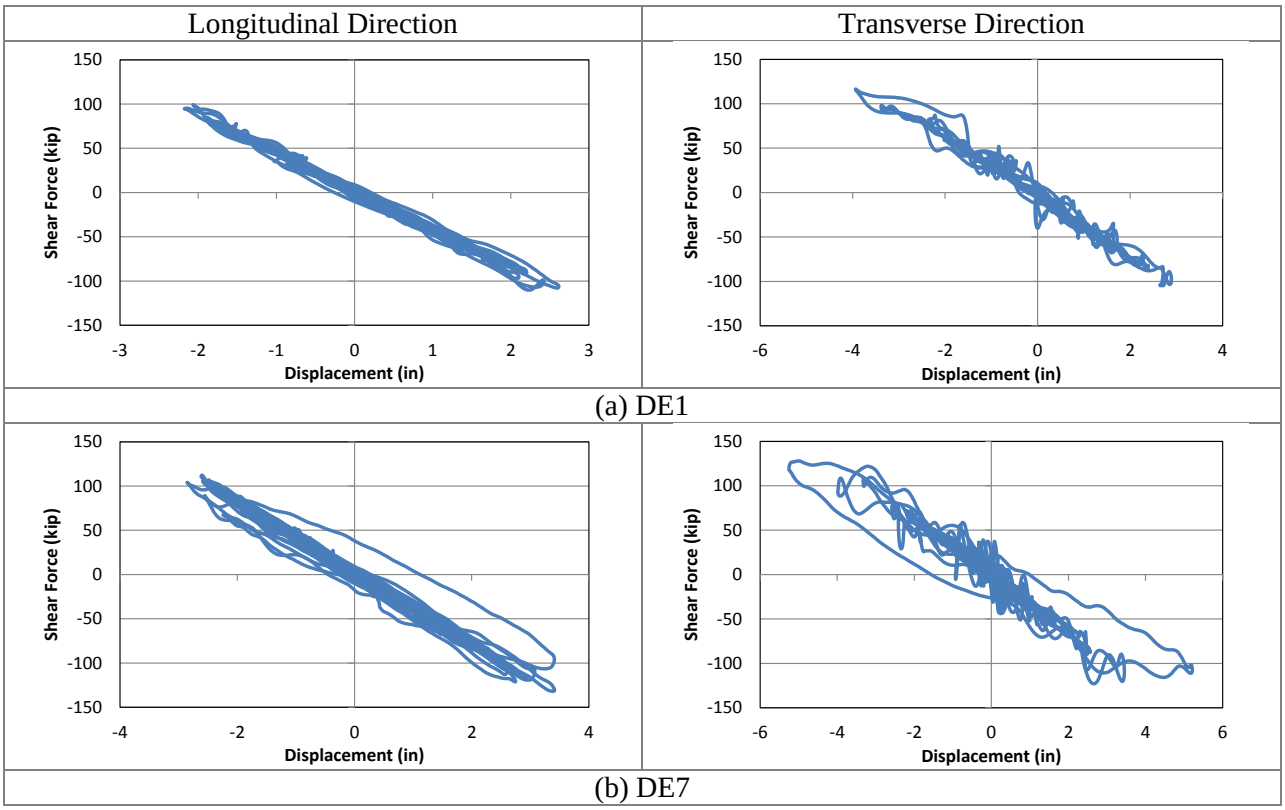

Figure 2-4 Column force-displacement plots from DE runs

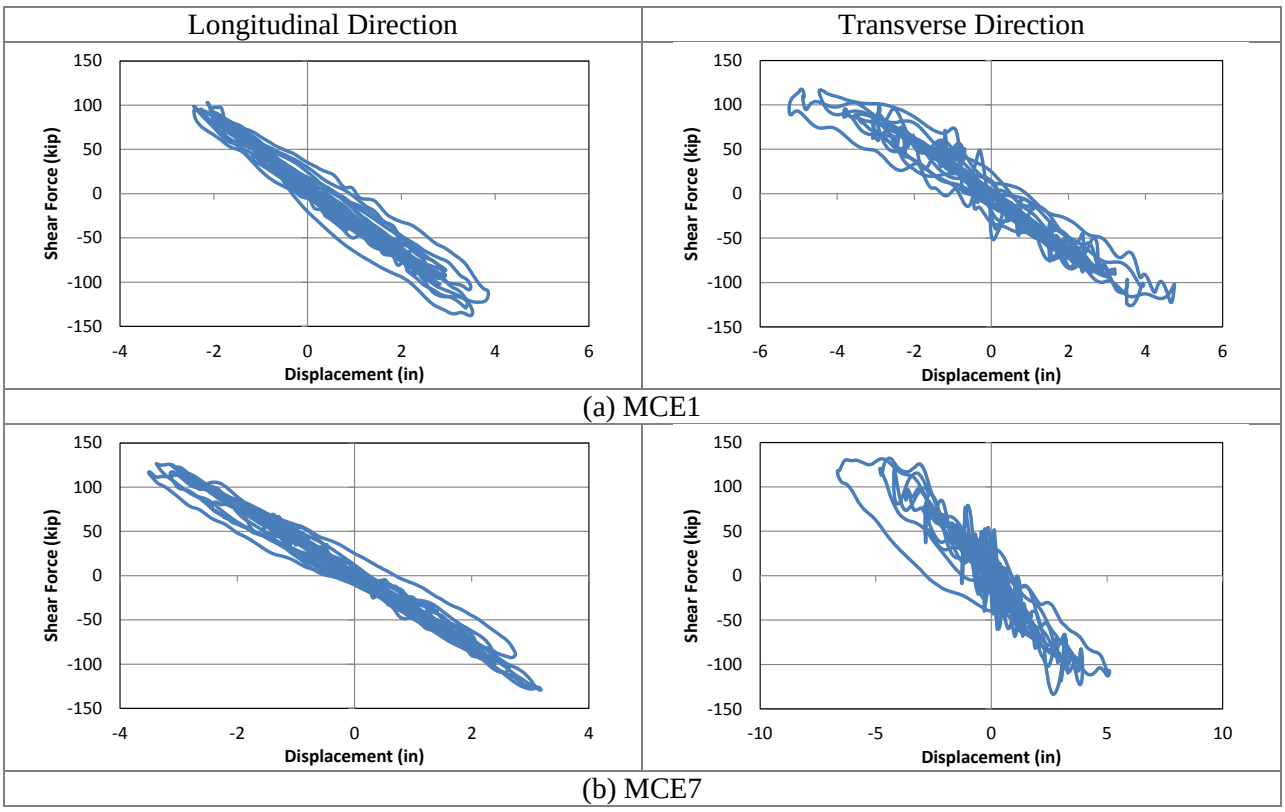

Figure 2-5 Column force-displacement plots from MCE runs

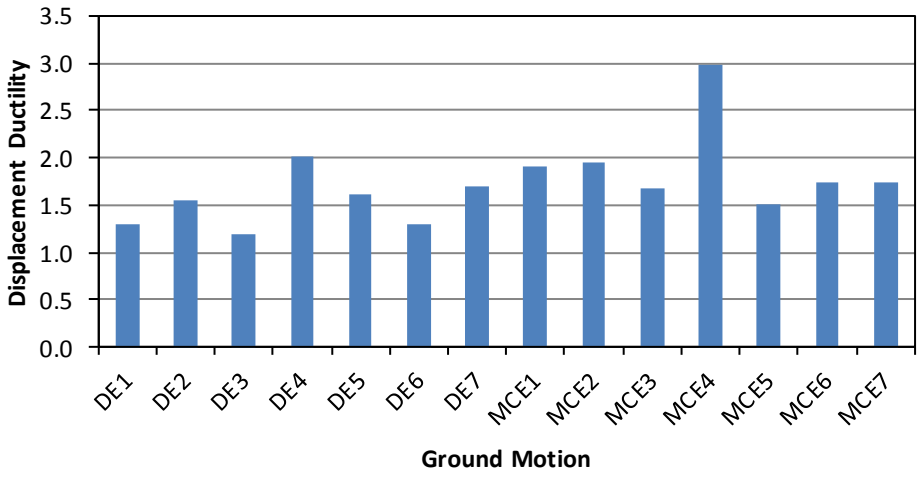

(a) ductility ratios in the longitudinal direction

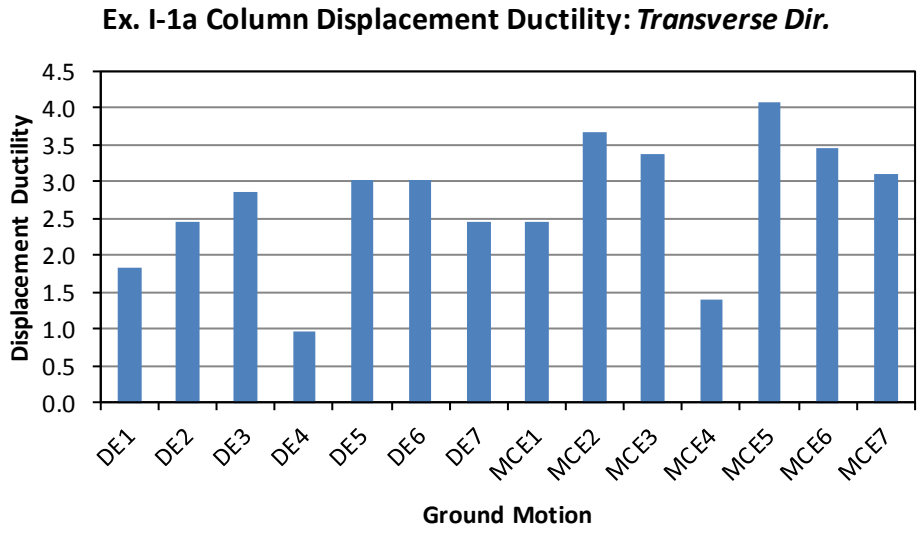

(b) ductility ratios in the transverse direction

Figure 2-6 Summary of column Displacement ductility

Chapter 3 Critical Bridge with Single-Column Piers Designed using Type 1 Strategy (Example I-1b)

3.1 Bridge Description

The overall geometry of Ex. I-1b is described in Section 1.3.1. From the final design iteration, the reinforced concrete (R/C) column diameter is 6.5 ft with longitudinal and transverse steel ratios of 2.4% and 1.1%. The pier cap is 7 ft wide, and it is tapered with depth starting from 3 ft-4 in. at the ends to 5 ft at the center. Figure 3-1 shows the elevation of Ex. I-1b at piers. The cross-frames are of X-type pattern with diagonal members made of WT7x34 while the top and bottom chords are 2L4x4x1/2 double angles.

3.2 Computational Model

The computational model is shown in Figure 3-2. The equivalent concrete section properties of superstructure are summarized in Table 3-1. Local axes of the superstructure are shown in Figure 3-1. Deck cracking was accounted for in the calculation of these properties by using 54% of the gross concrete modulus of elasticity (E_c).

For nonlinear response history analysis, the cross-frames were modeled with multi-linear plastic link elements with force-deformation relationship shown in Figure 1-5 to account for inelasticity in case it occurred. Calculation of expected force and deformations are shown in Section 3.6.

Table 3-1 Ex. I-1b superstructure equivalent concrete section properties

Area, A (in^2)	6,028
Moment of inertia about horizontal axis, I_2 (in^4)	4,660,235
Moment of inertia about vertical axis, I_3 (in^4)	69,386,665
Torsional constant, J (in^4)	102,071

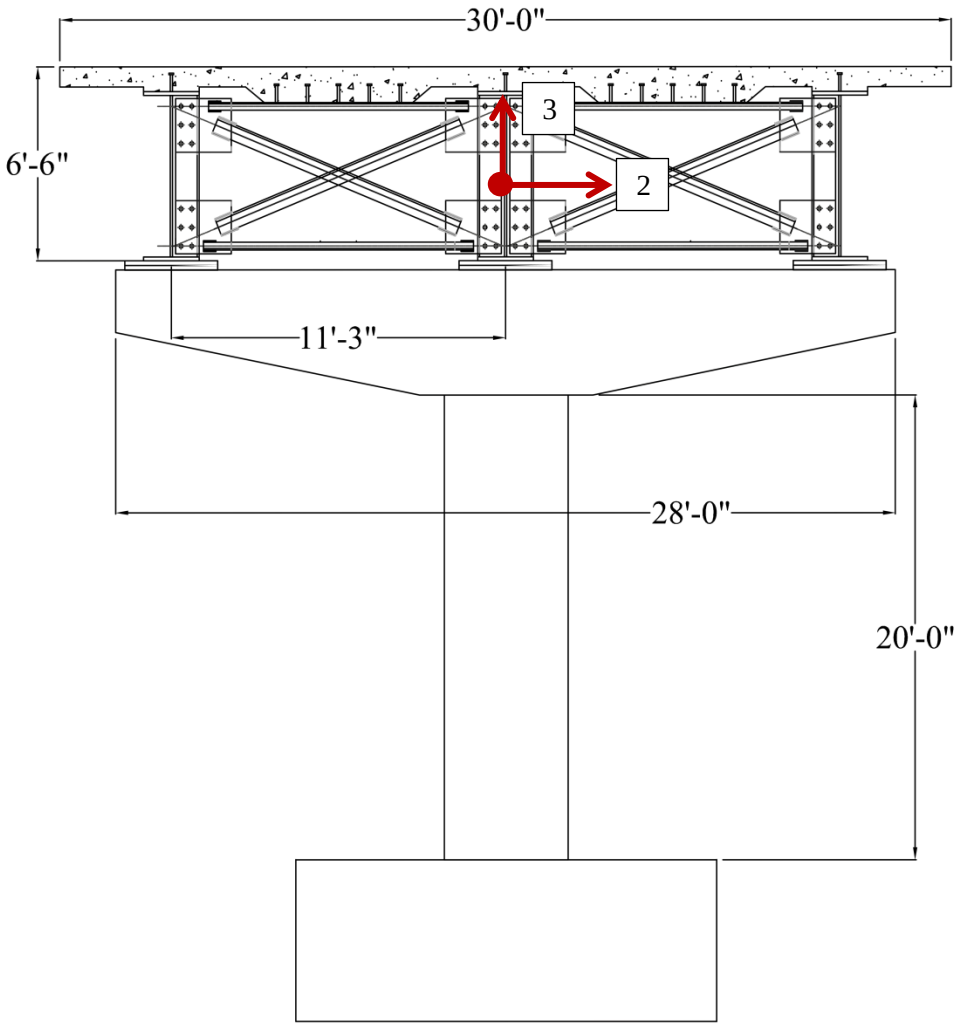

Figure 3-1 Elevation at piers of Ex. I-1b

3.3 Analysis

3.3.1 Gravity Loads – DC and DW

The total *DC* load (i.e. total bridge dead load) is 2,076 kips and the total *DW* load is 378 kips. The reactions at the base of column due to these loads are 876 kips and 152 kips, respectively. These loads were used to calculate the effective section properties of the columns, as illustrated in Section 3.3.2 *Steps 1* and *2*.

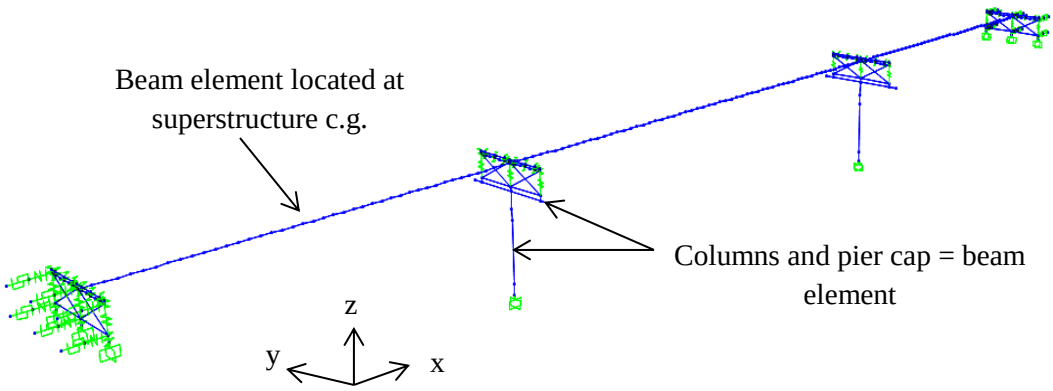

(a) 3D view of model

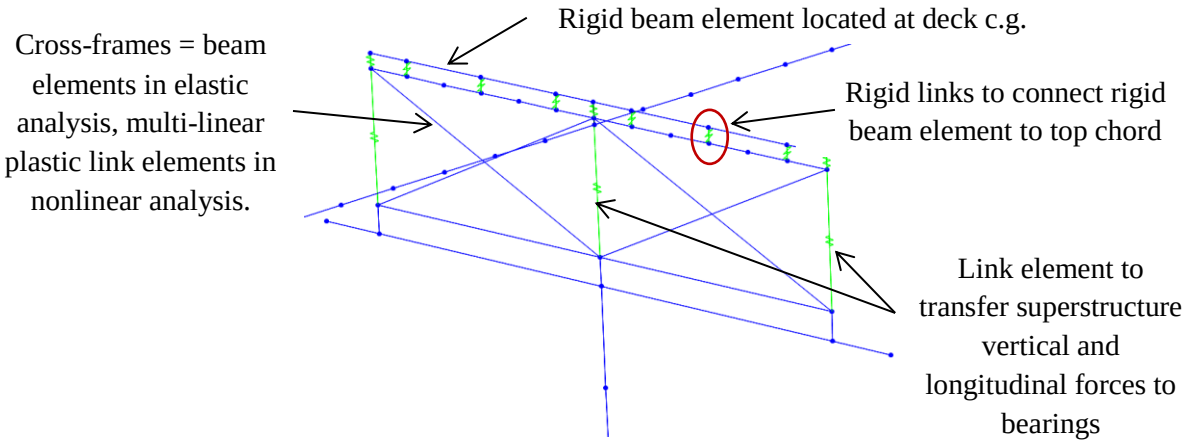

(b) Detail at piers

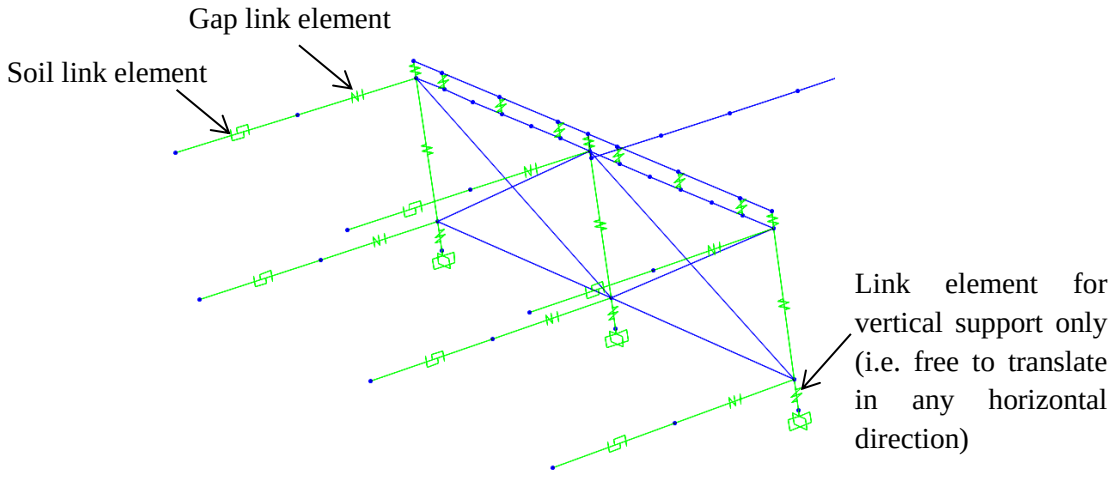

(c) Detail at abutments

Figure 3-2 Analytical model of Ex. I-1b

3.3.2 Earthquake Loads – EQ

Step 1: Calculate column axial loads due to gravity loads, P_{col}. This will be used to determine the effective moment of inertia, I_e, of columns. $$P_{col} = 1.25P_{DC} + 1.5P_{DW}$$		$$P_{col} = 1.25(876) + 1.5(152) = 1{,}323\ kips$$
Step 2: Determine effective moment of inertia, I_e. This is accomplished through section analysis of the column. The required parameters are: column diameter, longitudinal and transverse reinforcements, axial load, and material properties of concrete and steel reinforcement. The calculated I_e is assigned to the beam elements representing the column in the model.		The following are the column properties: D = 6.5 ft ρ_l = 2.4% (72 - #11) ρ_s = 1.1% (#8 @ 4.0 in.) f'_c = 4 ksi f_y = 60 ksi P_{col} = 1,323 kips From section analysis: I_e/I_g = 0.54
Step 3: Estimate soil displacement, Δ_{soil}, and calculate the effective abutment stiffness, K_e. The joint gap is included in the calculation of this stiffness, as shown in the figure below. 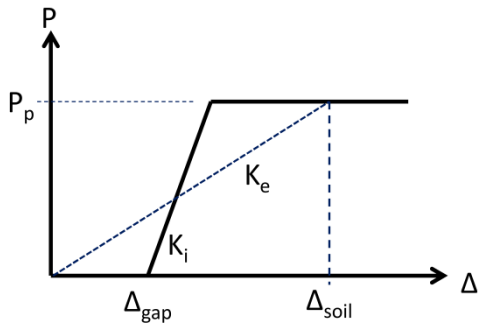 Figure 3-3 Abutment force-displacement The soil passive resistance, P_p, and initial soil stiffness, K_i, are calculated based on the recommended values in Caltrans SDC. $$P_p = 5.0A_e(h/5.5)\ \ (kips)$$ $$K_i = 50w(h/5.5)\ \ (kip/in)$$ where A_e (ft^2) is the effective backwall area, h (ft) is the backwall height, and w is the backwall		Δ_{soil} = 2.8 in. $$P_p = 5.0(6.5x30)(6.5/5.5) = 1{,}152\ kips$$ $$K_i = 50(30)(6.5/5.5) = 1{,}773\ kip/in$$ Check Δ_{soil} against Δ_{gap} + Δ_y to determine if the soil is yielding. $$\Delta_{gap} + \Delta_y = 2 + \frac{1{,}152}{1{,}773} = 2 + 0.65 = 2.65\ in$$ Since this is smaller than Δ_{soil}, the soil is yielding and the effective stiffness is: $$K_e = \frac{1{,}152}{2.8} = 411\ kip/in$$ $$1/2K_e = 206\ kip/in$$

<table>
<tr>
<td>width.

Under EQ in longitudinal direction, only one abutment is engaged in one direction. To account for this in elastic analyses such as modal and response spectrum analysis, half of K_e is applied to both abutments.

This $1/2K_e$ is then distributed to the link elements representing the soil. The gap link elements shown in Figure 3-2c were assigned with high stiffness with no opening during elastic analysis.</td>
<td></td>
<td>Since there are 6 soil springs at each abutment, the effective stiffness assigned to each is:

$(1/2K_e)/6 = 34\ kip/in$</td>
</tr>
<tr>
<td>Step 4: Perform modal analysis and determine the required number of modes needed for multimode spectral analysis.

After the effective stiffnesses of the elements are determined, modal analysis is performed to determine the fundamental vibration periods and the required number of modes needed in the response spectrum analysis. The AASHTO Specifications requires that the total number of modes used should ensure participation of at least 90% of the total bridge mass.</td>
<td></td>
<td>Table 3-2 shows the result of modal analysis. Although only the first 5 modes are shown in this table, a total of 30 modes were used in the response spectrum analysis with total mass participation of 100% in both the longitudinal and transverse directions.

The first mode with period of 1.09 sec is in-plane deck rotation; the second with period of 0.85 sec is the transverse translation mode; and the fourth with period of 0.49 sec is the longitudinal translation mode. The vertical vibration mode is the third mode with period of 0.58 sec.

Table 3-2 Modal periods and mass participation

<table>
<tr><th>Mode No</th><th>Period Sec</th><th>Mass Participation x-dir</th><th>y-dir</th></tr>
<tr><td>1</td><td>1.09</td><td>0.000</td><td>0.000</td></tr>
<tr><td>2</td><td>0.85</td><td>0.000</td><td>0.861</td></tr>
<tr><td>3</td><td>0.58</td><td>0.000</td><td>0.000</td></tr>
<tr><td>4</td><td>0.49</td><td>0.000</td><td>0.069</td></tr>
<tr><td>5</td><td>0.49</td><td>0.956</td><td>0.000</td></tr>
</table>
</td>
</tr>
<tr>
<td>Step 5: Perform response spectrum analysis in the longitudinal direction (EQ_x), determine Δ_{soil}, and check against the initial value in Step 3.

The design spectrum is applied in the longitudinal direction. Multimode spectral analysis is used and the modal responses are combined using the Complete Quadratic Combination (CQC).</td>
<td></td>
<td>From response spectrum analysis, Δ_{soil} = 2.78 in. Therefore, no further iteration is needed.</td>
</tr>
</table>

Step 6: Obtain the column forces due to EQ_x.

These forces will be combined with the forces due to EQ_y to determine the design forces.

Table 3-3 Column forces due to EQ_x

Load	P (kip)	M_x (k-ft)	M_y (k-ft)
EQ_x	27	0	21,817

The seismic base shear of the bridge in the longitudinal direction is 2,780 kips.

Step 7: Perform response spectrum analysis in the transverse direction (EQ_y) and determine the column forces.

Table 3-4 Column forces due to EQ_y

Load	P (kip)	M_x (k-ft)	M_y (k-ft)
EQ_y	0	20,766	0

The seismic base shear of the bridge in the transverse direction is 1,354 kips.

3.3.3 Design Loads

The 100%-30% combination was used to combine the EQ_x and EQ_y forces. The results are shown in Table 3-5.

Table 3-5 Combination of forces due to EQ_x and EQ_y

Load/Combination	P (kip)	M_x (k-ft)	M_y (k-ft)
EQ_x	27	0	21,817
EQ_y	0	20,766	0
EQ_1: $1.0EQ_x + 0.3EQ_y$	27	6,230	21,817
EQ_2: $0.3EQ_x + 1.0EQ_y$	8	20,766	6,545

The response modification factor, R, is then applied to EQ_1 and EQ_2 column moments. For bridge with single-column piers and under Critical category, R for columns is equal to 1.5. The resulting forces are then combined with DC and DW forces to determine the design forces. The load factors are based on Extreme Event I load combination and the result is shown in Table 3-6.

Table 3-6 Design loads for columns

Load/Combination	P (kip)	M_x (k-ft)	M_y (k-ft)
DC	876	0	0
DW	152	0	0
EQ_1/R	27	4,153	14,545
EQ_2/R	8	13,844	4,363
$LC1$: $1.25DC + 1.5DW + 1.0EQ_1/R$	1,350	4,153	14,545
$LC2$: $1.25DC + 1.5DW + 1.0EQ_2/R$	1,331	13,844	4,363

3.4 Design of Columns

Step 1: Determine the design axial load and resultant moment from Section 3.3.3.

Table 3-7 Design axial load and resultant moment

Load Combination	P (kip)	M_{res} (kip-ft)
LC1	1,350	15,126
LC2	1,331	14,515

Step 2: Develop the axial force-moment (P-M) interaction curve and check if the design loads are inside the P-M curve.

The AASHTO ϕ factors are used in the interaction curve.

From the final iteration the column properties are:

D = 6.5 ft
ρ_l = 2.4% (72 - #11)
ρ_s = 1.1% (#8 @ 4.0 in.)
f'_c = 4 ksi
f_y = 60 ksi

The design loads are within the boundaries of P-M interaction curve as shown below. Thus, the selected column size and reinforcement are adequate.

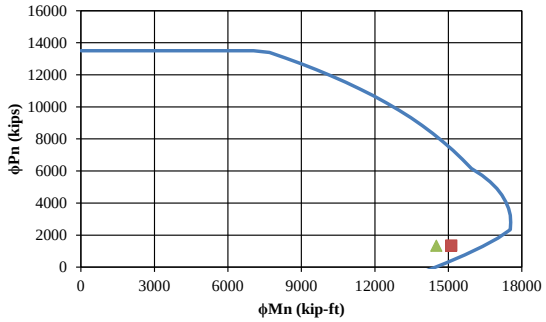

Step 3: Determine the plastic shear resistance, V_p, of the column.

This V_p will be used to design the column transverse reinforcement and cross-frames. For single-column piers, V_p is calculated using the equation:

$$V_p = \frac{M_p}{H} = \frac{1.3M_n}{H}$$

where M_n is the nominal moment and H is the

Using the design axial loads in Table 3-7, determine the nominal moment from interaction curve.

- for P = 1,350 kips, M_n = 18,287 kip-ft
- for P = 1,331 kips M_n = 18,261 kips.

The larger nominal moment is 18,287 kip-ft thus it will be used to calculate V_p.

height from the base of the column to the bearings. M_n is determined from interaction curve based on the axial load, P, in the column. Note that the ϕ factors are included in the values in the interaction curve, thus these values are to be divided by ϕ to get the nominal values. The 1.3 factor is to account for material overstrength.		$V_p = \frac{1.3(18287)}{25} = 951\ kips$
Step 4: Determine the column shear resistance and compare against the plastic shear resistance. The shear resistance can be calculated using the Simplified Procedure described in AASHTO Specifications Art. 5.8.3.4.1. For simplicity and to be conservative, the contribution of concrete to the shear resistance is not included in the calculations. $$V_n = \frac{A_v f_y d_v}{s}$$ where: $A_v = 2A_{sh}$ $d_v = 0.9d_e$ $d_e = \frac{D}{2} + \frac{D_r}{\pi}$ A_{sh} = area of one leg of transverse reinforcement; f_y is the yield stress of transverse reinforcement; s is the spacing of transverse reinforcement; D is the diameter of column; D_r is the diameter of the circle passing through the centers of longitudinal reinforcement.		The transverse reinforcement is #8 rebar spaced at 4.0 in. on center. The longitudinal reinforcement is #11 rebar. The concrete cover is 2.0 in. $A_v = 2(0.79) = 1.58\ in^2$ $D_r = 78 - 2 - 2 - 1 - 1 - 1.375 = 70.625\ in$ $d_e = \frac{78}{2} + \frac{70.625}{\pi} = 61.48\ in$ $d_v = 0.9(61.48) = 55.33\ in$ $V_n = \frac{1.58(60)(55.33)}{4} = 1{,}311\ kips$ $\phi V_n = 0.9(1{,}311) = 1{,}181\ kips$ The demand-resistance ratio is: $\frac{D}{C} = \frac{951}{1{,}181} = 0.81\ < 1.0, ok!$
Step 5: Check the transverse reinforcement. The volumetric ratio of transverse reinforcement shall satisfy (AASHTO Specifications Art. 5.10.11.4.1d): $$\rho_s \geq 0.12\frac{f_c'}{f_y}$$ The spacing of transverse reinforcement shall satisfy (AASHTO Specifications Art. 5.10.11.4.1e):		ρ_s = 1.1% (#8 @ 4.0 in.) f_y = 60 ksi f'_c = 4 ksi $\rho_s = 0.01 \geq 0.12\left(\frac{4}{60}\right) = 0.008\ \ ok!$ $s = 4.0 \leq \begin{cases} 78/4 = 19.5 \\ 4.0 \end{cases} \quad ok!$

$s \leq \begin{cases} D/4 \\ 4.0 \end{cases}$		

3.5 Seismic Design of Cross-Frames

For Type 1 design strategy, the inelasticity is to be limited in the columns. The components along the seismic load path such as cross-frames are designed and detailed to remain elastic.

Step 1: Determine the axial force in each of the cross-frame diagonal members. $$P_{XF} = \frac{V_{XF}}{2N\cos\theta} = \frac{V_p}{2N\cos\theta}$$ where V_p is the column plastic shear, N is the number of panels, and θ is the angle of the diagonal member measured from the horizontal.		V_p = 951 kips N = 2 panels θ = 26 degrees $P_{XF} = \frac{951}{2(2)(\cos 26)} = 265\ kips$
Step 2: Cross-frame member section properties Note that the size of the cross-frames may be governed by slenderness requirements.		Section: *WT 7x34* F_y = 50 ksi A_g = 10 in^2 r_x = 1.81 in. I_x = 32.6 in^4 e = 1.29 in. L = 149.85 in.
Step 3: Calculate the tensile resistance $$\phi P_r = 0.95 F_y A_g$$		$\phi P_r = 0.95(50)(10) = 475\ kips > 265\ kips$
Step 4: Calculate the compressive resistance Under seismic loading, the cross-frames are primary members in the transverse direction as they transmit the deck seismic forces to the bearings. The limiting slenderness ratio for primary members is 120 (AASHTO Specifications Art. 6.9.3). The compressive resistance is calculated according to AASHTO Specifications Art. 6.9.2.1,		*Kl* = 1.0(149.85) = 149.85 *Kl/r* = 149.85/1.81 = 82.79

6.9.4.1.1, and 6.9.4.1.2 $$P_e = \frac{\pi^2 E}{\left(\frac{Kl}{r}\right)^2_{eff}} A_g$$ $$P_o = QF_yA_g$$ The slender element reduction factor, *Q*, is equal to 1.0 when: for flanges: $$\frac{b}{2t_f} \leq 0.56\sqrt{\frac{E}{F_y}}$$ for stem: $$\frac{d}{t_w} \leq 0.75\sqrt{\frac{E}{F_y}}$$ ○ If $P_e/P_o \geq 0.44$ $$\phi P_n = 0.9\left[0.658^{(P_o/P_e)}\right]P_o$$ ○ If $P_e/P_o < 0.44$ $$\phi P_n = 0.9(0.877P_e)$$		$P_e = \frac{\pi^2(29{,}000)}{82.79^2}(10) = 418\ kips$ $\frac{b}{2t_f} = 6.97 < 0.56\sqrt{\frac{29000}{50}} = 13.5$ $\frac{d}{t_w} = 16.9 < 0.75\sqrt{\frac{29000}{50}} = 18.1$ Therefore, $Q = 1.0$ $P_o = 1.0(50)(10) = 500\ kips$ $\frac{P_e}{P_o} = \frac{418}{500} = 0.835 \geq 0.44$ $\phi P_n = 0.9\left[0.658^{1/0.835}\right](500) = 303\ kips > 265\ kips, ok!$
Step 5: Calculate the minimum nominal shear resistance of the cross-frames and check against V_p of column. $$V_{XF\_min} = (2P_n)N\cos\theta$$ In this equation, only the nominal compressive resistance, P_n, is used to determine the minimum nominal shear resistance. Note that P_n is smaller than the tensile resistance, P_r, which means buckling would occur first in any of the diagonal members before yielding is reached. Thus, V_{XF} is the minimum nominal shear force before inelasticity starts to occur in the cross-frames. Since this is Type 1 design strategy, V_p should be less than V_{XF}.		$V_{XF\_min} = 2\left(\frac{303}{0.9}\right)2\cos 26 = 1{,}210\ kip > V_p = 951\ kips, ok!$

3.6 Cross-Frame Properties for Nonlinear Analysis

It is not expected to have inelasticity in the cross-frames using Type I design strategy. However, the expected force and displacement resistance of the cross-frames are calculated for use in the design evaluation in case that inelasticity occurred in the analysis.

Step 1: Calculate the expected tensile yield and displacement resistance. The expected yield resistance is: $$P_{ye} = F_{ye}A_g$$ where F_{ye} is the expected yield stress and is equal to R_yF_y. For WT section with A992 Gr 50, R_y = 1.1. The effective axial stiffness is: $$K_{XF\_e} = \frac{EA_e}{L}$$ where E is the modulus of elasticity of steel which is 29,000 ksi, A_e is the effective area calculated using Eqn. (1-12), and L is the total length of the diagonal member. The expected yield displacement is then calculated as: $$\Delta_{ye} = \frac{P_{ye}}{K_{XF\_e}}$$		*L8x4x3/4* F_{ye} = 1.1(50) = 55 ksi A_g = 10 in^2 I_x = 32.6 in^4 e = 1.29 in. distance from connected flange of WT to its c.g. $P_{ye} = 55(10) = 550\ kips$ $A_e = \frac{10(32.6)}{32.6 + 10(1.29)^2} = 6.62\ in^2$ $K_{XF\_e} = \frac{29{,}000(6.62)}{149.85} = 1{,}281\ kip/in$ $\Delta_{ye} = \frac{550}{1{,}281} = 0.43\ in$

Step 2: Calculate the expected compressive resistance and associated displacement. The *Kl/r* and P_e are the same as that calculated in Section 3.5 *Step 4*. The expected yield strength is used to calculate P_o. $$P_o = F_{ye}A_g$$ The expected compressive resistance is then calculated as: ○ If $P_e/P_o \geq 0.44$ $$P_{nc} = \left[0.658^{(P_o/P_e)}\right]P_o$$ ○ If $P_e/P_o < 0.44$ $$P_{nc} = 0.877P_e$$ The corresponding displacement is: $$\Delta_{nc} = \frac{P_{nc}}{K_{XF\_e}}$$		$P_o = 55(10) = 550\ kips$ $\frac{P_e}{P_o} = \frac{418}{550} = 0.76 < 0.44$ $P_n = \left[0.658^{1/0.76}\right](550) = 317\ kips$ $\Delta_{nc} = \frac{317}{1{,}281} = 0.25\ in.$

3.7 Design Summary

The total weight of Ex. I-1b is 2,076 kips. From modal and response spectrum analyses, the periods, forces, and displacements are:

Parameter	Longitudinal Direction	Transverse Direction
Fundamental period, T (sec)	0.49	0.58
Base shear, V_b (kip)	2,780	1,354
Column displacement demand, Δ_{col} (in)	1.85	1.84
Column shear demand, V_{col} (in)	853	677
Deck displacement demand, Δ_{deck} (in)	2.8	3.2

The column properties are:

Diameter, D	6.5 ft
Longitudinal reinforcement	72 - #11 (ρ_l = 2.4%)
Transverse reinforcement	#8 @ 4.0 in. (ρ_s = 1.1%)
Effective moment of inertia, I_e	$0.54I_g$
Plastic shear resistance, V_p	951 kips

The cross-frame diagonal member section properties are:

Section	WT7x34
Area, A	10 in^2
Tensile resistance, ϕP_r	450 kips
Compressive resistance, ϕP_n	303 kips
Min. nominal shear resistance, V_{XF_min}	1,210 kips
Expected tensile resistance, P_{ye}	550 kips
Expected compression resistance, P_{nc}	317 kips

3.8 Nonlinear Evaluation

Example I-1b was analyzed using the ground motions described in Section 1.8.1. The ground motions were scaled to represent the Design (DE) and MCE Earthquake levels. There were seven DE analyses and seven MCE analyses for a total of fourteen analyses. Because of this, only the column force-displacement plots from DE1, DE7, MCE1 and MCE7 are shown in Figure 3-4 and Figure 3-5 to represent the results. However, the column ductility ratios for all runs are shown in Figure 3-6. Nonlinearity was not observed in the support cross-frames.

The yield displacements were calculated according to Section 1.8.2. Since the expected material properties were used in the nonlinear analyses, the yield displacements were also calculated using these properties. The yield displacements are 1.15 in. and 1.22 in. in the longitudinal and transverse directions, respectively.

In the longitudinal direction, the average ductility ratios were 1.5 from DE runs and 1.8 from MCE runs. In the transverse direction, the respective ductility ratios were 1.6 and 2.1. The ductility ratios are smaller compared to those in Ex. I-1a because the columns in Ex. I-1b are designed for an R-factor of 1.5.

In the transverse direction, the average column base shear forces were 634 kips from DE runs and 705 kips from MCE runs. The respective average of total bearing forces in the transverse direction were 576 kips and 641 kips. Thus, for this bridge, the inertia force in the pier cap is about 10% of the column base shear. The average of resultant shear forces at the base of the column were 819 kips from DE runs and 906 kips from MCE runs. From Section 3.7, the plastic shear resistance of the column is 951 kips.

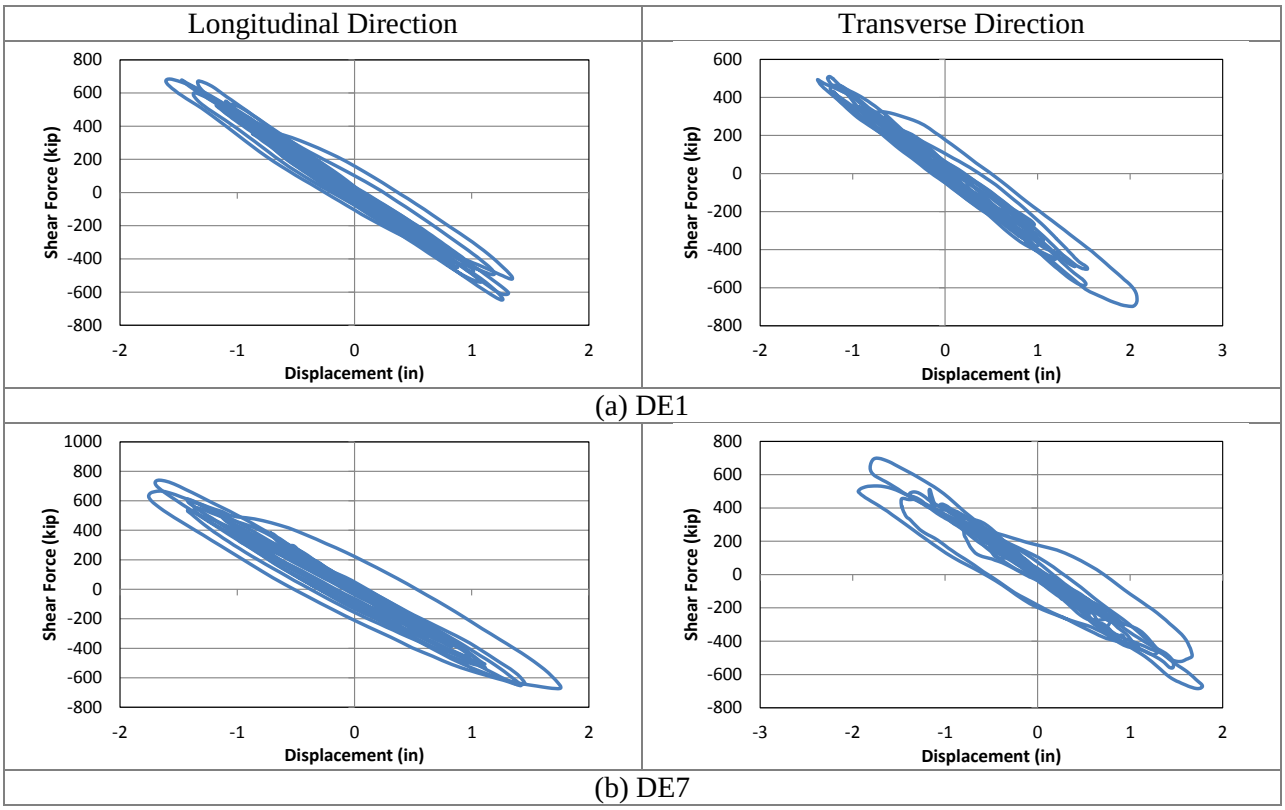

Figure 3-4 Column force-displacement plots from DE runs

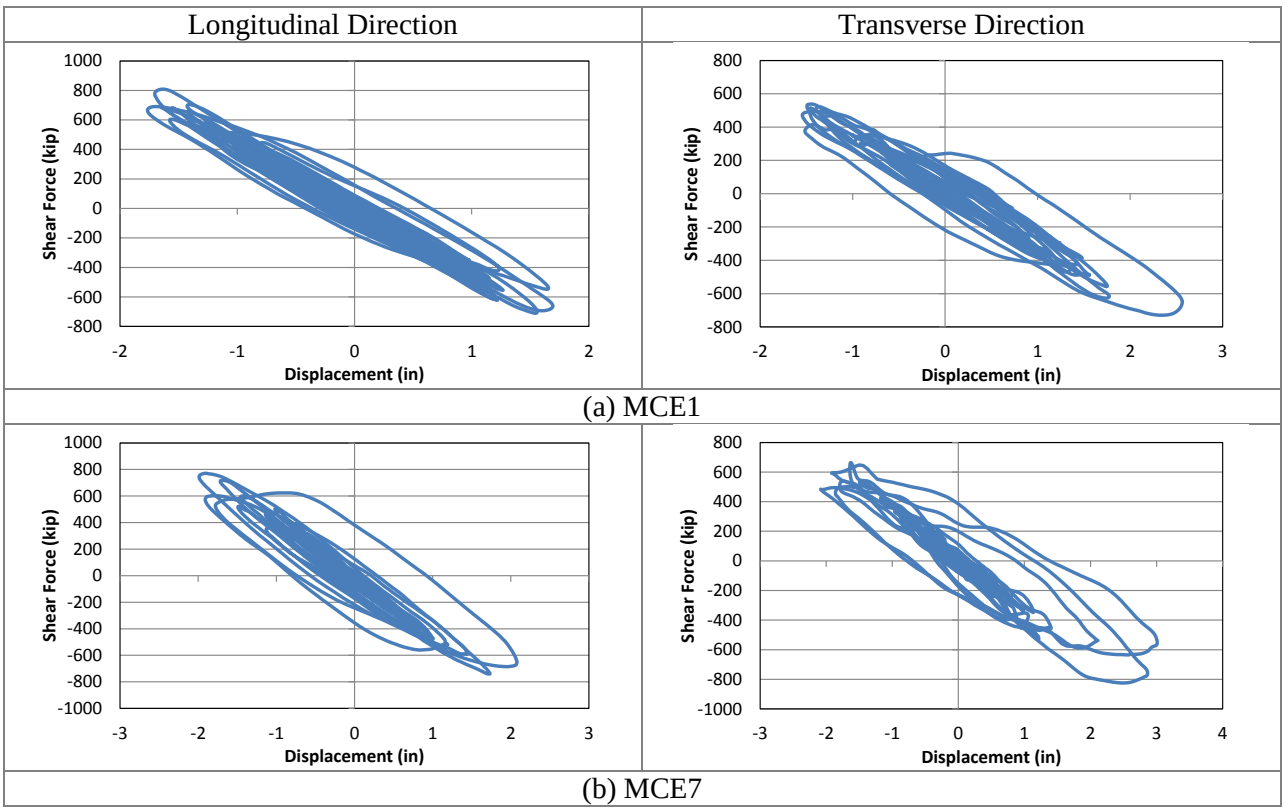

Figure 3-5 Column force-displacement plots from MCE runs

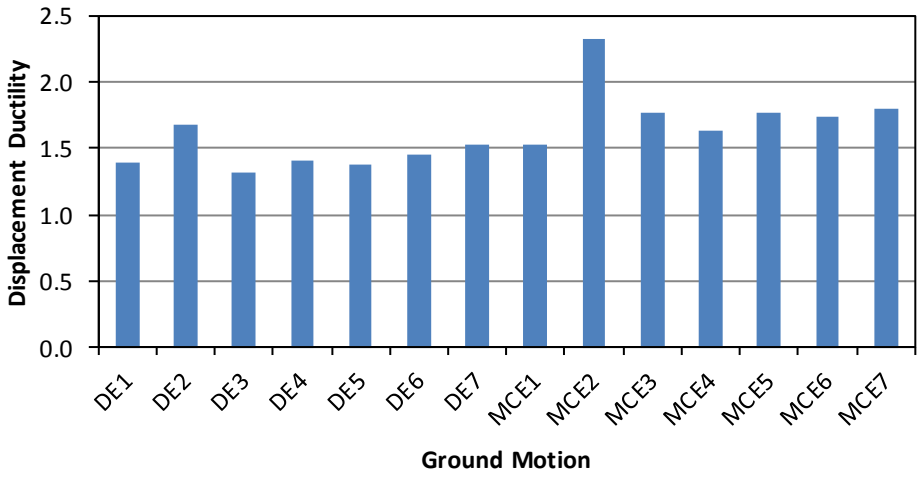

(a) ductility ratios in the longitudinal direction

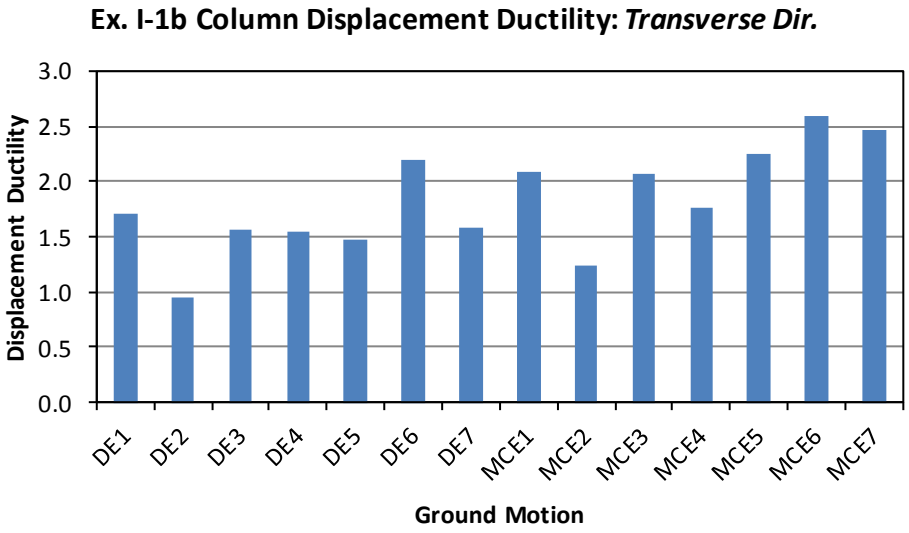

(b) ductility ratios in the transverse direction

Figure 3-6 Summary of column Displacement ductility

Chapter 4 Bridge with Single-Column Piers Designed using Type 2 Strategy (Example I-2)

4.1 Bridge Description

The overall geometry of Ex. I-2 is described in Section 1.3.1. From the final design iteration, the reinforced concrete (R/C) column diameter is 5 ft-6 in. with 2.5% longitudinal reinforcement and 1% transverse reinforcement. The pier cap is 6 ft-6 in. wide, and it is tapered with depth starting from 3 ft-4 in. at the ends to 5 ft at the center. Figure 4-1 shows the elevation of at piers. The cross-frames are of X-type pattern with diagonal members made of L3x3x3/8 single angles while the top and bottom chords are 2L2x2x1/4 double angles.

4.2 Computational Model

The computational model is shown in Figure 4-2. The equivalent concrete section properties of superstructure are summarized in Table 4-1. Local axes of the superstructure are shown in Figure 4-1. Deck cracking was accounted for in the calculation of these properties by using 50% of the gross concrete modulus of elasticity (E_c).

For elastic analysis, only one of the diagonal members of the cross-frames is included in the model as shown in Figure 4-2b. This is because the cross-frames are designed and detailed to yield and buckle under the design earthquake. Under transverse loading, in each cross-frame panel, one diagonal is under tension and the other is in compression. Consequently, the diagonal in compression would buckle and its stiffness becomes essentially close to zero.

For nonlinear response history analysis, the cross-frames were modeled with multi-linear plastic link elements with force-deformation relationship shown in Figure 1-5. The two cross-frame diagonal members are modeled because buckling is accounted for in the definition of link force-deformation relationship. Calculation of expected force and deformations are shown in Sections 4.5 and 4.6.

Table 4-1 Ex. I-2 superstructure equivalent concrete section properties

Area, A (in^2)	6,028
Moment of inertia about horizontal axis, I_2 (in^4)	4,660,235
Moment of inertia about vertical axis, I_3 (in^4)	69,386,665
Torsional constant, J (in^4)	102,071

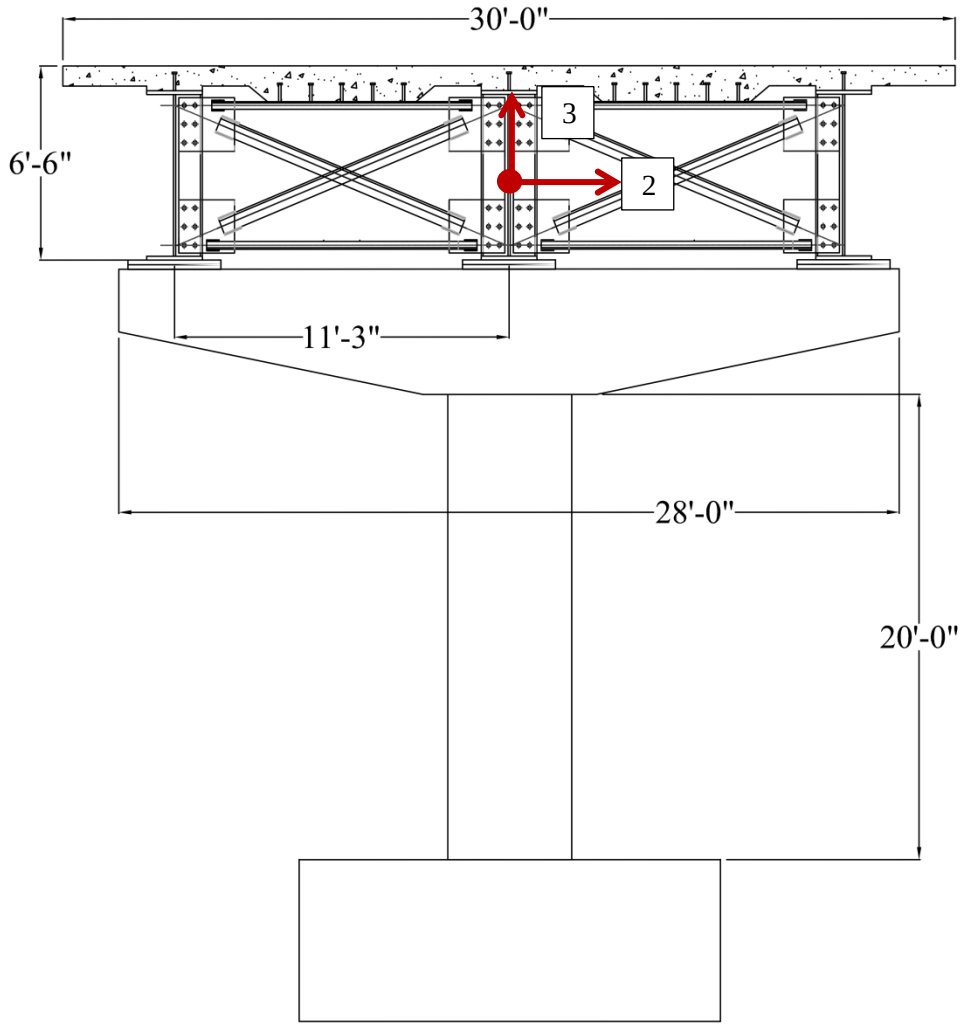

Figure 4-1 Elevation at piers of Ex. I-2

4.3 Analysis

4.3.1 Gravity Loads – DC and DW

The total *DC* load (i.e. total bridge dead load) is 2,014 kips and the total *DW* load is 378 kips. The reactions at the base of column due to these loads are 846 kips and 152 kips, respectively. These loads were used to calculate the effective section properties of the columns, as illustrated in Section 4.3.2 *Steps 1* and *2*.

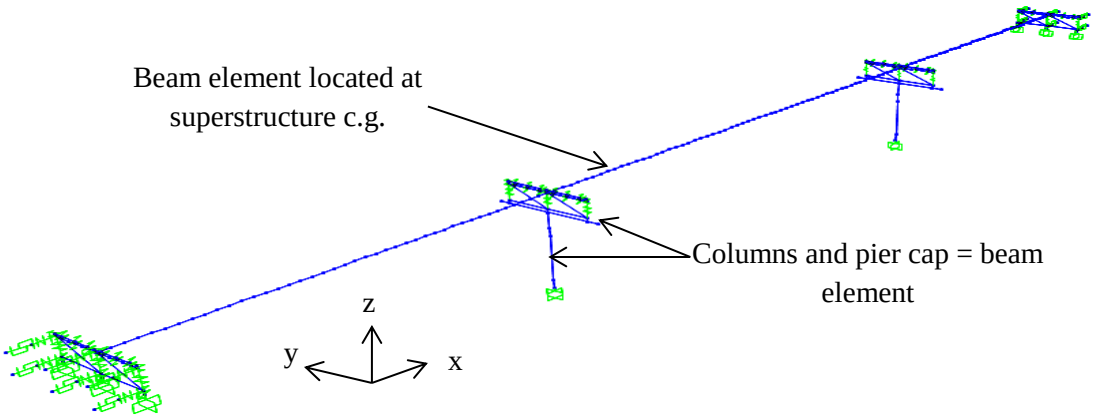

(a) 3D view of model

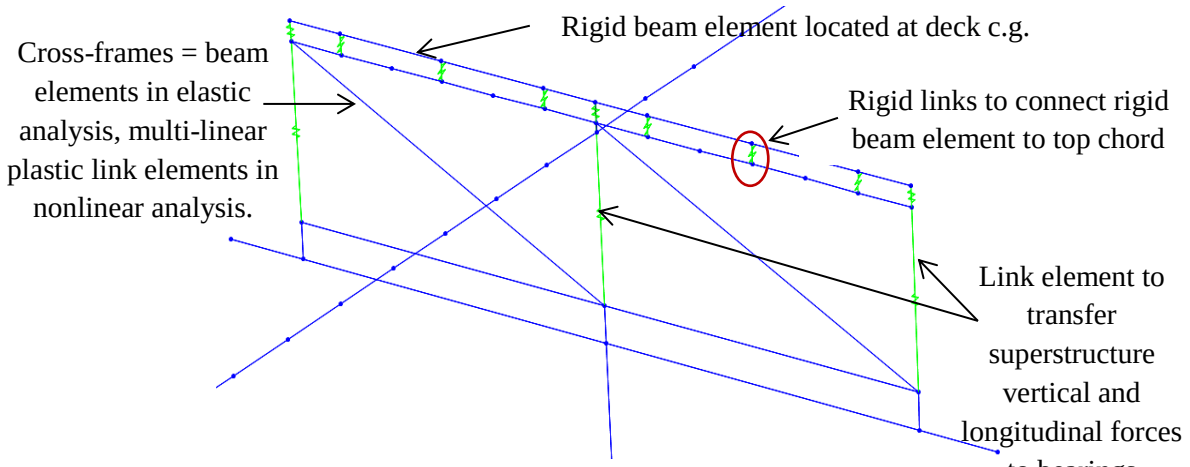

(b) Detail at piers

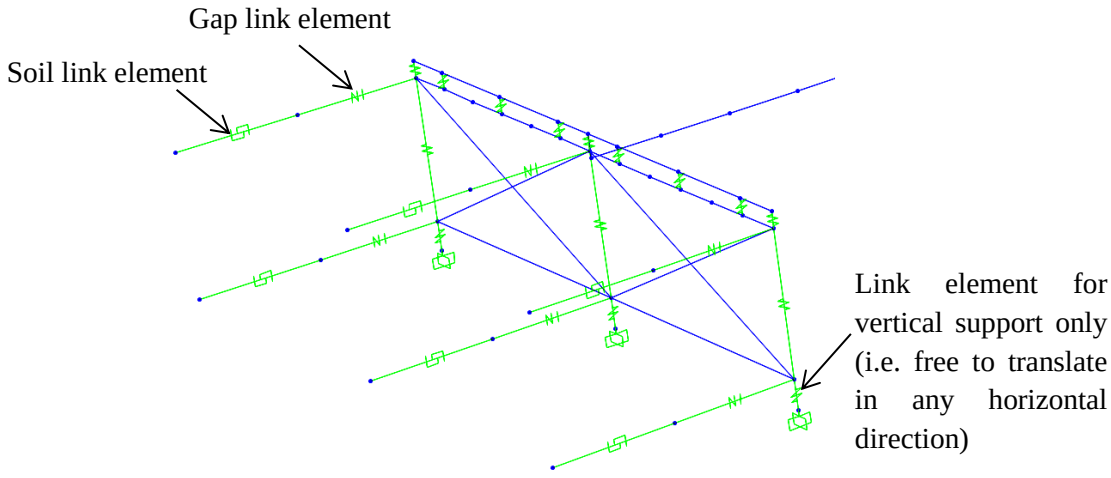

(c) Detail at abutments

Figure 4-2 Analytical model of Ex. I-2

4.3.2 Earthquake Loads – EQ

Step 1: Calculate column axial loads due to gravity loads, P_{col}. This will be used to determine the effective moment of inertia, I_e, of columns. $$P_{col} = 1.25P_{DC} + 1.5P_{DW}$$		$$P_{col} = 1.25(846) + 1.5(152) = 1{,}286\ kips$$
Step 2: Determine effective moment of inertia, I_e. This is accomplished through section analysis of the column. The required parameters are: column diameter, longitudinal and transverse reinforcements, axial load, and material properties of concrete and steel reinforcement. The calculated I_e is assigned to the beam elements representing the column in the model.		The following are the column properties: D = 5.5 ft ρ_l = 2.5% (54 - #11) ρ_s = 1% (#6 @ 3.0 in.) f'_c = 4 ksi f_y = 60 ksi P_{col} = 1,286 kips From section analysis: I_e/I_g = 0.56
Step 3: Estimate soil displacement, Δ_{soil}, and calculate the effective abutment stiffness, K_e. The joint gap is included in the calculation of this stiffness, as shown in the figure below. 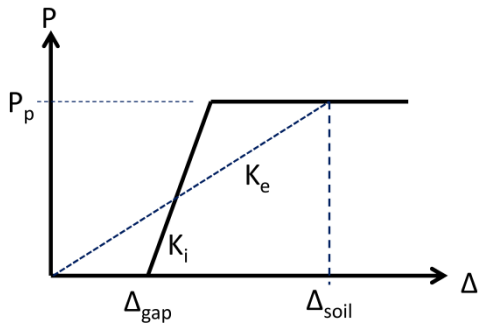 Figure 4-3 Abutment force-displacement The soil passive resistance, P_p, and initial soil stiffness, K_i, are calculated based on the recommended values in Caltrans SDC. $$P_p = 5.0A_e(h/5.5)\ \ (kips)$$ $$K_i = 50w(h/5.5)\ \ (kip/in)$$ where A_e (ft^2) is the effective backwall area, h (ft) is the backwall height, and w is the backwall		Δ_{soil} = 3.15 in. $$P_p = 5.0(6.5x30)(6.5/5.5) = 1{,}152\ kips$$ $$K_i = 50(30)(6.5/5.5) = 1{,}773\ kip/in$$ Check Δ_{soil} against Δ_{gap} + Δ_y to determine if the soil is yielding. $$\Delta_{gap} + \Delta_y = 2 + \frac{1{,}152}{1{,}773} = 2 + 0.65 = 2.65\ in$$ Since this is smaller than Δ_{soil}, the soil is yielding and the effective stiffness is: $$K_e = \frac{1{,}152}{3.15} = 366\ kip/in$$ $$1/2K_e = 183\ kip/in$$

<table>
<tr>
<td>width.

Under EQ in longitudinal direction, only one abutment is engaged in one direction. To account for this in elastic analyses such as modal and response spectrum analysis, half of K_e is applied to both abutments.

This $1/2K_e$ is then distributed to the link elements representing the soil. The gap link elements shown in Figure 4-2c were assigned with high stiffness with no opening during elastic analysis.</td>
<td></td>
<td>Since there are 6 soil springs at each abutment, the effective stiffness assigned to each is:

$(1/2K_e)/6 = 30.48\ kip/in$</td>
</tr>
<tr>
<td>Step 4: Perform modal analysis and determine the required number of modes needed for multimode spectral analysis.

After the effective stiffnesses of the elements are determined, modal analysis is performed to determine the fundamental vibration periods and the required number of modes needed in the response spectrum analysis. The AASHTO Specifications requires that the total number of modes used should ensure participation of at least 90% of the total bridge mass.</td>
<td></td>
<td>Table 4-2 shows the result of modal analysis. Although only the first 5 modes are shown in this table, a total of 30 modes were used in the response spectrum analysis with total mass participation of 100% in both the longitudinal and transverse directions.

The first mode with period of 1.58 sec is in-plane deck rotation; the second with period of 1.22 sec is the transverse translation mode; and the third with period of 0.58 sec is the longitudinal translation mode. The vertical vibration mode is the fourth mode with period of 0.58 sec.

Table 4-2 Modal periods and mass participation

<table>
<tr><th rowspan="2">Mode No</th><th rowspan="2">Period Sec</th><th colspan="2">Mass Participation</th></tr>
<tr><th>x-dir</th><th>y-dir</th></tr>
<tr><td>1</td><td>1.58</td><td>0.000</td><td>0.000</td></tr>
<tr><td>2</td><td>1.22</td><td>0.000</td><td>0.921</td></tr>
<tr><td>3</td><td>0.58</td><td>0.969</td><td>0.000</td></tr>
<tr><td>4</td><td>0.58</td><td>0.000</td><td>0.000</td></tr>
<tr><td>5</td><td>0.51</td><td>0.000</td><td>0.013</td></tr>
</table>
</td>
</tr>
<tr>
<td>Step 5: Perform response spectrum analysis in the longitudinal direction (EQ_x), determine Δ_{soil}, and check against the initial value in Step 3.

The design spectrum is applied in the longitudinal direction. Multimode spectral analysis is used and the modal responses are combined using the Complete Quadratic Combination (CQC).</td>
<td></td>
<td>From response spectrum analysis, Δ_{soil} = 3.13 in. This is within 5% of the assumed displacement in Step 3, thus no further iteration is needed.</td>
</tr>
</table>

Step 6: Obtain the column forces due to EQ_x.

These forces will be used to design the columns.

Table 4-3 Column forces due to EQ_x

Load	P (kip)	M_x (k-ft)	M_y (k-ft)
EQ_x	21	0	13,039

The seismic base shear of the bridge in the longitudinal direction is 2,150 kips.

Step 7: Obtain the column forces due to EQ_y.

Table 4-4 Column forces due to EQ_y

Load	P (kip)	M_x (k-ft)	M_y (k-ft)
EQ_y	0	14,894	0

The seismic base shear of the bridge in the longitudinal direction is 973 kips.

4.3.3 Design Loads

A proposed *R* factor of 1.5 is applied to moments from earthquake analysis. The forces based on Extreme Event I load combination is shown below.

Table 4-5 Design loads for columns

Load/Combination	P (kip)	M_x (k-ft)	M_y (k-ft)
DC	846	0	0
DW	152	0	0
EQ_x	21	0	13,039
EQ_y	0	14,894	0
EQ_1: $1.0EQ_x + 0.3EQ_y$	21	4,468	13,039
EQ_2: $0.3EQ_x + 1.0EQ_y$	6	14,894	3,912
EQ_1/R	21	2,979	8,693
EQ_2/R	6	9,929	2,608
LC1: $1.25DC + 1.5DW + 1.0EQ_1$	1,307	2,979	8,693
LC1: $1.25DC + 1.5DW + 1.0EQ_2$	1,292	9,929	2,608

4.4 Design of Columns

Step 1: Determine the design axial load and resultant moment from Section 4.3.3.

Table 4-6 Design axial load and resultant moment

Load Combination	P (kip)	M_{res} (kip-ft)
LC1	1,307	9,189
LC2	1,292	10,266

Step 2: Develop the axial force-moment (P-M) interaction curve and check if the design loads are inside the P-M curve.

The AASHTO ϕ factors are used in the interaction curve.

From the final iteration the column properties are:

D = 5.5 ft
ρ_l = 2.5% (54 - #11)
ρ_s = 1% (#6 @ 3.0 in.)
f'_c = 4 ksi
f_y = 60 ksi

The design loads are within the boundaries of P-M interaction curve as shown below. Thus, the selected column size and reinforcement are adequate.

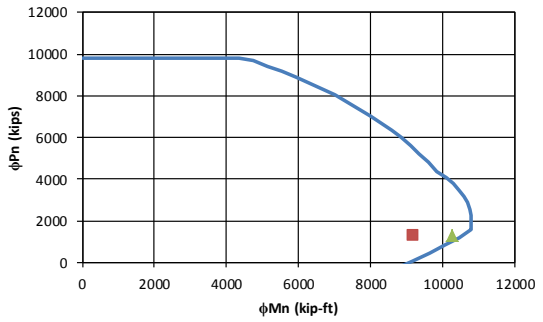

Step 3: Determine the plastic shear resistance, V_p, of the column.

This V_p will be used to design the column transverse reinforcement and cross-frames. For single-column piers, V_p is calculated using the equation:

$$V_p = \frac{M_p}{H} = \frac{1.3M_n}{H}$$

Using the design axial loads in Table 4-6, determine the nominal moment from interaction curve.

- for P = 1,307 kips, M_n = 11,734 kip-ft
- for P = 1,292 kips, M_n = 11,720 kip-ft

This larger nominal moment of 11,734 kip-ft will be used to calculate V_p.

where M_n is the nominal moment and H is the height from the base of the column to the bearings. M_n is determined from interaction curve based on the axial load, P, in the column. Note that the ϕ factors are included in the values in the interaction curve, thus these values are to be divided by ϕ to get the nominal values. The 1.3 factor is to account for material overstrength.		$V_p = \frac{1.3(11{,}734)}{25.42} = 600\ kips$
Step 4: Determine the column shear resistance and compare against the plastic shear resistance. The shear resistance can be calculated using the Simplified Procedure described in AASHTO Specifications Art. 5.8.3.4.1. For simplicity and to be conservative, the contribution of concrete to the shear resistance is not included in the calculations. $$V_n = \frac{A_v f_y d_v}{s}$$ where: $A_v = 2A_{sh}$ $d_v = 0.9 d_e$ $d_e = \frac{D}{2} + \frac{D_r}{\pi}$ A_{sh} = area of one leg of transverse reinforcement; f_y is the yield stress of transverse reinforcement; s is the spacing of transverse reinforcement; D is the diameter of column; D_r is the diameter of the circle passing through the centers of longitudinal reinforcement.		The transverse reinforcement is #6 rebar spaced at 3.0 in. on center. The longitudinal reinforcement is #11 rebar. The concrete cover is 2.0 in. $A_v = 2(0.44) = 0.88\ in^2$ $D_r = 66 - 2 - 2 - 0.75 - 0.75 - 1.375 = 59.125\ in$ $d_e = \frac{66}{2} + \frac{59.125}{\pi} = 51.82\ in$ $d_v = 0.9(51.82) = 46.64\ in$ $V_n = \frac{0.88(60)(46.64)}{3} = 821\ kips$ $\phi V_n = 0.9(821) = 739\ kips$ The demand-resistance ratio is: $\frac{D}{C} = \frac{600}{739} = 0.81 < 1.0, ok!$

Step 5: Check the transverse reinforcement. The volumetric ratio of transverse reinforcement shall satisfy (AASHTO Specifications Art. 5.10.11.4.1d): $$\rho_s \geq 0.12\frac{f_c'}{f_y}$$ The spacing of transverse reinforcement shall satisfy (AASHTO Specifications Art. 5.10.11.4.1e): $$s \leq \begin{cases} D/4 \\ 4.0 \end{cases}$$		ρ_s = 1% (#6 @ 3.0 in.) f_y = 60 ksi f'_c = 4 ksi $\rho_s = 0.021 \geq 0.12\left(\frac{4}{60}\right) = 0.008 \quad ok!$ $s = 3.0 \leq \begin{cases} 66/4 = 16.5 \\ 4.0 \end{cases} \quad ok!$

4.5 Design of Ductile End Cross-Frames

In the proposed Type 2 seismic design, the cross-frames are designed such that their resistance is less than the column nominal shear resistance in the transverse direction so the inelasticity will be limited to the cross-frames in that direction.

Step 1: Determine cross-frame force based on nominal shear resistance of the column. The cross-frame shear force is equal to nominal shear resistance of column in the transverse direction. $$V_{XF} = V_n = \frac{V_p}{1.3}$$ where V_p is the column plastic shear resistance. The corresponding cross-frame diagonal member axial force with *R* factor applied is: $$P_{XF1} = \frac{V_{XF}}{RN\cos\theta}$$ where *N* is the number of panels, θ is the angle of the diagonal from the horizontal, and *R* is the cross-frame modification factor and is equal to 4.0. In this equation, only one diagonal is assumed resisting the shear force. This is because, in a panel, one diagonal is in tension and the other one is in compression. The compression diagonal is expected to buckle in which case its post-buckling resistance is considerably smaller, thus the resistance is largely due to the yield resistance of the diagonal in tension.		V_p = 600 kips $N = 2$ $\theta = 26^o$ $V_{XF} = \frac{600}{1.3} = 461.54\ kips$ $P_{XF1} = \frac{461.54}{4(2)\cos 26} = 64\ kips$
Step 2: Determine the cross-frame force from response spectrum analysis in the transverse direction. $$P_{XF2} = \frac{P_{EQY}}{R}$$		$P_{XF2} = \frac{249}{4} = 62\ kips$
Step 3: The design cross-frame force is the smaller of P_{XF1} or P_{XF2}.		P_{XF} = 62 kips
Step 4: Determine cross-frame size.		A36 single angle

The required area is: $$A = \frac{P_{XF}}{F_y}$$ where F_y is the nominal yield stress of the cross-frame. The nominal value is used since P_{XF} was calculated from nominal shear force. Note that the size of the cross-frame may be governed by the compactness and slenderness requirements shown in *Step 5*.		F_y = 36 ksi $A = \frac{62}{36} = 1.72\ in^2$ Use *L3x3x3/8* A_g = 2.11 in^2 r_z = 0.581 in I = 1.75 in^4 x = 0.884 in. distance from connected leg of angle to its c.g. L = 149.85 in
Step 5: Check the compactness and slenderness ratios. The diagonal members of ductile cross-frames shall satisfy (proposed AASHTO Specifications Art. 6.16.4.5.2a): $$\frac{b}{t} \leq 0.3\sqrt{\frac{E}{F_y}}$$ The slenderness ratio shall satisfy (proposed AASHTO Specifications Art. 6.16.4.5.2b): $$\frac{Kl}{r} \leq 4.0\sqrt{\frac{E}{F_y}}$$ where K is 0.85, l is taken as one-half of the length of the diagonal member due to biased buckling, r is the radius of gyration normal to the plane of buckling and is equal to r_z for single angle members.		$\frac{3}{3/8} = 8.0 \leq 0.3\sqrt{\frac{29{,}000}{36}} = 8.51, \quad ok!$ $\frac{0.85(149.85/2)}{0.581} = 109.61 \leq 4\sqrt{\frac{29{,}000}{36}} = 113.53, \quad ok!$
Step 6: Calculate the expected yield resistance. $$P_{ye} = F_{ye}A_g$$ where F_{ye} is the expected yield stress and is equal to R_yF_y. For A36 steel sections, R_y = 1.5.		F_{ye} = 1.5(36) = 54 ksi $P_{ye} = (54)(2.11) = 113.94\ kips$
Step 7: Calculate the expected compressive		

resistance. The compressive resistance is calculated according to AASHTO Specifications Art. 6.9.2.1, 6.9.4.1.1, and 6.9.4.1.2 $$P_e = \frac{\pi^2 E}{\left(\frac{Kl}{r_z}\right)^2} A_g$$ $$P_o = F_{ye} A_g$$ ○ If $P_e/P_o \geq 0.44$ $$P_{nc} = \left[0.658^{(P_o/P_e)}\right] P_o$$ ○ If $P_e/P_o < 0.44$ $$P_{nc} = 0.877 P_e$$		$P_e = \frac{\pi^2(29{,}000)}{(109.61)^2}(2.11) = 50.27\ kips$ $P_o = 54.0(2.11) = 113.94\ kips$ $\frac{P_e}{P_o} = \frac{50.27}{113.94} = 0.441$ $P_{nc} = \left[0.658^{(1/0.441)}\right](113.94) = 44.11\ kips$
Step 8: Calculate the maximum expected lateral resistance of the cross-frames and compare against the column nominal shear resistance. The maximum lateral resistance is the maximum of: $$V_{lat1} = (P_t + 0.3P_{nc}) N \cos\theta$$ $$V_{lat2} = 2P_{nc} N \cos\theta$$ where P_t = $1.2P_{ye}$ is the tensile resistance of the diagonal member. The 1.5 factor is to account for the upper bound of tensile resistance. The $0.3P_{nc}$ is the post-buckling resistance of the diagonal member. V_{lat1} typically governs particularly with relatively slender diagonal members. V_{lat2} may govern in cases when the diagonal members are short and stocky. The cross-frame maximum lateral resistance is compared against the column nominal shear resistance to ensure elastic columns.		$P_t = 1.2(113.94) = 136.73\ kips$ $V_{lat1} = [136.73 + 0.3(44.11)]2\cos 26 = 270\ kips$ $V_{lat2} = [2(44.11)]2\cos 26 = 158.58\ kips$ Therefore, V_{lat} = 270 kips $V_{lat} = 270\ kips < V_p/1.3 = 523/1.3 = 420\ kips \quad ok!$
***Step 9*:** Determine the superstructure drift and check against limit. After the cross-frame designed, the superstructure drift is determined. The superstructure lateral displacement is calculated using the equation:		$A_e = \frac{2.11(1.75)}{1.75 + 2.11(0.884)^2} = 1.09\ in^2$

$$\Delta_{lat} = \frac{P_{EQY} L}{E A_e \cos\theta}$$ where, P_{EQY} is the force in the cross-frame diagonal member determined from response spectrum analysis in the transverse direction and A_e is the effective area calculated using Eqn. (1-12). The superstructure lateral drift should not exceed 4% (proposed AASHTO Specification Art. 6.16.4.5.1).		$\Delta_{lat} = \frac{249(149.85)}{29{,}000(1.09)\cos 26} = 1.31\ in.$ $Drift = \frac{1.31}{65} = 2\% < 4\%, ok!$

4.6 Cross-Frame Properties for Nonlinear Analysis

The expected force and displacement resistance of the cross-frames are calculated for use in the design evaluation.

Step 1: Calculate the expected tensile yield displacement. The expected yield resistance is calculated in Section 4.5 *Step 6*. The effective axial stiffness is: $$K_{XF\_e} = \frac{E A_e}{L}$$ where E is the modulus of elasticity of steel which is 29,000 ksi, A_e is the effective area calculated using Eqn. (1-12), and L is the total length of the diagonal member. The expected yield displacement is then calculated as: $$\Delta_{ye} = \frac{P_{ye}}{K_{XF\_e}}$$		*L3x3x3/8* P_{ye} = 113.94 kips A_g = 2.11 in^2 I = 1.75 in^4 x = 0.884 in. distance from connected leg of angle to its c.g. $A_e = \frac{2.11(1.75)}{1.75 + 2.11(0.884)^2} = 1.09\ in^2$ $K_{XF\_e} = \frac{29{,}000(1.09)}{149.85} = 210.25\ kip/in$ $\Delta_{ye} = \frac{113.94}{210.25} = 0.54\ in$
Step 2: Calculate the expected compressive displacement. The expected compressive resistance is calculated in Section 4.5 *Step 7*.		P_{nc} = 44.11 kips

The corresponding displacement is: $\Delta_{nc} = \frac{P_{nc}}{K_{XF\_e}}$		$\Delta_{nc} = \frac{44.11}{210.25} = 0.21\ in.$

4.7 Design Summary

The total weight of Ex. I-2 is 2,014 kips. From modal and response spectrum analyses, the periods, forces, and displacements are:

Parameter	Longitudinal Direction	Transverse Direction
Fundamental period, T (sec)	0.58	1.22
Base shear, V_b (kip)	2,150	973
Column displacement demand, Δ_{col} (in)	2.11	2.48
Column shear demand, V_{col} (in)	522	487
Deck displacement demand, Δ_{deck} (in)	3.18	5.78

The column properties are:

Diameter, D	5.5 ft
Longitudinal reinforcement	54 - #11 (ρ_l = 2.5%)
Transverse reinforcement	#6 @ 3.0 in. (ρ_s = 1%)
Effective moment of inertia, I_e	$0.56I_g$
Plastic shear resistance, V_p	600 kips

The cross-frame diagonal member section properties are:

Section	L3x3x3/8 (A36)
Area, A_g	2.11 in^2
Slenderness ratio, *KL/r*	109.61
Width-thickness ratio, *b/t*	8.0
Expected tensile yield resistance, P_{ye}	114 kips
Expected compressive resistance, P_{nc}	44 kips
Lateral resistance of cross-frames, V_{lat}	270 kips

4.8 Nonlinear Evaluation

Example I-2 was analyzed using the ground motions described in Section 1.8.1. The ground motions were scaled to represent the Design (DE) and MCE Earthquake levels. There were seven DE runs and seven MCE runs for a total of fourteen runs. Because of this, only the column force-displacement plots from DE1, DE7, MCE1 and MCE7 are shown in Figure 4-4 and Figure 4-5 to represent the results. However, the column ductility ratios for all runs are shown in Figure 4-6.

The yield displacements were calculated according to Section 1.8.2. Since the expected material properties were used in the nonlinear analyses, the yield displacements were also calculated using these properties. The yield displacements are 1.42 in. and 1.51 in. in the longitudinal and transverse directions, respectively.

In the longitudinal direction, the average ductility ratios were 1.5 from DE runs and 1.8 from MCE runs. In the transverse direction, the respective ductility ratios were 1.0 and 1.2. The longitudinal ductility ratios are comparable to those from Ex. I-1b while the transverse ductility ratios are lower. The yielding cross-frames limited the seismic forces transmitted to the column in the transverse.

Figure 4-7 and Figure 4-8 shows the superstructure force-displacement in the transverse direction under DE1, DE7, MCE1, and MCE7. As shown, there was significant yielding in the support cross-frames. It can be observed that the transverse shear force in the superstructure is about the same as the column transverse base shear, with the superstructure shear force slightly less. The average of total bearing forces in the transverse direction was 257 kips under DE and 274 kips under MCE. From Section 4.7, the lateral resistance of the cross-frames is 270 kips. The total bearing force under MCE is slightly higher because of strain hardening in the cross-frames. The average column base shear forces in the transverse directions were 318 kips under DE and 354 kips under MCE. Thus, for this bridge, the inertia force in the pier cap is about 20% of the base shear.

The average of resultant column base shear forces were 530 kips under DE and 582 kips under MCE. From Section 4.7, the plastic shear resistance of the column is 600 kips. Thus, the column response is essentially elastic.

The average lateral displacement of the superstructure under DE was 2.37 in. (3.6% drift). This is about two times larger than the displacement calculated from the cross-frame design shown in Section 4.5 Step 9 (the displacement is 1.31 in. and the drift is 2%). This difference is attributed to the larger contribution of the higher modes to the superstructure transverse response. Although the spectral acceleration of the selected ground motions are close to the design spectrum at fundamental period in transverse direction (1.22 sec as shown in Table 4-2), the ground motions have larger spectral accelerations at higher modes, as can be observed in Figure 1-8.

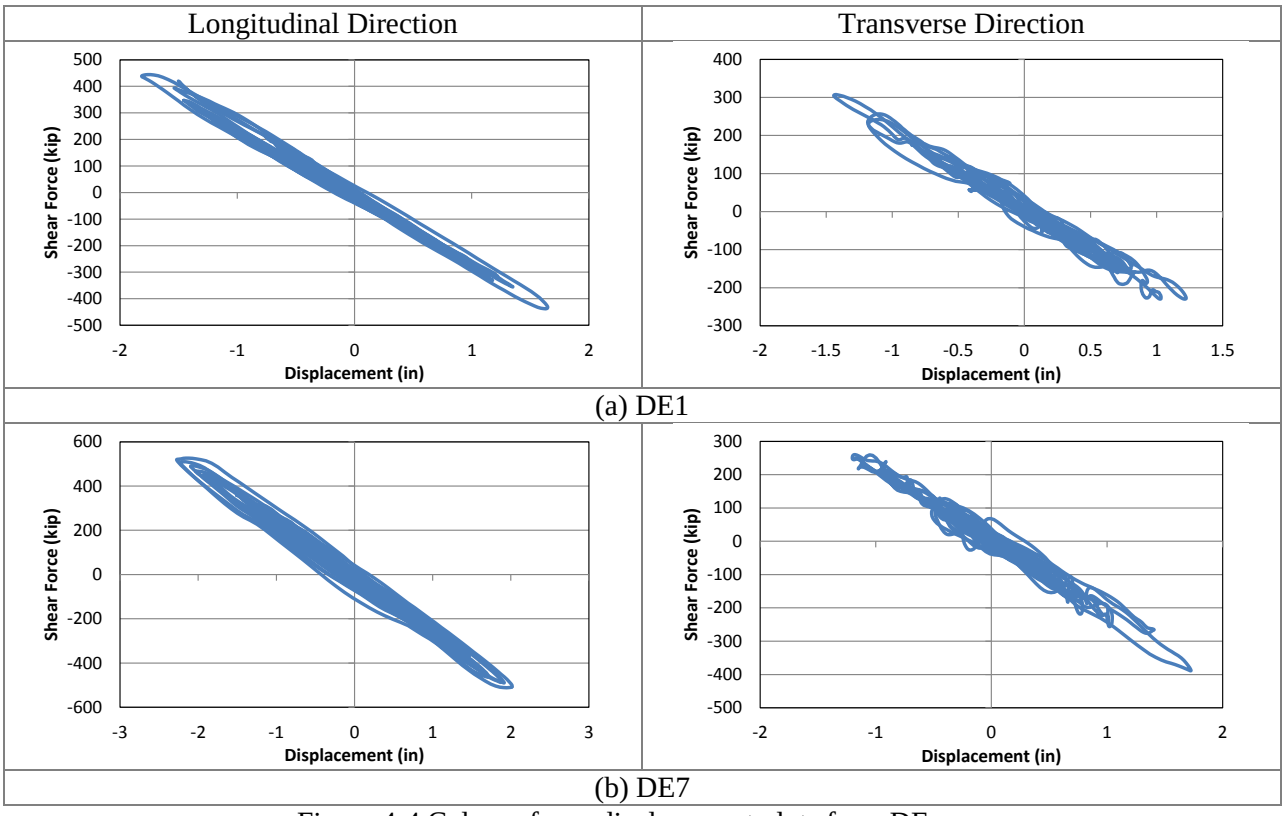

Figure 4-4 Column force-displacement plots from DE runs

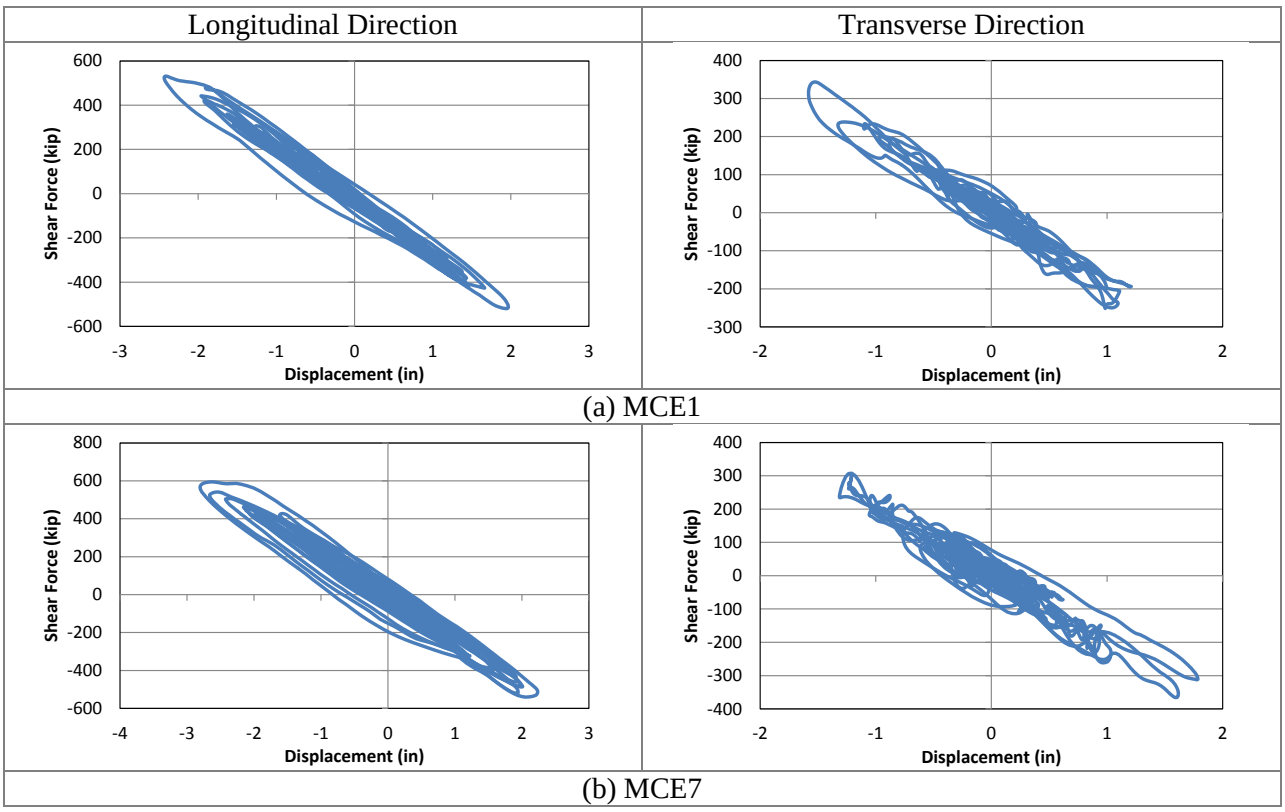

Figure 4-5 Column force-displacement plots from MCE runs

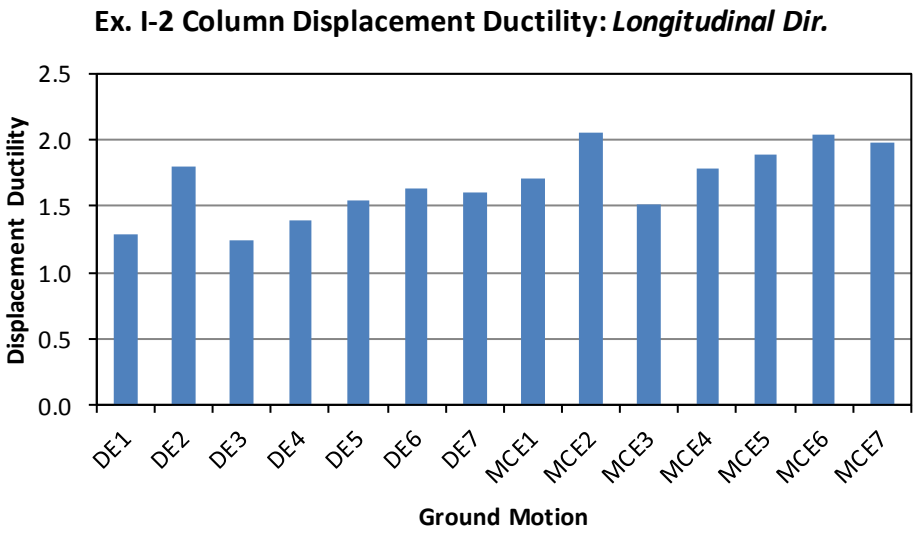

(a) ductility ratios in the longitudinal direction

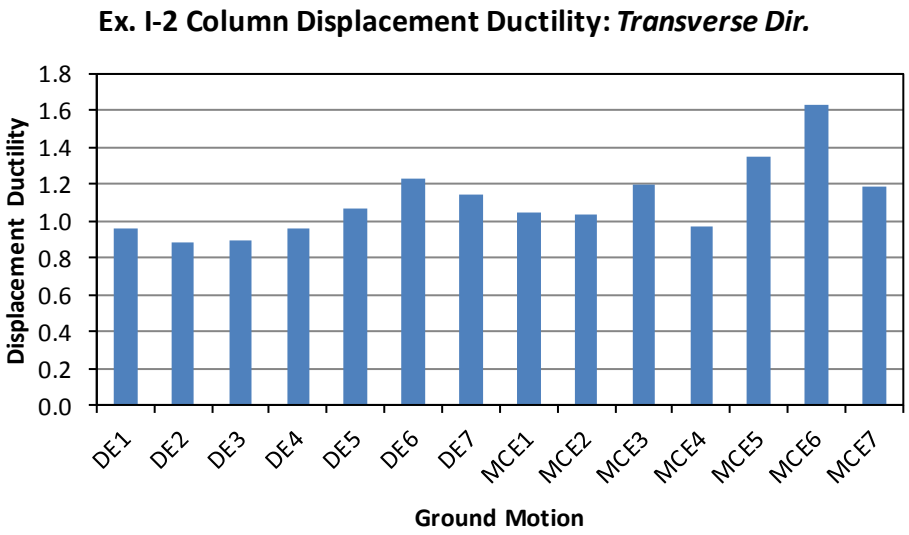

(b) ductility ratios in the transverse direction

Figure 4-6 Summary of column Displacement ductility

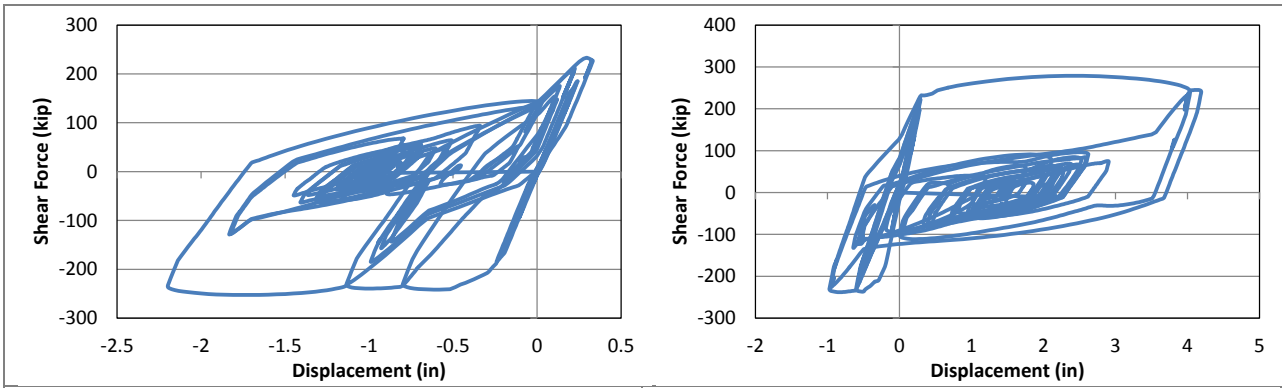

(a) DE1 (b) DE7

Figure 4-7 Superstructure force-displacement in the transverse direction from DE runs

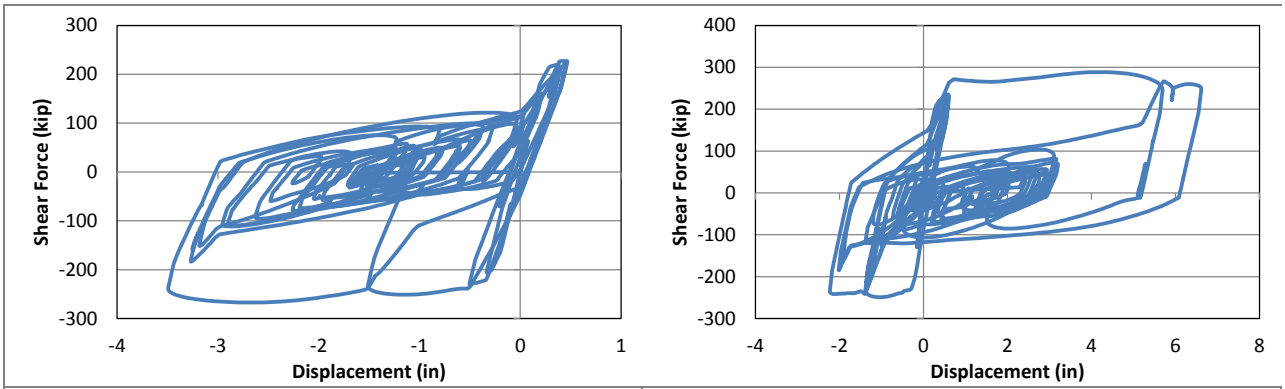

(a) MCE1 (b) MCE7

Figure 4-8 Superstructure force-displacement in the transverse direction from MCE runs

Chapter 5 Bridge with Two-Column Piers Designed using Type 1 Strategy (Example II-1a)

5.1 Bridge Description

The overall geometry of Ex. II-1a is described in Section 1.3.2. From the final design iteration, the reinforced concrete (R/C) column diameter is 4 ft with 1% longitudinal steel ratio and 1.4% transverse steel ratio. The rectangular pier cap is 5 ft wide and 4 ft deep. The pier cap is 60 ft long and the center-to-center distance between the columns is 40 ft. Figure 5-1 shows the elevation at piers. The cross-frames are of X-type pattern with diagonal members made of L8x8x5/8 single angles while the top and bottom chords are 2L4x4x1/2 double angles.

5.2 Computational Model

The computational model is shown in Figure 5-2. The equivalent concrete section properties of superstructure are summarized in Table 5-1. Local axes of the superstructure are shown in Figure 5-1. Deck cracking was accounted for in the calculation of these properties by using 50% of the gross concrete modulus of elasticity (E_c).

For nonlinear response history analysis, the cross-frames were modeled with multi-linear plastic link element with force-deformation relationship shown in Figure 1-5 to account for inelasticity in case it occurred. Calculation of expected force and deformations are shown in Section 5.6.

Table 5-1 Ex.II-1a superstructure section properties

Area, A (in^2)	16,195
Moment of inertia about horizontal axis, I_2 (in^4)	10,316,084
Moment of inertia about vertical axis, I_3 (in^4)	8.22×10^8
Torsional constant, J (in^4)	285,124

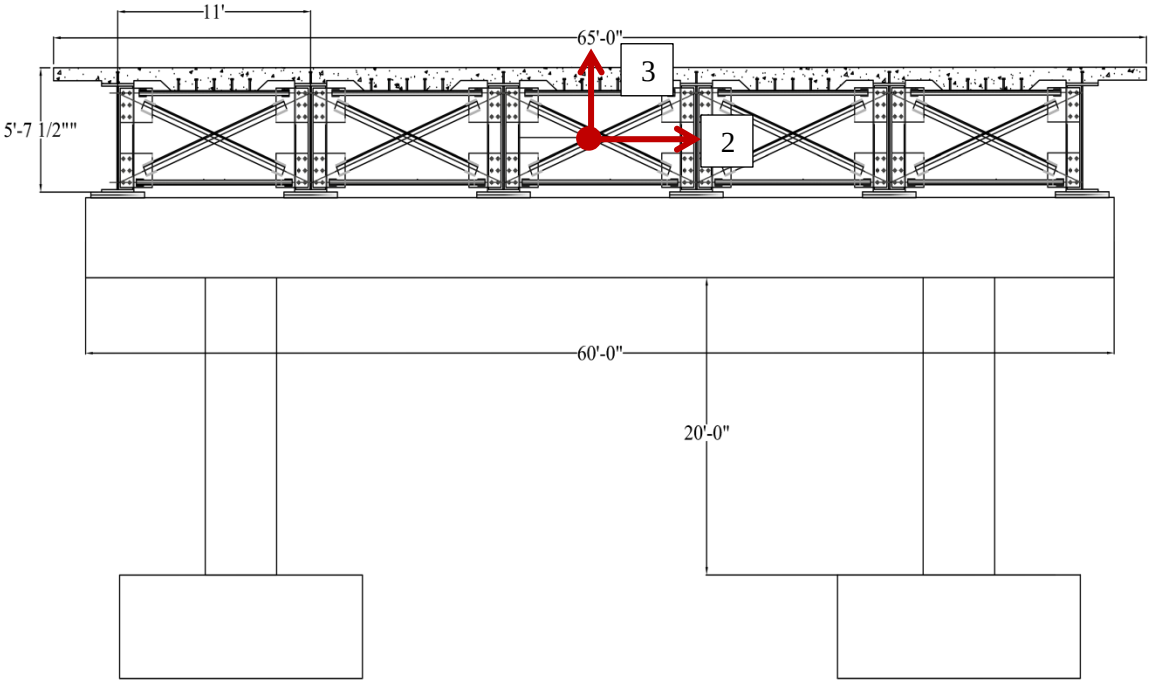

Figure 5-1 Elevation at pier of Ex. II-1a

5.3 Analysis

5.3.1 Gravity Loads – DC and DW

The total *DC* load (i.e. total bridge dead load) is 3,933 kips and the total *DW* load is 844 kips. The reactions at the base of each column due to these loads are 801 kips and 166 kips, respectively. These loads were used to calculate the effective section properties of the columns, as illustrated in Section 5.3.2 Steps *1* and *2*.

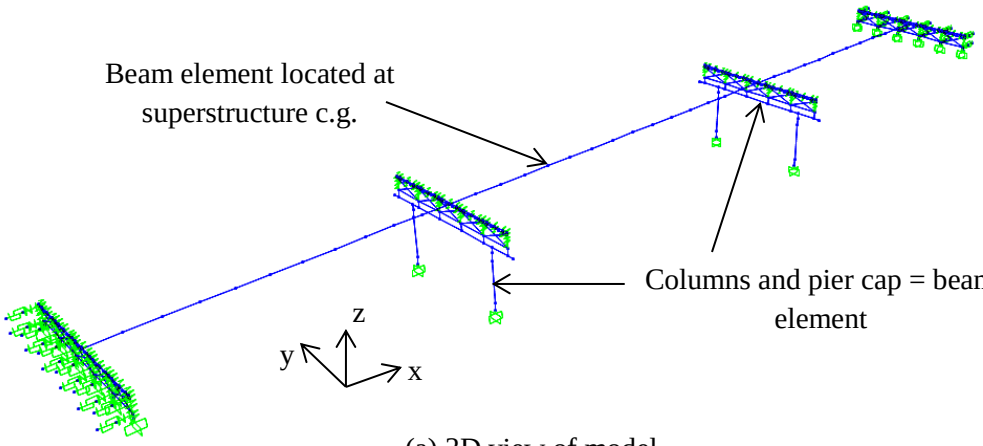

(a) 3D view of model

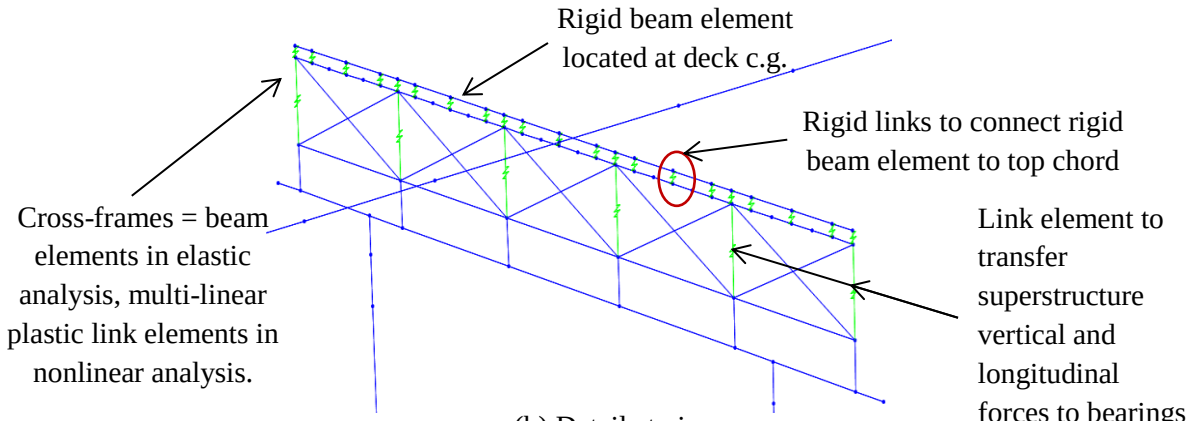

(b) Detail at piers

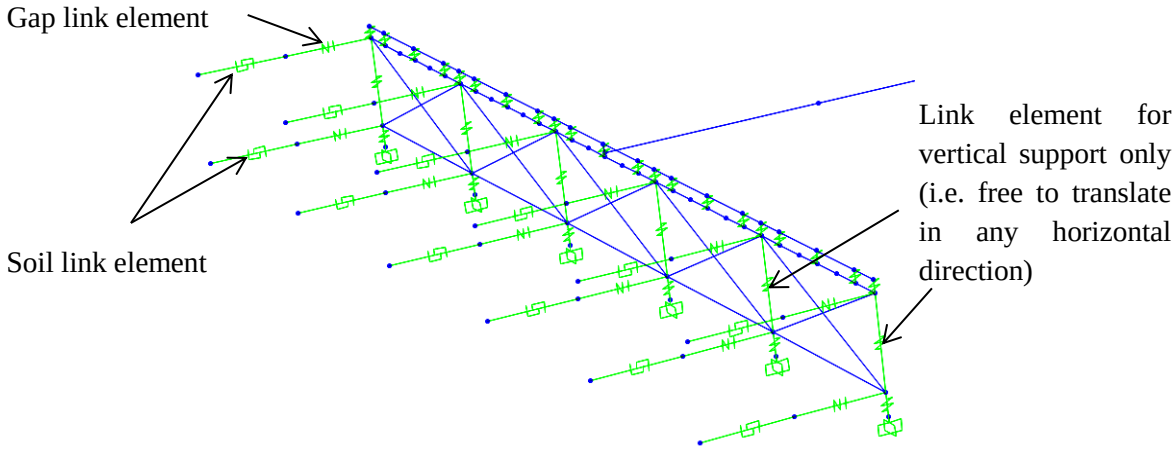

(c) Detail at abutments

Figure 5-2 Analytical model of Ex. II-1a

5.3.2 Earthquake Loads – EQ

Step 1: Calculate column axial loads due to gravity loads, P_{col}. This will be used to determine the effective moment of inertia, I_e, of columns. $$P_{col} = 1.25P_{DC} + 1.5P_{DW}$$		$$P_{col} = 1.25(801) + 1.5(166) = 1{,}250\ kips$$
Step 2: Determine effective moment of inertia, I_e. This is accomplished through section analysis of the column. The required parameters are: column diameter, longitudinal and transverse reinforcements, axial load, and material properties of concrete and steel reinforcement. The calculated I_e is assigned to the beam elements representing the column in the model.		The following are the column properties: D = 4 ft ρ_l = 1% (12 - #11) ρ_s = 1.4% (#6 @ 3.0 in.) f'_c = 4 ksi f_y = 60 ksi P_{col} = 1,250 kips From section analysis: I_e/I_g = 0.38
Step 3: Estimate soil displacement, Δ_{soil}, and calculate the effective abutment stiffness, K_e. The joint gap is included in the calculation of this stiffness, as shown in the figure below. 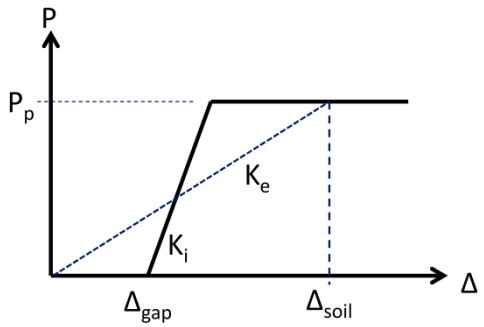 Figure 5-3 Abutment force-displacement The soil passive resistance, P_p, and initial soil stiffness, K_i, are calculated based on the recommended values in Caltrans SDC. $$P_p = 5.0A_e(h/5.5)\ \ (kips)$$ $$K_i = 50w(h/5.5)\ \ (kip/in)$$ where A_e (ft^2) is the effective backwall area, h (ft) is the backwall height, and w is the backwall		Δ_{soil} = 5.0 in. $$P_p = 5.0(5.625x65)(5.625/5.5) = 1{,}870\ kips$$ $$K_i = 50(65)(5.625/5.5) = 3{,}324\ kip/in$$ Check Δ_{soil} against Δ_{gap} + Δ_y to determine if the soil is yielding. $$\Delta_{gap} + \Delta_y = 2 + \frac{1{,}870}{3{,}324} = 2 + 0.56 = 2.56\ in$$ Since this is smaller than Δ_{soil}, the soil is yielding and the effective stiffness is: $$K_e = \frac{1{,}870}{5.0} = 374\ kip/in$$ $$1/2K_e = 187\ kip/in$$

width. Under *EQ* in longitudinal direction, only one abutment is engaged in one direction. To account for this in elastic analyses such as modal and response spectrum analysis, half of K_e is applied to both abutments. This $1/2K_e$ is then distributed to the link elements representing the soil. The gap link elements shown in Figure 5-2c were assigned with high stiffness with no opening during elastic analysis.		Since there are 12 soil springs at each abutment, the effective stiffness assigned to each is: $(1/2K_e)/12 = 15.58\ kip/in$
Step 4: Perform modal analysis and determine the required number of modes needed for multimode spectral analysis. After the effective stiffnesses of the elements are determined, modal analysis is performed to determine the fundamental vibration periods and the required number of modes needed in the response spectrum analysis. The AASHTO Specifications requires that the total number of modes used should ensure participation of at least 90% of the total bridge mass.		Table 5-2 shows the result of modal analysis. Although only the first 5 modes are shown in this table, a total of 30 modes were used in the response spectrum analysis with total mass participation of 100% in both the longitudinal and transverse directions. The first mode with period of 0.94 sec is longitudinal translation mode; the second with period of 0.94 sec is in-plane deck rotation mode; and the third with period of 0.68 sec is the transverse translation mode. The vertical vibration mode is the fourth mode with period of 0.34 sec. Table 5-2 Modal periods and mass participation Mode No | Period Sec | Mass Participation x-dir | Mass Participation y-dir 1 | 0.94 | 0.981 | 0.000 2 | 0.92 | 0.000 | 0.000 3 | 0.68 | 0.000 | 0.980 4 | 0.34 | 0.000 | 0.000 5 | 0.24 | 0.000 | 0.006
Step 5: Perform response spectrum analysis in the longitudinal direction (EQ_x), determine Δ_{soil}, and check against the initial value in *Step 3*. The design spectrum is applied in the longitudinal direction. Multimode spectral analysis is used and the modal responses are combined using the Complete Quadratic Combination (CQC).		From response spectrum analysis, Δ_{soil} = 5.05 in. Therefore, no further iteration is needed.

Step 6: Obtain the column forces due to EQ_x.

These forces will be combined with the forces due to EQ_y to determine the design forces.

Table 5-3 Column forces due to EQ_x

Load	P (kip)	M_x (k-ft)	M_y (k-ft)
EQ_x	17	0	5,317

The seismic base shear of the bridge in the longitudinal direction is 2,676 kips.

Step 7: Perform response spectrum analysis in the transverse direction (EQ_y) and determine the column forces.

Table 5-4 Column forces due to EQ_y

Load	P (kip)	M_x (k-ft)	M_y (k-ft)
EQ_y	858	9,369	0

The seismic base shear of the bridge in the transverse direction is 3,731 kips.

5.3.3 Design Loads

The 100%-30% combination was used to combine the EQ_x and EQ_y forces. The results are shown in Table 5-5.

Table 5-5 Combination of forces due to EQ_x and EQ_y

Load/Combination	P (kip)	M_x (k-ft)	M_y (k-ft)
EQ_x	17	0	5,317
EQ_y	858	9,369	0
EQ_1: $1.0EQ_x + 0.3EQ_y$	274	2,811	5,317
EQ_2: $0.3EQ_x + 1.0EQ_y$	863	9,369	1,595

The response modification factor, R, is then applied to EQ_1 and EQ_2 moments. For bridge with multi-column piers, R for columns is equal to 5.0. The resulting forces are then combined with DC and DW forces to determine the design forces. The load factors are based on Extreme Event I load combination and the result is shown in Table 5-6.

Table 5-6 Design loads for columns

Load/Combination	P (kip)	M_x (k-ft)	M_y (k-ft)
DC	801	0	0
DW	166	0	0
EQ_1/R	274	562	1,063
EQ_2/R	863	1,874	319
$LC1$: $1.25DC + 1.5DW + 1.0EQ_1$	1,524	562	1,063
$LC2$: $1.25DC + 1.5DW + 1.0EQ_2$	2,113	1,874	319

5.4 Design of Columns

Step 1: Determine the design axial load and resultant moment from Section 5.3.3.

Table 5-7 Design axial load and resultant moment

Load Combination	P (kip)	M_{res} (kip-ft)
LC1	1,524	1,202
LC2	2,113	1,901

Step 2: Develop the axial force-moment (P-M) interaction curve and check if the design loads are inside the P-M curve.

The AASHTO ϕ factors are used in the interaction curve.

From the final iteration the column properties are:

D = 4 ft
ρ_l = 1% (12 - #11)
ρ_s = 1.4% (#6 @ 3.0 in.)
f'_c = 4 ksi
f_y = 60 ksi

The design loads are within the boundaries of P-M interaction curve as shown below. Thus, the selected column size and reinforcement are adequate.

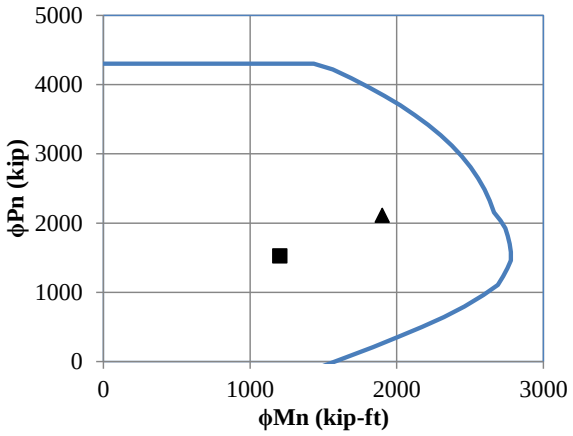

Step 3: Determine the plastic shear resistance, F_p, of the piers in transverse direction

The plastic moment resistance, M_p, of column is a function of its axial load. In multi-column pier, due to frame action, there is variation in column axial loads resulting in different plastic moment capacities. Calculation of F_p is therefore an iterative process. The calculation of F_p is outlined

in the procedure below. ***Step 3.1:*** Start the calculation process by using the column axial load, *P*, obtained from *LC1*. The following procedure, up to *Step 3.7*, is repeated to calculate F_p based on *P* from *LC2*. The maximum F_p calculated from *LC1* and *LC2* will be used to design the transverse reinforcement and cross-frames ***Step 3.2:*** Based on this *P*, determine M_n from the interaction curve. ***Step 3.3:*** Determine M_p and V_p. $$M_p = 1.3M_n$$ where the 1.3 factor is to account for column overstrength. $$V_p = \frac{2M_p}{H}$$ where *H* is the column clear height. This equation is based on double-curvature behavior. This behavior is typically assumed for a multi-column pier because the cap beam is much stiffer than the columns. ***Step 3.4:*** Calculate F_p and ΔP. The following equations are based on the free-body diagram for a two-column pier shown in Figure 5-4.		From Table 5-7, P = 1,524 kips. Since this *P* was from response spectrum analysis, both columns of the pier have the same *P*. By interpolating on the points of the interaction curve, M_n = 3,197 kip-ft for P = 1,524 kips. M_p = 1.3(3,197) = 4,156 kip-ft V_p = 2(4,156)/20 = 416 kips

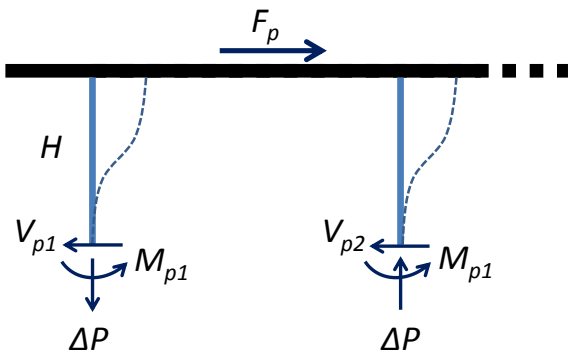

Figure 5-4 Forces in a two-column pier

$$F_p = V_{p1} + V_{p2}$$

$$\Delta P = \frac{(V_{p1} + V_{p2})H - (M_{p1} + M_{p2})}{L}$$

where L is the distance between the two columns.

F_p = 416 + 416 = 832 kips

$$\Delta P = \frac{(416 + 416)20 - (4{,}156 + 4{,}156)}{40} = 208\ kips$$

Step 3.5: Update the axial load in the columns.

$$P_1 = P - \Delta P$$

$$P_2 = P + \Delta P$$

Where P_1 is the updated axial load in left column and P_p is updated axial load in right column.

P_1 = 1,524 – 208 = 1,315 kips

P_2 = 1,524 + 208 = 1,731 kips

Step 3.6: Update the M_n, M_p, and V_p in the columns.

The new plastic moments and shears are determined using P_1 and P_2.

- For P_1 = 1,315 kips
  M_{n1} = 3,058 kip-ft from interaction curve
  M_{p1} = 1.3(3,058)= 3,975 kip-ft
  V_{p1} = 2(3,975)/20 = 398 kips
- For P_2 = 1,731 kips
  M_{n2} = 3,324 kip-ft from interaction curve
  M_{p2} = 1.3(3,324) = 4,321 kip-ft
  V_{p2} = 2(4,321)/20 = 432 kips

Step 3.7: Calculate the new F_p and ΔP and compare against that in *Step 3.4*.

F_p = 398 + 432 = 830 kips

If F_p in this step is within 5% of that in *Step 3.4*, further iteration is not necessary. Otherwise, repeat *Steps 3.4* to *3.7*.		$\Delta P = \frac{(398 + 432)20 - (3{,}975 + 4{,}321)}{40}$ $= 208\ kips$ Since F_p and ΔP are within 5% of previous, further iteration is not necessary.
Step 3.8: Repeat Steps *3.1* to *3.7* using P from *LC2*.		The calculations were started using P = 2,113 kips from *LC2* in Table 5-7. The results of the last iteration are: M_{p1} = 4,410 kip-ft V_{p1} = 441 kips M_{p2} = 4,571 kip-ft V_p = 457 kips F_p = 868 kips
Step 3.9: Determine the maximum F_p and the maximum column plastic shear resistance. This is the maximum of the results from *Steps 3.7* and *3.8*. The results will be used to design the column transverse reinforcement and cross-frames.		From the results of *Steps 3.7* and *3.8*: V_p = 457 kips (maximum V_p per column) F_p = 868 kips (maximum F_p for the pier)
Step 4: Determine the column shear resistance and compare against the plastic shear resistance. The shear resistance can be calculated using the Simplified Procedure described in AASHTO Specifications Art. 5.8.3.4.1. For simplicity and to be conservative, the contribution of concrete to the shear resistance is not included in the calculations. $V_n = \frac{A_v f_y d_v}{s}$ where:		The transverse reinforcement is #6 rebar spaced at 3.0 in. on center. The longitudinal reinforcement is #11 rebar. The concrete cover is 2.0 in. $A_v = 2(0.44) = 0.88\ in^2$ $D_r = 48 - 2 - 2 - 0.75 - 0.75 - 1.375$ $= 41.125\ in$ $d_e = \frac{48}{2} + \frac{41.125}{\pi} = 37.09\ in$ $d_v = 0.9(37.09) = 33.38\ in$

$A_v = 2A_{sh}$ $d_v = 0.9d_e$ $d_e = \frac{D}{2} + \frac{D_r}{\pi}$ A_{sh} = area of one leg of transverse reinforcement; f_y is the yield stress of transverse reinforcement; s is the spacing of transverse reinforcement; D is the diameter of column; D_r is the diameter of the circle passing through the centers of longitudinal reinforcement.		$V_n = \frac{0.88(60)(33.38)}{3} = 587\ kips$ $\phi V_n = 0.9(587) = 529\ kips$ The maximum V_p = 457 kips per column. The demand-resistance ratio is: $\frac{D}{C} = \frac{457}{529} = 0.86\ < 1.0, ok!$
Step 5: Check the transverse reinforcement. The volumetric ratio of transverse reinforcement shall satisfy (AASHTO Specifications Art. 5.10.11.4.1d): $\rho_s \geq 0.12\frac{f_c'}{f_y}$ The spacing of transverse reinforcement shall satisfy (AASHTO Specifications Art. 5.10.11.4.1e): $s \leq \begin{cases} D/4 \\ 4.0 \end{cases}$		ρ_s = 1.4% (#6 @ 3.0 in.) f_y = 60 ksi f'_c = 4 ksi $\rho_s = 0.014 \geq 0.12\left(\frac{4}{60}\right) = 0.008\ \ ok!$ $s = 3.0 \leq \begin{cases} 66/4 = 16.5 \\ 4.0 \end{cases}\ \ ok!$

5.5 Seismic Design of Cross-Frames

For Type 1 design strategy, the inelasticity is to be limited in the columns. The components along the seismic load path such as cross-frames are designed and detailed to remain elastic.

Step 1: Determine the axial force in each of the cross-frame diagonal members. $$P_{XF} = \frac{V_{XF}}{2N\cos\theta} = \frac{F_p}{2N\cos\theta}$$ where F_p is the pier plastic shear resistance, N is the number of panels, and θ is the angle of the diagonal member measured from the horizontal.		F_p = 868 kips N = 5 panels θ = 22 degrees $P_{XF} = \frac{868}{2(5)(\cos 22)} = 93.62\ kips$
Step 2: Cross-frame member section properties Note that the size of the cross-frames may be governed by slenderness requirements.		Section: *L8x8x5/8* F_y = 36 ksi A_g = 9.61 in^2 $r_x = r_y$ = 2.48 in. L = 142.62 in.
Step 3: Calculate the tensile resistance $$\phi P_r = 0.95 F_y A_g$$		$\phi P_r = 0.95(36)(9.61) = 328.66\ kips > 93.62\ kips$
Step 4: Calculate the compressive resistance Under seismic loading, the cross-frames are primary members in the transverse direction as they transmit the deck seismic forces to the bearings. The limiting slenderness ratio for primary members is 120 (AASHTO Specifications Art. 6.9.3). Equal-leg single angle sections will be used as diagonal members. The slenderness ratio is calculated according to AASHTO Specifications Art. 6.9.4.4. ○ If $l/r_x \leq 80$ $$\left(\frac{KL}{r}\right)_{eff} = 72 + 0.75\frac{l}{r_x}$$ ○ If $l/r_x > 80$		l/r_x = 142.62/2.48 = 57.51 < 80 $\left(\frac{KL}{r}\right)_{eff} = 72 + 0.75(57.51) = 115.13 < 120\ ok!$

$$\left(\frac{KL}{r}\right)_{eff} = 32 + 1.25\frac{l}{r_x}$$

The compressive resistance is calculated according to AASHTO Specifications Art. 6.9.2.1, 6.9.4.1.1, and 6.9.4.1.2

$$P_e = \frac{\pi^2 E}{\left(\frac{Kl}{r}\right)^2_{eff}} A_g$$

$$P_o = QF_yA_g$$

The slender element reduction factor, *Q*, is equal to 1.0 when:

$$\frac{b}{t} \leq 0.45\sqrt{\frac{E}{F_y}}$$

- If $P_e/P_o \geq 0.44$

$$\phi P_n = 0.9\left[0.658^{(P_o/P_e)}\right]P_o$$

- If $P_e/P_o < 0.44$

$$\phi P_n = 0.9(0.877P_e)$$

Note that although the calculations shown here is for single angle sections, unequal-leg single angles and double angles may be also used as diagonal members of cross-frames.

$$P_e = \frac{\pi^2(29{,}000)}{115.13^2}(9.61) = 207.51\ kips$$

$$\frac{b}{t} = \frac{8}{5/8} = 12.8 \leq 0.45\sqrt{\frac{29{,}000}{36}} = 12.8, Q = 1.0$$

$$P_o = 1.0(36)(9.61) = 345.96\ kips$$

$$\frac{P_e}{P_o} = \frac{207.51}{345.96} = 0.60 \geq 0.44$$

$$\phi P_n = 0.9\left[0.658^{1/0.60}\right](345.96) = 155.0\ kips > 93.62\ kips, ok!$$

The resistance of the selected section, *L8x8x5/8*, is much larger than the demand. However, this section was selected due to limit on slenderness ratio.

Step 5: Calculate the minimum nominal shear resistance of the cross-frames and check against V_p of column.

$$V_{XF\_min} = (2P_n)N\cos\theta$$

In this equation, only the compression resistance, P_n, is used to determine the minimum nominal shear resistance. Note that P_n is smaller than the tension resistance, P_r, which means buckling would occur first in any of the diagonal members before yielding is reached. Thus, V_{XF} is the minimum shear force before inelasticity starts to occur in the cross-frames. Since this is Type 1 design – inelasticity is accommodated in the columns only – F_p should be less than V_{XF}.

$$V_{XF\_min} = 2\left(\frac{155.0}{0.9}\right)5\cos 22 = 1{,}597\ kips > F_p = 868\ kips, ok!$$

As can be seen above, the slenderness ratio is the governing parameter in the design of elastic support cross-frames.

5.6 Cross-Frame Properties for Nonlinear Analysis

The expected force and displacement resistance of the cross-frames are calculated for use in the design evaluation.

Step 1: Calculate the expected tensile yield and displacement resistance. The expected yield resistance is: $$P_{ye} = F_{ye}A_g$$ where F_{ye} is the expected yield stress and is equal to R_yF_y. For A36 steel sections, R_y = 1.5. The effective axial stiffness is: $$K_{XF\_e} = \frac{EA_e}{L}$$ where E is the modulus of elasticity of steel which is 29,000 ksi, A_e is the effective area calculated using Eqn. (1-12), and L is the total length of the diagonal member. The expected yield displacement is then calculated as: $$\Delta_{ye} = \frac{P_{ye}}{K_{XF\_e}}$$		*L8x8x5/8* F_{ye} = 1.5(36) = 54 ksi A_g = 9.61 in^2 I = 59.6 in^4 e = 2.21 in. distance from connected leg of angle to its c.g. $P_{ye} = 54(9.61) = 518.94\ kips$ $A_e = \frac{9.61(59.6)}{59.6 + 9.61(2.21)^2} = 5.38\ in^2$ $K_{XF\_e} = \frac{29{,}000(5.38)}{142.62} = 1{,}093.18\ kip/in$ $\Delta_{ye} = \frac{518.94}{1{,}093.18} = 0.47\ in$
Step 2: Calculate the expected compressive resistance and associated displacement. The $(Kl/r)_{eff}$ and P_e is the same as that calculated in Section 5.5 *Step 4*. The expected yield strength is used to calculate P_o. $$P_o = QF_{ye}A_g$$ The expected compressive resistance is then calculated as: ○ If $P_e/P_o \geq 0.44$ $$P_{nc} = \left[0.658^{(P_o/P_e)}\right]P_o$$ ○ If $P_e/P_o < 0.44$		$P_o = 54(9.61) = 518.94\ kips$ $\frac{P_e}{P_o} = \frac{207.51}{518.94} = 0.40 < 0.44$ $P_{nc} = 0.877(207.51) = 181.99\ kips$

$P_{nc} = 0.877P_e$ The corresponding displacement is: $\Delta_{nc} = \frac{P_{nc}}{K_{XF\_e}}$		$\Delta_{nc} = \frac{181.99}{1{,}093.18} = 0.17\ in.$

5.7 Design Summary

The total weight of Ex. II-1a is 3,933 kips. From modal and response spectrum analyses, the periods, forces, and displacements are:

Parameter	Longitudinal Direction	Transverse Direction
Fundamental period, T (sec)	0.94	0.68
Base shear, V_b (kip)	2,676	3,731
Column displacement demand, Δ_{col} (in)	3.73	3.17
Column shear demand, V_{col} (kip)	225	933
Pier base shear demand, F_b (kip)	450	1,866
Deck displacement demand, Δ_{deck} (in)	5.06	3.37

The column properties are:

Diameter, D	4 ft
Longitudinal reinforcement	12 - #11 (ρ_l = 1%)
Transverse reinforcement	#6 @ 3.0 in. (ρ_s = 1.4%)
Effective moment of inertia, I_e	$0.38I_g$
Column plastic shear resistance, V_p	457 kips
Pier plastic shear resistance, F_p	898 kips

The cross-frame diagonal member section properties are:

Section	L8x8x5/8 (A36)
Area, A	9.61 in^2
Slenderness ratio, KL/r	115.13
Width-thickness ratio, b/t	12.8
Tensile resistance, ϕP_r	329 kips
Compressive resistance, ϕP_n	155 kips
Min. nominal shear resistance, V_{XF_min}	1,597 kips
Expected tensile yield resistance, P_{ye}	519 kips
Expected compressive resistance, P_{nc}	182 kips

5.8 Nonlinear Evaluation

Example II-1a was analyzed using the ground motions described in Section 1.8.1. The ground motions were scaled to represent the Design (DE) and MCE Earthquake levels. There were seven DE runs and seven MCE runs for a total of fourteen runs. Because of this, only the column force-displacement plots from DE1, DE7, MCE1 and MCE7 are shown in Figure 5-5 and Figure 5-6 to represent the results. However, the column ductility ratios for all runs are shown in Figure 5-7. Nonlinearity was not observed in the support cross-frames.

The yield displacements were calculated according to Section 1.8.2. Since the expected material properties were used in the nonlinear analyses, the yield displacements were also calculated using these properties. The yield displacements are 1.91 in. and 0.88 in. in the longitudinal and transverse directions, respectively.

In the longitudinal direction, the average ductility ratios were 1.7 from DE runs and 2.3 from MCE runs. In the transverse direction, the respective ductility ratios were 3.8 and 5.2. The smaller ductility in the longitudinal direction is due to the contribution of abutment soil in the response. The column response in this direction is single-curvature resulting in yield displacement that is about three times the yield displacement in transverse direction. Thus, the ductility demand in the transverse direction is larger even though the displacements in both directions are about the same. Yielding is also apparent in the hysteresis loops in the transverse direction.

The average of total bearing forces in the transverse direction were 902 kips under DE and 1,010 kips under MCE. These are smaller than the minimum nominal resistance of the cross-frames shown in Section 5.7 thus the cross-frames were elastic. The average of pier base shear forces in the transverse direction were 980 kips under DE and 1,091 kips under MCE. Thus, for this bridge, the inertia force in the pier cap is about 8% of the pier base shear.

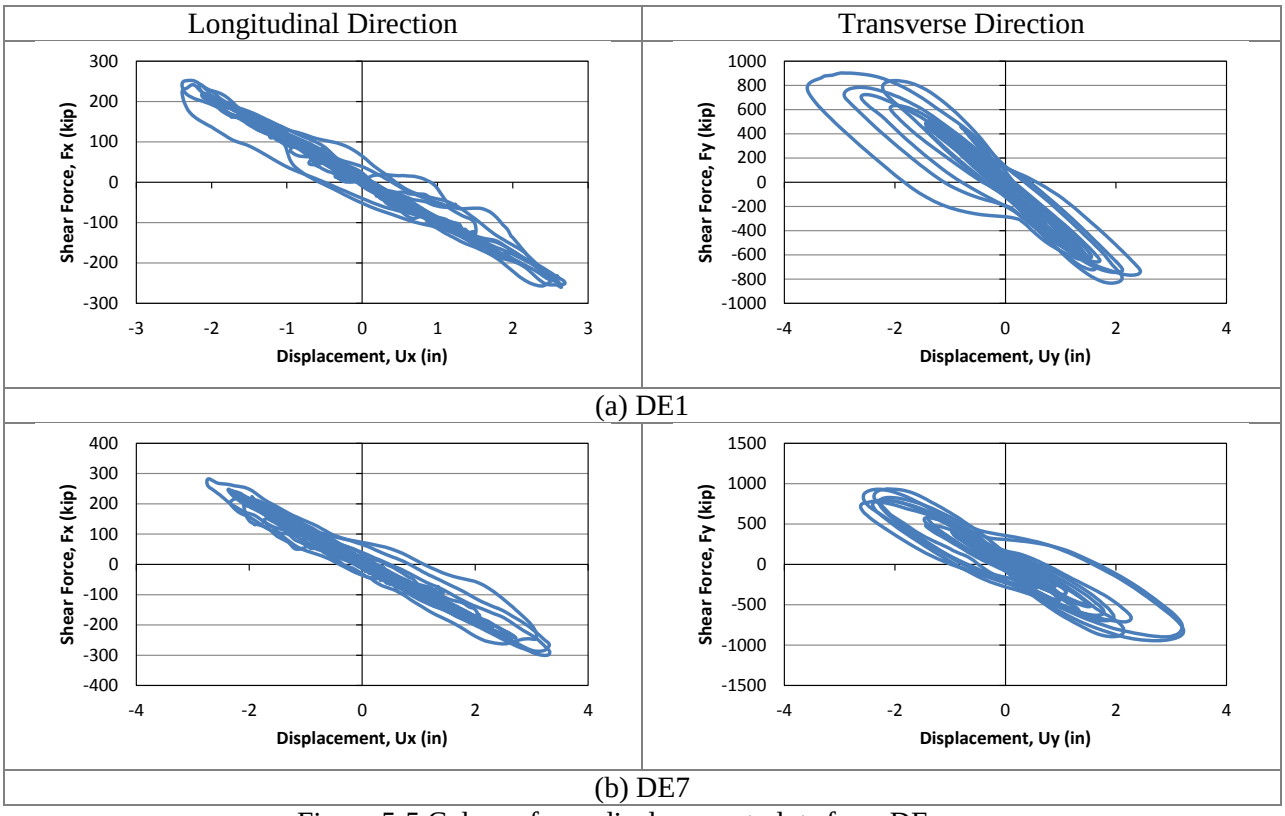

Figure 5-5 Column force-displacement plots from DE runs

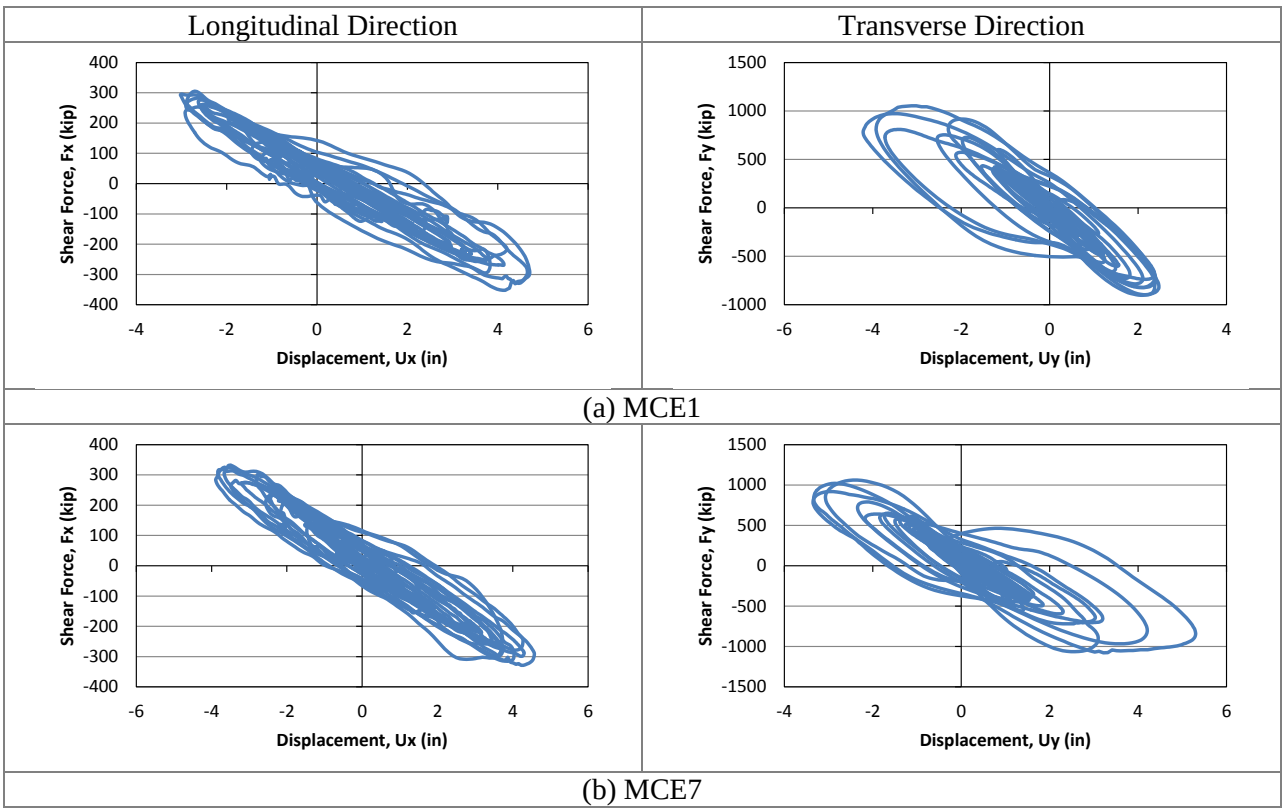

Figure 5-6 Column force-displacement plots from MCE runs

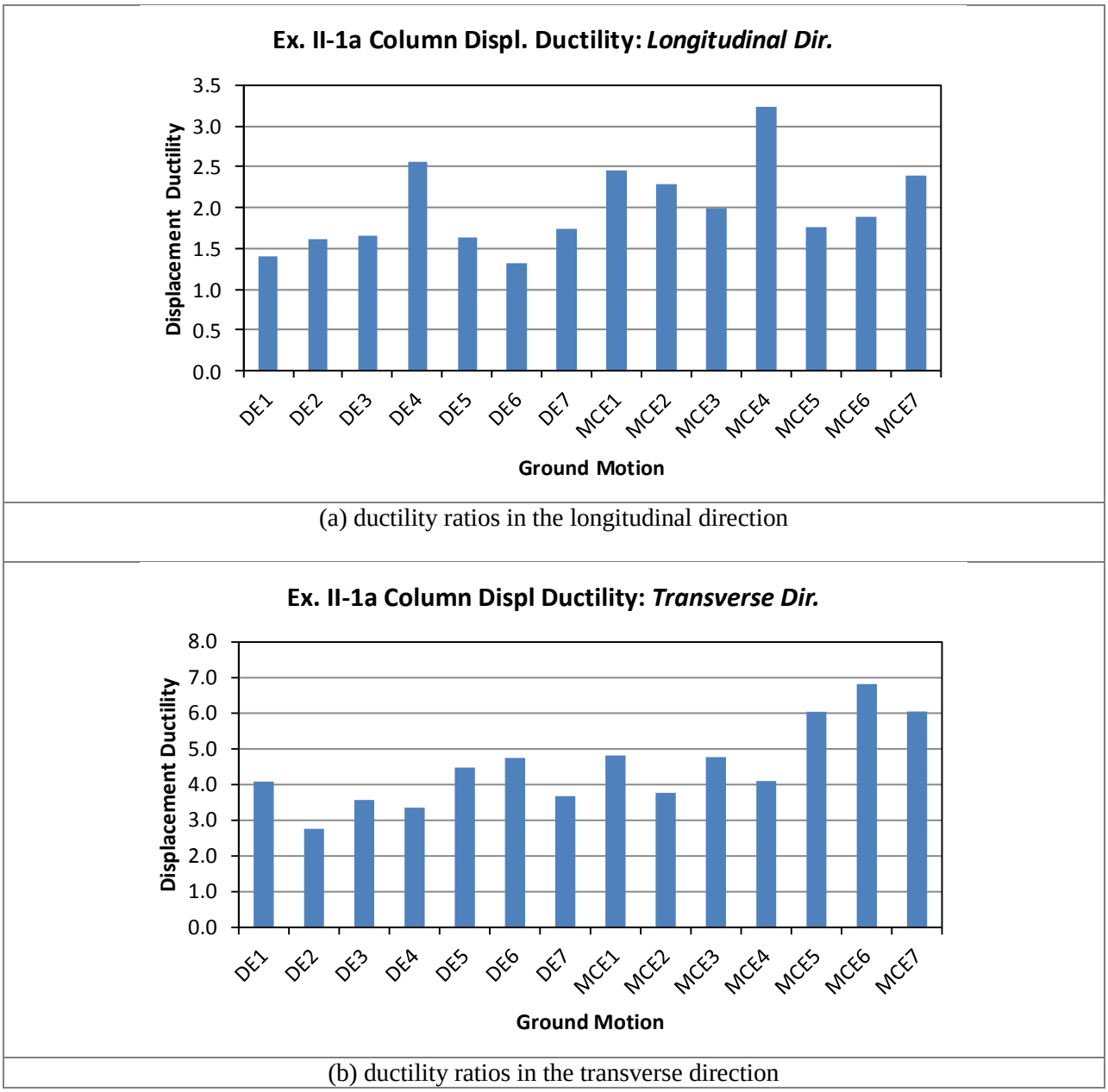

(a) ductility ratios in the longitudinal direction

(b) ductility ratios in the transverse direction

Figure 5-7 Summary of column Displacement ductility

Chapter 6 Critical Bridge with Two-Column Piers Designed using Type 1 Strategy (Example II-1b)

6.1 Bridge Description

The overall geometry of Ex. II-1b is described in Section 1.3.2. From the final design iteration, the reinforced concrete (R/C) column diameter is 6.5 ft with 2.4% longitudinal steel ratio and 2.5% transverse steel ratio. The rectangular pier cap is 7 ft wide and 5 ft deep. The pier cap is 60 ft long and the center-to-center distance between the columns is 40 ft. shows the elevation at piers. The cross-frames are of X-type pattern with diagonal members made of WT 9x54 while the top and bottom chords are 2L5x5x1/2 double angles.

6.2 Computational Model

The computational model is shown in Figure 6-1. The equivalent concrete section properties of superstructure are summarized in Table 6-1. Local axes of the superstructure are shown in Figure 6-1. Deck cracking was accounted for in the calculation of these properties by using 50% of the gross concrete modulus of elasticity (E_c).

For nonlinear response history analysis, the cross-frames were modeled with multi-linear plastic link element with force-deformation relationship shown in Figure 1-5 to account for inelasticity in case it occurred. Calculation of expected force and deformations are shown in Section 6.6.

Table 6-1 Ex.II-1b superstructure section properties

Area, A (in^2)	16,195
Moment of inertia about horizontal axis, I_2 (in^4)	10,316,084
Moment of inertia about vertical axis, I_3 (in^4)	8.22×10^8
Torsional constant, J (in^4)	285,124

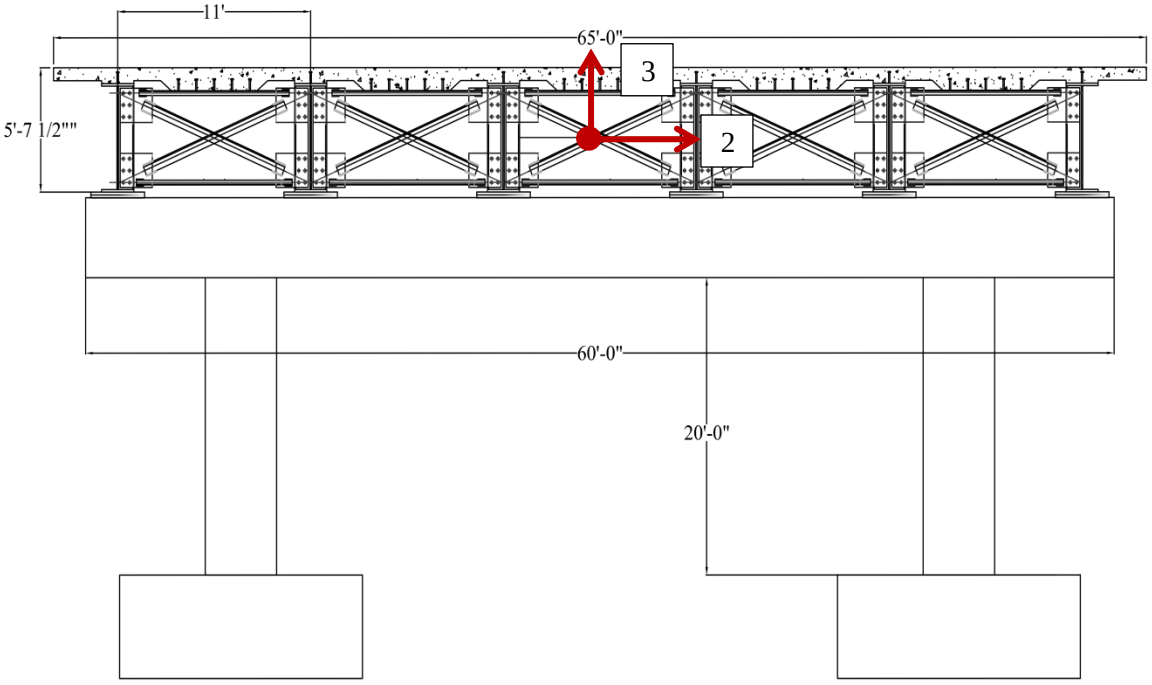

Figure 6-1 Elevation at pier of Ex. II-1b

6.3 Analysis

6.3.1 Gravity Loads – DC and DW

The total *DC* load (i.e. total bridge dead load) is 4,573 kips and the total *DW* load is 844 kips. The reactions at the base of each column due to these loads are 959 kips and 166 kips, respectively. These loads were used to calculate the effective section properties of the columns, as illustrated in Section 6.3.2 Steps *1* and *2*.

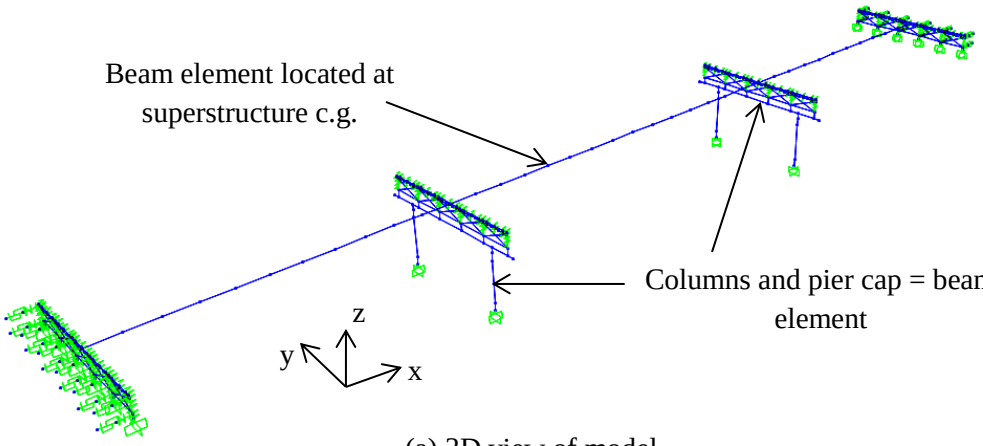

(a) 3D view of model

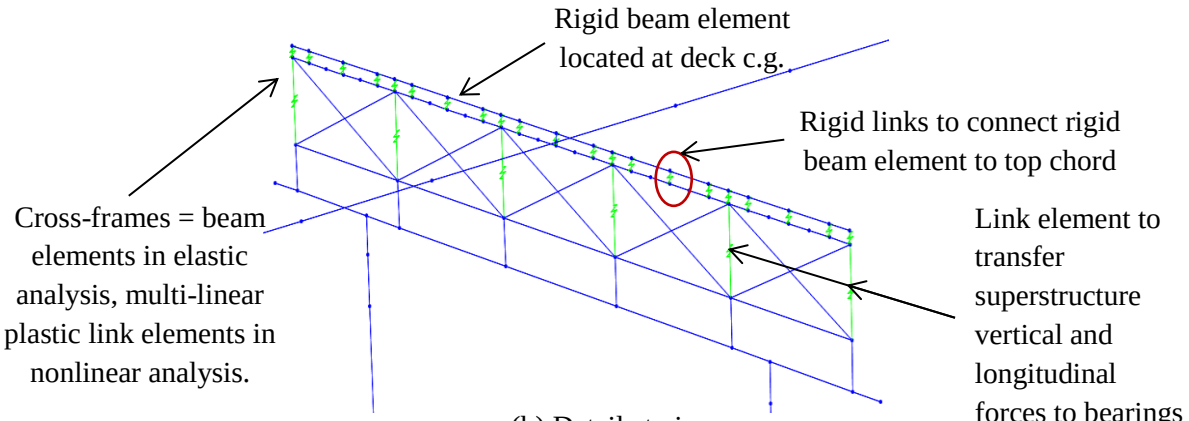

(b) Detail at piers

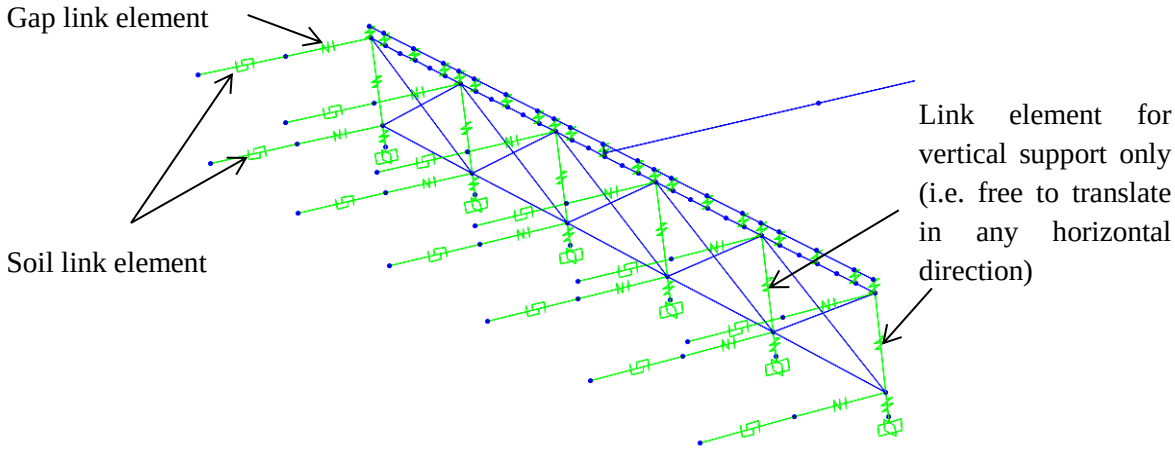

(c) Detail at abutments

Figure 6-2 Analytical model of Ex. II-1b

6.3.2 Earthquake Loads – EQ

Step 1: Calculate column axial loads due to gravity loads, P_{col}. This will be used to determine the effective moment of inertia, I_e, of columns. $$P_{col} = 1.25P_{DC} + 1.5P_{DW}$$		$$P_{col} = 1.25(959) + 1.5(166) = 1{,}448\ kips$$
Step 2: Determine effective moment of inertia, I_e. This is accomplished through section analysis of the column. The required parameters are: column diameter, longitudinal and transverse reinforcements, axial load, and material properties of concrete and steel reinforcement. The calculated I_e is assigned to the beam elements representing the column in the model.		The following are the column properties: D = 6.5 ft ρ_l = 2.4% (72 - #11) ρ_s = 2.5% (#8 @ 1.75 in.) f'_c = 4 ksi f_y = 60 ksi P_{col} = 1,448 kips From section analysis: I_e/I_g = 0.54
Step 3: Estimate soil displacement, Δ_{soil}, and calculate the effective abutment stiffness, K_e. The joint gap is included in the calculation of this stiffness, as shown in the figure below. 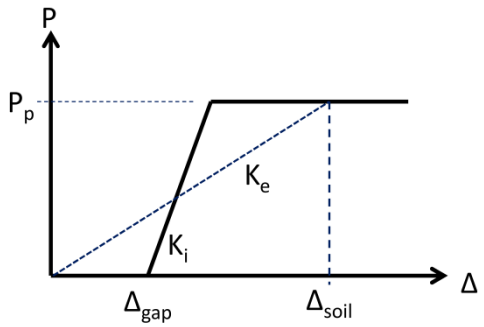 Figure 6-3 Abutment force-displacement The soil passive resistance, P_p, and initial soil stiffness, K_i, are calculated based on the recommended values in Caltrans SDC. $$P_p = 5.0A_e(h/5.5)\ \ (kips)$$ $$K_i = 50w(h/5.5)\ \ (kip/in)$$ where A_e (ft^2) is the effective backwall area, h (ft) is the backwall height, and w is the backwall		Δ_{soil} = 3.0 in. $$P_p = 5.0(5.625x65)(5.625/5.5) = 1{,}870\ kips$$ $$K_i = 50(65)(5.625/5.5) = 3{,}324\ kip/in$$ Check Δ_{soil} against Δ_{gap} + Δ_y to determine if the soil is yielding. $$\Delta_{gap} + \Delta_y = 2 + \frac{1{,}870}{3{,}324} = 2 + 0.56 = 2.56\ in$$ Since this is smaller than Δ_{soil}, the soil is yielding and the effective stiffness is: $$K_e = \frac{1{,}870}{3.0} = 623\ kip/in$$ $$1/2K_e = 312\ kip/in$$

width. Under *EQ* in longitudinal direction, only one abutment is engaged in one direction. To account for this in elastic analyses such as modal and response spectrum analysis, half of K_e is applied to both abutments. This $1/2K_e$ is then distributed to the link elements representing the soil. The gap link elements shown in Figure 5-2c were assigned with high stiffness with no opening during elastic analysis.		Since there are 12 soil springs at each abutment, the effective stiffness assigned to each is: $(1/2K_e)/12 = 26\ kip/in$
Step 4: Perform modal analysis and determine the required number of modes needed for multimode spectral analysis. After the effective stiffnesses of the elements are determined, modal analysis is performed to determine the fundamental vibration periods and the required number of modes needed in the response spectrum analysis. The AASHTO Specifications requires that the total number of modes used should ensure participation of at least 90% of the total bridge mass.		Table 6-2 shows the result of modal analysis. Although only the first 5 modes are shown in this table, a total of 30 modes were used in the response spectrum analysis with total mass participation of 100% in both the longitudinal and transverse directions. The second mode with period of 0.57 sec is longitudinal translation mode; the third with period of 0.45 sec is in-plane deck rotation mode; and the fourth with period of 0.35 sec is the transverse translation mode. The vertical vibration mode is the first mode with period of 0.57 sec. Table 6-2 Modal periods and mass participation Mode No | Period Sec | Mass Participation x-dir | Mass Participation y-dir 1 | 0.57 | 0.000 | 0.000 2 | 0.51 | 0.955 | 0.000 3 | 0.45 | 0.000 | 0.000 4 | 0.35 | 0.000 | 0.774 5 | 0.34 | 0.002 | 0.000
Step 5: Perform response spectrum analysis in the longitudinal direction (EQ_x), determine Δ_{soil}, and check against the initial value in *Step 3*. The design spectrum is applied in the longitudinal direction. Multimode spectral analysis is used and the modal responses are combined using the Complete Quadratic Combination (CQC).		From response spectrum analysis, Δ_{soil} = 2.96 in. Therefore, no further iteration is needed.

Step 6: Obtain the column forces due to EQ_x.

These forces will be combined with the forces due to EQ_y to determine the design forces.

Table 6-3 Column forces due to EQ_x

Load	P (kip)	M_x (k-ft)	M_y (k-ft)
EQ_x	36	0	24,766

The seismic base shear of the bridge in the longitudinal direction is 5,722 kips.

Step 7: Perform response spectrum analysis in the transverse direction (EQ_y) and determine the column forces.

Table 6-4 Column forces due to EQ_y

Load	P (kip)	M_x (k-ft)	M_y (k-ft)
EQ_y	1,580	17,777	0

The seismic base shear of the bridge in the transverse direction is 6,681 kips.

6.3.3 Design Loads

The 100%-30% combination was used to combine the EQ_x and EQ_y forces. The results are shown in Table 5-5.

Table 6-5 Combination of forces due to EQ_x and EQ_y

Load/Combination	P (kip)	M_x (k-ft)	M_y (k-ft)
EQ_x	36	0	24,766
EQ_y	1,580	17,777	0
EQ_1: $1.0EQ_x + 0.3EQ_y$	510	5,331	24,766
EQ_2: $0.3EQ_x + 1.0EQ_y$	1,591	17,777	7,430

The response modification factor, *R*, is then applied to EQ_1 and EQ_2 moments. For a critical bridge with multi-column piers, *R* for columns is equal to 1.5. The resulting forces are then combined with *DC* and *DW* forces to determine the design forces. The load factors are based on Extreme Event I load combination and the result is shown in Table 6-6.

Table 6-6 Design loads for columns

Load/Combination	P (kip)	M_x (k-ft)	M_y (k-ft)
DC	959	0	0
DW	166	0	0
EQ_1/R	510	3,554	16,511
EQ_2/R	1,591	11,851	4,953
LC1: $1.25DC + 1.5DW + 1.0EQ_1$	1,959	3,554	16,511
LC2: $1.25DC + 1.5DW + 1.0EQ_2$	3,040	11,851	4,953

6.4 Design of Columns

Step 1: Determine the design axial load and resultant moment from Section 5.3.3.

Table 6-7 Design axial load and resultant moment

Load Combination	P (kip)	M_{res} (kip-ft)
LC1	1,959	16,889
LC2	3,040	12,844

Step 2: Develop the axial force-moment (P-M) interaction curve and check if the design loads are inside the P-M curve.

The AASHTO ϕ factors are used in the interaction curve.

From the final iteration the column properties are:

D = 6.5 ft
ρ_l = 2.4% (72 - #11)
ρ_s = 2.5% (#8 @ 1.75 in.)
f'_c = 4 ksi
f_y = 60 ksi

The design loads are within the boundaries of P-M interaction curve as shown below. Thus, the selected column size and reinforcement are adequate.

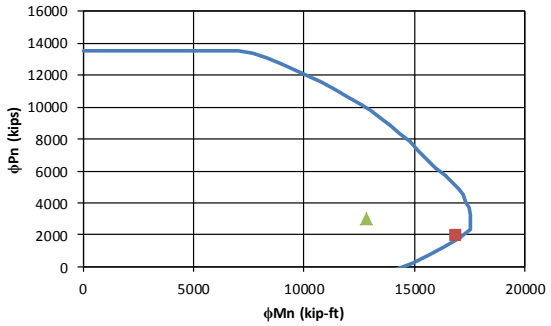

Step 3: Determine the plastic shear resistance, F_p, of the piers in transverse direction

The plastic moment resistance, M_p, of column is a function of its axial load. In multi-column pier, due to frame action, there is variation in column axial loads resulting in different plastic moment capacities. Calculation of F_p is therefore an iterative process. The calculation of F_p is outlined in the procedure below.

Step 3.1: Start the calculation process by using the column axial load, *P*, obtained from *LC1*. The following procedure, up to *Step 3.7*, is repeated to calculate F_p based on *P* from *LC2*. The maximum F_p calculated from *LC1* and *LC2* will be used to design the transverse reinforcement and cross-frames		From Table 6-7, P = 1,959 kips. Since this P was from response spectrum analysis, both columns of the pier have the same P.
Step 3.2: Based on this *P*, determine M_n from the interaction curve.		By interpolating on the points of the interaction curve, M_n = 19,006 kip-ft for P = 1,959 kips.
Step 3.3: Determine M_p and V_p. $$M_p = 1.3M_n$$ where the 1.3 factor is to account for column overstrength. $$V_p = \frac{2M_p}{H}$$ where H is the column clear height. This equation is based on double-curvature behavior. This behavior is typically assumed for a multi-column pier because the cap beam is much stiffer than the columns.		M_p = 1.3(19,006) = 24,708 kip-ft V_p = 2(24,708)/20 = 2,471 kips
Step 3.4: Calculate F_p and ΔP. The following equations are based on the free-body diagram for a two-column pier shown in Figure 6-4.		

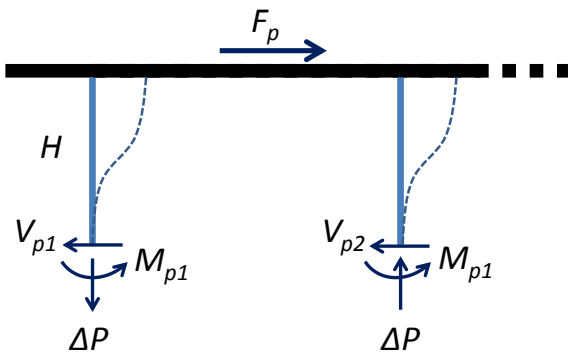

Figure 6-4 Forces in a two-column pier

$$F_p = V_{p1} + V_{p2}$$

$$\Delta P = \frac{(V_{p1} + V_{p2})H - (M_{p1} + M_{p2})}{L}$$

where L is the distance between the two columns.

F_p = 2,471 + 2,471 = 4,942 kips

$$\Delta P = \frac{(2{,}471 + 2{,}471)20 - (24{,}708 + 24{,}708)}{40} = 1{,}236\ kips$$

Step 3.5: Update the axial load in the columns.

$$P_1 = P - \Delta P$$

$$P_2 = P + \Delta P$$

Where P_1 is the updated axial load in left column and P_p is updated axial load in right column.

P_1 = 1,959 – 1,236 = 723 kips

P_2 = 1,959 + 1,236 = 3,195 kips

Step 3.6: Update the M_n, M_p, and V_p in the columns.

The new plastic moments and shears are determined using P_1 and P_2.

- For P_1 = 723 kips
  M_{n1} = 17,341 kip-ft from interaction curve
  M_{p1} = 1.3(17,341)=22,544 kip-ft
  V_{p1} = 2(22,544)/20 = 2,254 kips
- For P_2 = 3,195 kips
  M_{n2} = 19,477 kip-ft from interaction curve
  M_{p2} = 1.3(19,477) = 25,320 kip-ft
  V_{p2} = 2(25,320)/20 = 2,532 kips

Step 3.7: Calculate the new F_p and ΔP and compare against that in *Step 3.4*.

F_p = 2,254 + 2,532 = 4,786 kips

If F_p in this step is within 5% of that in *Step 3.4*, further iteration is not necessary. Otherwise, repeat *Steps 3.4* to *3.7*.		$\Delta P = \frac{(2{,}254 + 2{,}532)20 - (22{,}544 + 25{,}320)}{40}$ $= 1{,}196\ kips$ Since F_p and ΔP are within 5% of previous, further iteration is not necessary.
Step 3.8: Repeat Steps *3.1* to *3.7* using *P* from *LC2*.		The calculations were started using *P* = 3,040 kips from *LC2* in Table 6-7. The results of the last iteration are: M_{p1} = 24,518 kip-ft V_{p1} = 2,452 kips M_{p2} = 24,931 kip-ft V_{p2} = 2,493 kips F_p = 4,945 kips
Step 3.9: Determine the maximum F_p and the maximum column plastic shear resistance. This is the maximum of the results from *Steps 3.7* and *3.8*. The results will be used to design the column transverse reinforcement and cross-frames.		From the results of *Steps 3.7* and *3.8*: V_p = 2,532 kips (maximum V_p per column) F_p = 4,945 kips (maximum F_p for the pier)
Step 4: Determine the column shear resistance and compare against the plastic shear resistance. The shear resistance can be calculated using the Simplified Procedure described in AASHTO Specifications Art. 5.8.3.4.1. For simplicity and to be conservative, the contribution of concrete to the shear resistance is not included in the calculations. $V_n = \frac{A_v f_y d_v}{s}$ where:		The transverse reinforcement is #8 rebar spaced at 1.75 in. on center. The longitudinal reinforcement is #11 rebar. The concrete cover is 2.0 in. $A_v = 2(0.79) = 1.58\ in^2$ $D_r = 78 - 2 - 2 - 1 - 1 - 1.375 = 70.625\ in$ $d_e = \frac{78}{2} + \frac{70.625}{\pi} = 61.48\ in$ $d_v = 0.9(61.48) = 55.33\ in$

$A_v = 2A_{sh}$ $d_v = 0.9d_e$ $d_e = \frac{D}{2} + \frac{D_r}{\pi}$ A_{sh} = area of one leg of transverse reinforcement; f_y is the yield stress of transverse reinforcement; s is the spacing of transverse reinforcement; D is the diameter of column; D_r is the diameter of the circle passing through the centers of longitudinal reinforcement.		$V_n = \frac{1.58(60)(55.33)}{1.5} = 2{,}997\ kips$ $\phi V_n = 0.9(2{,}997) = 2{,}698\ kips$ The maximum V_p = 2,532 kips per column. The demand-resistance ratio is: $\frac{D}{C} = \frac{2{,}532}{2{,}698} = 0.94\ < 1.0, ok!$
Step 5: Check the transverse reinforcement. The volumetric ratio of transverse reinforcement shall satisfy (AASHTO Specifications Art. 5.10.11.4.1d): $\rho_s \geq 0.12\frac{f_c'}{f_y}$ The spacing of transverse reinforcement shall satisfy (AASHTO Specifications Art. 5.10.11.4.1e): $s \leq \begin{cases} D/4 \\ 4.0 \end{cases}$		ρ_s = 2.5% (#8 @ 1.75 in.) f_y = 60 ksi f'_c = 4 ksi $\rho_s = 0.014 \geq 0.12\left(\frac{4}{60}\right) = 0.008\ \ ok!$ $s = 1.75 \leq \begin{cases} 78/4 = 19.5 \\ 4.0 \end{cases}\ \ ok!$

6.5 Seismic Design of Cross-Frames

For Type 1 design strategy, the inelasticity is to be limited in the columns. The components along the seismic load path such as cross-frames are designed and detailed to remain elastic.

Step 1: Determine the axial force in each of the cross-frame diagonal members. $$P_{XF} = \frac{V_{XF}}{2N\cos\theta} = \frac{F_p}{2N\cos\theta}$$ where F_p is the pier plastic shear resistance, N is the number of panels, and θ is the angle of the diagonal member measured from the horizontal.		F_p = 4,945 kips N = 5 panels θ = 22 degrees $P_{XF} = \frac{4{,}945}{2(5)(\cos 22)} = 533\ kips$
Step 2: Cross-frame member section properties Note that the size of the cross-frames may be governed by slenderness requirements.		Section: *WT9x65* F_y = 50 ksi A_g = 19.2 in^2 r_x = 2.58 in. I_x = 127 in. e = 2.02 in. L = 142.62 in.
Step 3: Calculate the tensile resistance $$\phi P_r = 0.95 F_y A_g$$		$\phi P_r = 0.95(50)(19.2) = 912\ kips > 533\ kips$
Step 4: Calculate the compressive resistance Under seismic loading, the cross-frames are primary members in the transverse direction as they transmit the deck seismic forces to the bearings. The limiting slenderness ratio for primary members is 120 (AASHTO Specifications Art. 6.9.3). The compressive resistance is calculated according to AASHTO Specifications Art. 6.9.2.1, 6.9.4.1.1, and 6.9.4.1.2 $$P_e = \frac{\pi^2 E}{\left(\frac{Kl}{r}\right)^2_{eff}} A_g$$		*Kl* = 1.0(142.62) = 142.62 *Kl/r* = 142.62/2.58 = 55.28 < 120 $P_e = \frac{\pi^2(29{,}000)}{55.28^2}(19.2) = 1{,}798\ kips$

$$P_o = QF_yA_g$$ The slender element reduction factor, *Q*, is equal to 1.0 when: for flanges: $$\frac{b}{2t_f} \leq 0.56\sqrt{\frac{E}{F_y}}$$ for stem: $$\frac{d}{t_w} \leq 0.75\sqrt{\frac{E}{F_y}}$$ ○ If $P_e/P_o \geq 0.44$ $$\phi P_n = 0.9\left[0.658^{(P_o/P_e)}\right]P_o$$ ○ If $P_e/P_o < 0.44$ $$\phi P_n = 0.9(0.877P_e)$$		$$\frac{b}{2t_f} = 4.65 < 0.56\sqrt{\frac{29000}{50}} = 13.5$$ $$\frac{d}{t_w} = 14.4 < 0.75\sqrt{\frac{29000}{50}} = 18.1$$ Therefore, $Q = 1.0$ $$P_o = 1.0(50)(19.2) = 960\ kips$$ $$\frac{P_e}{P_o} = \frac{1,798}{960} = 1.87 \geq 0.44$$ $$\phi P_n = 0.9\left[0.658^{1/1.87}\right](960) = 692\ kips > 533\ kips, ok!$$
Step 5: Calculate the minimum nominal shear resistance of the cross-frames and check against V_p of column. $$V_{XF\_min} = (2P_n)N\cos\theta$$ In this equation, only the compression resistance, P_n, is used to determine the minimum nominal shear resistance. Note that P_n is smaller than the tension resistance, P_r, which means buckling would occur first in any of the diagonal members before yielding is reached. Thus, V_{XF} is the minimum shear force before inelasticity starts to occur in the cross-frames. Since this is Type 1 design – inelasticity is accommodated in the columns only – V_p should be less than V_{XF}.		$$V_{XF\_min} = 2\left(\frac{692}{0.9}\right)5\cos 22 = 7,129\ kips > F_p = 4,945\ kips, ok!$$ As can be seen above, the slenderness ratio is the governing parameter in the design of elastic support cross-frames.

6.6 Cross-Frame Properties for Nonlinear Analysis

The expected force and displacement resistance of the cross-frames are calculated for use in the design evaluation.

Step 1: Calculate the expected tensile yield and displacement resistance. The expected yield resistance is: $$P_{ye} = F_{ye}A_g$$ where F_{ye} is the expected yield stress and is equal to R_yF_y. For WT section with A992 Gr 50, R_y = 1.1. The effective axial stiffness is: $$K_{XF\_e} = \frac{EA_e}{L}$$ where E is the modulus of elasticity of steel which is 29,000 ksi, A_e is the effective area calculated using Eqn. (1-12), and L is the total length of the diagonal member. The expected yield displacement is then calculated as: $$\Delta_{ye} = \frac{P_{ye}}{K_{XF\_e}}$$		*WT9x65* F_{ye} = 1.1(50) = 55 ksi A_g = 19.2 in^2 I_x = 127 in^4 e = 2.02 in. distance from connected flange of WT to its c.g. $P_{ye} = 55(19.2) = 1{,}056\ kips$ $A_e = \frac{19.2(127)}{127 + 19.2(2.03)^2} = 11.83\ in^2$ $K_{XF\_e} = \frac{29{,}000(11.83)}{142.62} = 2{,}405.47\ kip/in$ $\Delta_{ye} = \frac{1{,}056}{2{,}405.47} = 0.44\ in$

Step 2: Calculate the expected compressive resistance and associated displacement. The $(Kl/r)_{eff}$ and P_e is the same as that calculated in Section 5.5 *Step 4*. The expected yield strength is used to calculate P_o. $$P_o = QF_{ye}A_g$$ The expected compressive resistance is then calculated as: ○ If $P_e/P_o \geq 0.44$ $$P_{nc} = \left[0.658^{(P_o/P_e)}\right]P_o$$ ○ If $P_e/P_o < 0.44$ $$P_{nc} = 0.877P_e$$ The corresponding displacement is: $$\Delta_{nc} = \frac{P_{nc}}{K_{XF\_e}}$$		$P_o = 55(19.2) = 1{,}056\ kips$ $\frac{P_e}{P_o} = \frac{1{,}798}{1{,}056} = 1.70 < 0.44$ $P_n = \left[0.658^{1/1.70}\right](1{,}056) = 826\ kips$ $\Delta_{nc} = \frac{826}{2{,}405.47} = 0.34\ in.$

6.7 Design Summary

The total weight of Ex. II-1b is 4,573 kips. From modal and response spectrum analyses, the periods, forces, and displacements are:

Parameter	Longitudinal Direction	Transverse Direction
Fundamental period, T (sec)	0.51	0.35
Base shear, V_b (kip)	5,722	6,681
Column displacement demand, Δ_{col} (in)	2.0	0.9
Column shear demand, V_{col} (kip)	989	1,670
Pier base shear demand, F_b (kip)	196	3,340
Deck displacement demand, Δ_{deck} (in)	2.97	0.97

The column properties are:

Diameter, D	6.5 ft
Longitudinal reinforcement	72 - #11 (ρ_l = 2.4%)
Transverse reinforcement	#8 @ 1.75 in. (ρ_s = 2.5%)
Effective moment of inertia, I_e	$0.54I_g$
Column plastic shear resistance, V_p	2,543 kips
Pier plastic shear resistance, F_p	4,945 kips

The cross-frame diagonal member section properties are:

Section	WT9x65
Area, A	19.2 in^2
Tensile resistance, ϕP_r	912 kips
Compressive resistance, ϕP_n	692 kips
Min. nominal shear resistance, V_{XF_min}	7,129 kips
Expected tensile yield resistance, P_{ye}	1,056 kips
Expected compressive resistance, P_{nc}	826 kips

6.8 Nonlinear Evaluation

Example II-1b was analyzed using the ground motions described in Section 1.8.1. The ground motions were scaled to represent the Design (DE) and MCE Earthquake levels. There were seven DE runs and seven MCE runs for a total of fourteen runs. Because of this, only the column force-displacement plots from DE1, DE7, MCE1 and MCE7 are shown in Figure 6-5 and Figure 6-6 to represent the results. However, the column ductility ratios for all runs are shown in Figure 6-7. Nonlinearity was not observed in the support cross-frames.

The yield displacements were calculated according to Section 1.8.2. Since the expected material properties were used in the nonlinear analyses, the yield displacements were also calculated using these properties. The yield displacements are 1.17 in. and 0.53 in. in the longitudinal and transverse directions, respectively.

In the longitudinal direction, the average ductility ratios were 1.6 from DE runs and 1.9 from MCE runs. In the transverse direction, the respective ductility ratios were 2.0 and 2.9. The smaller ductility in the longitudinal direction is due to the contribution of abutment soil in the response. The column response in this direction is single-curvature resulting in yield displacement that is more than three times the yield displacement in transverse direction. Thus, the ductility demand in the transverse direction is larger even though the displacements in both directions are about the same. Yielding is apparent in the hysteresis loops in the transverse direction, particularly at MCE.

The average of total bearing forces in the transverse direction were 3,372 kips under DE and 4,019 kips under MCE. These are smaller than the minimum nominal resistance of the cross-frames shown in Section 6.7 thus the cross-frames were elastic. The average of pier base shear forces in the transverse direction were 3,826 kips under DE and 4,616 kips under MCE. Thus, for this bridge, the inertia force in the pier cap is about 12% of the pier base shear.

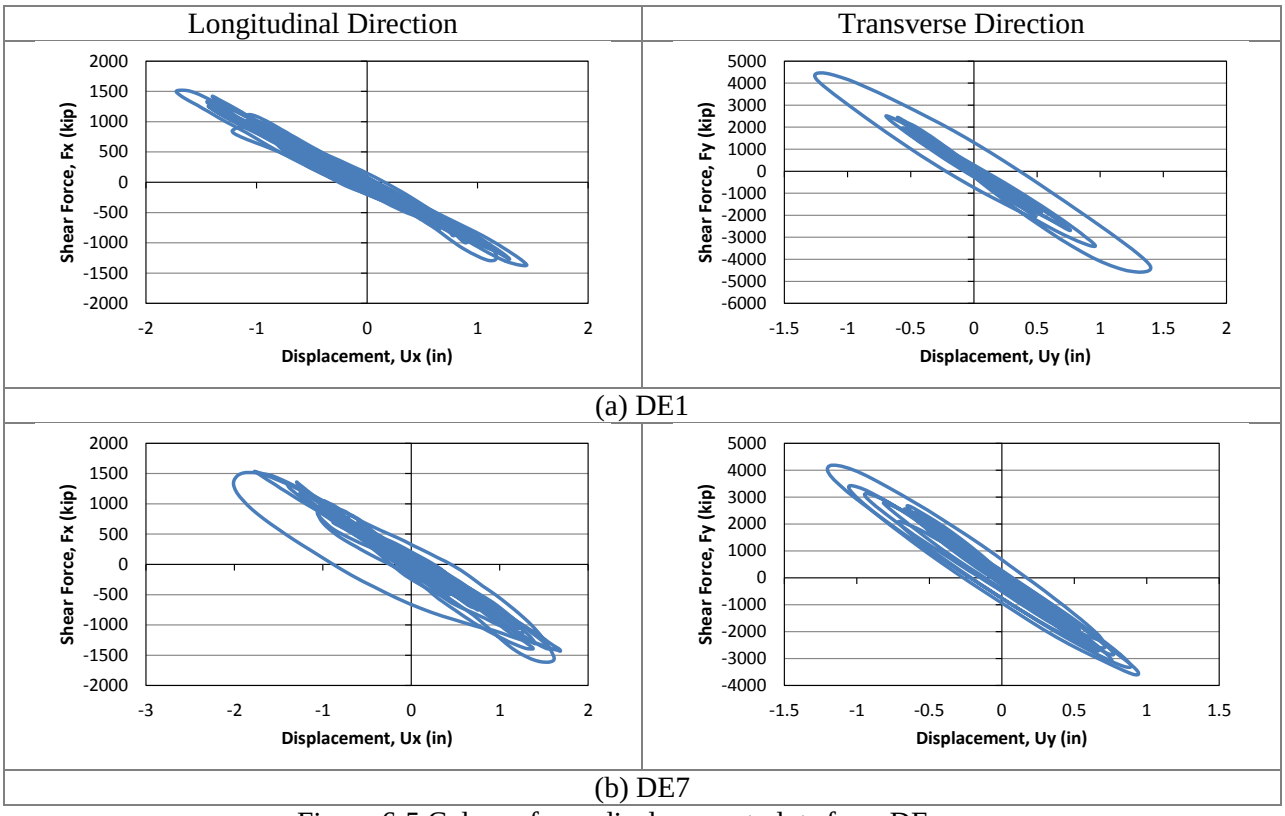

Figure 6-5 Column force-displacement plots from DE runs

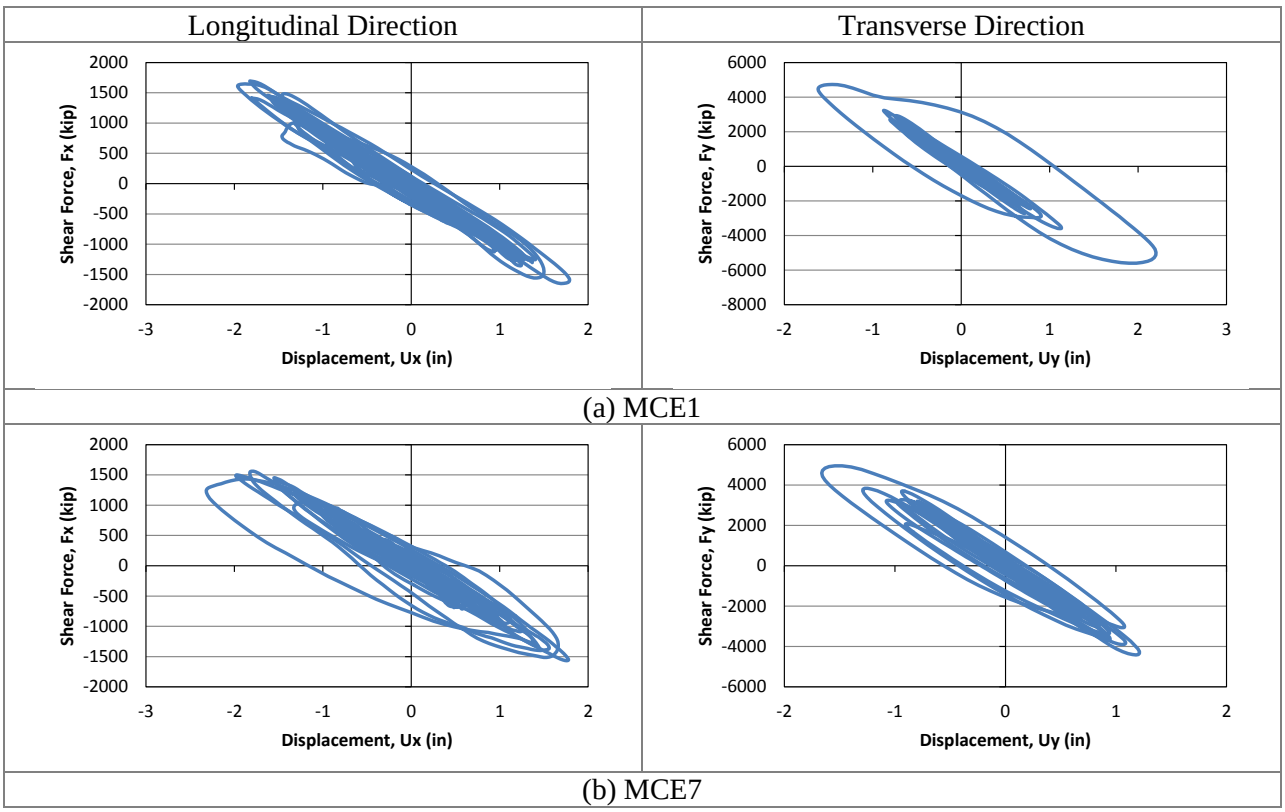

Figure 6-6 Column force-displacement plots from MCE runs

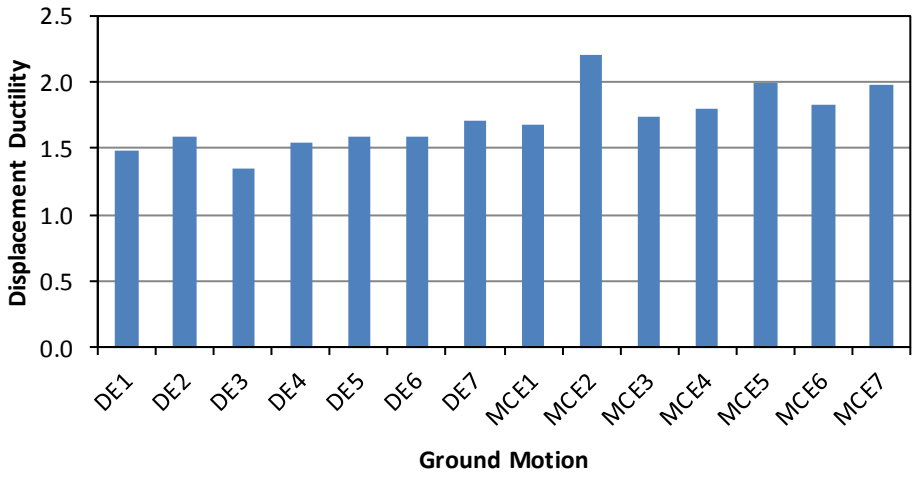

(a) ductility ratios in the longitudinal direction

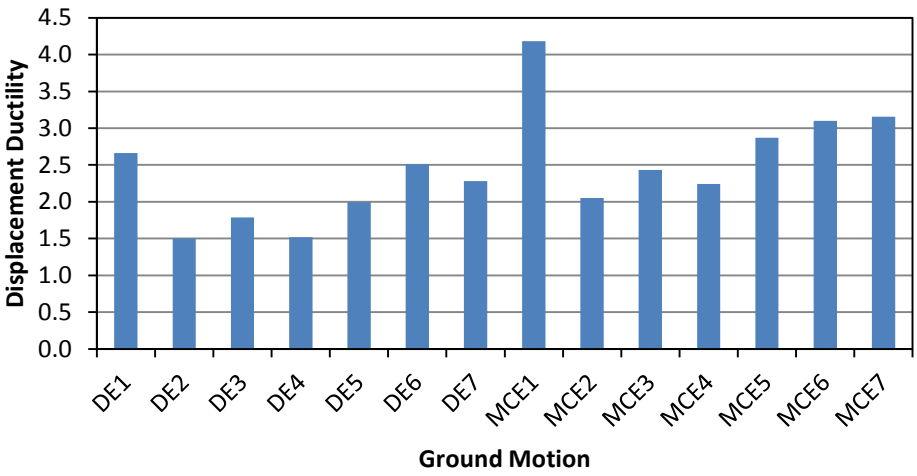

(b) ductility ratios in the transverse direction

Figure 6-7 Summary of column Displacement ductility

Chapter 7 Bridge with Two-Column Piers Designed using Type 2 Strategy (Example II-2)

7.1 Bridge Description

The overall geometry of Ex. II-2 is described in Section 1.3.2. From the final design iteration, the reinforced concrete (R/C) column diameter is 5 ft-6in. with 2.8% longitudinal steel ratio and 2.6% transverse steel ratio. The rectangular pier cap is 6 ft-6in. wide and 5 ft-6 in. deep. The pier cap is 60 ft long and the center-to-center distance between the columns is 40 ft. Figure 7-1 shows the elevation at piers. The cross-frames are of X-type pattern with diagonal members made of L4x4x1/2 single angles while the top and bottom chords are 2L2x2x1/4 double angles.

7.2 Computational Model

The computational model is shown in Figure 7-2. The equivalent concrete section properties of superstructure are summarized in Table 7-1. Local axes of the superstructure are shown in Figure 7-1. Deck cracking was accounted for in the calculation of these properties by using 50% of the gross concrete modulus of elasticity (E_c).

For elastic analysis, only one of the diagonal members of the cross-frames is included in the model as shown in Figure 7-2b. This is because the cross-frames are designed and detailed to yield and buckle under the design earthquake. Under transverse loading, in each cross-frame panel, one diagonal is under tension and the other is in compression. Consequently, the diagonal in compression would buckle and its stiffness becomes essentially zero.

For nonlinear response history analysis, the cross-frames were modeled with multi-linear plastic link elements with force-deformation relationship shown in Figure 1-5. The two cross-frame diagonal members are modeled because buckling is accounted for in the definition of link force-deformation relationship. Calculation of expected force and deformations are shown in Sections 7.5 and 7.6.

Table 7-1 Ex.II-1 superstructure section properties

Area, A (in^2)	16,195
Moment of inertia about horizontal axis, I_2 (in^4)	10,316,084
Moment of inertia about vertical axis, I_3 (in^4)	8.22×10^8
Torsional constant, J (in^4)	285,124

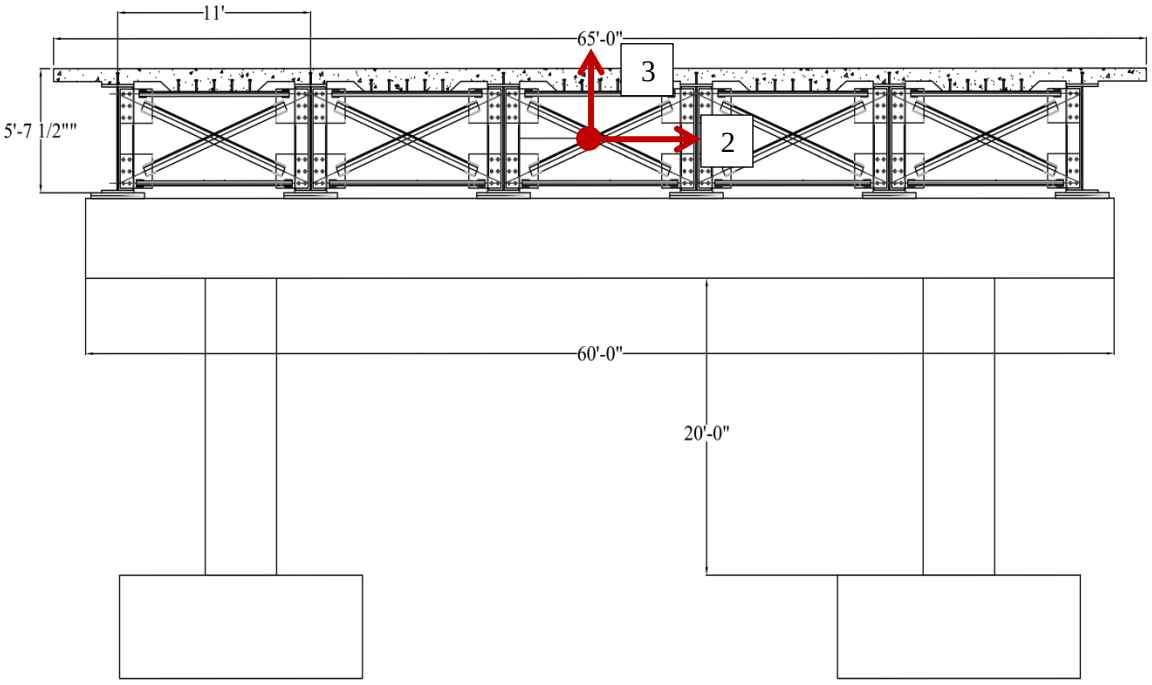

Figure 7-1 Elevation at pier of Ex. II-2

7.3 Analysis

7.3.1 Gravity Loads – DC and DW

The total *DC* load (i.e. total bridge dead load) is 3,933 kips and the total *DW* load is 844 kips. The reactions at the base of each column due to these loads are 904 kips and 166 kips, respectively. These loads were used to calculate the effective section properties of the columns, as illustrated in Section 7.3.2 Steps *1* and *2*.

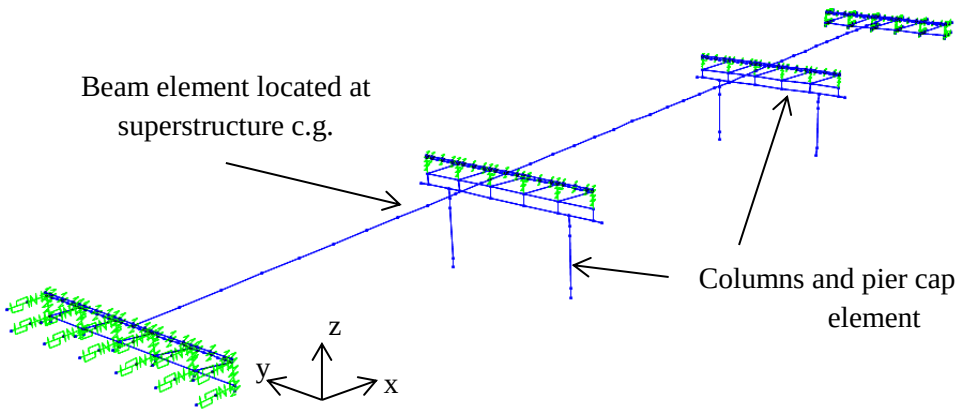

(a) 3D view of model

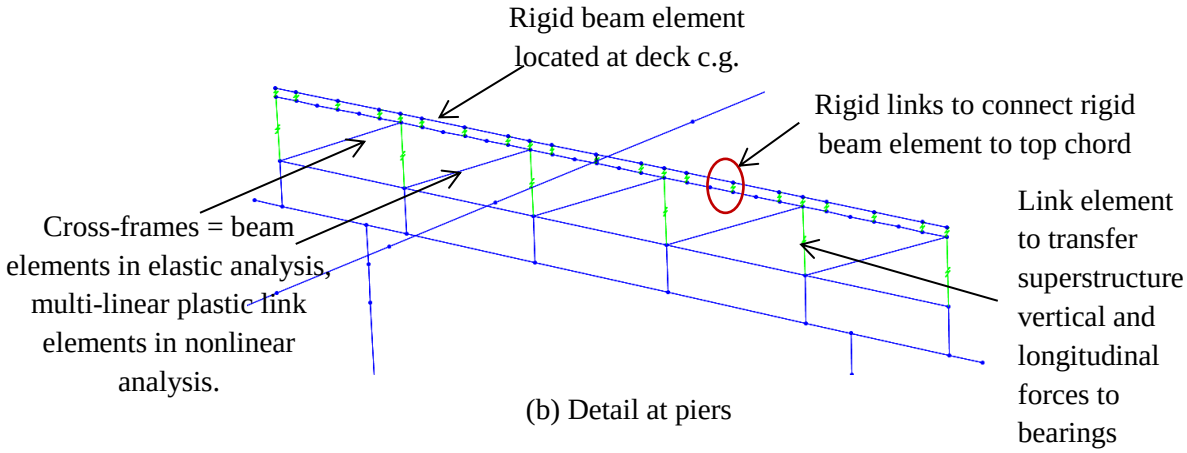

(b) Detail at piers

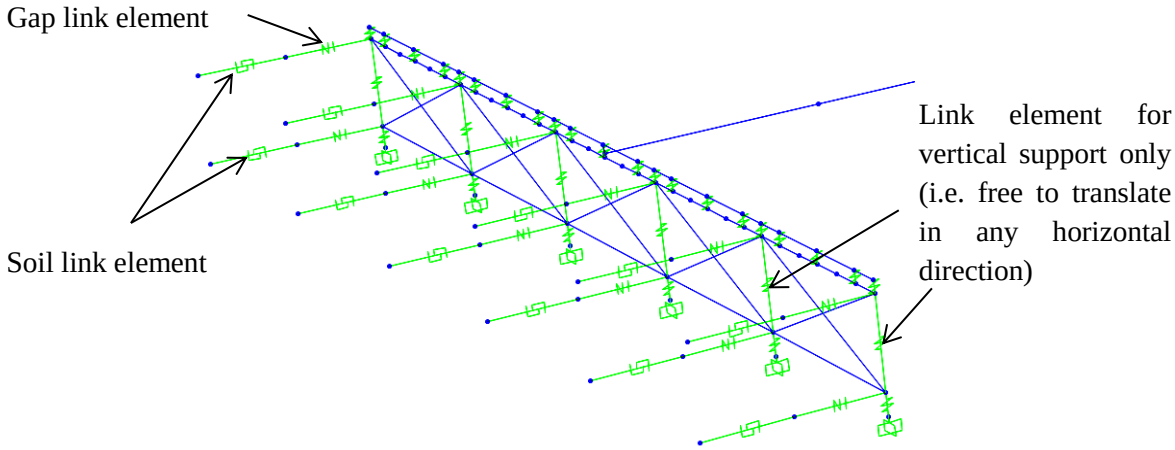

(c) Detail at abutments

Figure 7-2 Analytical model of Ex. II-2

7.3.2 Earthquake Loads – EQ

Step 1: Calculate column axial loads due to gravity loads, P_{col}. This will be used to determine the effective moment of inertia, I_e, of columns. $$P_{col} = 1.25P_{DC} + 1.5P_{DW}$$		$$P_{col} = 1.25(904) + 1.5(166) = 1{,}379\ kips$$
Step 2: Determine effective moment of inertia, I_e. This is accomplished through section analysis of the column. The required parameters are: column diameter, longitudinal and transverse reinforcements, axial load, and material properties of concrete and steel reinforcement. The calculated I_e is assigned to the beam elements representing the column in the model.		The following are the column properties: D = 5.5 ft ρ_l = 2.8% (66 - #11) ρ_s = 2.6% (#8 @ 2.0 in.) f'_c = 4 ksi f_y = 60 ksi P_{col} = 1,379 kips From section analysis: I_e/I_g = 0.57
Step 3: Estimate soil displacement, Δ_{soil}, and calculate the effective abutment stiffness, K_e. The joint gap is included in the calculation of this stiffness, as shown in the figure below. 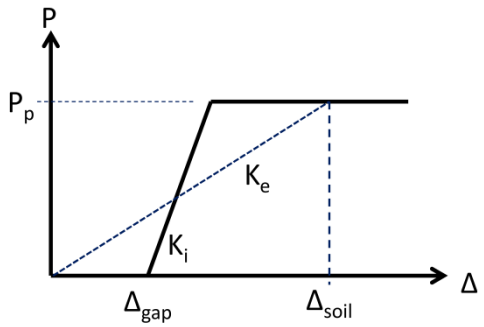 Figure 7-3 Abutment force-displacement The soil passive resistance, P_p, and initial soil stiffness, K_i, are calculated based on the recommended values in Caltrans SDC. $$P_p = 5.0A_e(h/5.5)\ \ (kips)$$ $$K_i = 50w(h/5.5)\ \ (kip/in)$$ where A_e (ft^2) is the effective backwall area, h (ft) is the backwall height, and w is the backwall		Δ_{soil} = 3.3 in. $$P_p = 5.0(5.625x65)(5.625/5.5) = 1{,}870\ kips$$ $$K_i = 50(65)(5.625/5.5) = 3{,}324\ kip/in$$ Check Δ_{soil} against Δ_{gap} + Δ_y to determine if the soil is yielding. $$\Delta_{gap} + \Delta_y = 2 + \frac{1{,}870}{3{,}324} = 2 + 0.56 = 2.56\ in$$ Since this is smaller than Δ_{soil}, the soil is yielding and the effective stiffness is: $$K_e = \frac{1{,}870}{3.3} = 566.67\ kip/in$$ $$1/2K_e = 283.33\ kip/in$$

width.

Under *EQ* in longitudinal direction, only one abutment is engaged in one direction. To account for this in elastic analyses such as modal and response spectrum analysis, half of K_e is applied to both abutments.

This $1/2K_e$ is then distributed to the link elements representing the soil. The gap link elements shown in Figure 7-2c were assigned with high stiffness with no opening during elastic analysis.

Since there are 12 soil springs at each abutment, the effective stiffness assigned to each is:

$(1/2K_e)/12 = 23.61\ kip/in$

Step 4: Perform modal analysis and determine the required number of modes needed for multimode spectral analysis.

After the effective stiffnesses of the elements are determined, modal analysis is performed to determine the fundamental vibration periods and the required number of modes needed in the response spectrum analysis. The AASHTO Specifications requires that the total number of modes used should ensure participation of at least 90% of the total bridge mass.

Table 7-2 shows the result of modal analysis. Although only the first 5 modes are shown in this table, a total of 30 modes were used in the response spectrum analysis with total mass participation of 100% in both the longitudinal and transverse directions.

The first mode with period of 0.64 sec is in-plane deck rotation; the second with period of 0.61 sec is the longitudinal translation mode; the third with period of 0.57 sec is the vertical vibration mode; and the fourth with period of 0.48 sec is the longitudinal translation mode.

The vibration periods in this example are shorter than those in Ex. II-1 because of larger columns.

Table 7-2 Modal periods and mass participation

Mode No	Period Sec	Mass Participation x-dir	Mass Participation y-dir
1	0.64	0.000	0.000
2	0.61	0.967	0.000
3	0.57	0.000	0.000
4	0.48	0.000	0.887
5	0.34	0.000	0.000

Step 5: Perform response spectrum analysis in the longitudinal direction (EQ_x), determine Δ_{soil}, and check against the initial value in *Step 3*.

The design spectrum is applied in the longitudinal direction. Multimode spectral analysis is used and the modal responses are combined using the Complete Quadratic Combination (CQC).

From response spectrum analysis, Δ_{soil} = 3.26 in. This is within 5% of the assumed displacement in *Step 3*, thus no further iteration is needed.

Step 6: Obtain the column forces due to EQ_x.

These forces will be used to design the columns.

Table 7-3 Column forces due to EQ_x

Load	P (kip)	M_x (k-ft)	M_y (k-ft)
EQ_x	0	0	16,526

The seismic base shear in the longitudinal direction is 4,351 kips.

Step 7: Obtain the column forces due to EQ_y.

Table 7-4 Column forces due to EQ_y

Load	P (kip)	M_x (k-ft)	M_y (k-ft)
EQ_y	1,376	14,173	0

The seismic base shear of the bridge in the transverse direction is 5,569 kips.

7.3.3 Design Loads

A proposed *R* factor of 1.5 is applied to column moments from earthquake analysis. The forces based on Extreme Event I load combination is shown in Table 7-5.

Table 7-5 Design loads for columns

Load/Combination	P (kip)	M_x (k-ft)	M_y (k-ft)
DC	904	0	0
DW	166	0	0
EQ_x	16	0	16,526
EQ_y	1,376	14,173	0
EQ_1: $1.0EQ_x + 0.3EQ_y$	429	4,252	16,526
EQ_2: $0.3EQ_x + 1.0EQ_y$	1,381	14,173	4,958
EQ_1/R	429	2,835	11,017
EQ_2/R	1,381	9,449	3,305
LC1: $1.25DC + 1.5DW + 1.0EQ_1$	1,808	2,835	11,017
LC1: $1.25DC + 1.5DW + 1.0EQ_2$	2,760	9,449	3,305

7.4 Design of Columns

Step 1: Determine the design axial load and resultant moment from Section 7.3.3.

Table 7-6 Design axial load and resultant moment

Load Combination	P (kip)	M_{res} (kip-ft)
LC1	1,808	11,376
LC2	2,760	10,010

Step 2: Develop the axial force-moment (P-M) interaction curve and check if the design loads are inside the P-M curve.

The AASHTO ϕ factors are used in the interaction curve.

From the final iteration the column properties are:

D = 5.5 ft
ρ_l = 2.8% (61 - #11)
ρ_s = 2.6% (#8 @ 2.0 in.)
f'_c = 4 ksi
f_y = 60 ksi

The design loads are within the boundaries of P-M interaction curve as shown below. Thus, the selected column size and reinforcement are adequate.

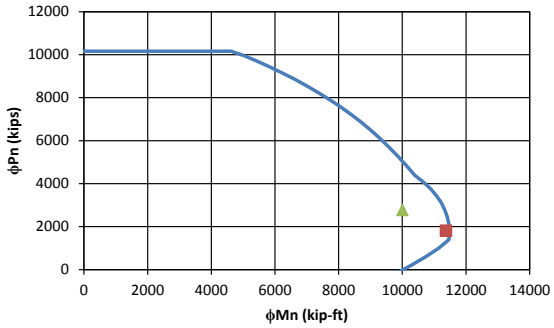

Step 3: Determine the plastic shear resistance, F_p, of the piers in transverse direction

The plastic moment resistance, M_p, of column is a function of its axial load. In multi-column pier, due to frame action, there is variation in column axial loads resulting in different plastic moment capacities. Calculation of F_p is therefore an iterative process. The calculation of F_p is outlined in the procedure below.

Step 3.1: Start the calculation process by using the column axial load, *P*, obtained from *LC1*.

From Table 7-6, P = 1,808 kips.

Since this P was from response spectrum analysis, both columns of the pier have the same P.

Step 3.2: Based on this *P*, determine M_n from the interaction curve.

By interpolating on the points of the interaction curve, M_n = 12,751 kip-ft for P = 1,808 kips.

Step 3.3: Determine M_p and V_p.

$$M_p = 1.3M_n$$

M_p = 1.3(12,751) = 16,576 kip-ft

where the 1.3 factor is to account for column overstrength.

$$V_p = \frac{2M_p}{H}$$

V_p = 2(16,576)/20 = 1,658 kips

where H is the column clear height. This equation is based on double-curvature behavior. This behavior is typically assumed for a multi-column pier because the cap beam is much stiffer than the columns.

Step 3.4: Calculate F_p and ΔP.

The following equations are based on the free-body diagram for a two-column pier shown in Figure 7-4.

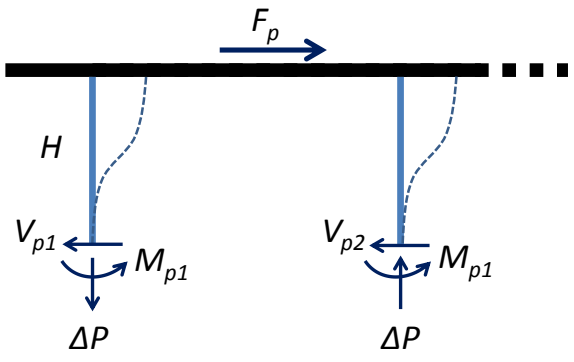

Figure 7-4 Forces in a two-column pier

$$F_p = V_{p1} + V_{p2}$$ $$\Delta P = \frac{(V_{p1} + V_{p2})H - (M_{p1} + M_{p2})}{L}$$ where L is the distance between the two columns.		F_p = 1,658 + 1,658 = 3,316 kips $$\Delta P = \frac{(1{,}658 + 1{,}658)20 - (16{,}576 + 16{,}576)}{40} = 829\ kips$$
Step 3.5: Update the axial load in the columns. $$P_1 = P - \Delta P$$ $$P_2 = P + \Delta P$$ Where P_1 is the updated axial load in left column and P_p is updated axial load in right column.		P_1 = 1,808 – 829 = 979 kips P_2 = 1,808 + 829 = 2,637 kips
Step 3.6: Update the M_n, M_p, and V_p in the columns. The new plastic moments and shears are determined using P_1 and P_2.		• For P_1 = 979 kips M_{n1} = 12,366 kip-ft from interaction curve M_{p1} = 1.3(12,366) = 16,076 kip-ft V_{p1} = 2(16,076)/20 = 1,608 kips • For P_2 = 2,637 kips M_{n2} = 12,631 kip-ft from interaction curve M_{p2} = 1.3(12,631) = 16,420 kip-ft V_{p2} = 2(17,268)/20 = 1,642 kips
Step 3.7: Calculate the new F_p and ΔP and compare against that in *Step 3.4*. If F_p in this step is within 5% of that in *Step 3.4*, further iteration is not necessary. Otherwise, repeat *Steps 3.4* to *3.7*.		F_p = 1,608 + 1,642 = 3,250 kips $$\Delta P = \frac{(1{,}608 + 1{,}642)20 - (16{,}076 + 16{,}420)}{40} = 812\ kips$$ Since F_p and ΔP are within 5% of previous, further iteration is not necessary.
Step 3.8: Repeat Steps *3.1* to *3.7* using P from *LC2*.		The calculations were started using P = 2,760 kips from *LC2* in Table 6-6. The results of the last iteration are: M_{p1} = 16,567 kip-ft

		V_{p1} = 1,657 kips M_{p2} = 15,876 kip-ft V_{p2} = 1,588 kips F_p = 3,245 kips
Step 3.9: Determine the maximum F_p and the maximum column plastic shear resistance. This is the maximum of the results from *Steps 3.7* and *3.8*. The results will be used to design the column transverse reinforcement and cross-frames.		From the results of *Steps 3.7* and *3.8*: V_p = 1,657 kips (maximum V_p per column) F_p = 3,250 kips (maximum F_p for the pier)
Step 4: Determine the column shear resistance and compare against the plastic shear resistance. The shear resistance can be calculated using the Simplified Procedure described in AASHTO Specifications Art. 5.8.3.4.1. For simplicity and to be conservative, the contribution of concrete to the shear resistance is not included in the calculations. $$V_n = \frac{A_v f_y d_v}{s}$$ where: $A_v = 2A_{sh}$ $d_v = 0.9d_e$ $d_e = \frac{D}{2} + \frac{D_r}{\pi}$ A_{sh} = area of one leg of transverse reinforcement; f_y is the yield stress of transverse reinforcement; s is the spacing of transverse reinforcement; D is the diameter of column; D_r is the diameter of the circle passing through the centers of longitudinal reinforcement.		The transverse reinforcement is #8 rebar spaced at 2.0 in. on center. The longitudinal reinforcement is #11 rebar. The concrete cover is 2.0 in. $A_v = 2(0.79) = 1.58\ in^2$ $D_r = 66 - 2 - 2 - 0.75 - 0.75 - 1.375$ $= 59.125\ in$ $d_e = \frac{66}{2} + \frac{59.125}{\pi} = 51.82\ in$ $d_v = 0.9(51.82) = 46.64\ in$ $V_n = \frac{1.58(60)(46.64)}{2} = 2{,}211\ kips$ $\phi V_n = 0.9(2{,}211) = 1{,}990\ kips$ The maximum V_p = 1,657 kips per column. The demand-resistance ratio is: $\frac{D}{C} = \frac{1{,}657}{1{,}990} = 0.83 < 1.0, ok!$

Step 5: Check the transverse reinforcement. The volumetric ratio of transverse reinforcement shall satisfy (AASHTO Specifications Art. 5.10.11.4.1d): $$\rho_s \geq 0.12\frac{f_c'}{f_y}$$ The spacing of transverse reinforcement shall satisfy (AASHTO Specifications Art. 5.10.11.4.1e): $$s \leq \begin{cases} D/4 \\ 4.0 \end{cases}$$		ρ_s = 2.6% (#8 @ 2.0 in.) f_y = 60 ksi f'_c = 4 ksi $\rho_s = 0.026 \geq 0.12\left(\frac{4}{60}\right) = 0.008 \quad ok!$ $s = 2.0 \leq \begin{cases} 66/4 = 16.5 \\ 4.0 \end{cases} \quad ok!$

7.5 Design of Ductile Cross-Frames

In the proposed Type 2 seismic design, the cross-frames are designed such that their resistance is less than the column nominal shear resistance in the transverse direction so the inelasticity will be limited to the cross-frames in that direction.

Step 1: Determine cross-frame force based on nominal shear resistance of the pier. The cross-frame shear force is equal to nominal shear resistance of pier in the transverse direction. $$V_{XF} = F_n = \frac{F_p}{1.3}$$ where F_p is the pier plastic shear resistance. The corresponding cross-frame diagonal member axial force with *R* factor applied is: $$P_{XF1} = \frac{V_{XF}}{RN\cos\theta}$$ where *N* is the number of panels, θ is the angle of the diagonal from the horizontal, and *R* is the cross-frame modification factor and is equal to 4.0. In this equation, only one diagonal is assumed resisting the shear force. This is because, in a panel, one diagonal is in tension and the other one is in compression. The compression diagonal is expected to buckle in which case its post-buckling resistance is considerably smaller, thus the resistance is largely due to the yield resistance of the diagonal in tension.		F_p = 3,250 kips $N = 5$ $\theta = 22^o$ $V_{XF} = \frac{3{,}250}{1.3} = 2{,}500\ kips$ $P_{XF1} = \frac{2{,}500}{4(5)\cos 22} = 135\ kips$
Step 2: Determine the cross-frame force from response spectrum analysis in the transverse direction. $$P_{XF2} = \frac{P_{EQY}}{R}$$		$P_{XF2} = \frac{569}{4} = 142\ kips$
Step 3: The design cross-frame force is the smaller of P_{XF1} or P_{XF2}.		P_{XF} = 135 kips
Step 4: Determine cross-frame size. The required area is:		A36 single angle F_y = 36 ksi

$$A = \frac{P_{XF}}{F_y}$$ where F_y is the nominal yield stress of the cross-frame. The nominal value is used since P_{XF} was calculated from nominal shear force. Note that the size of the cross-frame may be governed by the compactness and slenderness requirements shown in *Step 5*.		$A = \frac{135}{36} = 3.76\ in^2$ Use *L4x4x1/2* A_g = 3.75 in^2 r_z = 0.776 in I = 5.52 in^4 x = 1.18 in. distance from connected leg of angle to its c.g. L = 142.62 in
Step 5: Check the compactness and slenderness ratios. The diagonal members of ductile cross-frames shall satisfy (proposed AASHTO Specifications Art. 6.16.4.5.2a): $$\frac{b}{t} \le 0.3\sqrt{\frac{E}{F_y}}$$ The slenderness ratio shall satisfy (proposed AASHTO Specifications Art. 6.16.4.5.2b): $$\frac{Kl}{r} \le 4.0\sqrt{\frac{E}{F_y}}$$ where K is 0.85, l is taken as one-half of the length of the diagonal member due to biased buckling, r is the radius of gyration normal to the plane of buckling and is equal to r_z for single angle members.		$$\frac{4}{1/2} = 8.0 \le 0.3\sqrt{\frac{29{,}000}{36}} = 8.51, \quad ok!$$ $$\frac{0.85(142.62/2)}{0.776} = 78.11 \le 4\sqrt{\frac{29{,}000}{36}} = 113.53, \quad ok!$$
Step 6: Calculate the expected yield resistance. $$P_{ye} = F_{ye}A_g$$ where F_{ye} is the expected yield stress and is equal to R_yF_y. For A36 steel sections, R_y = 1.5.		F_{ye} = 1.5(36) = 54 ksi $P_{ye} = (54)(3.75) = 202.5\ kips$
Step 7: Calculate the expected compressive resistance. The compressive resistance is calculated		

according to AASHTO Specifications Art. 6.9.2.1, 6.9.4.1.1, and 6.9.4.1.2 $$P_e = \frac{\pi^2 E}{\left(\frac{Kl}{r_z}\right)^2} A_g$$ $$P_o = F_{ye} A_g$$ ○ If $P_e/P_o \geq 0.44$ $$P_{nc} = \left[0.658^{(P_o/P_e)}\right] P_o$$ ○ If $P_e/P_o < 0.44$ $$P_{nc} = 0.877 P_e$$		$$P_e = \frac{\pi^2(29{,}000)}{(78.11)^2}(3.75) = 175.92\ kips$$ $$P_o = 54(3.75) = 202.5\ kips$$ $$\frac{P_e}{P_o} = \frac{175.92}{202.5} = 0.869 > 0.44$$ $$P_{nc} = \left[0.658^{(1/0.869)}\right](202.5) = 125.10\ kips$$
Step 8: Calculate the maximum expected lateral resistance of the cross-frames and compare against the pier nominal shear resistance. The maximum lateral resistance is the maximum of: $$V_{lat1} = (P_t + 0.3P_{nc}) N \cos\theta$$ $$V_{lat2} = 2P_{nc} N \cos\theta$$ where P_t = $1.2P_{ye}$ is the tensile resistance of the diagonal member. The 1.5 factor is to account for the upper bound of tensile resistance. The $0.3P_{nc}$ is the post-buckling resistance of the diagonal member. V_{lat1} typically governs particularly with relatively slender diagonal members. V_{lat2} may govern in cases when the diagonal members are short and stocky. The cross-frame maximum lateral resistance is compared against the pier nominal shear resistance to ensure elastic columns.		$$P_t = 1.2(202.5) = 243\ kips$$ $$V_{lat1} = [243 + 0.3(125.10)]5\cos 22 = 1{,}301\ kips$$ $$V_{lat2} = [2(125.10)]5\cos 22 = 1{,}159.91\ kips$$ Therefore, V_{lat} = 1,301 kips $$V_{lat} = 1{,}301\ kips < F_p/1.3 = 3{,}250/1.3 = 2{,}500\ kips \quad ok!$$
***Step 9*:** Determine the superstructure drift and check against limit. After the cross-frame designed, the superstructure drift is determined. The superstructure lateral displacement is calculated using the equation:		$$A_e = \frac{3.75(5.52)}{5.52 + 3.75(1.18)^2} = 1.93\ in^2$$

$$\Delta_{lat} = \frac{P_{EQY} L}{E A_e \cos\theta}$$ where, P_{EQY} is the force in the cross-frame diagonal member determined from response spectrum analysis in the transverse direction and A_e is the effective area calculated using Eqn. (1-12). The superstructure lateral drift should not exceed 4% (proposed AASHTO Specification Art. 6.16.4.5.1).		$$\Delta_{lat} = \frac{568.86(142.62)}{29{,}000(1.93)\cos 22} = 1.56\ in.$$ $$Drift = \frac{1.56}{54} = 2.9\% < 4\%, ok!$$

7.6 Cross-Frame Properties for Nonlinear Analysis

The expected force and displacement resistance of the cross-frames are calculated for use in the design evaluation.

Step 1: Calculate the expected tensile yield displacement. The expected yield resistance is calculated in Section 7.5 *Step 6*. The effective axial stiffness is: $$K_{XF\_e} = \frac{E A_e}{L}$$ where E is the modulus of elasticity of steel which is 29,000 ksi, A_e is the effective area calculated using Eqn. (1-12), and L is the total length of the diagonal member. The expected yield displacement is then calculated as: $$\Delta_{ye} = \frac{P_{ye}}{K_{XF\_e}}$$		*L4x4x1/2* P_{ye} = 202.5 kips A_g = 3.75 in^2 I = 5.52 in^4 x = 1.18 in. distance from connected leg of angle to its c.g. $$A_e = \frac{3.75(5.52)}{5.52 + 3.75(1.18)^2} = 1.93\ in^2$$ $$K_{XF\_e} = \frac{29{,}000(1.93)}{142.62} = 391.85\ kip/in$$ $$\Delta_{ye} = \frac{202.5}{391.85} = 0.52\ in$$
Step 2: Calculate the expected compressive displacement. The expected compressive resistance is calculated in Section 7.5 *Step 7*.		P_{nc} = 125.10 kips

The corresponding displacement is: $\Delta_{nc} = \frac{P_{nc}}{K_{XF\_e}}$		$\Delta_{nc} = \frac{125.10}{391.85} = 0.32\ in.$

7.7 Design Summary

The total weight of Ex. II-2 is 4,340 kips. From modal and response spectrum analyses, the periods, forces, and displacements are:

Parameter	Longitudinal Direction	Transverse Direction
Fundamental period, T (sec)	0.61	0.48
Base shear, V_b (kip)	4,351	5,569
Column displacement demand, Δ_{col} (in)	2.2	1.0
Column shear demand, V_{col} (kip)	660	1,387
Pier base shear demand, F_b (kip)	1,320	2,774
Deck displacement demand, Δ_{deck} (in)	3.35	2.25

The column properties are:

Diameter, D	5.5 ft
Longitudinal reinforcement	61 - #11 (ρ_l = 2.8%)
Transverse reinforcement	#8 @ 2 in. (ρ_s = 2.6%)
Effective moment of inertia, I_e	$0.57I_g$
Column plastic shear resistance, V_p	1,657 kips
Pier plastic shear resistance, F_p	3,250 kips

The cross-frame diagonal member section properties are:

Section	L4x4x1/2 (A36)
Area, A_g	3.75 in^2
Slenderness ratio, KL/r	78.11
Width-thickness ratio, b/t	8.0
Expected tensile yield resistance, P_{ye}	202.5 kips
Expected compressive resistance, P_{nc}	125.10 kips
Lateral resistance of cross-frames, V_{lat}	1,301 kips

7.8 Nonlinear Evaluation

Example II-2 was analyzed using the ground motions described in Section 1.8.1. The ground motions were scaled to represent the Design (DE) and MCE Earthquake levels. There were seven DE runs and seven MCE runs for a total of fourteen runs. Because of this, only the column force-displacement plots from DE1, DE7, MCE1 and MCE7 are shown in Figure 7-5 and Figure 7-6 to represent the results. However, the column ductility ratios for all runs are shown in Figure 7-7.

The yield displacements were calculated according to Section 1.8.2. Since the expected material properties were used in the nonlinear analyses, the yield displacements were also calculated using these properties. The yield displacements are 1.47 in. and 0.66 in. in the longitudinal and transverse directions, respectively.

In the longitudinal direction, the average ductility ratios were 1.6 from DE runs and 1.9 from MCE runs. In the transverse direction, the respective ductility ratios were 1.3 and 1.4. The longitudinal ductility ratios are comparable to those from Ex. II-1b while the transverse ductility ratios are about half. The yielding cross-frames limited the seismic forces transmitted to the column in the transverse direction resulting in lower ductility ratios. The columns were elastic even at MCE.

Figure 7-8 and Figure 7-9 shows the superstructure force-displacement in the transverse direction under DE1, DE7, MCE1, and MCE7. As shown, there was significant yielding in the support cross-frames. It can be observed that the transverse shear force in the superstructure is about the same as the column transverse base shear, with the superstructure shear force slightly less.

The average of total bearing forces in the transverse direction was 1,543 kips under DE and 1,554 kips under MCE. This is larger than the cross-frame lateral resistance shown in Section 7.7 because the cross-frames did not yield and buckle and at the same time which, in turn, is due to flexibility of the pier cap. Note that the tensile and post-buckling resistances of the cross-frame were used in the calculation of lateral resistance. The average column base shear forces in the transverse directions were 1,920 kips under DE and 2,065 kips under MCE. These are below the pier plastic resistance of 3,250 kips shown in Section 7.7. For this bridge, the inertia force in the pier cap is about 20% of the base shear.

The average lateral displacement of the superstructure under DE was 2.02 in. (3.7% drift). This is larger than the displacement calculated from the cross-frame design shown in Section 7.5 Step 9 (the displacement is 1.56 in. and the drift is 2.9%). This difference is attributed to the larger contribution of the higher modes to the superstructure transverse response. Figure 1-8 shows that the selected ground motions have higher spectral accelerations at short periods.

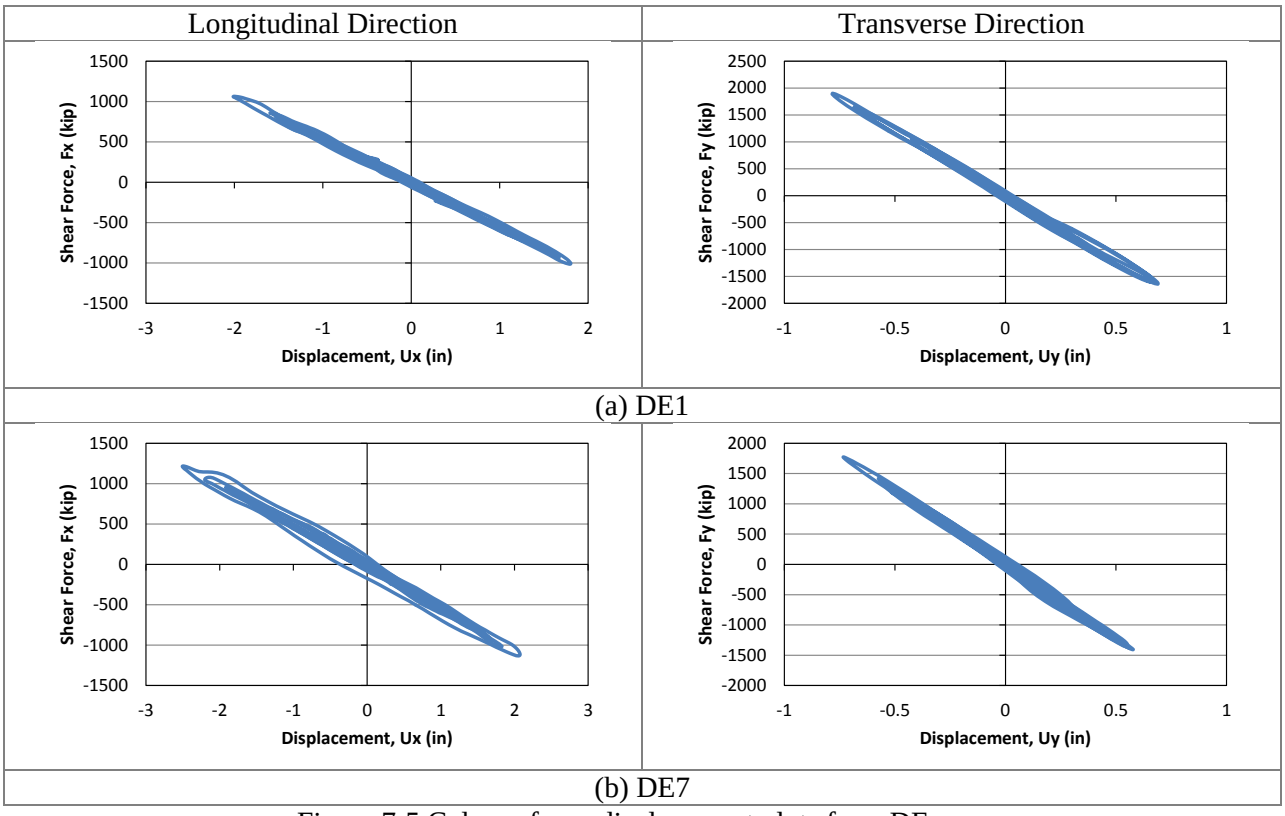

Figure 7-5 Column force-displacement plots from DE runs

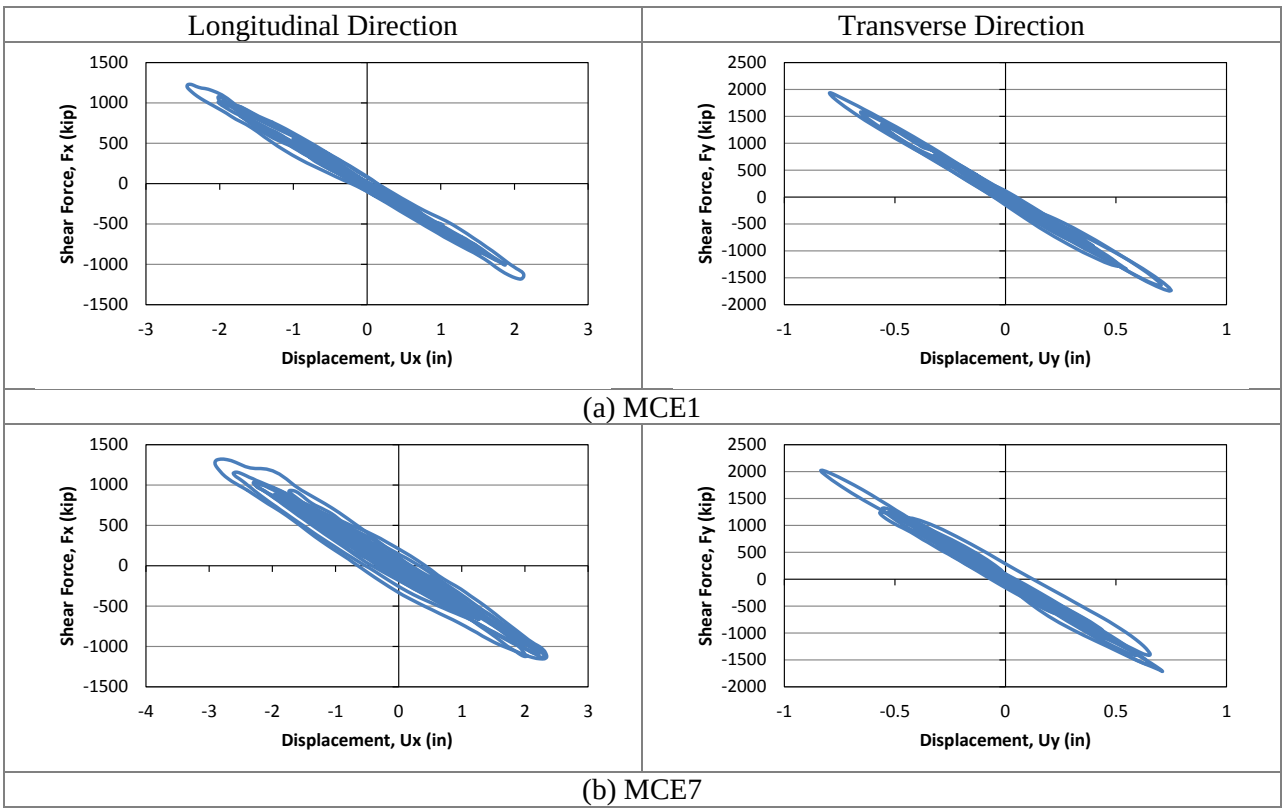

Figure 7-6 Column force-displacement plots from MCE runs

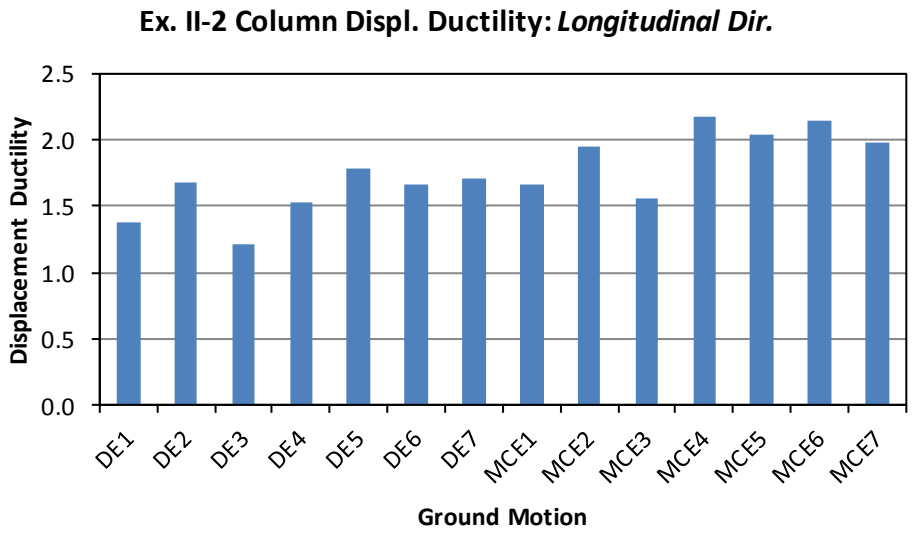

(a) ductility ratios in the longitudinal direction

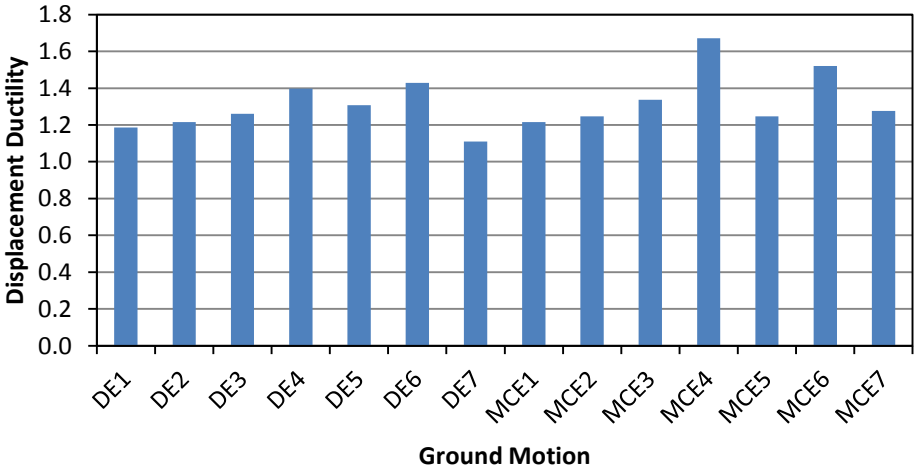

(b) ductility ratios in the transverse direction

Figure 7-7 Summary of column Displacement ductility

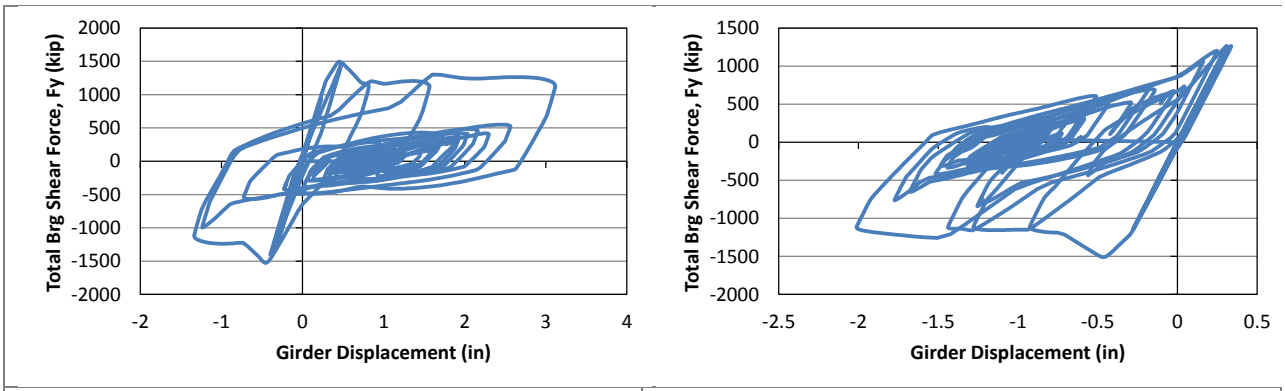

(a) DE1 (b) DE7

Figure 7-8 Superstructure force-displacement in the transverse direction from DE runs

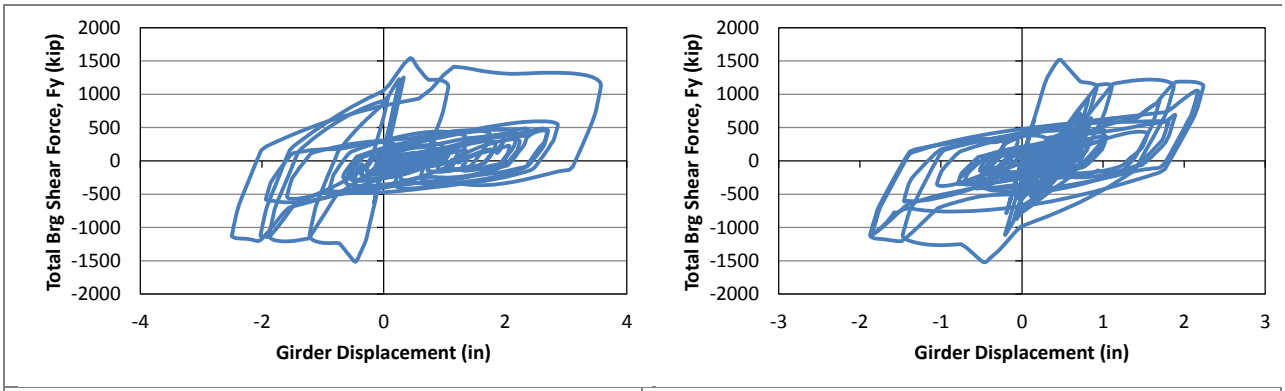

(a) MCE1 (b) MCE7

Figure 7-9 Superstructure force-displacement in the transverse direction from MCE runs

Chapter 8 Bridge with Wall Piers Design using Type 1 Strategy (Example III-1)

8.1 Bridge Description

The overall geometry of Ex. III-1 is described in Section 1.3.3. From the final design iteration, the reinforced concrete (R/C) wall pier is 40 ft wide and 4 ft thick. The vertical and horizontal steel reinforcement ratios are both 0.69% (#9 spaced at 6 in.). Figure 8-1 shows the elevation at piers. The cross-frames are of X-type pattern with diagonal members made of L8x8x1 single angles while the top and bottom chords are 2L4x4x1/2 double angles.

8.2 Computational Model

The extruded view of the computational model is shown in Figure 8-2 and details of the model are shown in Figure 8-3. The equivalent concrete section properties of superstructure are summarized in Table 8-1. Local axes of the superstructure are shown in Figure 8-1. Deck cracking was accounted for in the calculation of these properties by using 50% of the gross concrete modulus of elasticity (E_c).

The wall pier was modeled as a vertical beam element as shown in Figure 8-3a. The top of wall is then connected to a horizontal rigid beam element where the link elements representing the bearings are connected as shown in Figure 8-3b. To ensure correct modeling of the boundary condition at the top of the wall, the nodes of the horizontal beam element are assigned with rigid constraint such that there is no relative deformation and rotation between them.

For nonlinear response history analysis, the cross-frames were modeled with multi-linear plastic link element with force-deformation relationship shown in Figure 1-5 to account for inelasticity in case it occurred. Calculation of expected force and deformations are shown in Section 8.6.

Table 8-1 Ex.II-1 superstructure section properties

Area, A (in^2)	16,195
Moment of inertia about horizontal axis, I_2 (in^4)	10,316,084
Moment of inertia about vertical axis, I_3 (in^4)	8.22 x 10^8
Torsional constant, J (in^4)	285,124

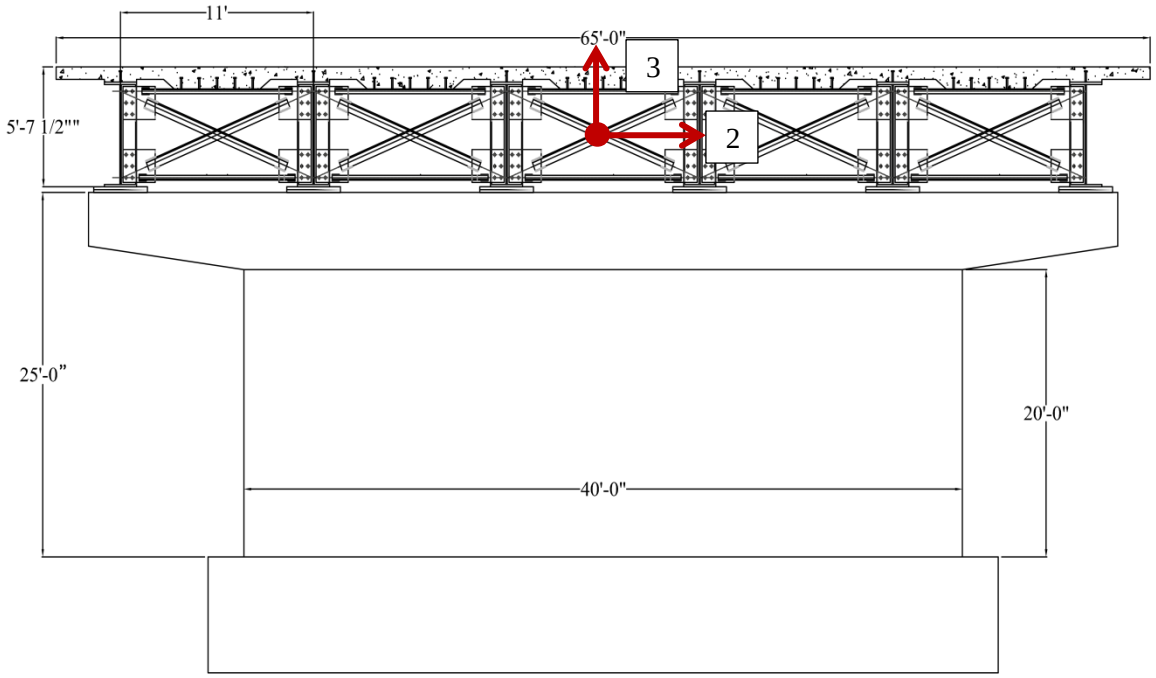

Figure 8-1 Elevation at pier of Ex. III-1

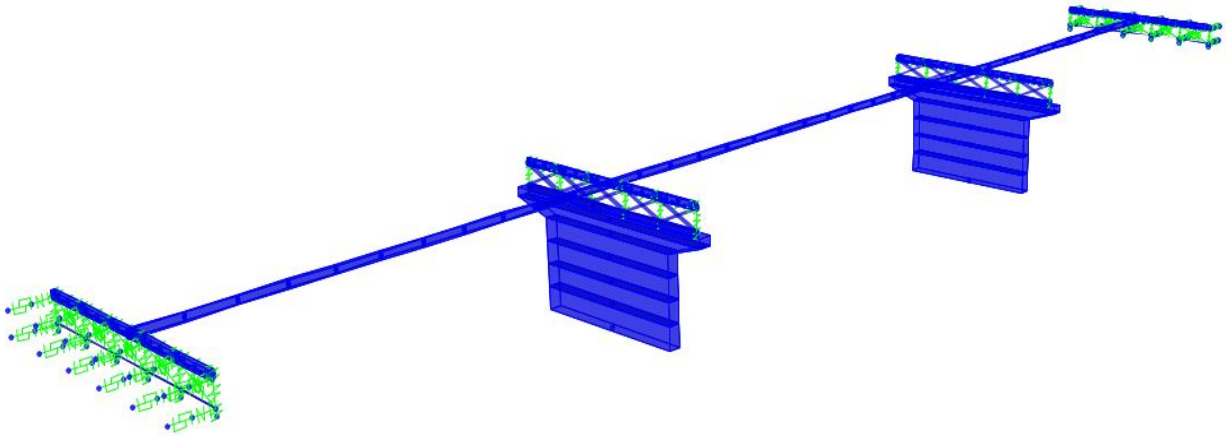

Figure 8-2 Extruded view of analytical model of Ex. III-1

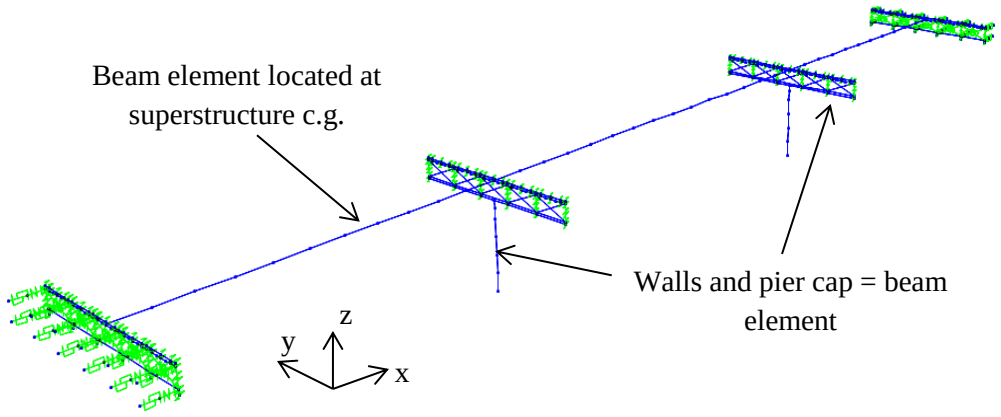

(a) 3D view of model

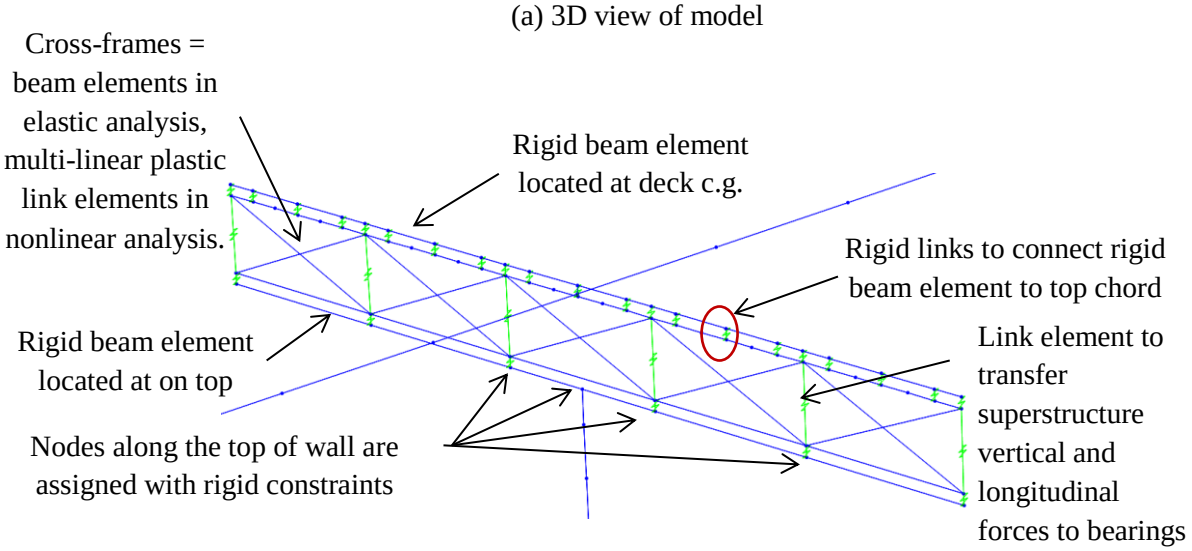

(b) Detail at piers

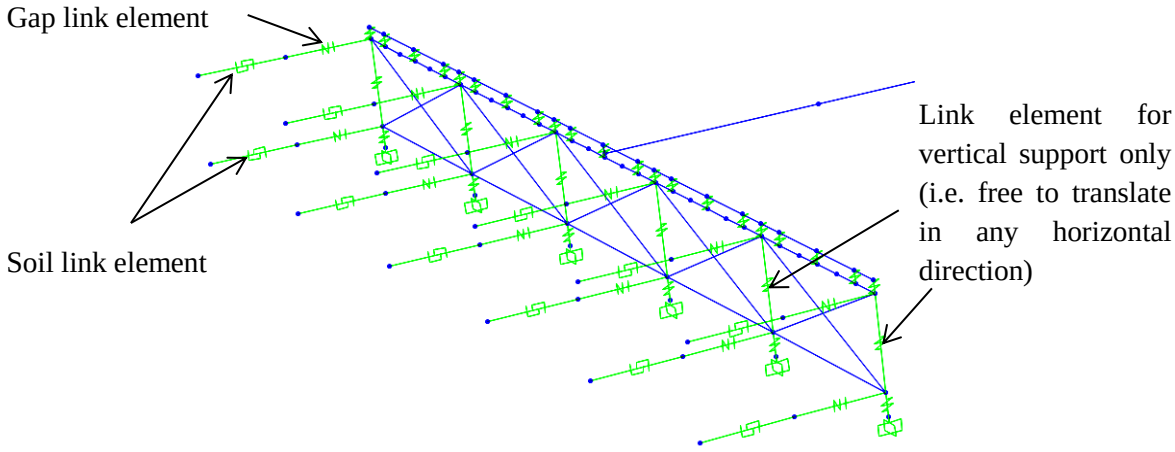

(c) Detail at abutments

Figure 8-3 Analytical model of Ex. III-1

8.3 Analysis

8.3.1 Gravity Loads – DC and DW

The total *DC* load (i.e. total bridge dead load) is 4,704 kips and the total *DW* load is 844 kips. The reactions at the base of wall due to these loads are 1,991 kips and 332 kips, respectively. These loads were used to calculate the effective section properties, as illustrated in Section 8.3.2 Steps *1* and *2*.

8.3.2 Earthquake Loads – EQ

Step 1: Calculate wall axial loads due to gravity loads, P_{col}. This will be used to determine the effective moment of inertia, I_e, of columns. $P_{col} = 1.25P_{DC} + 1.5P_{DW}$		$P_{col} = 1.25(1{,}991) + 1.5(332) = 2{,}987\ kips$
Step 2: Determine effective moment of inertia, I_e. This is accomplished through section analysis of the wall. The required parameters are: wall dimensions, longitudinal and transverse reinforcements, axial load, and material properties of concrete and steel reinforcement. The calculated I_e is assigned to the beam elements representing the wall pier in the model.		The following are the column properties: w = 40 ft t = 4 ft ρ_v = 0.69% (#9 at 6 in. both face for a total of 158 - #9) ρ_h = 0.69% (#9 @ 6 in.) f'_c = 4 ksi f_y = 60 ksi P_{col} = 2,787 kips From section analysis: I_e/I_g = 0.24
Step 3: Estimate soil displacement, Δ_{soil}, and calculate the effective abutment stiffness, K_e. The joint gap is included in the calculation of this stiffness, as shown in the figure below. 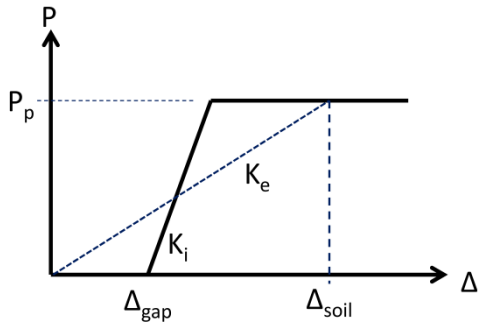 		Δ_{soil} = 3.75 in. $P_p = 5.0(5.625x65)(5.625/5.5) = 1{,}870\ kips$ $K_i = 50(65)(5.625/5.5) = 3{,}324\ kip/in$ Check Δ_{soil} against $\Delta_{gap} + \Delta_y$ to determine if the soil is yielding. $\Delta_{gap} + \Delta_y = 2 + \frac{1{,}870}{3{,}324} = 2 + 0.56 = 2.56\ in$

Figure 8-4 Abutment force-displacement

The soil passive resistance, P_p, and initial soil stiffness, K_i, are calculated based on the recommended values in Caltrans SDC.

$$P_p = 5.0A_e(h/5.5) \quad (kips)$$

$$K_i = 50w(h/5.5) \quad (kip/in)$$

where A_e (ft^2) is the effective backwall area, h (ft) is the backwall height, and w is the backwall width.

Under *EQ* in longitudinal direction, only one abutment is engaged in one direction. To account for this in elastic analyses such as modal and response spectrum analysis, half of K_e is applied to both abutments.

This $1/2K_e$ is then distributed to the link elements representing the soil. The gap link elements shown in Figure 8-3c were assigned with high stiffness with no opening during elastic analysis.

Since this is smaller than Δ_{soil}, the soil is yielding and the effective stiffness is:

$$K_e = \frac{1{,}870}{3.75} = 475\ kip/in$$

$$1/2K_e = 237\ kip/in$$

Since there are 12 soil springs at each abutment, the effective stiffness assigned to each is:

$$(1/2K_e)/12 = 19.78\ kip/in$$

Step 4: Perform modal analysis and determine the required number of modes needed for multimode spectral analysis.

After the effective stiffnesses of the elements are determined, modal analysis is performed to determine the fundamental vibration periods and the required number of modes needed in the response spectrum analysis. The AASHTO Specifications requires that the total number of modes used should ensure participation of at least 90% of the total bridge mass.

Table 8-2 shows the result of modal analysis. Although only the first 7 modes are shown in this table, a total of 30 modes were used in the response spectrum analysis with total mass participation of 100% in both the longitudinal and transverse directions.

The first mode with period of 0.67 sec is longitudinal translation mode; the second with period of 0.57 sec is the vertical vibration mode; the transverse translation modes are the fifth and seventh modes with periods of 0.30 sec and 0.17 sec, respectively.

Table 8-2 Modal periods and mass participation

Mode	Period	Mass Participation	
No	Sec	x-dir	y-dir
1	0.67	0.900	0.000
2	0.57	0.000	0.000
3	0.35	0.000	0.000
4	0.34	0.000	0.000
5	0.30	0.000	0.420
6	0.29	0.000	0.000
7	0.17	0.000	0.390

Step 5: Perform response spectrum analysis in the longitudinal direction (EQ_x), determine Δ_{soil}, and check against the initial value in *Step 3*.

The design spectrum is applied in the longitudinal direction. Multimode spectral analysis is used and the modal responses are combined using the Complete Quadratic Combination (CQC).

From response spectrum analysis, Δ_{soil} = 3.72 in. This is within less than 5% of the assumed value, thus, no further iteration is needed.

Step 6: Obtain the column forces due to EQ_x.

These forces will be combined with the forces due to EQ_y to determine the design forces.

Table 8-3 Column forces due to EQ_x

Load	P (kip)	M_x (k-ft)	M_y (k-ft)
EQ_x	37	0	27,326

The seismic base shear of the bridge in the longitudinal direction is 4,014 kips.

Step 7: Perform response spectrum analysis in the transverse direction (EQ_y) and determine the column forces.

Table 8-4 Column forces due to EQ_y

Load	P (kip)	M_x (k-ft)	M_y (k-ft)
EQ_y	0	75,952	0

The seismic base shear of the bridge in the transverse direction is 5,095 kips.

8.3.3 Design Loads

The 100%-30% combination was used to combine the EQ_x and EQ_y forces. The results are shown in Table 8-5.

Table 8-5 Combination of forces due to EQ_x and EQ_y

Load/Combination	P (kip)	M_x (k-ft)	M_y (k-ft)
EQ_x	37	0	27,326
EQ_y	0	75,952	0
EQ_1: $1.0EQ_x + 0.3EQ_y$	37	22,786	27,326
EQ_2: $0.3EQ_x + 1.0EQ_y$	11	75,952	8,198

The response modification factor, *R*, is then applied to EQ_1 and EQ_2 moments. The piers are designed as wall in both directions thus *R* is equal to 2.0. The resulting forces are then combined with *DC* and *DW* forces to determine the design forces. The load factors are based on Extreme Event I load combination and the result is shown in Table 8-6.

Table 8-6 Design loads

Load/Combination	P (kip)	F_x (kip)	F_y (kip)	M_x (k-ft)	M_y (k-ft)
DC	1,991	0	0	0	0
DW	332	0	0	0	0
EQ_1/R	37	568	382	11,393	13,663
EQ_2/R	11	171	1,274	37,976	4,099
LC1: $1.25DC + 1.5DW + 1.0EQ_1$	3,024	568	382	11,393	13,663
LC2: $1.25DC + 1.5DW + 1.0EQ_2$	2,998	171	1,274	37,976	4,099

8.4 Design of Wall Pier

Step 1: Determine the design axial load and resultant moment from Section 8.3.3.

Table 8-7 Design axial load and resultant moment

Load Comb.	P (kip)	M_x (kip-ft)	M_y (kip-ft)	M_{res} (kip-ft)
LC1	3,024	11,393	13,663	17,790
LC2	2,998	37,976	4,099	38,197

Step 2: Develop the axial force-moment (P-M) interaction curve and check if the design loads are inside the P-M curve.

The AASHTO ϕ factors are used in the interaction curve.

Since the pier is rectangular, an interaction curve needs to be developed for each load combination.

From the final iteration the wall properties are:

w = 40 ft
t = 4 ft
ρ_v = 0.69% (#9 @ 6 in. = 158 - #8) vertical reinf.
ρ_h = 0.69% (#9 @ 6 in.) horizontal reinf.
f'_c = 4 ksi
f_y = 60 ksi

For *LC1*:

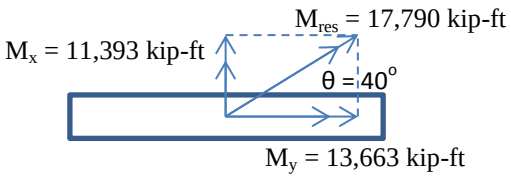

The interaction curve for $\theta = 40^o$ is:

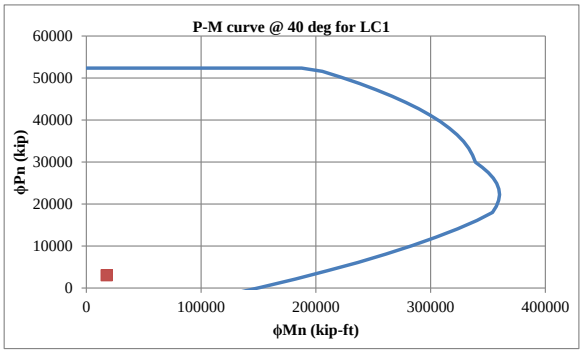

Since the design of the wall section is governed by the forces in the weak axis direction, the capacity in this direction is also checked against the forces due to earthquake in longitudinal direction EQ_x.		For *LC2*: 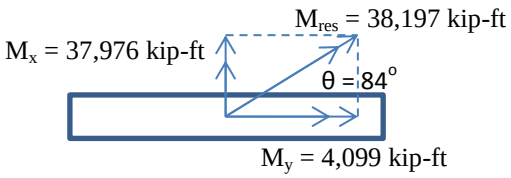 The interaction curve for $\theta = 84^o$ is: 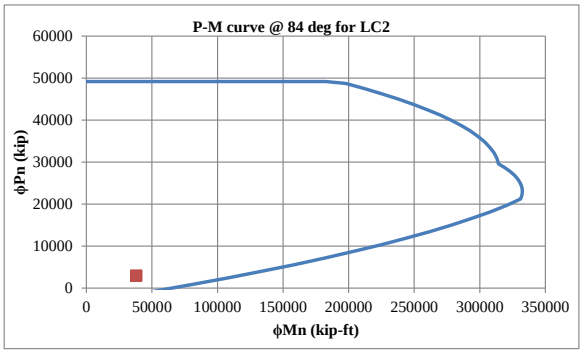 For EQ_x: P = 3,024 M_y = 13,663 kip-ft (R = 2) The interaction curve for $\theta = 0^o$ is: 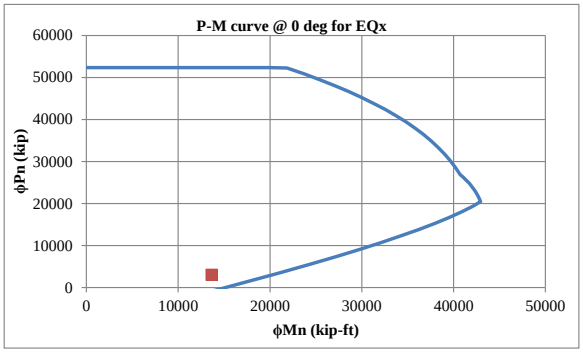 Therefore, selected section and its reinforcement are adequate.
Step 3: Determine shear resistance in the transverse direction. Transverse direction is the strong direction of the wall.		ρ_h = 0.0069 b = 48 in. d = 472 in.

The factored shear resistance, V_r, of the wall pier is taken as the lesser of (AASHTO Specifications Art. 5.10.11.4.2): $V_r = 0.253\sqrt{f_c'}bd$ and $V_r = 0.9\left[0.063\sqrt{f_c'} + \rho_h f_y\right]bd$ where ρ_h is the horizontal steel reinforcement ratio.		$V_r = 0.253\sqrt{4}(48)(472) = 11{,}464\ kips$ $V_r = 0.9\left[0.063\sqrt{4} + 0.0069(60)\right](48)(472)$ $= 11{,}011\ kips$ Therefore, V_r = 11,011 kips The maximum shear demand is 1,274 kips from Table 8-6. $\frac{D}{C} = \frac{1{,}274}{11{,}011} = 0.12\ < 1.0, ok!$
Step 5: Check the vertical and horizontal reinforcements. The minimum vertical and horizontal reinforcement ratio shall satisfy (AASHTO Specifications Art. 5.10.11.4.2): $\rho_{v,h} \geq 0.0025$ The spacing of vertical and horizontal reinforcement shall satisfy (AASHTO Specifications Art. 5.10.11.4.2): $s \leq 18\ in.$		$\rho_v = 0.0069 > 0.0025\ \ ok!$ $\rho_h = 0.0069 > 0.0025\ \ ok!$ $s = 6\ in. \leq 18\ in.\quad ok!$

8.5 Seismic Design of Cross-Frames

Step 1: Determine the design cross-frame force. Designing the cross-frames based on shear resistance of wall pier may result in large uneconomical section due to large shear resistance of wall piers. Therefore, in this case, the diagonal member design force is taken as the lesser of: $P_{XF} = \frac{V_n}{2N\cos\theta} = \frac{V_r/(\phi = 0.9)}{2N\cos\theta}$ and $P_{XF} = P_{EQY}$ where N is the number of cross-frame panels, θ is the angle of the diagonal member measured from the horizontal, and P_{EQY} is the force in the diagonal member from response spectrum analysis in the transverse direction.		V_r = 11,011 kips N = 5 panels θ = 22 degrees $P_{XF} = \frac{11{,}011/0.9}{2(5)(\cos 22)} = 1{,}320\ kips$ From response spectrum analysis in the transverse direction: $P_{XF} = 221\ kips$ Therefore, the design axial load in the diagonal member is: $P_{XF} = 221\ kips$
Step 2: Cross-frame member section properties. Note that the size of the cross-frames may be governed by slenderness requirements.		Section: *L8x8x1* F_y = 36 ksi A_g = 15.0 in^2 $r_x = r_y$ = 2.43 in. r_z = 1.56 in. L = 142.62 in.
Step 3: Calculate the tensile resistance $\phi P_r = 0.95 F_y A_g$		$\phi P_r = 0.95(36)(15.0) = 513\ kips > 221\ kips$
Step 4: Calculate the compressive resistance Under seismic loading, the cross-frames are primary members in the transverse direction as they transmit the deck seismic forces to the bearings. The limiting slenderness ratio for primary members is 120 (AASHTO Specifications Art. 6.9.3). Equal-leg single angle sections will be used as diagonal members. The slenderness ratio is calculated according to AASHTO Specifications		l/r_x = 142.62/2.43 = 58.69 < 80 $\left(\frac{KL}{r}\right)_{eff} = 72 + 0.75(58.69) = 116.02 < 120\ ok!$

Art. 6.9.4.4. ○ If $l/r_x \leq 80$ $$\left(\frac{KL}{r}\right)_{eff} = 72 + 0.75\frac{l}{r_x}$$ ○ If $l/r_x > 80$ $$\left(\frac{KL}{r}\right)_{eff} = 32 + 1.25\frac{l}{r_x}$$ The compressive resistance is calculated according to AASHTO Specifications Art. 6.9.2.1, 6.9.4.1.1, and 6.9.4.1.2 $$P_e = \frac{\pi^2 E}{\left(\frac{Kl}{r}\right)^2_{eff}} A_g$$ $$P_o = QF_yA_g$$ The slender element reduction factor, *Q*, is equal to 1.0 when: $$\frac{b}{t} \leq 0.45\sqrt{\frac{E}{F_y}}$$ ○ If $P_e/P_o \geq 0.44$ $$\phi P_n = 0.9\left[0.658^{(P_o/P_e)}\right]P_o$$ ○ If $P_e/P_o < 0.44$ $$\phi P_n = 0.9(0.877P_e)$$ Note that although the calculations shown here is for single angle sections, double angles may be also used as diagonal members of cross-frames under Type 1 design strategy.		$P_e = \frac{\pi^2(29{,}000)}{116.02^2}(15.0) = 318.95\ kips$ $\frac{b}{t} = \frac{8}{1} = 8.0 \leq 0.45\sqrt{\frac{29{,}000}{36}} = 12.77, Q = 1.0$ $P_o = 1.0(36)(15) = 540\ kips$ $\frac{P_e}{P_o} = \frac{318.95}{540} = 0.591 \geq 0.44$ $\phi P_n = 0.9\left[0.658^{1/0.591}\right](540) = 239.37\ kips > 221\ kips, ok!$
Step 5: Calculate the minimum nominal shear resistance of the cross-frames $$V_{XF\_min} = (2P_n)N\cos\theta$$ In this equation, only the compression resistance, P_n, is used to determine the minimum nominal shear resistance. Note that P_n is smaller than the		$V_{XF\_min} = 2\left(\frac{239.37}{0.9}\right)5\cos 22 = 2{,}466 kips$ This is less than the nominal shear resistance of the wall pier:

tensile resistance, P_r, which means buckling would occur first in any of the diagonal members before yielding is reached. Thus, V_{XF} is the minimum shear force before inelasticity starts to occur in the cross-frames. Although this is Type 1 design strategy, V_{XF} may be less than shear resistance of the wall pier. As noted in *Step 1*, in cases where the pier shear resistance is very large, the cross-frames are designed based on the response spectrum analysis. This means that cross-frames may become inelastic before shear resistance of pier is reached.		$V_n = \frac{11{,}011}{0.9} = 12{,}234\ kips$

8.6 Cross-Frame Properties for Nonlinear Analysis

The expected force and displacement resistance of the cross-frames are calculated for use in the design evaluation.

Step 1: Calculate the expected tensile yield and displacement resistance. The expected yield resistance is: $$P_{ye} = F_{ye}A_g$$ where F_{ye} is the expected yield stress and is equal to R_yF_y. For A36 steel sections, R_y = 1.5. The effective axial stiffness is: $$K_{XF\_e} = \frac{EA_e}{L}$$ where E is the modulus of elasticity of steel which is 29,000 ksi, A_e is the effective area calculated using Eqn. (1-12), and L is the total length of the diagonal member. The expected yield displacement is then calculated as: $$\Delta_{ye} = \frac{P_{ye}}{K_{XF\_e}}$$		*L8x8x1* F_{ye} = 1.5(36) = 54 ksi A_g = 15.0 in^2 I = 89.1 in^4 x = 2.40 in. distance from connected leg of angle to its c.g. $P_{ye} = 54(15) = 810\ kips$ $A_e = \frac{15.0(89.1)}{89.1 + 15.0(2.40)^2} = 7.62\ in^2$ $K_{XF\_e} = \frac{29{,}000(7.62)}{142.62} = 1{,}548.49\ kip/in$ $\Delta_{ye} = \frac{810}{1{,}548.49} = 0.52\ in$

Step 2: Calculate the expected compressive resistance and associated displacement. The $(Kl/r)_{eff}$ and P_e is the same as that calculated in Section 8.5 *Step 4*. The expected yield strength is used to calculate P_o. $$P_o = QF_{ye}A_g$$ The expected compressive resistance is then calculated as: ○ If $P_e/P_o \geq 0.44$ $$P_{nc} = \left[0.658^{(P_o/P_e)}\right]P_o$$ ○ If $P_e/P_o < 0.44$ $$P_{nc} = 0.877P_e$$ The corresponding displacement is: $$\Delta_{nc} = \frac{P_{nc}}{K_{XF\_e}}$$		$P_o = 1.0(54)(15.0) = 810\ kips$ $\frac{P_e}{P_o} = \frac{318.95}{810} = 0.394 < 0.44$ $P_{nc} = 0.877(318.95) = 279.72\ kips$ $\Delta_{nc} = \frac{279.72}{1{,}548.49} = 0.181\ in.$

8.7 Design Summary

The total weight of Ex. III-1 is 4,383 kips. From modal and response spectrum analyses, the periods, forces, and displacements are:

Parameter	Longitudinal Direction	Transverse Direction
Fundamental period, T (sec)	0.67	0.31
Base shear, V_b (kip)	4,014	5,151
Pier displacement, Δ_{pier} (in)	4.76	0.21
Pier Base Shear, F_b (kip)	1,136	2,576
Deck displacement, Δ_{deck} (in)	3.74	0.61

The wall pier properties are:

Width, w	40 ft
Thickness, t	4 ft
Vertical reinforcement	#9 @ 6 in. (total 158 - #8) (ρ_v = 0.69%)
Horizontal reinforcement	#9 @ 6 in. (ρ_h = 0.69%)
Factored shear resistance, V_r	11,011 kips

The cross-frame diagonal member section properties are:

Section	L8x8x1 (A36)
Area, A	15.0 in^2
Slenderness ratio, *KL/r*	116.02
Width-thickness ratio, *b/t*	8.0
Tensile resistance, ϕP_r	513 kips
Compressive resistance, ϕP_n	239 kips
Min. nominal shear resistance, V_{XF_min}	2,466 kips
Expected tensile yield resistance, P_{ye}	810 kips
Expected compressive resistance, P_{nc}	280 kips

8.8 Nonlinear Evaluation

Example III-1 was analyzed using the ground motions described in Section 1.8.1. The ground motions were scaled to represent the Design (DE) and MCE Earthquake levels. There were seven DE runs and seven MCE runs for a total of fourteen runs. Because of this, only the column force-displacement plots from DE1, DE7, MCE1 and MCE7 are shown in Figure 8-5 and Figure 8-6 to represent the results. However, the column ductility ratios in the longitudinal direction for all runs are shown in Figure 8-7. Only the results in longitudinal direction are shown here because the transverse displacements were small and piers were elastic. The cross-frames remained elastic in all runs.

The yield displacements were calculated according to Section 1.8.2. Since the expected material properties were used in the nonlinear analyses, the yield displacements were also calculated using these properties. The yield displacement in the longitudinal direction is 2.07 in. The average ductility ratios were 1.8 from DE runs and 2.5 from MCE runs.

The negative stiffness observed in the hysteresis plots was not due to instability in the structure or computational error in the analysis. Rather, it is attributed to the coupled biaxial response of the column. This phenomenon was observed when the response is elastic and depends on the frequency content of the input motion and period of the structure (Monzon et al. 2013b).

Figure 8-8 shows the transverse base shear forces in the wall piers. The average base shear at DE runs was 3,500 kips and at MCE it was 4,800 kips which were below the transverse shear resistance of the wall pier shown in Section 8.7. The average of total bearing shear forces in the transverse direction were 3,207 kips under DE and 4,393 kips under MCE. These are below the expected lateral resistance of the cross-frames which is equal to 4,896 kips, thus the cross-frame were elastic.

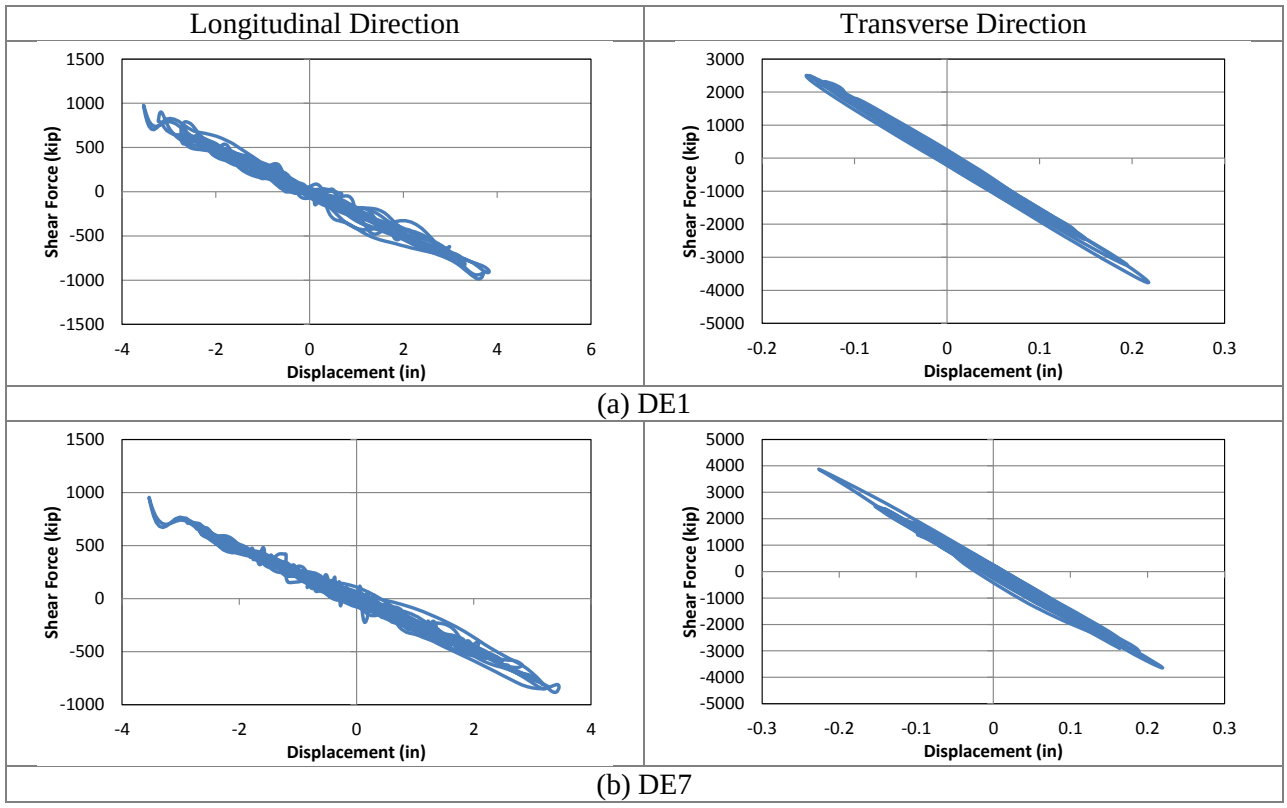

(a) DE1

(b) DE7

Figure 8-5 Column force-displacement plots from DE runs

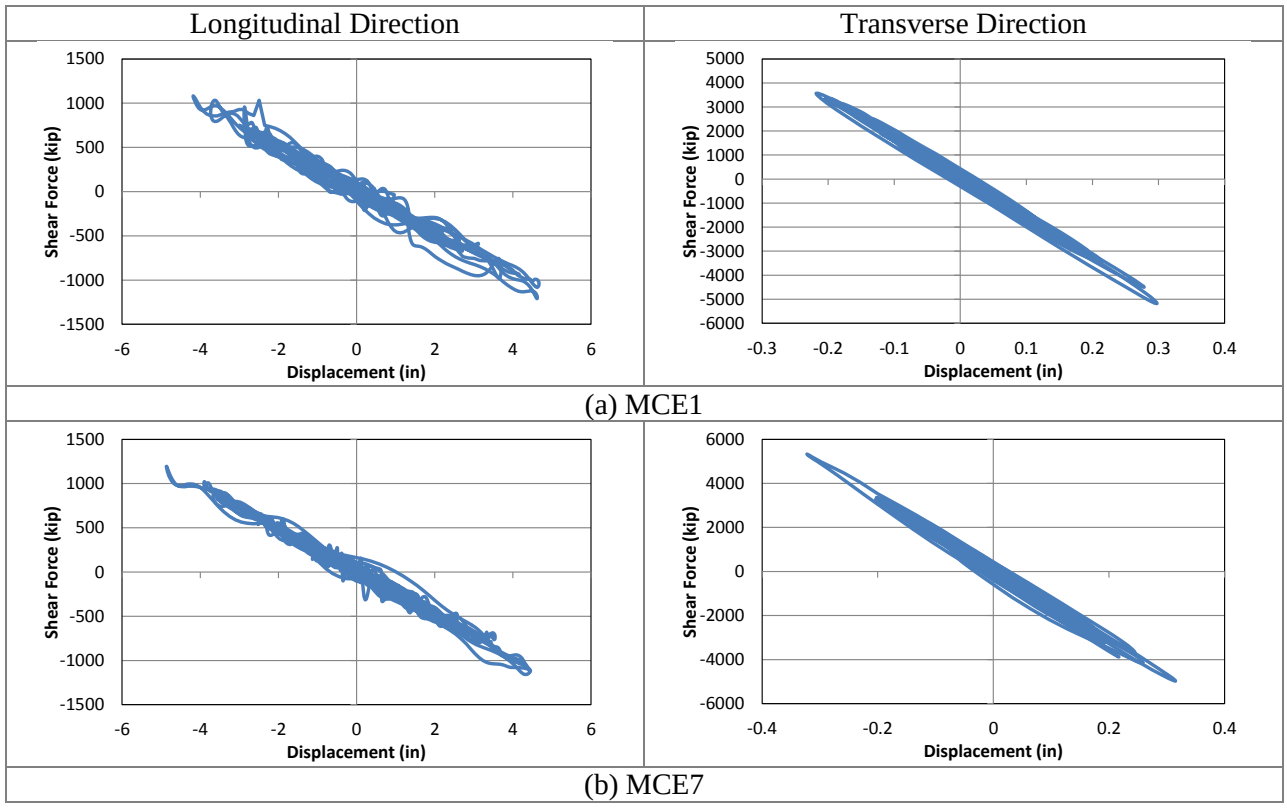

(a) MCE1

(b) MCE7

Figure 8-6 Column force-displacement plots from MCE runs

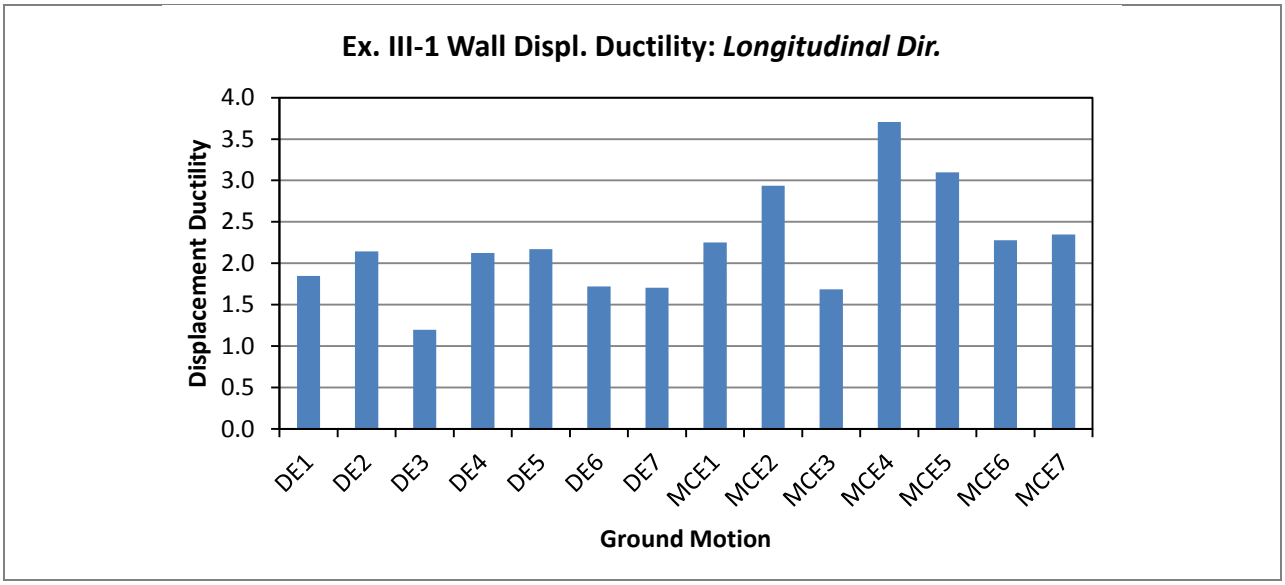

Figure 8-7 Summary of column displacement ductility in the longitudinal direction

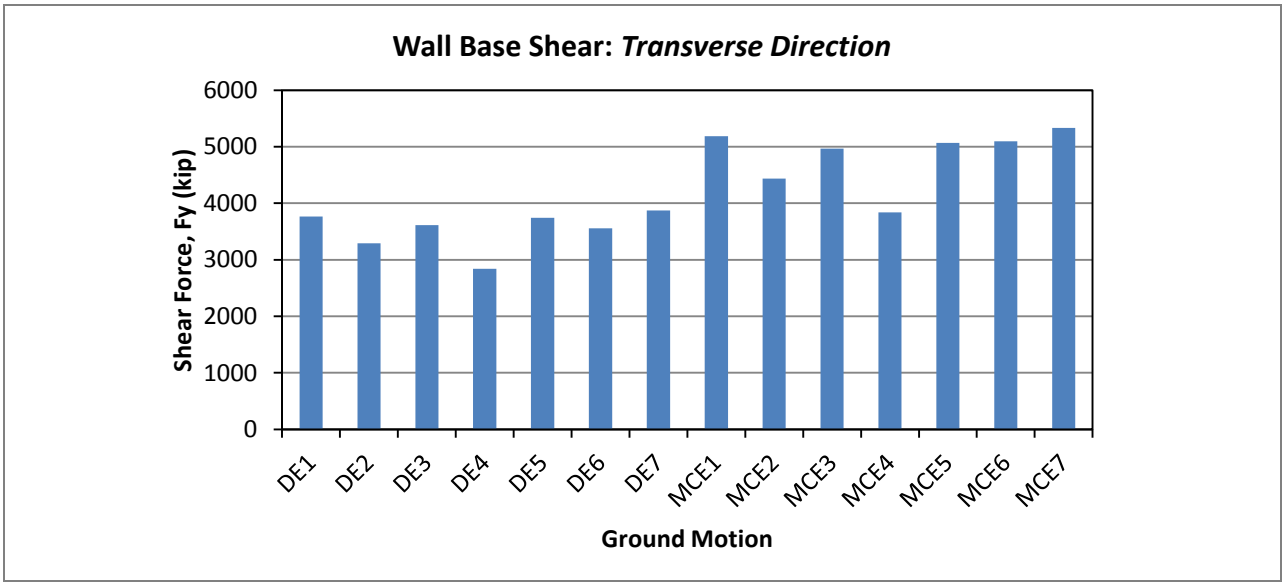

Figure 8-8 Summary of wall base shear in the transverse direction

Chapter 9 Bridge with Wall Piers Designed using Type 2 Strategy (Example III-2)

9.1 Bridge Description

The overall geometry of Ex. III-2 is described in Section 1.3.3. From the final design iteration, the reinforced concrete (R/C) wall pier is 40 ft wide and 4 ft thick. The vertical and horizontal steel reinforcement ratios are both 0.69% (#9 spaced at 6 in.). Figure 9-1 shows the elevation at piers. The cross-frames are of X-type pattern with diagonal members made of L4x4x3/4 single angles while the top and bottom chords are 2L2x2x3/8 double angles

9.2 Computational Model

The extruded view of the computational model is shown in Figure 9-2 and details of the model are shown in Figure 9-3. The equivalent concrete section properties of superstructure are summarized in Table 9-1. Local axes of the superstructure are shown in Figure 9-1. Deck cracking was accounted for in the calculation of these properties by using 50% of the gross concrete modulus of elasticity (E_c).

For elastic analysis, only one of the diagonal members of the cross-frames is included in the model as shown in Figure 9-3b. This is because the cross-frames are designed and detailed to yield and buckle under the design earthquake. Under transverse loading, in each cross-frame panel, one diagonal is under tension and the other is in compression. Consequently, the diagonal in compression would buckle and its stiffness becomes essentially close to zero.

For nonlinear response history analysis, the cross-frames were modeled with multi-linear plastic link elements with force-deformation relationship shown in Figure 1-5. The two cross-frame diagonal members are modeled because buckling is accounted for in the definition of link force-deformation relationship. Calculation of expected force and deformations are shown in Sections 9.5 and 9.6.

Table 9-1 Ex.II-1 superstructure section properties

Area, A (in^2)	16,195
Moment of inertia about horizontal axis, I_2 (in^4)	10,316,084
Moment of inertia about vertical axis, I_3 (in^4)	8.22×10^8
Torsional constant, J (in^4)	285,124

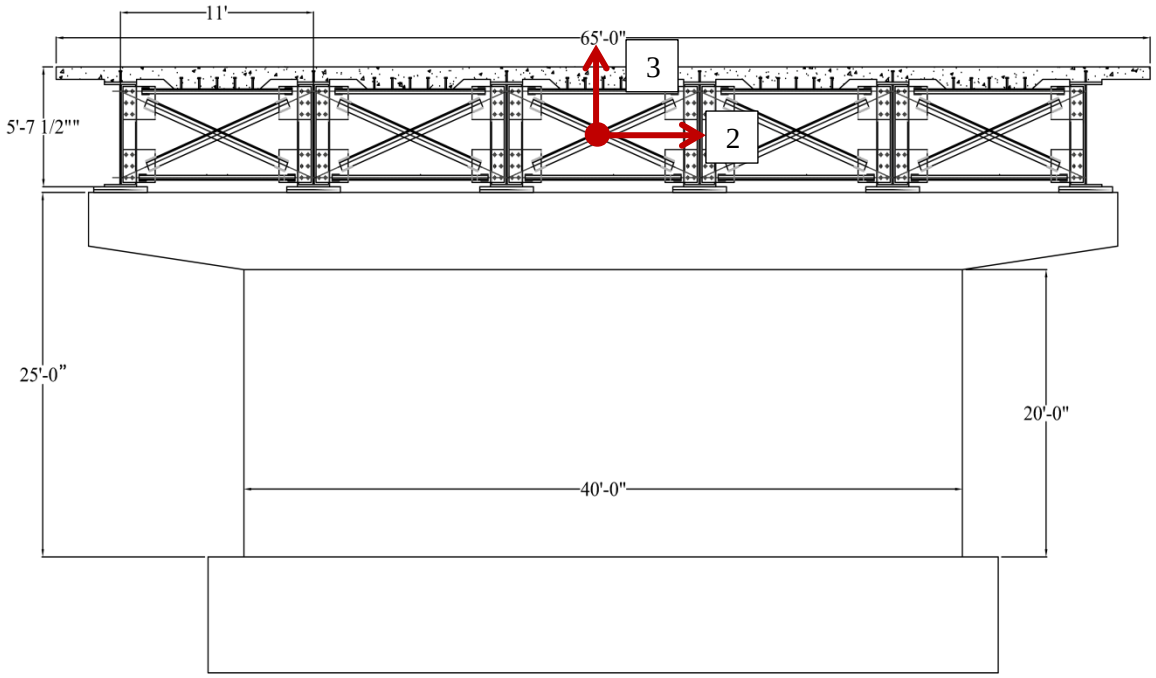

Figure 9-1 Elevation at piers of Ex. III-2

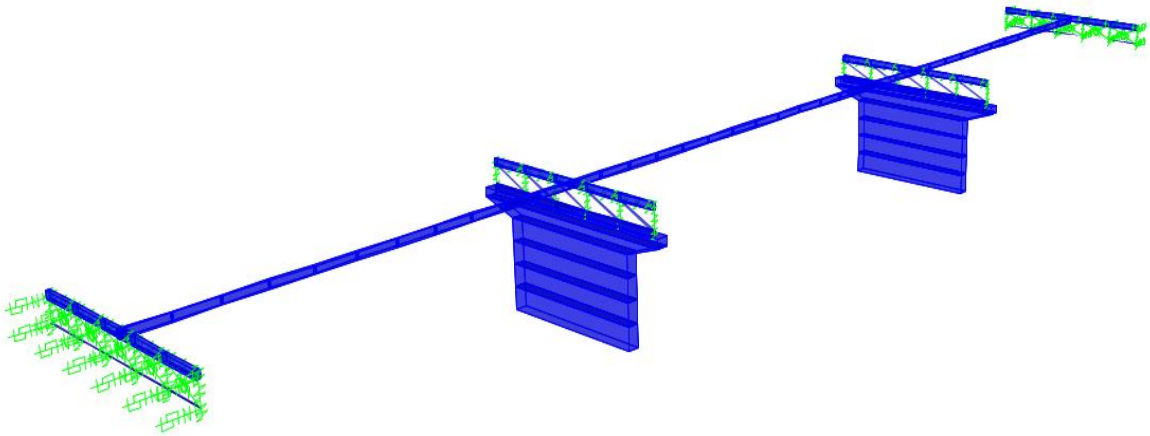

Figure 9-2 Extruded view of analytical model of Ex. III-2

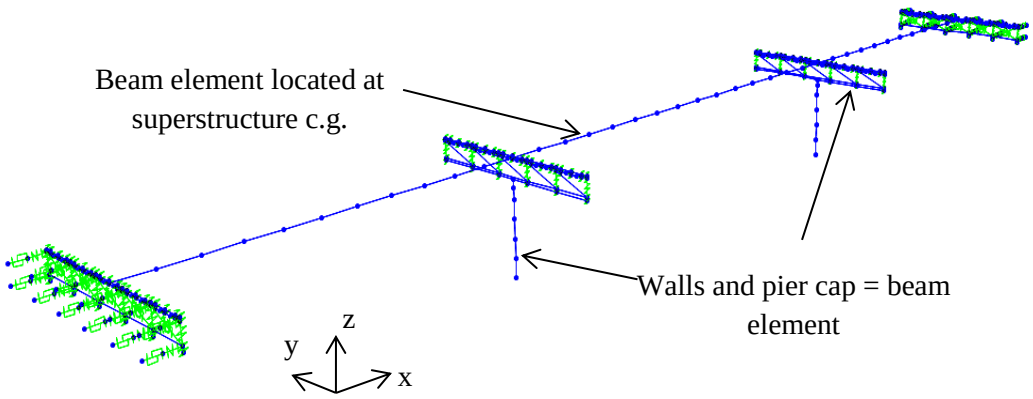

(a) 3D view of model

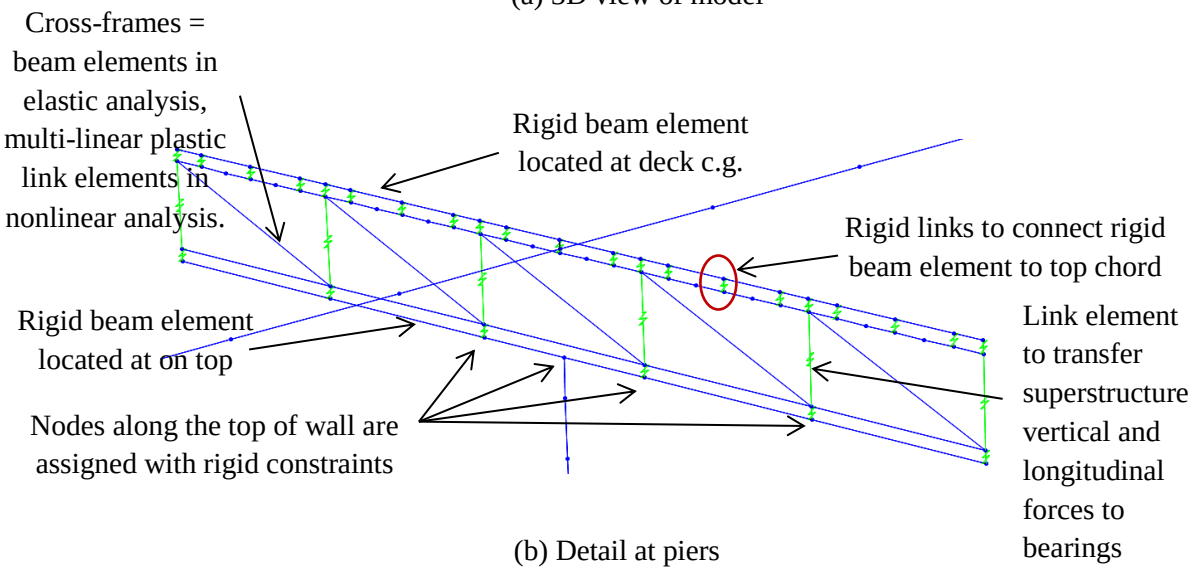

(b) Detail at piers

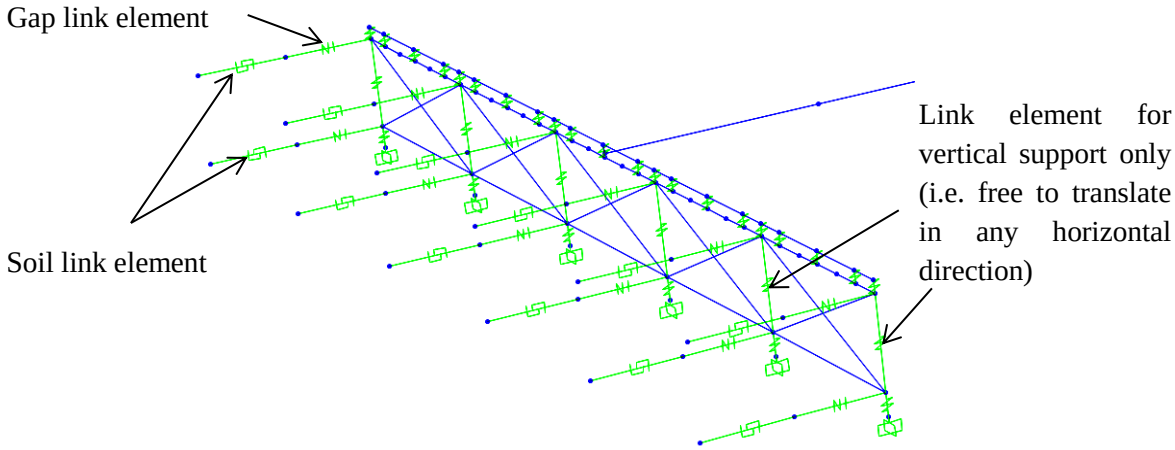

(c) Detail at abutments

Figure 9-3 Analytical model of Ex. III-2

9.3 Analysis

9.3.1 Gravity Loads – DC and DW

The total *DC* load (i.e. total bridge dead load) is 4,704 kips and the total *DW* load is 844 kips. The reactions at the base of wall due to these loads are 1,991 kips and 332 kips, respectively. These loads were used to calculate the effective section properties, as illustrated in Section 9.3.2 Steps *1* and *2*.

9.3.2 Earthquake Loads – EQ

Step 1: Calculate wall axial loads due to gravity loads, P_{col}. This will be used to determine the effective moment of inertia, I_e, of columns. $P_{col} = 1.25P_{DC} + 1.5P_{DW}$		$P_{col} = 1.25(1{,}991) + 1.5(332) = 2{,}987\ kips$
Step 2: Determine effective moment of inertia, I_e. This is accomplished through section analysis of the wall. The required parameters are: wall dimensions, longitudinal and transverse reinforcements, axial load, and material properties of concrete and steel reinforcement. The calculated I_e is assigned to the beam elements representing the wall pier in the model.		The following are the column properties: w = 40 ft t = 4 ft ρ_v = 0.69% (#9 at 6 in. both face for a total of 158 - #9) ρ_h = 0.69% (#9 @ 6 in.) f'_c = 4 ksi f_y = 60 ksi P_{col} = 2,787 kips From section analysis: I_e/I_g = 0.24
Step 3: Estimate soil displacement, Δ_{soil}, and calculate the effective abutment stiffness, K_e. The joint gap is included in the calculation of this stiffness, as shown in the figure below. 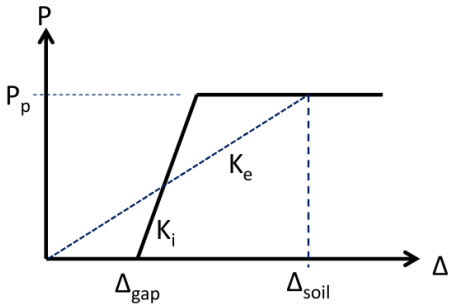 Figure 9-4 Abutment force-displacement		Δ_{soil} = 3.75 in. $P_p = 5.0(5.625x65)(5.625/5.5) = 1{,}870\ kips$ $K_i = 50(65)(5.625/5.5) = 3{,}324\ kip/in$ Check Δ_{soil} against $\Delta_{gap} + \Delta_y$ to determine if the soil is yielding. $\Delta_{gap} + \Delta_y = 2 + \frac{1{,}870}{3{,}324} = 2 + 0.56 = 2.56\ in$

The soil passive resistance, P_p, and initial soil stiffness, K_i, are calculated based on the recommended values in Caltrans SDC.

$$P_p = 5.0A_e(h/5.5) \quad (kips)$$

$$K_i = 50w(h/5.5) \quad (kip/in)$$

where A_e (ft^2) is the effective backwall area, h (ft) is the backwall height, and w is the backwall width.

Under *EQ* in longitudinal direction, only one abutment is engaged in one direction. To account for this in elastic analyses such as modal and response spectrum analysis, half of K_e is applied to both abutments.

This $1/2K_e$ is then distributed to the link elements representing the soil. The gap link elements shown in Figure 8-3c were assigned with high stiffness with no opening during elastic analysis.

Since this is smaller than Δ_{soil}, the soil is yielding and the effective stiffness is:

$$K_e = \frac{1{,}870}{3.75} = 475\ kip/in$$

$$1/2K_e = 237\ kip/in$$

Since there are 12 soil springs at each abutment, the effective stiffness assigned to each is:

$$(1/2K_e)/12 = 19.78\ kip/in$$

Step 4: Perform modal analysis and determine the required number of modes needed for multimode spectral analysis.

After the effective stiffnesses of the elements are determined, modal analysis is performed to determine the fundamental vibration periods and the required number of modes needed in the response spectrum analysis. The AASHTO Specifications requires that the total number of modes used should ensure participation of at least 90% of the total bridge mass.

Table 9-2 shows the result of modal analysis. Although only the first 5 modes are shown in this table, a total of 30 modes were used in the response spectrum analysis with total mass participation of 100% in both the longitudinal and transverse directions.

The first mode with period of 0.67 sec is longitudinal translation mode; the second with period of 0.57 sec is the vertical vibration mode; the transverse translation mode is the fourth mode with period of 0.39 sec. This transverse mode is mainly due to deformation in the support cross-frames. The third mode with a period of 0.52 sec is in-plane torsional mode.

Table 9-2 Modal periods and mass participation

Mode	Period	Mass Participation	
No	Sec	x-dir	y-dir
1	0.67	0.904	0.000
2	0.57	0.000	0.000
3	0.52	0.000	0.000
4	0.39	0.000	0.722
5	0.34	0.000	0.000

<table>
<tr>
<td>Step 5: Perform response spectrum analysis in the longitudinal direction (EQ_x), determine Δ_{soil}, and check against the initial value in Step 3.

The design spectrum is applied in the longitudinal direction. Multimode spectral analysis is used and the modal responses are combined using the Complete Quadratic Combination (CQC).</td>
<td></td>
<td>From response spectrum analysis, Δ_{soil} = 3.72 in. This is within less than 5% of the assumed value, thus, no further iteration is needed.</td>
</tr>
<tr>
<td>Step 6: Obtain the column forces due to EQ_x.

These forces will be combined with the forces due to EQ_y to determine the design forces.</td>
<td></td>
<td>Table 9-3 Column forces due to EQ_x
<table><tr><td>Load</td><td>P (kip)</td><td>M_x (k-ft)</td><td>M_y (k-ft)</td></tr><tr><td>EQ_x</td><td>37</td><td>0</td><td>27,326</td></tr></table>The seismic base shear of the bridge in the longitudinal direction is 4,014 kips.</td>
</tr>
<tr>
<td>Step 6: Obtain the column forces due to EQ_y.</td>
<td></td>
<td>Table 9-4 Column forces due to EQ_y
<table><tr><td>Load</td><td>P (kip)</td><td>M_x (k-ft)</td><td>M_y (k-ft)</td></tr><tr><td>EQ_y</td><td>0</td><td>86,468</td><td>0</td></tr></table>The seismic base shear of the bridge in the longitudinal direction is 5,771 kips.</td>
</tr>
</table>

9.3.3 Design Loads

A proposed *R* factor of 1.5 is applied to the moments from earthquake analysis. The forces based on Extreme Event I load combination is shown in Table 9-5.

Table 9-5 Design loads for wall pier

Load/Combination	P (kip)	M_x (k-ft)	M_y (k-ft)
DC	1,991	0	0
DW	332	0	0
EQ_x	37	0	27,326
EQ_y	0	86,468	0
EQ_1: $1.0EQ_x + 0.3EQ_y$	37	25,940	27,326
EQ_2: $0.3EQ_x + 1.0EQ_y$	11	86,468	8,198
EQ_1/R	37	17,293	18,217
EQ_2/R	11	57,645	5,465
LC1: $1.25DC + 1.5DW + 1.0EQ_1$	3,024	17,293	18,217
LC1: $1.25DC + 1.5DW + 1.0EQ_2$	2,998	57,645	5,465

9.4 Design of Wall Pier

Step 1: Determine the design axial load and resultant moment from Section 9.3.3.

Table 9-6 Design axial load and resultant moment

Load Comb.	P (kip)	M_x (kip-ft)	M_y (kip-ft)
LC1	3,024	17,293	18,217
LC2	2,998	57,645	5,465

Step 2: Develop the axial force-moment (P-M) interaction curve and check if the design loads are inside the P-M curve.

The AASHTO ϕ factors are used in the interaction curve.

From the final iteration the wall properties are:

w = 40 ft
t = 4 ft
ρ_v = 0.69% (#9 @ 6 in. = 158 - #8) vertical reinf.
ρ_h = 0.69% (#9 @ 6 in.) horizontal reinf.
f'_c = 4 ksi

Since the pier is rectangular, an interaction curve needs to be developed for each load combination.

f_y = 60 ksi

For *LC1*:

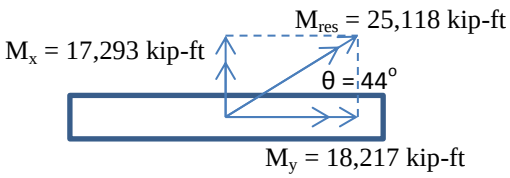

Note: the x- and y-axes are based on global axes.

The interaction curve for $\theta = 46^o$ is:

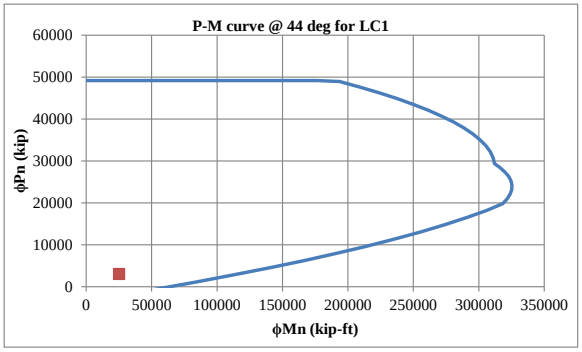

For *LC2*:

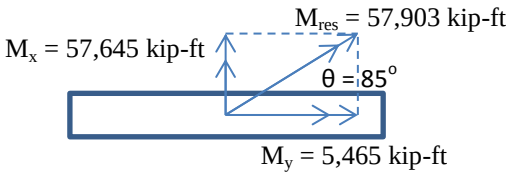

The interaction curve for $\theta = 85^o$ is:

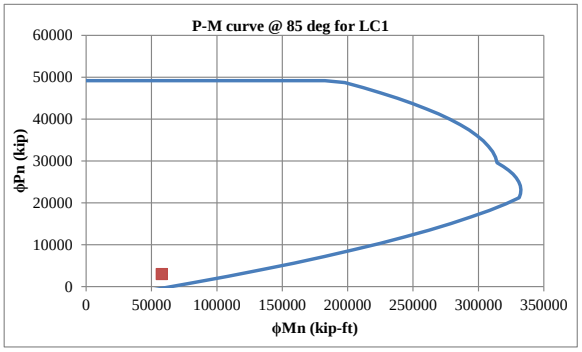

Since the design of the wall section is governed by the forces in the weak axis direction, the capacity in this direction is also checked against the forces due to earthquake in longitudinal direction EQ_x.		For EQ_x: P = 3,024 M_y = 18,217 kip-ft (R = 1.5) The interaction curve for $\theta = 0^o$ is: 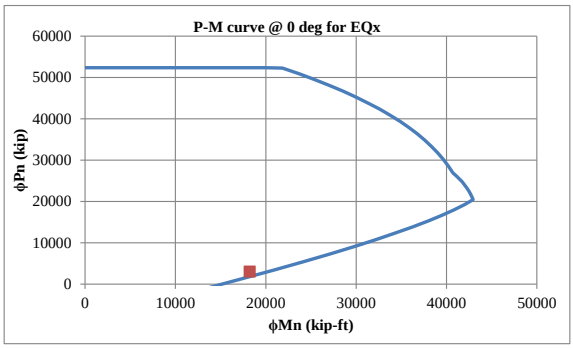 Therefore, selected section and its reinforcement are adequate.
Step 3: Determine shear resistance in the transverse direction. Transverse direction is the strong direction of the wall. The factored shear resistance, V_r, of the wall pier is taken as the lesser of (AASHTO Specifications Art. 5.10.11.4.2): $V_r = 0.253\sqrt{f_c'}bd$ and $V_r = 0.9\left[0.063\sqrt{f_c'} + \rho_h f_y\right]bd$ where ρ_h is the horizontal steel reinforcement ratio.		ρ_h = 0.0069 b = 48 in. d = 472 in. $V_r = 0.253\sqrt{4}(48)(472) = 11{,}464\ kips$ $V_r = 0.9\left[0.063\sqrt{4} + 0.0069(60)\right](48)(472)$ $= 11{,}011\ kips$ Therefore, V_r = 11,011 kips
Step 5: Check the vertical and horizontal reinforcements. The minimum vertical and horizontal reinforcement ratio shall satisfy (AASHTO Specifications Art. 5.10.11.4.2): $\rho_{v,h} \geq 0.0025$ The spacing of vertical and horizontal		$\rho_v = 0.0069 > 0.0025 \quad ok!$ $\rho_h = 0.0069 > 0.0025 \quad ok!$

reinforcement shall satisfy (AASHTO Specifications Art. 5.10.11.4.2): $s \leq 18\ in.$		$s = 6\ in. \leq 18\ in. \quad ok!$

9.5 Design of Ductile Cross-Frames

Step 1: Determine cross-frame force based on nominal shear resistance of the pier. The cross-frame shear force is equal to nominal shear resistance of pier in the transverse direction. $$V_{XF} = F_n = \frac{V_r}{\phi = 0.9}$$ where V_r is the factored shear resistance of wall pier. The corresponding cross-frame diagonal member axial force with *R* factor applied is: $$P_{XF1} = \frac{V_{XF}}{RN\cos\theta}$$ where *N* is the number of panels, θ is the angle of the diagonal from the horizontal, and *R* is the cross-frame modification factor and is equal to 4.0. In this equation, only one diagonal is assumed resisting the shear force. This is because, in a panel, one diagonal is in tension and the other one is in compression. The compression diagonal is expected to buckle in which case its post-buckling resistance is considerably smaller, thus the resistance is largely due to the yield resistance of the diagonal in tension.		V_r = 11,011 kips *N = 5* $\theta = 22^o$ $V_{XF} = \frac{11{,}011}{0.9} = 12{,}234\ kips$ $P_{XF1} = \frac{12{,}234}{4(5)\cos 22} = 660\ kips$
Step 2: Determine the cross-frame force from response spectrum analysis in the transverse direction. $$P_{XF2} = \frac{P_{EQY}}{R}$$		$P_{XF2} = \frac{609.72}{4} = 152.43\ kips$
Step 3: The design cross-frame force is the smaller of P_{XF1} or P_{XF2}. In bridges with wall piers, it is expected that P_{XF2} would govern due to large shear resistance of wall.		P_{XF} = 152.43 kips
Step 4: Determine cross-frame size. The required area is:		A36 single angle F_y = 36 ksi

$$A = \frac{P_{XF}}{F_y}$$ where F_y is the nominal yield stress of the cross-frame. The nominal value is used since P_{XF} was calculated from nominal shear force. Note that the size of the cross-frame may be governed by the compactness and slenderness requirements shown in *Step 5*.		$A = \frac{152.43}{36} = 4.23\ in^2$ Use *L4x4x3/4* A_g = 5.44 in^2 r_z = 0.774 in I = 7.62 in^4 x = 1.27 in. distance from connected leg of angle to its c.g. L = 142.62 in
Step 5: Check the compactness and slenderness ratios. The diagonal members of ductile cross-frames shall satisfy (proposed AASHTO Specifications Art. 6.16.4.5.2a): $$\frac{b}{t} \le 0.3\sqrt{\frac{E}{F_y}}$$ The slenderness ratio shall satisfy (proposed AASHTO Specifications Art. 6.16.4.5.2b): $$\frac{Kl}{r} \le 4.0\sqrt{\frac{E}{F_y}}$$ where K is 0.85, l is taken as one-half of the length of the diagonal member due to biased buckling, r is the radius of gyration normal to the plane of buckling and is equal to r_z for single angle members.		$\frac{4}{3/4} = 5.33 \le 0.3\sqrt{\frac{29{,}000}{36}} = 8.51, \quad ok!$ $\frac{0.85(142.62/2)}{0.774} = 78.31 \le 4\sqrt{\frac{29{,}000}{36}} = 113.53, \quad ok!$
Step 6: Calculate the expected yield resistance. $$P_{ye} = F_{ye}A_g$$ where F_{ye} is the expected yield stress and is equal to R_yF_y. For A36 steel sections, R_y = 1.5.		F_{ye} = 1.5(36) = 54 ksi $P_{ye} = 54(5.44) = 293.76\ kips$
Step 7: Calculate the expected compressive resistance. The compressive resistance is calculated		

according to AASHTO Specifications Art. 6.9.2.1, 6.9.4.1.1, and 6.9.4.1.2 $$P_e = \frac{\pi^2 E}{\left(\frac{Kl}{r_z}\right)^2} A_g$$ $$P_o = QF_{ye}A_g$$ The slender element reduction factor, *Q*, is equal to 1.0 when: $$\frac{b}{t} \leq 0.45\sqrt{\frac{E}{F_{ye}}}$$ ○ If $P_e/P_o \geq 0.44$ $$P_{nc} = \left[0.658^{(P_o/P_e)}\right]P_o$$ ○ If $P_e/P_o < 0.44$ $$P_{nc} = 0.877P_e$$		$P_e = \frac{\pi^2(29{,}000)}{(78.31)^2}(5.44) = 253.90\ kips$ $\frac{b}{t} = 5.3 \leq 0.45\sqrt{\frac{29{,}000}{54}} = 10.43, thus\ Q = 1.0$ $P_o = 1.0(54)(5.44) = 293.76\ kips$ $\frac{P_e}{P_o} = \frac{253.90}{293.76} = 0.864 > 0.44$ $P_{nc} = \left[0.658^{(1/0.864)}\right](293.76) = 181.00\ kips$
Step 8: Calculate the maximum expected lateral resistance of the cross-frames and compare against the pier nominal shear resistance. The maximum lateral resistance is the maximum of: $$V_{lat1} = (P_t + 0.3P_{nc})N\cos\theta$$ $$V_{lat2} = 2P_{nc}N\cos\theta$$ where $P_t = 1.2P_{ye}$ is the tensile resistance of the diagonal member. The 1.5 factor is to account for the upper bound of tensile resistance. The $0.3P_{nc}$ is the post-buckling resistance of the diagonal member. V_{lat1} typically governs particularly with relatively slender diagonal members. V_{lat2} may govern in cases when the diagonal members are short and stocky. The cross-frame maximum lateral resistance is compared against the pier nominal shear resistance to ensure elastic response.		$P_t = 1.5(293.76) = 440.64\ kips$ $V_{lat1} = [440.64 + 0.3(181.00)](5)\cos 22 = 2{,}294.50\ kips$ $V_{lat2} = [2(181.00)](5)\cos 22 = 1{,}678.20\ kips$ Therefore, V_{lat} = 2,295 kips $V_{lat} = 2{,}295\ kips < V_r/0.9 = 11{,}011/0.9 = 12{,}234\ kips \quad ok!$
***Step 9*:** Determine the superstructure drift and check against limit.		

After the cross-frame designed, the superstructure drift is determined. The superstructure lateral displacement is calculated using the equation: $$\Delta_{lat} = \frac{P_{EQY} L}{E A_e \cos\theta}$$ where, P_{EQY} is the force in the cross-frame diagonal member determined from response spectrum analysis in the transverse direction and A_e is the effective area calculated using Eqn. (1-12). The superstructure lateral drift should not exceed 4% (proposed AASHTO Specification Art. 6.16.4.5.1).		$A_e = \frac{5.44(7.62)}{7.62 + 5.44(1.27)^2} = 2.53\ in^2$ $\Delta_{lat} = \frac{609.72(142.62)}{29{,}000(2.53)\cos 22} = 1.28\ in.$ $Drift = \frac{1.28}{54} = 2.4\% < 4\%, ok!$

9.6 Cross-Frame Properties for Nonlinear Analysis

The expected force and displacement resistance of the cross-frames are calculated for use in the design evaluation.

Step 1: Calculate the expected tensile yield displacement. The expected yield resistance is calculated in Section 9.5 *Step 6*. The effective axial stiffness is: $$K_{XF\_e} = \frac{E A_e}{L}$$ where E is the modulus of elasticity of steel which is 29,000 ksi, A_e is the effective area calculated using Eqn. (1-12), and L is the total length of the diagonal member. The expected yield displacement is then calculated as: $$\Delta_{ye} = \frac{P_{ye}}{K_{XF\_e}}$$		*L4x4x3/4* P_{ye} = 293.76 kips A_g = 5.44 in^2 I = 7.62 in^4 x = 1.27 in. distance from connected leg of angle to its c.g. $A_e = \frac{5.44(7.62)}{7.62 + 5.44(1.27)^2} = 2.53\ in^2$ $K_{XF\_e} = \frac{29{,}000(2.53)}{142.62} = 514.14\ kip/in$ $\Delta_{ye} = \frac{293.76}{514.14} = 0.57\ in$
Step 2: Calculate the expected compressive displacement.		

The expected compressive resistance is calculated in Section 9.5 *Step 7*. The corresponding displacement is: $\Delta_{nc} = \frac{P_{nc}}{K_{XF\_e}}$		P_{nc} = 181.00 kips $\Delta_{nc} = \frac{181.00}{514.14} = 0.35\ in.$

9.7 Design Summary

The total weight of Ex. III-2 is 4,374 kips. From modal and response spectrum analyses, the periods, forces, and displacements are:

Parameter	Longitudinal Direction	Transverse Direction
Fundamental period, T (sec)	0.67	0.39
Base shear, V_b (kip)	4,014	5,771
Pier displacement, Δ_{pier} (in)	3.57	0.15
Pier Base Shear, F_b (kip)	1,136	2,885
Deck displacement, Δ_{deck} (in)	3.74	1.39

The wall pier properties are:

Width, w	40 ft
Thickness, t	4 ft
Vertical reinforcement	#9 @ 6 in. (total 158 - #9) (ρ_v = 0.69%)
Horizontal reinforcement	#9 @ 6 in. (ρ_h = 0.69%)
Factored shear resistance, V_r	11,011 kips

The cross-frame diagonal member section properties are:

Section	L4x4x3/4 (A36)
Area, A	5.44 in^2
Expected tensile yield resistance, P_{ye}	294 kips
Expected compressive resistance, P_{nc}	181 kips
Maximum lateral resistance, V_{lat}	2,295 kips

9.8 Nonlinear Evaluation

Example III-2 was analyzed using the ground motions described in Section 1.8.1. The ground motions were scaled to represent the Design (DE) and MCE Earthquake levels. There were seven DE runs and seven MCE runs for a total of fourteen runs. Because of this, only the column force-displacement plots from DE1, DE7, MCE1 and MCE7 are shown in Figure 9-5 and Figure 9-6 to represent the results. However, the column ductility ratios in the longitudinal direction for all runs are shown in Figure 9-7. Only the results in longitudinal direction are shown here because the transverse displacements were small and piers were elastic.

The yield displacements were calculated according to Section 1.8.2. Since the expected material properties were used in the nonlinear analyses, the yield displacements were also calculated using these properties. The yield displacement in the longitudinal direction is 2.07 in. The average ductility ratios were 1.8 from DE runs and 2.5 from MCE runs which are the same as those from Example III-1.

The negative stiffness observed in the hysteresis plots was not due to instability in the structure or computational error in the analysis. Rather, it is attributed to the coupled biaxial response of the column. This phenomenon was observed when the response is elastic and depends on the frequency content of the input motion and period of the structure (Monzon et al. 2013b).

Figure 9-8 shows the transverse base shear forces in the wall piers. Both DE and MCE runs have an average base shear of 2,700 kips. They were the same because the yielding cross-frames limited the seismic force in the transverse direction. At DE, this base shear is 75% of the base shear from Example III-1. At MCE, it is 57% of the base shear from Example III-1. The average of total bearing forces under DE and MCE is both 2,224 kips which is about the same as the expected lateral resistance of the cross-frames shown in Section 9.7.

Figure 9-9 and Figure 9-10 shows the superstructure force-displacement in the transverse direction under DE1, DE7, MCE1, and MCE7. As shown, there was significant yielding in the support cross-frames. It can be observed that the transverse shear force in the superstructure is about the same as the column transverse base shear, with the superstructure shear force slightly less. The difference is attributed to the inertia force in the wall pier.

The average lateral displacement of the superstructure under DE was 1.61 in. (3% drift). This is larger than the displacement calculated from the cross-frame design shown in Section 9.5 Step 9 (the displacement is 1.28 in. and the drift is 2.4%). This difference is attributed to the larger contribution of the higher modes to the superstructure transverse response. Figure 1-8 shows that the selected ground motions have higher spectral accelerations at short periods.

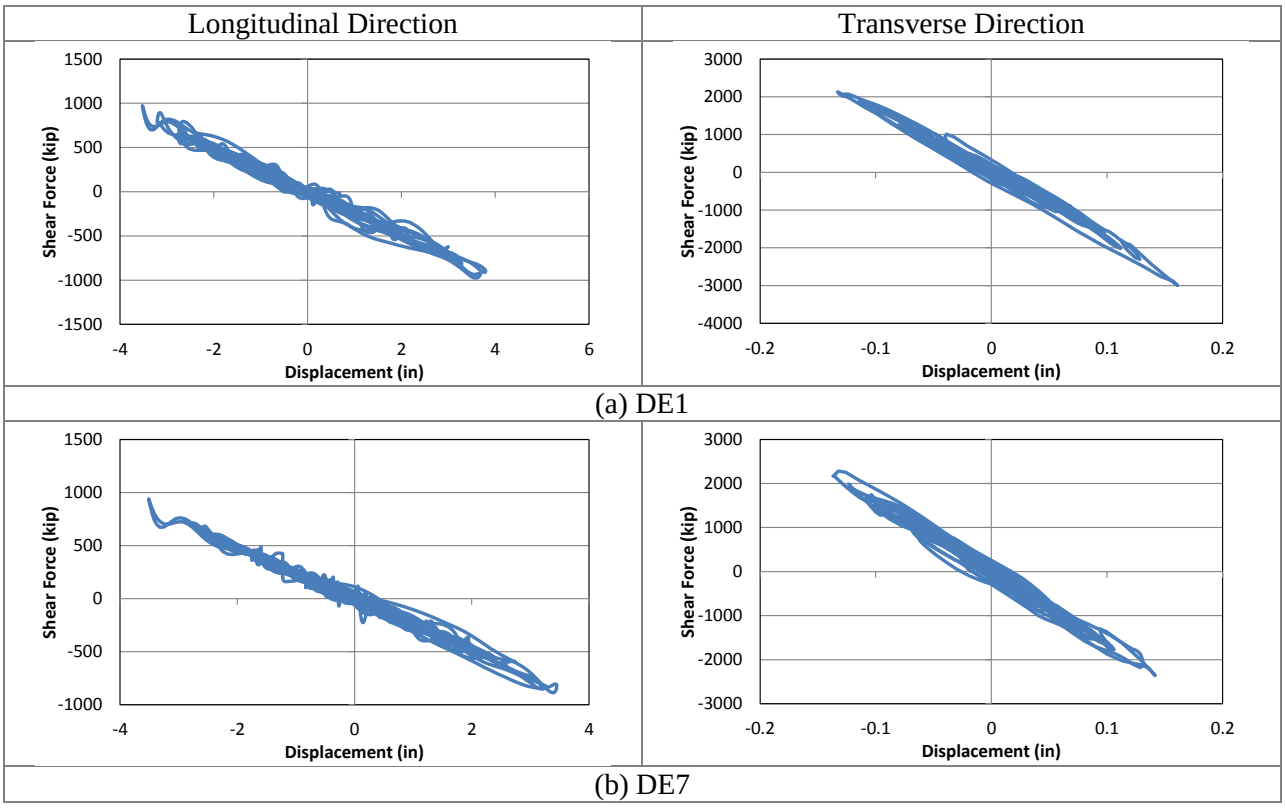

(a) DE1

(b) DE7

Figure 9-5 Column force-displacement plots from DE runs

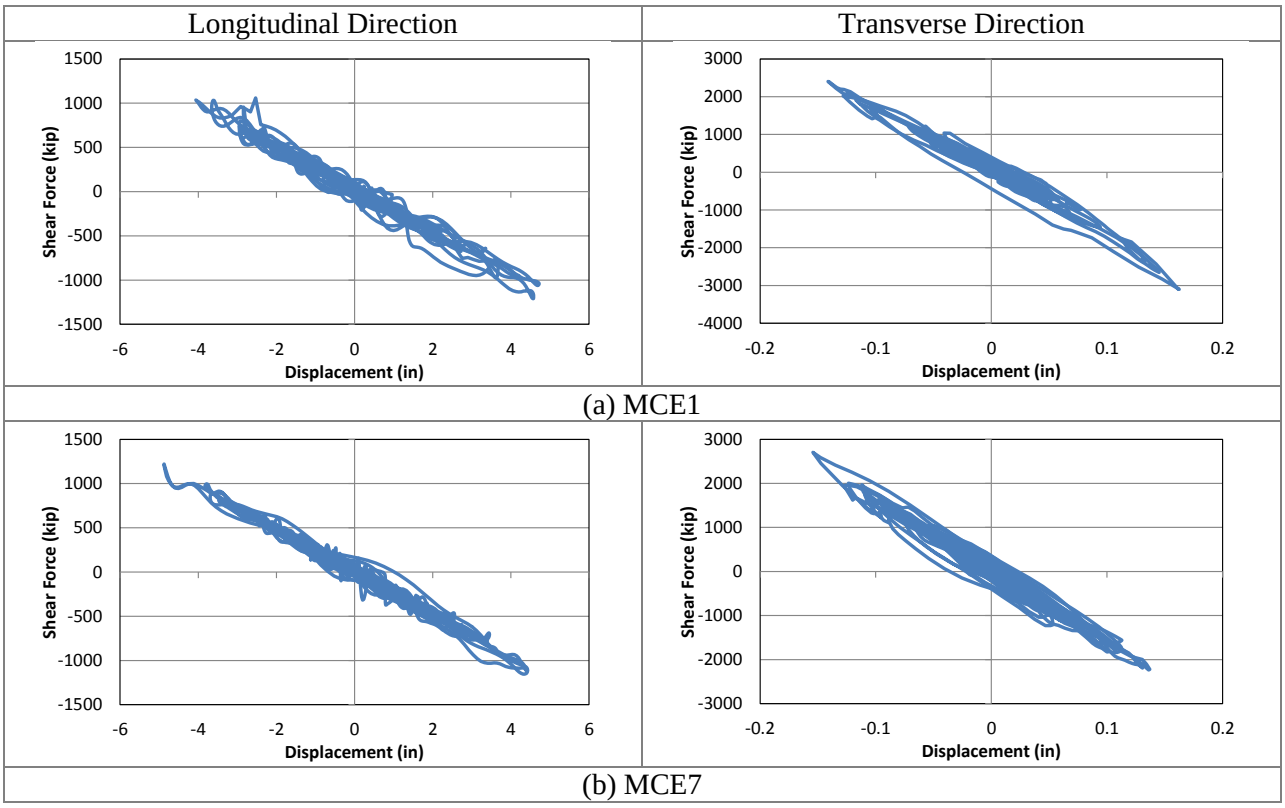

(a) MCE1

(b) MCE7

Figure 9-6 Column force-displacement plots from MCE runs

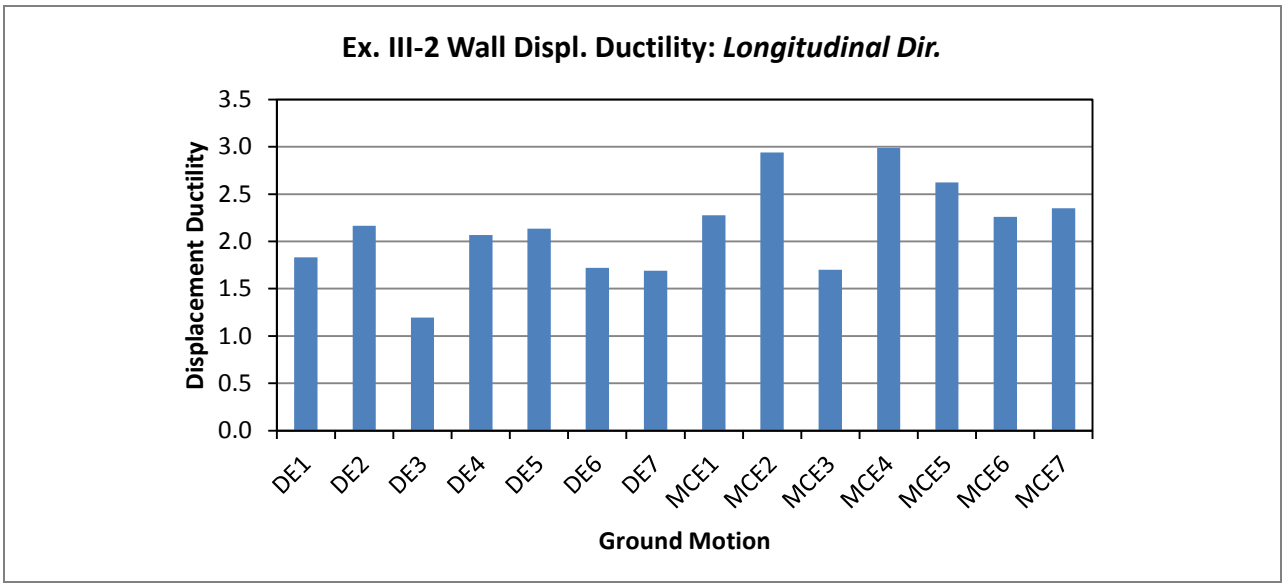

Figure 9-7 Summary of column displacement ductility in the longitudinal direction

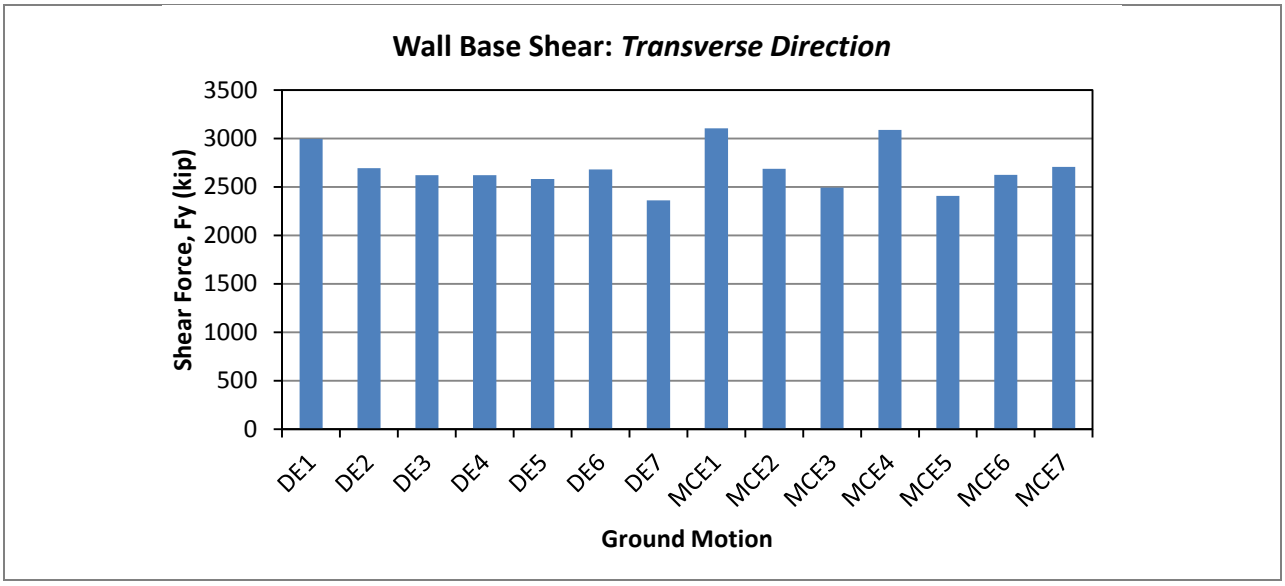

Figure 9-8 Summary of wall base shear in the transverse direction

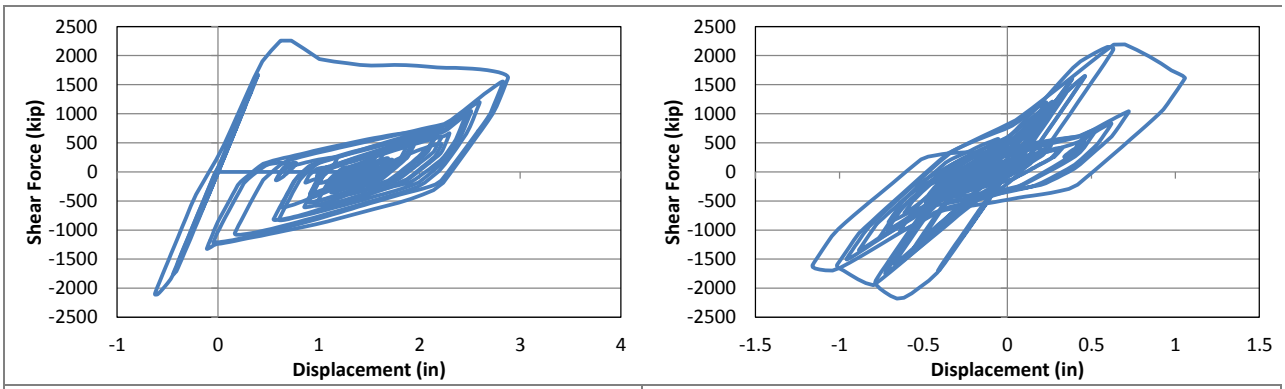

(a) DE1 (b) DE7

Figure 9-9 Superstructure force-displacement in the transverse direction from DE runs

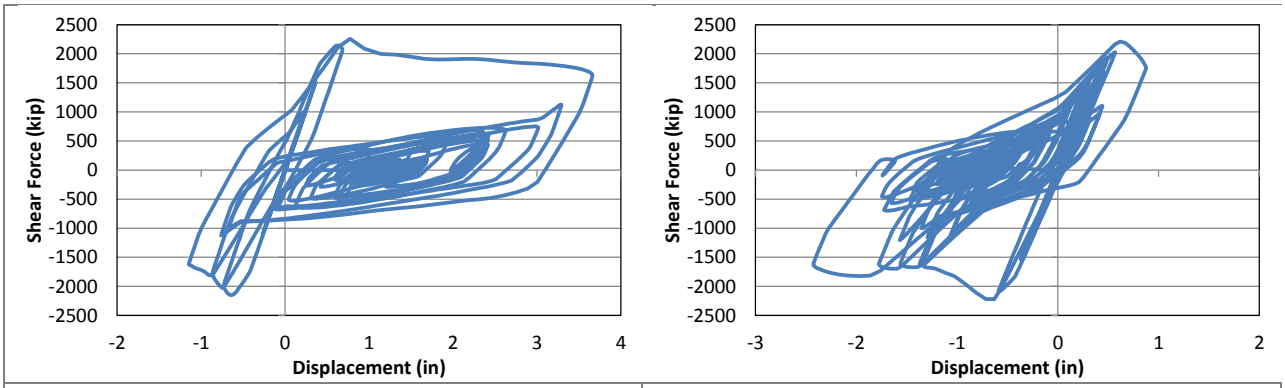

(a) MCE1 (b) MCE7

Figure 9-10 Superstructure force-displacement in the transverse direction from MCE runs

Chapter 10 Summary of Design and Nonlinear Evaluation

10.1 Overview

The DECF system is one of the several techniques that can be used to reduce ductility in the columns and may be used to protect the columns from damage during an earthquake. One advantage of this system over other forms of seismic protection is the smaller superstructure and substructure displacements. However, the beneficial effect of DECF is diminished when: (a) the pier is designed flexible and (b) when the pier has large ductility demand (i.e. large *R* factor) in the longitudinal direction. The DECF system works effectively when it is more flexible than the pier below it. If the pier is more flexible, then it will yield before the cross-frames undergo inelasticity. The benefit of the DECF is also diminished when the piers are designed to have large ductility demand in the longitudinal direction. In such case, the bridge response would be dominated by the longitudinal response and the columns would yield even though the DECF system limits the transverse seismic forces transferred to the columns.

Experimental and analytical investigations showed that DECF reduces the force and displacement demand in the transverse direction of the substructure. However, the DECF is ineffective in the longitudinal direction for a straight bridge due to its location and orientation. The nonlinear analysis of bridges designed using Type 2 strategy showed that the bridge response in one direction affects the total response. For example, the reduction of force in the column in the transverse direction reduces the overall (resultant) force in the column. This overall response is important particularly when minimal damage or bridge serviceability is required after an earthquake.

The nonlinear analysis of the design examples showed that the bridge responded as intended indicating the adequacy of the proposed design procedure for Type 2 strategy. There was minimal yielding in the columns such that they are considered essentially elastic even under the MCE-level earthquakes.

10.2 Design Examples Summary

The design using Types 1 and 2 strategies are summarized in Table 10-1 and the bridge response from elastic multimodal spectral analysis is summarized Table 10-2. For bridges with single and two-column piers, two bridges were designed using the Type 1 strategy – a bridge under operational category of ‘Other’ and a bridge under ‘Critical’ category. The bridges in the former were designed based on R-factor of 3.0 (for single-column pier) and 5.0 (for two-column pier) while in the latter the R-factors were both 1.5. The two categories were used to show which bridge category the DECF is more effective. A more direct comparison between the responses of ‘Critical’ bridge with Type 1 strategy and bridge with Type 2 strategy can be made because the R-factor used in both is 1.5. For the bridge with wall piers, since the R-factors are about the same – 2.0 for ‘Other’ category and 1.5 for ‘Critical’ – only one example was designed with Type 1 strategy. The design using either category would result in the same design.

As shown in Table 10-1, Ex. I-1a and II-1a resulted in smaller column because of larger R-factor. However, bridges with Type 2 strategy (Ex. I-2 and II-2) has smaller column than the 'Critical' bridges with Type 1 strategy (Ex. I-1b and II-1b) even though both use the same R-factor of 1.5. The flexibility provided by DECF to the superstructure in the transverse direction reduced the overall demand in the column. On the other hand, the larger cross-frame size needed in Type 1 strategy increases the transverse bridge stiffness which further increases the seismic force that resulted in larger column.

Table 10-1 Summary of design

Pier Type	Example No.	Oper. Category	Design Strategy	Pier Size	Reinforcement		Support Cross-Frames
					Long.	Trans.	
Single-column	I-1a	Other	Type 1	4 ft diameter	1%	1%	L8x8x5/8
	I-1b	Critical	Type 1	6.5 ft diameter	2.4%	1.1%	WT7x34
	I-2	---	Type 2	5.5 ft diameter	2.5%	1%	L3x3x3/8
Two-column	II-1a	Other	Type 1	4 ft diameter	1%	1.4%	L8x8x5/8
	II-1b	Critical	Type 1	6.5 ft diameter	2.4%	2.5%	WT9x65
	II-2	---	Type 2	5.5 ft diameter	2.8%	2.6%	L4x4x1/2
Wall	III-1	Other	Type 1	40 ft wide, 4 ft thick	0.69%	0.69%	L8x8x1
	III-2	---	Type 2	40 ft wide, 4 ft thick	0.69%	0.69%	L4x4x3/4

Table 10-2 Summary of elastic seismic analysis

Example No.	Fundamental Period (sec)		Bridge Base Shear (kip)		Bridge Deck Displacement (in)	
	Longitudinal	Transverse	Longitudinal	Transverse	Longitudinal	Transverse
I-1a	0.92	2.23	1,285	524	4.92	11.58
I-1b	0.49	0.58	2,780	1,354	2.8	3.2
I-2	0.58	1.22	2,150	973	3.18	5.78
II-1a	0.94	0.68	2,676	3,731	5.06	3.37
II-1b	0.51	0.35	5,722	6,681	2.97	0.97
II-2	0.61	0.48	4,351	5,569	3.35	2.25
III-1	0.67	0.31	4,014	5,151	3.74	0.61
III-2	0.67	0.39	4,014	5,771	3.74	1.39

10.3 Summary of Nonlinear Evaluations

The displacement ductility ratios are primarily used to compare the seismic response of the design examples. Even though they the pier have the same number of columns, each example is essentially a different bridge thus it is not fair to directly compare response parameters such as column displacements. The bearing forces are used to show the benefit of allowing the cross-frames to go nonlinear. But the comparison can only be made between 'Critical' bridge with Type 1 strategy and bridge with Type 2 strategy because both use the same R-factor and the columns remained essentially elastic in most cases. For the two examples with wall piers, the bearing forces are the only parameter used to compare the response because both have the same wall size and the wall remained elastic. The superstructure response is summarized using the maximum drift ratios.

10.3.1 Bridge with Single-Column Piers

It is shown in Table 10-3 that the column displacement ductility ratios in the longitudinal direction are about the same. Even though the columns are of different sizes, the ductility demand in this direction is limited by the soil response at the abutments.

In the transverse direction, Ex. I-1a has the largest ductility demand because of smaller column. Only the column resist the seismic forces in this direction thus the response is dependent on the column flexibility only. The ductility demand in Ex. I-1b is considerably low such that the column can be considered as essentially elastic, but this is expected since the R-factor used in the design is equal to 1.50. However, the ductility demand in Ex. I-2 is smaller compared to Ex. I-1b and is even about half at MCE. The DECF in Ex. I-2 limited the transverse forces transferred to the column resulting in less ductility demand even though its column is more flexible than Ex. I-1b. This is evident in Table 10-4 where it shown that the total bearing force in Ex. I-2 is about half of that in Ex. I-1b. For Ex. I-1a the bearing forces at DE and MCE are about the same because of column yielding. In this example, it was the column plastic shear force that limited the bearing forces.

The superstructure transverse displacements and corresponding drift ratios for Ex. I-2 are shown in Figure 10-1. The average drifts were 3.6 % under DE and 6.4% under MCE. The corresponding ductility demands in the cross-frames were 3.9 and 6.9.

Table 10-3 Average column displacement ductility in bridges with single-column piers

Example	Average Column Displacement Ductility			
	Design EQ		MCE	
	Longitudinal	Transverse	Longitudinal	Transverse
I-1a	1.5	2.4	1.9	3.1
I-1b	1.5	1.6	1.8	2.1
I-2	1.5	1.0	1.9	1.2

Table 10-4 Average of total bearing force in the transverse direction

Example	Average $\sum V_{brg\_trans}$ (kips)	
	Design EQ	MCE
I-1a	126	128
I-1b	575	641
I-2	257	274

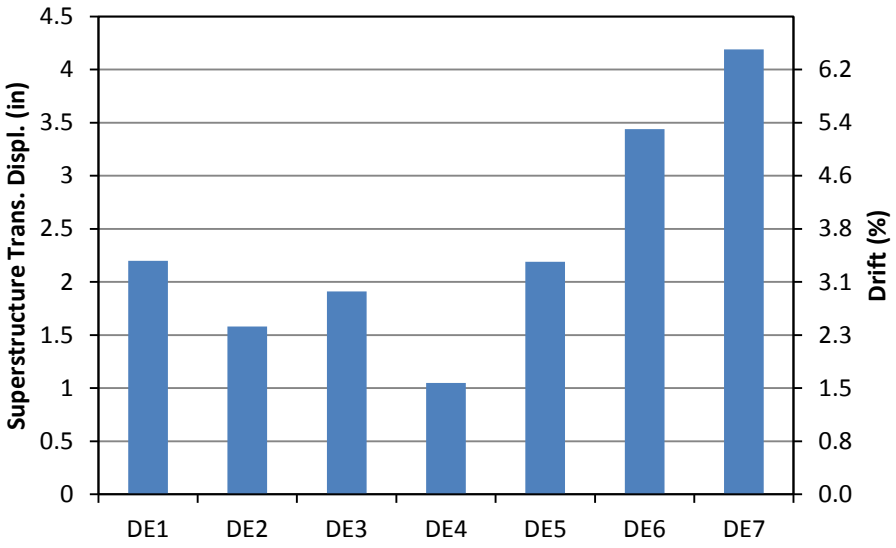

Figure 10-1 Summary of superstructure transverse displacement and drift ratios

10.3.2 Bridge with Two-Column Piers

The observations made in bridges with single-column pier are also true for bridges with two-column piers. The longitudinal ductility demands are about the same for all bridges. The transverse ductility demands in the column of bridge designed based on Type 2 strategy are about half of those in 'Critical' bridge designed based on Type 1 strategy. The total transverse bearing forces in Ex. II-2 are less than half of those in Ex. II-1b.

The superstructure transverse displacements and corresponding drift ratios for Ex. I-2 are shown in Figure 10-2. The average drifts were 3.7 % under DE and 5.3% under MCE. The corresponding ductility demands in the cross-frames were 3.6 and 5.1.

Table 10-5 Average column displacement ductility in bridges with two-column piers

Example	Average Column Displacement Ductility			
	Design EQ		MCE	
	Longitudinal	Transverse	Longitudinal	Transverse
II-1a	1.7	3.8	2.3	5.2
II-1b	1.6	2.0	1.9	2.9
II-2	1.6	1.3	1.9	1.4

Table 10-6 Average of total bearing force in the transverse direction

Example	Average $\sum V_{brg\_trans}$ (kips)	
	Design EQ	MCE
II-1a	902	1010
II-1b	3,372	4,018
II-2	1,534	1,554

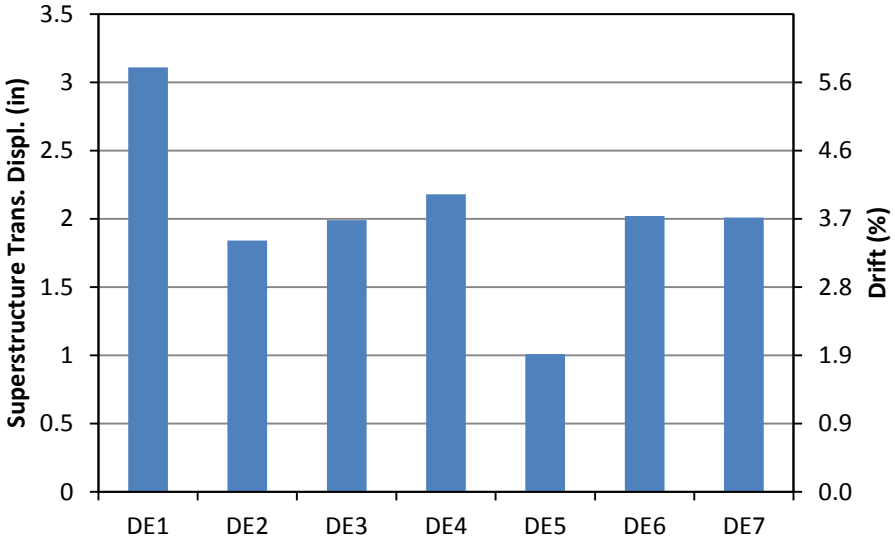

Figure 10-2 Summary of superstructure transverse displacement and drift ratios

10.3.3 Bridge with Wall Piers

In the longitudinal direction, the pier ductility demands in Ex. III-1 and III-2 are the same because both have the same pier size. In the transverse direction, the pier is stiff and has large shear capacity thus it remained elastic. The only difference between the two examples is the magnitude of transverse bearing

forces as shown in Table 10-7. In Ex. III-2, the bearing force was limited by the DECF and it was the same for both DE and MCE.

The superstructure transverse displacements and corresponding drift ratios for Ex. I-2 are shown in Figure 10-3. The average drifts were 3.0 % under DE and 4.8% under MCE. The corresponding ductility demands in the cross-frames were 2.6 and 4.2.

Table 10-7 Average of total bearing force in the transverse direction

Example	Average $\sum V_{brg\_trans}$ (kips)	
	Design EQ	MCE
III-1	3,206	4,393
II-2	2,224	2,224

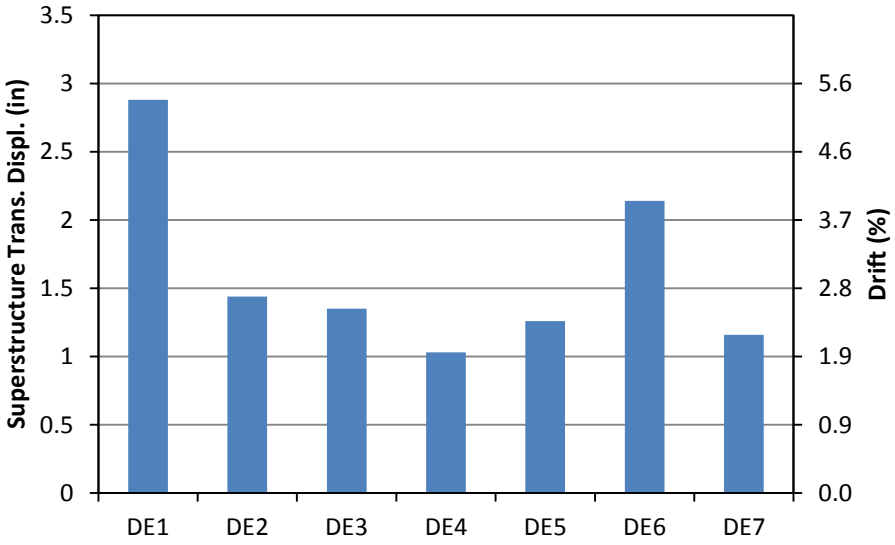

Figure 10-3 Summary of superstructure transverse displacement and drift ratios

10.4 Concluding Remarks

This report presents a proposed 'force-based' design procedure that will achieve an essentially elastic substructure and ductile superstructure. The reinforced concrete (R/C) substructure flexural resistance is designed for the combined effect of seismic forces similar to conventional seismic design with a force reduction factor equal to 1.5. Meanwhile, the shear resistance and the confinement requirements of the substructure are determined in a way similar to the seismic design of conventional bridges. To achieve a ductile superstructure, the horizontal resistance of the support cross frames is based on the lesser of the pier nominal shear resistance and the elastic seismic cross forces obtained from the response spectrum analysis, divided by a proposed response modification factor for ductile cross frames equal to 4. This will ensure that support cross frames will act as a 'fuse' and will not subject the substructure to forces that

may cause nonlinear response in that direction. To achieve a ductile response of support cross frames, the diagonal members, which are expected to undergo inelastic response, are detailed to have limits on width-to-thickness and slenderness ratios. The other cross frame components and the shear resistance of the substructure are then checked for a fully yielded and strain hardened support cross frame.

The nonlinear seismic evaluation of the design examples verified the seismic performance of bridge design according to the proposed Type 2 bridges. The inelasticity was concentrated at the support cross frames while the substructure remained elastic. Furthermore, this evaluation showed the substructure also remained essentially elastic even for ground motions at the MCE level. The main advantages of utilizing Type 2 design strategy can be realized in post-earthquake repair since the substructure will remain elastic while only the nonlinear elements that need to be replaced is the end cross frames. This performance may be also achieved by using Type 1 performance criteria with critical bridges, however, the size of the cross frames that is required for this design will be substantially larger than the one obtained using type 2. This will require larger cross frames, bearings, and foundation.

The nonlinear seismic analysis also showed that stiff substructure i.e. pier walls shows great advantages of using this strategy. The ductile end cross frames provide a "fuse" for the seismic forces and thus limits the force transfer to the pier wall and to its foundation. Furthermore, the seismic analysis of conventional design of example III-1 showed that the superstructure experienced nonlinear activity and subjected to the bearing to forces that are not designed for. The failure of these bearing may cause unseating of the superstructure if adequate support length was not provided on the top of the pier wall.

References

AASHTO. 2012. *AASHTO LRFD Bridge Design Specifications*, American Association of State Highway and Transportation Officials, Washington, D.C.

AASHTO. 2012. *AASHTO Guide Specifications for LRFD Bridge Seismic Design*, American Association of State Highway and Transportation Officials, Washington, D.C.

ASCE. 2010. *Minimum Design Loads for Buildings and Other Structures*, American Society of Civil Engineers, Reston, VA.

AISC. 2010a. *Specifications for Structural Steel Buildings*, American Institute of Steel Construction, Chicago, IL.

AISC. 2010b. *Seismic Provisions for Structural Steel Buildings*, American Institute of Steel Construction, Chicago, IL.

Alfawakhiri, F. and Bruneau, M. 2001. "Local versus Global Ductility Demands in Simple Bridges," *Journal of Structural Engineering*, 127(5), 554-560.

Astaneh-Asl, A., Goel, S.C. and Hanson, R.D., 1985, *Cyclic Out-of-Plane Buckling of Double Angle Bracing*. Report UCB/CE-STEEL-94/01. Department of Civil Engineering, University of California at Berkeley, Berkeley, CA.

Bahrami, H., Itani, A.M., and Buckle, I.G. 2010. *Guidelines for the Seismic Design of Ductile End Cross-Frames in Steel Girder Bridge Superstructures*, CCEER Report No. 09-04, Center for Civil Engineering Research, University of Nevada, Reno, NV.

Carden, L.P., Itani, A.M., and Buckle, I.G. 2005a. *Seismic Load Path in Steel Girder Bridge Superstructures*, CCEER Report No. 05-03, Center for Civil Engineering Research, University of Nevada, Reno, NV.

Carden, L.P., Itani, A.M., and Buckle, I.G. 2005b. *Seismic Performance of Steel Girder Bridge Superstructures with Ductile End Cross-Frames and Seismic Isolation*, CCEER Report No. 05-04, Center for Civil Engineering Research, University of Nevada, Reno, NV.

Carden, L.P., Garcia-Alvarez, F., Itani, A.M., and Buckle, I.G. 2006. "Cyclic Behavior of Single Angles for Ductile End Cross-Frames," *AISC Engineering Journal*, 2nd Quarter, 2006, 111-125.

CSI. 2012. *SAP2000*, Computers and Structures, Inc., Berkeley, CA>

Goel, S.C. and El-Tayem, A. 1986. "Cyclic Load Behavior of Angle X-Bracing," *Journal of Structural Engineering*, 112(11), 2528-2539.

Itani, A.M. and Goel, S.C. 1991. *Earthquake Resistant Design of Open Web Framing Systems*, Research Report No. UMCE 91-21, Department of Civil and Environmental Engineering, University of Michigan, Ann Arbor, MI.

Itani, A.M., Bruneau, M., Carden, L., and Buckle, I.G. 2004. "Seismic Behavior Steel Girder Bridge Superstructures," Journal of Bridge Engineering, 1(8), 243-249.

Monzon, E.V., Itani, A.M., and Buckle, I.G. 2013a. *Seismic Modeling and Analysis of Curved Steel Plate Girder Bridges*, CCEER Report No. 13-05, Center for Civil Engineering Research, University of Nevada, Reno, NV.

Monzon, E.V., Itani, A.M., and Buckle, I.G. 2013b. *Seismic Performance of Curved Steel Plate Girder Bridges with Seismic Isolation*, CCEER Report No. 13-06, Center for Civil Engineering Research, University of Nevada, Reno, NV.

PEER. 2013. *PEER Ground Motion Database*, Pacific Earthquake Engineering Research Center, Berkeley, CA.

LIST OF CCEER PUBLICATIONS

Report No. **Publication**

CCEER-84-1 Saiidi, M., and R. Lawver, "User's Manual for LZAK-C64, A Computer Program to Implement the Q-Model on Commodore 64," Civil Engineering Department, Report No. CCEER-84-1, University of Nevada, Reno, January 1984.

CCEER-84-1 Reprint Douglas, B., Norris, G., Saiidi, M., Dodd, L., Richardson, J. and Reid, W., "Simple Bridge Models for Earthquakes and Test Data," Civil Engineering Department, Report No. CCEER-84-1 Reprint, University of Nevada, Reno, January 1984.

CCEER-84-2 Douglas, B. and T. Iwasaki, "Proceedings of the First USA-Japan Bridge Engineering Workshop," held at the Public Works Research Institute, Tsukuba, Japan, Civil Engineering Department, Report No. CCEER-84-2, University of Nevada, Reno, April 1984.

CCEER-84-3 Saiidi, M., J. Hart, and B. Douglas, "Inelastic Static and Dynamic Analysis of Short R/C Bridges Subjected to Lateral Loads," Civil Engineering Department, Report No. CCEER-84-3, University of Nevada, Reno, July 1984.

CCEER-84-4 Douglas, B., "A Proposed Plan for a National Bridge Engineering Laboratory," Civil Engineering Department, Report No. CCEER-84-4, University of Nevada, Reno, December 1984.

CCEER-85-1 Norris, G. and P. Abdollaholiaee, "Laterally Loaded Pile Response: Studies with the Strain Wedge Model," Civil Engineering Department, Report No. CCEER-85-1, University of Nevada, Reno, April 1985.

CCEER-86-1 Ghusn, G. and M. Saiidi, "A Simple Hysteretic Element for Biaxial Bending of

R/C in NEABS-86," Civil Engineering Department, Report No. CCEER-86-1, University of Nevada, Reno, July 1986.

CCEER-86-2 Saiidi, M., R. Lawver, and J. Hart, "User's Manual of ISADAB and SIBA, Computer Programs for Nonlinear Transverse Analysis of Highway Bridges Subjected to Static and Dynamic Lateral Loads," Civil Engineering Department, Report No. CCEER-86-2, University of Nevada, Reno, September 1986.

CCEER-87-1 Siddharthan, R., "Dynamic Effective Stress Response of Surface and Embedded Footings in Sand," Civil Engineering Department, Report No. CCEER-86-2, University of Nevada, Reno, June 1987.

CCEER-87-2 Norris, G. and R. Sack, "Lateral and Rotational Stiffness of Pile Groups for Seismic Analysis of Highway Bridges," Civil Engineering Department, Report No. CCEER-87-2, University of Nevada, Reno, June 1987.

CCEER-88-1 Orie, J. and M. Saiidi, "A Preliminary Study of One-Way Reinforced Concrete Pier Hinges Subjected to Shear and Flexure," Civil Engineering Department, Report No. CCEER-88-1, University of Nevada, Reno, January 1988.

CCEER-88-2 Orie, D., M. Saiidi, and B. Douglas, "A Micro-CAD System for Seismic Design of Regular Highway Bridges," Civil Engineering Department, Report No. CCEER-88-2, University of Nevada, Reno, June 1988.

CCEER-88-3 Orie, D. and M. Saiidi, "User's Manual for Micro-SARB, a Microcomputer Program for Seismic Analysis of Regular Highway Bridges," Civil Engineering Department, Report No. CCEER-88-3, University of Nevada, Reno, October 1988.

CCEER-89-1 Douglas, B., M. Saiidi, R. Hayes, and G. Holcomb, "A Comprehensive Study of the Loads and Pressures Exerted on Wall Forms by the Placement of Concrete," Civil Engineering Department, Report No. CCEER-89-1, University of Nevada, Reno, February 1989.

CCEER-89-2 Richardson, J. and B. Douglas, "Dynamic Response Analysis of the Dominion Road Bridge Test Data," Civil Engineering Department, Report No. CCEER-89-2, University of Nevada, Reno, March 1989.

CCEER-89-2 Vrontinos, S., M. Saiidi, and B. Douglas, "A Simple Model to Predict the Ultimate Response of R/C Beams with Concrete Overlays," Civil Engineering Department, Report NO. CCEER-89-2, University of Nevada, Reno, June 1989.

CCEER-89-3 Ebrahimpour, A. and P. Jagadish, "Statistical Modeling of Bridge Traffic Loads - A Case Study," Civil Engineering Department, Report No. CCEER-89-3, University of Nevada, Reno, December 1989.

CCEER-89-4 Shields, J. and M. Saiidi, "Direct Field Measurement of Prestress Losses in Box Girder Bridges," Civil Engineering Department, Report No. CCEER-89-4, University of Nevada, Reno, December 1989.

CCEER-90-1 Saiidi, M., E. Maragakis, G. Ghusn, Y. Jiang, and D. Schwartz, "Survey and Evaluation of Nevada's Transportation Infrastructure, Task 7.2 - Highway Bridges, Final Report," Civil Engineering Department, Report No. CCEER 90-1, University of Nevada, Reno, October 1990.

CCEER-90-2 Abdel-Ghaffar, S., E. Maragakis, and M. Saiidi, "Analysis of the Response of Reinforced Concrete Structures During the Whittier Earthquake 1987," Civil Engineering Department, Report No. CCEER 90-2, University of Nevada, Reno, October 1990.

CCEER-91-1 Saiidi, M., E. Hwang, E. Maragakis, and B. Douglas, "Dynamic Testing and the Analysis of the Flamingo Road Interchange," Civil Engineering Department, Report No. CCEER-91-1, University of Nevada, Reno, February 1991.

CCEER-91-2 Norris, G., R. Siddharthan, Z. Zafir, S. Abdel-Ghaffar, and P. Gowda, "Soil-Foundation-Structure Behavior at the Oakland Outer Harbor Wharf," Civil

Engineering Department, Report No. CCEER-91-2, University of Nevada, Reno, July 1991.

CCEER-91-3 Norris, G., "Seismic Lateral and Rotational Pile Foundation Stiffnesses at Cypress," Civil Engineering Department, Report No. CCEER-91-3, University of Nevada, Reno, August 1991.

CCEER-91-4 O'Connor, D. and M. Saiidi, "A Study of Protective Overlays for Highway Bridge Decks in Nevada, with Emphasis on Polyester-Styrene Polymer Concrete," Civil Engineering Department, Report No. CCEER-91-4, University of Nevada, Reno, October 1991.

CCEER-91-5 O'Connor, D.N. and M. Saiidi, "Laboratory Studies of Polyester-Styrene Polymer Concrete Engineering Properties," Civil Engineering Department, Report No. CCEER-91-5, University of Nevada, Reno, November 1991.

CCEER-92-1 Straw, D.L. and M. Saiidi, "Scale Model Testing of One-Way Reinforced Concrete Pier Hinges Subject to Combined Axial Force, Shear and Flexure," edited by D.N. O'Connor, Civil Engineering Department, Report No. CCEER-92-1, University of Nevada, Reno, March 1992.

CCEER-92-2 Wehbe, N., M. Saiidi, and F. Gordaninejad, "Basic Behavior of Composite Sections Made of Concrete Slabs and Graphite Epoxy Beams," Civil Engineering Department, Report No. CCEER-92-2, University of Nevada, Reno, August 1992.

CCEER-92-3 Saiidi, M. and E. Hutchens, "A Study of Prestress Changes in A Post-Tensioned Bridge During the First 30 Months," Civil Engineering Department, Report No. CCEER-92-3, University of Nevada, Reno, April 1992.

CCEER-92-4 Saiidi, M., B. Douglas, S. Feng, E. Hwang, and E. Maragakis, "Effects of Axial Force on Frequency of Prestressed Concrete Bridges," Civil Engineering Department, Report No. CCEER-92-4, University of Nevada, Reno, August 1992.

CCEER-92-5 Siddharthan, R., and Z. Zafir, "Response of Layered Deposits to Traveling Surface Pressure Waves," Civil Engineering Department, Report No. CCEER-92-5, University of Nevada, Reno, September 1992.

CCEER-92-6 Norris, G., and Z. Zafir, "Liquefaction and Residual Strength of Loose Sands from Drained Triaxial Tests," Civil Engineering Department, Report No. CCEER-92-6, University of Nevada, Reno, September 1992.

CCEER-92-6-A Norris, G., Siddharthan, R., Zafir, Z. and Madhu, R. "Liquefaction and Residual Strength of Sands from Drained Triaxial Tests," Civil Engineering Department, Report No. CCEER-92-6-A, University of Nevada, Reno, September 1992.

CCEER-92-7 Douglas, B., "Some Thoughts Regarding the Improvement of the University of Nevada, Reno's National Academic Standing," Civil Engineering Department, Report No. CCEER-92-7, University of Nevada, Reno, September 1992.

CCEER-92-8 Saiidi, M., E. Maragakis, and S. Feng, "An Evaluation of the Current Caltrans Seismic Restrainer Design Method," Civil Engineering Department, Report No. CCEER-92-8, University of Nevada, Reno, October 1992.

CCEER-92-9 O'Connor, D., M. Saiidi, and E. Maragakis, "Effect of Hinge Restrainers on the Response of the Madrone Drive Undercrossing During the Loma Prieta Earthquake," Civil Engineering Department, Report No. CCEER-92-9, University of Nevada, Reno, February 1993.

CCEER-92-10 O'Connor, D., and M. Saiidi, "Laboratory Studies of Polyester Concrete: Compressive Strength at Elevated Temperatures and Following Temperature Cycling, Bond Strength to Portland Cement Concrete, and Modulus of Elasticity," Civil Engineering Department, Report No. CCEER-92-10, University of Nevada, Reno, February 1993.

CCEER-92-11 Wehbe, N., M. Saiidi, and D. O'Connor, "Economic Impact of Passage of Spent

Fuel Traffic on Two Bridges in Northeast Nevada," Civil Engineering Department, Report No. CCEER-92-11, University of Nevada, Reno, December 1992.

CCEER-93-1 Jiang, Y., and M. Saiidi, "Behavior, Design, and Retrofit of Reinforced Concrete One-way Bridge Column Hinges," edited by D. O'Connor, Civil Engineering Department, Report No. CCEER-93-1, University of Nevada, Reno, March 1993.

CCEER-93-2 Abdel-Ghaffar, S., E. Maragakis, and M. Saiidi, "Evaluation of the Response of the Aptos Creek Bridge During the 1989 Loma Prieta Earthquake," Civil Engineering Department, Report No. CCEER-93-2, University of Nevada, Reno, June 1993.

CCEER-93-3 Sanders, D.H., B.M. Douglas, and T.L. Martin, "Seismic Retrofit Prioritization of Nevada Bridges," Civil Engineering Department, Report No. CCEER-93-3, University of Nevada, Reno, July 1993.

CCEER-93-4 Abdel-Ghaffar, S., E. Maragakis, and M. Saiidi, "Performance of Hinge Restrainers in the Huntington Avenue Overhead During the 1989 Loma Prieta Earthquake," Civil Engineering Department, Report No. CCEER-93-4, University of Nevada, Reno, June 1993 (in final preparation).

CCEER-93-5 Maragakis, E., M. Saiidi, S. Feng, and L. Flournoy, "Effects of Hinge Restrainers on the Response of the San Gregorio Bridge during the Loma Prieta Earthquake," (in final preparation) Civil Engineering Department, Report No. CCEER-93-5, University of Nevada, Reno.

CCEER-93-6 Saiidi, M., E. Maragakis, S. Abdel-Ghaffar, S. Feng, and D. O'Connor, "Response of Bridge Hinge Restrainers during Earthquakes -Field Performance, Analysis, and Design," Civil Engineering Department, Report No. CCEER-93-6, University of Nevada, Reno, May 1993.

CCEER-93-7 Wehbe, N., Saiidi, M., Maragakis, E., and Sanders, D., "Adequacy of Three Highway Structures in Southern Nevada for Spent Fuel Transportation," Civil Engineering Department, Report No. CCEER-93-7, University of Nevada, Reno,

August 1993.

CCEER-93-8 Roybal, J., Sanders, D.H., and Maragakis, E., "Vulnerability Assessment of Masonry in the Reno-Carson City Urban Corridor," Civil Engineering Department, Report No. CCEER-93-8, University of Nevada, Reno, May 1993.

CCEER-93-9 Zafir, Z. and Siddharthan, R., "MOVLOAD: A Program to Determine the Behavior of Nonlinear Horizontally Layered Medium Under Moving Load," Civil Engineering Department, Report No. CCEER-93-9, University of Nevada, Reno, August 1993.

CCEER-93-10 O'Connor, D.N., Saiidi, M., and Maragakis, E.A., "A Study of Bridge Column Seismic Damage Susceptibility at the Interstate 80/U.S. 395 Interchange in Reno, Nevada," Civil Engineering Department, Report No. CCEER-93-10, University of Nevada, Reno, October 1993.

CCEER-94-1 Maragakis, E., B. Douglas, and E. Abdelwahed, "Preliminary Dynamic Analysis of a Railroad Bridge," Report CCEER-94-1, January 1994.

CCEER-94-2 Douglas, B.M., Maragakis, E.A., and Feng, S., "Stiffness Evaluation of Pile Foundation of Cazenovia Creek Overpass," Civil Engineering Department, Report No. CCEER-94-2, University of Nevada, Reno, March 1994.

CCEER-94-3 Douglas, B.M., Maragakis, E.A., and Feng, S., "Summary of Pretest Analysis of Cazenovia Creek Bridge," Civil Engineering Department, Report No. CCEER-94-3, University of Nevada, Reno, April 1994.

CCEER-94-4 Norris, G.M., Madhu, R., Valceschini, R., and Ashour, M., "Liquefaction and Residual Strength of Loose Sands from Drained Triaxial Tests," Report 2, Vol. 1&2, Civil Engineering Department, Report No. CCEER-94-4, University of Nevada, Reno, August 1994.

CCEER-94-5 Saiidi, M., Hutchens, E., and Gardella, D., "Prestress Losses in a Post-Tensioned R/C Box Girder Bridge in Southern Nevada," Civil Engineering Department, CCEER-94-5, University of Nevada, Reno, August 1994.

CCEER-95-1 Siddharthan, R., El-Gamal, M., and Maragakis, E.A., "Nonlinear Bridge Abutment , Verification, and Design Curves," Civil Engineering Department, CCEER-95-1, University of Nevada, Reno, January 1995.

CCEER-95-2 Ashour, M. and Norris, G., "Liquefaction and Undrained Response Evaluation of Sands from Drained Formulation," Civil Engineering Department, Report No. CCEER-95-2, University of Nevada, Reno, February 1995.

CCEER-95-3 Wehbe, N., Saiidi, M., Sanders, D. and Douglas, B., "Ductility of Rectangular Reinforced Concrete Bridge Columns with Moderate Confinement," Civil Engineering Department, Report No. CCEER-95-3, University of Nevada, Reno, July 1995.

CCEER-95-4 Martin, T.., Saiidi, M. and Sanders, D., "Seismic Retrofit of Column-Pier Cap Connections in Bridges in Northern Nevada," Civil Engineering Department, Report No. CCEER-95-4, University of Nevada, Reno, August 1995.

CCEER-95-5 Darwish, I., Saiidi, M. and Sanders, D., "Experimental Study of Seismic Susceptibility Column-Footing Connections in Bridges in Northern Nevada," Civil Engineering Department, Report No. CCEER-95-5, University of Nevada, Reno, September 1995.

CCEER-95-6 Griffin, G., Saiidi, M. and Maragakis, E., "Nonlinear Seismic Response of Isolated Bridges and Effects of Pier Ductility Demand," Civil Engineering Department, Report No. CCEER-95-6, University of Nevada, Reno, November 1995.

CCEER-95-7 Acharya, S.., Saiidi, M. and Sanders, D., "Seismic Retrofit of Bridge Footings and Column-Footing Connections," Civil Engineering Department, Report No. CCEER-95-7, University of Nevada, Reno, November 1995.

CCEER-95-8 Maragakis, E., Douglas, B., and Sandirasegaram, U., "Full-Scale Field Resonance Tests of a Railway Bridge," A Report to the Association of American Railroads, Civil Engineering Department, Report No. CCEER-95-8, University of Nevada, Reno, December 1995.

CCEER-95-9 Douglas, B., Maragakis, E. and Feng, S., "System Identification Studies on Cazenovia Creek Overpass," Report for the National Center for Earthquake Engineering Research, Civil Engineering Department, Report No. CCEER-95-9, University of Nevada, Reno, October 1995.

CCEER-96-1 El-Gamal, M.E. and Siddharthan, R.V., "Programs to Computer Translational Stiffness of Seat-Type Bridge Abutment," Civil Engineering Department, Report No. CCEER-96-1, University of Nevada, Reno, March 1996.

CCEER-96-2 Labia, Y., Saiidi, M. and Douglas, B., "Evaluation and Repair of Full-Scale Prestressed Concrete Box Girders," A Report to the National Science Foundation, Research Grant CMS-9201908, Civil Engineering Department, Report No. CCEER-96-2, University of Nevada, Reno, May 1996.

CCEER-96-3 Darwish, I., Saiidi, M. and Sanders, D., "Seismic Retrofit of R/C Oblong Tapered Bridge Columns with Inadequate Bar Anchorage in Columns and Footings," A Report to the Nevada Department of Transportation, Civil Engineering Department, Report No. CCEER-96-3, University of Nevada, Reno, May 1996.

CCEER-96-4 Ashour, M., Pilling, R., Norris, G. and Perez, H., "The Prediction of Lateral Load Behavior of Single Piles and Pile Groups Using the Strain Wedge Model," A Report to the California Department of Transportation, Civil Engineering Department, Report No. CCEER-96-4, University of Nevada, Reno, June 1996.

CCEER-97-1-A Rimal, P. and Itani, A. "Sensitivity Analysis of Fatigue Evaluations of Steel Bridges," Center for Earthquake Research, Department of Civil Engineering, University of Nevada, Reno, Nevada Report No. CCEER-97-1-A, September, 1997.

CCEER-97-1-B Maragakis, E., Douglas, B., and Sandirasegaram, U. "Full-Scale Field Resonance Tests of a Railway Bridge," A Report to the Association of American Railroads, Civil Engineering Department, University of Nevada, Reno, May, 1996.

CCEER-97-2 Wehbe, N., Saiidi, M., and D. Sanders, "Effect of Confinement and Flares on the Seismic Performance of Reinforced Concrete Bridge Columns," Civil Engineering Department, Report No. CCEER-97-2, University of Nevada, Reno, September 1997.

CCEER-97-3 Darwish, I., M. Saiidi, G. Norris, and E. Maragakis, "Determination of In-Situ Footing Stiffness Using Full-Scale Dynamic Field Testing," A Report to the Nevada Department of Transportation, Structural Design Division, Carson City, Nevada, Report No. CCEER-97-3, University of Nevada, Reno, October 1997.

CCEER-97-4-A Itani, A. "Cyclic Behavior of Richmond-San Rafael Tower Links," Center for Civil Engineering Earthquake Research, Department of Civil Engineering, University of Nevada, Reno, Nevada, Report No. CCEER-97-4, August 1997.

CCEER-97-4-B Wehbe, N., and M. Saiidi, "User's Manual for RCMC v. 1.2 : A Computer Program for Moment-Curvature Analysis of Confined and Unconfined Reinforced Concrete Sections," Center for Civil Engineering Earthquake Research, Department of Civil Engineering, University of Nevada, Reno, Nevada, Report No. CCEER-97-4, November, 1997.

CCEER-97-5 Isakovic, T., M. Saiidi, and A. Itani, "Influence of new Bridge Configurations on Seismic Performance," Department of Civil Engineering, University of Nevada, Reno, Report No. CCEER-97-5, September, 1997.

CCEER-98-1 Itani, A., Vesco, T. and Dietrich, A., "Cyclic Behavior of "as Built" Laced Members With End Gusset Plates on the San Francisco Bay Bridge," Center for Civil Engineering Earthquake Research, Department of Civil Engineering, University of Nevada, Reno, Nevada Report No. CCEER-98-1, March, 1998.

CCEER-98-2 G. Norris and M. Ashour, "Liquefaction and Undrained Response Evaluation of

Sands from Drained Formulation," Center for Civil Engineering Earthquake Research, Department of Civil Engineering, University of Nevada, Reno, Nevada, Report No. CCEER-98-2, May, 1998.

CCEER-98-3 Qingbin, Chen, B. M. Douglas, E. Maragakis, and I. G. Buckle, "Extraction of Nonlinear Hysteretic Properties of Seismically Isolated Bridges from Quick-Release Field Tests," Center for Civil Engineering Earthquake Research, Department of Civil Engineering, University of Nevada, Reno, Nevada, Report No. CCEER-98-3, June, 1998.

CCEER-98-4 Maragakis, E., B. M. Douglas, and C. Qingbin, "Full-Scale Field Capacity Tests of a Railway Bridge," Center for Civil Engineering Earthquake Research, Department of Civil Engineering, University of Nevada, Reno, Nevada, Report No. CCEER-98-4, June, 1998.

CCEER-98-5 Itani, A., Douglas, B., and Woodgate, J., "Cyclic Behavior of Richmond-San Rafael Retrofitted Tower Leg," Center for Civil Engineering Earthquake Research, Department of Civil Engineering, University of Nevada, Reno. Report No. CCEER-98-5, June 1998

CCEER-98-6 Moore, R., Saiidi, M., and Itani, A., "Seismic Behavior of New Bridges with Skew and Curvature," Center for Civil Engineering Earthquake Research, Department of Civil Engineering, University of Nevada, Reno. Report No. CCEER-98-6, October, 1998.

CCEER-98-7 Itani, A and Dietrich, A, "Cyclic Behavior of Double Gusset Plate Connections," Center for Civil Engineering Earthquake Research, Department of Civil Engineering, University of Nevada, Reno, Nevada, Report No. CCEER-98-5, December, 1998.

CCEER-99-1 Caywood, C., M. Saiidi, and D. Sanders, "Seismic Retrofit of Flared Bridge Columns with Steel Jackets," Civil Engineering Department, University of Nevada, Reno, Report No. CCEER-99-1, February 1999.

CCEER-99-2 Mangoba, N., M. Mayberry, and M. Saiidi, "Prestress Loss in Four Box Girder Bridges in Northern Nevada," Civil Engineering Department, University of Nevada, Reno, Report No. CCEER-99-2, March 1999.

CCEER-99-3 Abo-Shadi, N., M. Saiidi, and D. Sanders, "Seismic Response of Bridge Pier Walls in the Weak Direction," Civil Engineering Department, University of Nevada, Reno, Report No. CCEER-99-3, April 1999.

CCEER-99-4 Buzick, A., and M. Saiidi, "Shear Strength and Shear Fatigue Behavior of Full-Scale Prestressed Concrete Box Girders," Civil Engineering Department, University of Nevada, Reno, Report No. CCEER-99-4, April 1999.

CCEER-99-5 Randall, M., M. Saiidi, E. Maragakis and T. Isakovic, "Restrainer Design Procedures For Multi-Span Simply-Supported Bridges," Civil Engineering Department, University of Nevada, Reno, Report No. CCEER-99-5, April 1999.

CCEER-99-6 Wehbe, N. and M. Saiidi, "User's Manual for RCMC v. 1.2, A Computer Program for Moment-Curvature Analysis of Confined and Unconfined Reinforced Concrete Sections," Civil Engineering Department, University of Nevada, Reno, Report No. CCEER-99-6, May 1999.

CCEER-99-7 Burda, J. and A. Itani, "Studies of Seismic Behavior of Steel Base Plates," Civil Engineering Department, University of Nevada, Reno, Report No. CCEER-99-7, May 1999.

CCEER-99-8 Ashour, M. and G. Norris, "Refinement of the Strain Wedge Model Program," Civil Engineering Department, University of Nevada, Reno, Report No. CCEER-99-8, March 1999.

CCEER-99-9 Dietrich, A., and A. Itani, "Cyclic Behavior of Laced and Perforated Steel Members on the San Francisco-Oakland Bay Bridge," Civil Engineering Department, University, Reno, Report No. CCEER-99-9, December 1999.

CCEER 99-10 Itani, A., A. Dietrich, "Cyclic Behavior of Built Up Steel Members and their

Connections," Civil Engineering Department, University of Nevada, Reno, Report No. CCEER-99-10, December 1999.

CCEER 99-10-A Itani, A., E. Maragakis and P. He, "Fatigue Behavior of Riveted Open Deck Railroad Bridge Girders," Civil Engineering Department, University of Nevada, Reno, Report No. CCEER-99-10-A, August 1999.

CCEER 99-11 Itani, A., J. Woodgate, "Axial and Rotational Ductility of Built Up Structural Steel Members," Civil Engineering Department, University of Nevada, Reno, Report No. CCEER-99-11, December 1999.

CCEER-99-12 Sgambelluri, M., Sanders, D.H., and Saiidi, M.S., "Behavior of One-Way Reinforced Concrete Bridge Column Hinges in the Weak Direction," Department of Civil Engineering, University of Nevada, Reno, Report No. CCEER-99-12, December 1999.

CCEER-99-13 Laplace, P., Sanders, D.H., Douglas, B, and Saiidi, M, "Shake Table Testing of Flexure Dominated Reinforced Concrete Bridge Columns", Department of Civil Engineering, University of Nevada, Reno, Report No. CCEER-99-13, December 1999.

CCEER-99-14 Ahmad M. Itani, Jose A. Zepeda, and Elizabeth A. Ware "Cyclic Behavior of Steel Moment Frame Connections for the Moscone Center Expansion," Department of Civil Engineering, University of Nevada, Reno, Report No. CCEER-99-14, December 1999.

CCEER 00-1 Ashour, M., and Norris, G. "Undrained Lateral Pile and Pile Group Response in Saturated Sand," Civil Engineering Department, University of Nevada, Reno, Report No. CCEER-00-1, May 1999. January 2000.

CCEER 00-2 Saiidi, M. and Wehbe, N., "A Comparison of Confinement Requirements in Different Codes for Rectangular, Circular, and Double-Spiral RC Bridge

Columns," Civil Engineering Department, University of Nevada, Reno, Report No. CCEER-00-2, January 2000.

CCEER 00-3 McElhaney, B., M. Saiidi, and D. Sanders, "Shake Table Testing of Flared Bridge Columns With Steel Jacket Retrofit," Civil Engineering Department, University of Nevada, Reno, Report No. CCEER-00-3, January 2000.

CCEER 00-4 Martinovic, F., M. Saiidi, D. Sanders, and F. Gordaninejad, "Dynamic Testing of Non-Prismatic Reinforced Concrete Bridge Columns Retrofitted with FRP Jackets," Civil Engineering Department, University of Nevada, Reno, Report No. CCEER-00-4, January 2000.

CCEER 00-5 Itani, A., and M. Saiidi, "Seismic Evaluation of Steel Joints for UCLA Center for Health Science Westwood Replacement Hospital," Civil Engineering Department, University of Nevada, Reno, Report No. CCEER-00-5, February 2000.

CCEER 00-6 Will, J. and D. Sanders, "High Performance Concrete Using Nevada Aggregates," Civil Engineering Department, University of Nevada, Reno, Report No. CCEER-00-6, May 2000.

CCEER 00-7 French, C., and M. Saiidi, "A Comparison of Static and Dynamic Performance of Models of Flared Bridge Columns," Civil Engineering Department, University of Nevada, Reno, Report No. CCEER-00-7, October 2000.

CCEER 00-8 Itani, A., H. Sedarat, "Seismic Analysis of the AISI LRFD Design Example of Steel Highway Bridges," Civil Engineering Department, University of Nevada, Reno, Report No. CCEER 00-08, November 2000.

CCEER 00-9 Moore, J., D. Sanders, and M. Saiidi, "Shake Table Testing of 1960's Two Column Bent with Hinges Bases," Civil Engineering Department, University of Nevada, Reno, Report No. CCEER 00-09, December 2000.

CCEER 00-10 Asthana, M., D. Sanders, and M. Saiidi, "One-Way Reinforced Concrete Bridge Column Hinges in the Weak Direction," Civil Engineering Department, University of Nevada, Reno, Report No. CCEER 00-10, April 2001.

CCEER 01-1 Ah Sha, H., D. Sanders, M. Saiidi, "Early Age Shrinkage and Cracking of Nevada Concrete Bridge Decks," Civil Engineering Department, University of Nevada, Reno, Report No. CCEER 01-01, May 2001.

CCEER 01-2 Ashour, M. and G. Norris, "Pile Group program for Full Material Modeling a Progressive Failure," Civil Engineering Department, University of Nevada, Reno, Report No. CCEER 01-02, July 2001.

CCEER 01-3 Itani, A., C. Lanaud, and P. Dusicka, "Non-Linear Finite Element Analysis of Built-Up Shear Links," Civil Engineering Department, University of Nevada, Reno, Report No. CCEER 01-03, July 2001.

CCEER 01-4 Saiidi, M., J. Mortensen, and F. Martinovic, "Analysis and Retrofit of Fixed Flared Columns with Glass Fiber-Reinforced Plastic Jacketing," Civil Engineering Department, University of Nevada, Reno, Report No. CCEER 01-4, August 2001

CCEER 01-5 Not Published

CCEER 01-6 Laplace, P., D. Sanders, and M. Saiidi, "Experimental Study and Analysis of Retrofitted Flexure and Shear Dominated Circular Reinforced Concrete Bridge Columns Subjected to Shake Table Excitation," Civil Engineering Department, University of Nevada, Reno, Report No. CCEER 01-6, June 2001.

CCEER 01-7 Reppi, F., and D. Sanders, "Removal and Replacement of Cast-in-Place, Post-tensioned, Box Girder Bridge," Civil Engineering Department, University of Nevada, Reno, Report No. CCEER 01-7, December 2001.

CCEER 02-1 Pulido, C., M. Saiidi, D. Sanders, and A. Itani, "Seismic Performance and Retrofitting of Reinforced Concrete Bridge Bents," Civil Engineering Department, University of Nevada, Reno, Report No. CCEER 02-1, January 2002.

CCEER 02-2 Yang, Q., M. Saiidi, H. Wang, and A. Itani, "Influence of Ground Motion Incoherency on Earthquake Response of Multi-Support Structures," Civil Engineering Department, University of Nevada, Reno, Report No. CCEER 02-2, May 2002.

CCEER 02-3 M. Saiidi, B. Gopalakrishnan, E. Reinhardt, and R. Siddharthan, "A Preliminary Study of Shake Table Response of A Two-Column Bridge Bent on Flexible Footings,"
Civil Engineering Department, University of Nevada, Reno, Report No. CCEER 02-03,

June 2002.

CCEER 02-4 Not Published

CCEER 02-5 Banghart, A., Sanders, D., Saiidi, M., "Evaluation of Concrete Mixes for Filling the Steel Arches in the Galena Creek Bridge," Civil Engineering Department, University of Nevada, Reno, Report No. CCEER 02-05, June 2002.

CCEER 02-6 Dusicka, P., Itani, A., Buckle, I. G., "Cyclic Behavior of Shear Links and Tower Shaft Assembly of San Francisco – Oakland Bay Bridge Tower," Civil Engineering Department, University of Nevada, Reno, Report No. CCEER 02-06, July 2002.

CCEER 02-7 Mortensen, J., and M. Saiidi, "A Performance-Based Design Method for Confinement in Circular Columns," Civil Engineering Department, University of Nevada, Reno, Report No. CCEER 02-07, November 2002.

CCEER 03-1 Wehbe, N., and M. Saiidi, "User's manual for SPMC v. 1.0 : A Computer Program for Moment-Curvature Analysis of Reinforced Concrete Sections with Interlocking Spirals," Center for Civil Engineering Earthquake Research, Department of Civil Engineering, University of Nevada, Reno, Nevada, Report No. CCEER-03-1, May, 2003.

CCEER 03-2 Wehbe, N., and M. Saiidi, "User's manual for RCMC v. 2.0 : A Computer Program for Moment-Curvature Analysis of Confined and Unconfined

Reinforced Concrete Sections," Center for Civil Engineering Earthquake Research, Department of Civil Engineering, University of Nevada, Reno, Nevada, Report No. CCEER-03-2, June, 2003.

CCEER 03-3 Nada, H., D. Sanders, and M. Saiidi, "Seismic Performance of RC Bridge Frames with Architectural-Flared Columns," Civil Engineering Department, University of Nevada, Reno, Report No. CCEER 03-3, January 2003.

CCEER 03-4 Reinhardt, E., M. Saiidi, and R. Siddharthan, "Seismic Performance of a CFRP/ Concrete Bridge Bent on Flexible Footings," Civil Engineering Department, University of Nevada, Reno, Report No. CCEER 03-4, August 2003.

CCEER 03-5 Johnson, N., M. Saiidi, A. Itani, and S. Ladkany, "Seismic Retrofit of Octagonal Columns with Pedestal and One-Way Hinge at the Base," Center for Civil Engineering Earthquake Research, Department of Civil Engineering, University of Nevada, Reno, Nevada, and Report No. CCEER-03-5, August 2003.

CCEER 03-6 Mortensen, C., M. Saiidi, and S. Ladkany, "Creep and Shrinkage Losses in Highly Variable Climates," Center for Civil Engineering Earthquake Research, Department of Civil Engineering, University of Nevada, Reno, Report No. CCEER-03-6, September 2003.

CCEER 03- 7 Ayoub, C., M. Saiidi, and A. Itani, "A Study of Shape-Memory-Alloy-Reinforced Beams and Cubes," Center for Civil Engineering Earthquake Research, Department of Civil Engineering, University of Nevada, Reno, Nevada, Report No. CCEER-03-7, October 2003.

CCEER 03-8 Chandane, S., D. Sanders, and M. Saiidi, "Static and Dynamic Performance of RC Bridge Bents with Architectural-Flared Columns," Center for Civil Engineering Earthquake Research, Department of Civil Engineering, University of Nevada, Reno, Nevada, Report No. CCEER-03-8, November 2003.

CCEER 04-1 Olaegbe, C., and Saiidi, M., "Effect of Loading History on Shake Table Performance of A Two-Column Bent with Infill Wall," Center for Civil Engineering Earthquake Research, Department of Civil Engineering, University of Nevada, Reno, Nevada, Report No. CCEER-04-1, January 2004.

CCEER 04-2 Johnson, R., Maragakis, E., Saiidi, M., and DesRoches, R., "Experimental Evaluation of Seismic Performance of SMA Bridge Restrainers," Center for Civil Engineering Earthquake Research, Department of Civil Engineering, University of Nevada, Reno, Nevada, Report No. CCEER-04-2, February 2004.

CCEER 04-3 Moustafa, K., Sanders, D., and Saiidi, M., "Impact of Aspect Ratio on Two-Column Bent Seismic Performance," Center for Civil Engineering Earthquake Research, Department of Civil Engineering, University of Nevada, Reno, Nevada, Report No. CCEER-04-3, February 2004.

CCEER 04-4 Maragakis, E., Saiidi, M., Sanchez-Camargo, F., and Elfass, S., "Seismic Performance of Bridge Restrainers At In-Span Hinges," Center for Civil Engineering Earthquake Research, Department of Civil Engineering, University of Nevada, Reno, Nevada, Report No. CCEER-04-4, March 2004.

CCEER 04-5 Ashour, M., Norris, G. and Elfass, S., "Analysis of Laterally Loaded Long or Intermediate Drilled Shafts of Small or Large Diameter in Layered Soil," Center for Civil Engineering Earthquake Research, Department of Civil Engineering, University of Nevada, Reno, Nevada, Report No. CCEER-04-5, June 2004.

CCEER 04-6 Correal, J., Saiidi, M. and Sanders, D., "Seismic Performance of RC Bridge Columns Reinforced with Two Interlocking Spirals," Center for Civil Engineering Earthquake Research, Department of Civil Engineering, University of Nevada, Reno, Nevada, Report No. CCEER-04-6, August 2004.

CCEER 04-7 Dusicka, P., Itani, A. and Buckle, I., "Cyclic Response and Low Cycle Fatigue Characteristics of Plate Steels," Center for Civil Engineering Earthquake Research, Department of Civil Engineering, University of Nevada, Reno, Nevada, Report No. CCEER-04-7, November 2004.

CCEER 04-8 Dusicka, P., Itani, A. and Buckle, I., "Built-up Shear Links as Energy Dissipaters for Seismic Protection of Bridges," Center for Civil Engineering Earthquake Research, Department of Civil Engineering, University of Nevada, Reno, Nevada, Report No. CCEER-04-8, November 2004.

CCEER 04-9 Sureshkumar, K., Saiidi, S., Itani, A. and Ladkany, S., "Seismic Retrofit of Two-Column Bents with Diamond Shape Columns," Center for Civil Engineering Earthquake Research, Department of Civil Engineering, University of Nevada, Reno, Nevada, Report No. CCEER-04-9, November 2004.

CCEER 05-1 Wang, H. and Saiidi, S., "A Study of RC Columns with Shape Memory Alloy and Engineered Cementitious Composites," Center for Civil Engineering Earthquake Research, Department of Civil Engineering, University of Nevada, Reno, Nevada, Report No. CCEER-05-1, January 2005.

CCEER 05-2 Johnson, R., Saiidi, S. and Maragakis, E., "A Study of Fiber Reinforced Plastics for Seismic Bridge Restrainers," Center for Civil Engineering Earthquake Research, Department of Civil Engineering, University of Nevada, Reno, Nevada, Report No. CCEER-05-2, January 2005.

CCEER 05-3 Carden, L.P., Itani, A.M., Buckle, I.G, "Seismic Load Path in Steel Girder Bridge Superstructures," Center for Civil Engineering Earthquake Research, Department of Civil Engineering, University of Nevada, Reno, Nevada, Report No. CCEER-05-3, January 2005.

CCEER 05-4 Carden, L.P., Itani, A.M., Buckle, I.G, "Seismic Performance of Steel Girder Bridge Superstructures with Ductile End Cross Frames and Seismic Isolation," Center for Civil Engineering Earthquake Research, Department of Civil Engineering, University of Nevada, Reno, Nevada, Report No. CCEER-05-4, January 2005.

CCEER 05-5 Goodwin, E., Maragakis, M., Itani, A. and Luo, S., "Experimental Evaluation of the Seismic Performance of Hospital Piping Subassemblies," Center for Civil Engineering Earthquake Research, Department of Civil Engineering, University of Nevada, Reno, Nevada, Report No. CCEER-05-5, February 2005.

CCEER 05-6 Zadeh M. S., Saiidi, S, Itani, A. and Ladkany, S., "Seismic Vulnerability Evaluation and Retrofit Design of Las Vegas Downtown Viaduct," Center for Civil Engineering Earthquake Research, Department of Civil Engineering, University of Nevada, Reno, Nevada, Report No. CCEER-05-6, February 2005.

CCEER 05-7 Phan, V., Saiidi, S. and Anderson, J., "Near Fault (Near Field) Ground Motion Effects on Reinforced Concrete Bridge Columns," Center for Civil Engineering Earthquake Research, Department of Civil Engineering, University of Nevada, Reno, Nevada, Report No. CCEER-05-7, August 2005.

CCEER 05-8 Carden, L., Itani, A. and Laplace, P., "Performance of Steel Props at the UNR Fire Science Academy subjected to Repeated Fire," Center for Civil Engineering

Earthquake Research, Department of Civil Engineering, University of Nevada, Reno, Nevada, Report No. CCEER-05-8, August 2005.

CCEER 05-9 Yamashita, R. and Sanders, D., "Shake Table Testing and an Analytical Study of Unbonded Prestressed Hollow Concrete Column Constructed with Precast Segments," Center for Civil Engineering Earthquake Research, Department of Civil Engineering, University of Nevada, Reno, Nevada, Report No. CCEER-05-9, August 2005.

CCEER 05-10 Not Published

CCEER 05-11 Carden, L., Itani., A., and Peckan, G., "Recommendations for the Design of Beams and Posts in Bridge Falsework," Center for Civil Engineering Earthquake Research, Department of Civil Engineering, University of Nevada, Reno, Nevada, Report No. CCEER-05-11, October 2005.

CCEER 06-01 Cheng, Z., Saiidi, M., and Sanders, D., "Development of a Seismic Design Method for Reinforced Concrete Two-Way Bridge Column Hinges," Center for Civil Engineering Earthquake Research, Department of Civil Engineering, University of Nevada, Reno, Nevada, Report No. CCEER-06-01, February 2006.

CCEER 06-02 Johnson, N., Saiidi, M., and Sanders, D., "Large-Scale Experimental and Analytical Studies of a Two-Span Reinforced Concrete Bridge System," Center for Civil Engineering Earthquake Research, Department of Civil Engineering, University of Nevada, Reno, Nevada, Report No. CCEER-06-02, March 2006.

CCEER 06-03 Saiidi, M., Ghasemi, H. and Tiras, A., "Seismic Design and Retrofit of Highway Bridges," Proceedings, Second US-Turkey Workshop, Center for Civil Engineering Earthquake Research, Department of Civil Engineering, University of Nevada, Reno, Nevada, Report No. CCEER-06-03, May 2006.

CCEER 07-01 O'Brien, M., Saiidi, M. and Sadrossadat-Zadeh, M., "A Study of Concrete Bridge Columns Using Innovative Materials Subjected to Cyclic Loading," Center for Civil Engineering Earthquake Research, Department of Civil Engineering, University of Nevada, Reno, Nevada, Report No. CCEER-07-01, January 2007.

CCEER 07-02 Sadrossadat-Zadeh, M. and Saiidi, M., "Effect of Strain rate on Stress-Strain Properties and Yield Propagation in Steel Reinforcing Bars," Center for Civil Engineering Earthquake Research, Department of Civil Engineering, University of Nevada, Reno, Nevada, Report No. CCEER-07-02, January 2007.

CCEER 07-03 Sadrossadat-Zadeh, M. and Saiidi, M., "Analytical Study of NEESR-SG 4-Span Bridge Model Using OpenSees," Center for Civil Engineering Earthquake Research, Department of Civil Engineering, University of Nevada, Reno, Nevada, Report No. CCEER-07-03, January 2007.

CCEER 07-04 Nelson, R., Saiidi, M. and Zadeh, S., "Experimental Evaluation of Performance of Conventional Bridge Systems," Center for Civil Engineering Earthquake Research, Department of Civil Engineering, University of Nevada, Reno, Nevada, Report No. CCEER-07-04, October 2007.

CCEER 07-05 Bahen, N. and Sanders, D., "Strut-and-Tie Modeling for Disturbed Regions in Structural Concrete Members with Emphasis on Deep Beams," Center for Civil Engineering Earthquake Research, Department of Civil Engineering, University of Nevada, Reno, Nevada, Report No. CCEER-07-05, December 2007.

CCEER 07-06 Choi, H., Saiidi, M. and Somerville, P., "Effects of Near-Fault Ground Motion and Fault-Rupture on the Seismic Response of Reinforced Concrete Bridges," Center for Civil Engineering Earthquake Research, Department of Civil Engineering, University of Nevada, Reno, Nevada, Report No. CCEER-07-06, December 2007.

CCEER 07-07 Ashour M. and Norris, G., "Report and User Manual on Strain Wedge Model Computer Program for Files and Large Diameter Shafts with LRFD Procedure," Center for Civil Engineering Earthquake Research, Department of Civil Engineering, University of Nevada, Reno, Nevada, Report No. CCEER-07-07, October 2007.

CCEER 08-01 Doyle, K. and Saiidi, M., "Seismic Response of Telescopic Pipe Pin Connections," Center for Civil Engineering Earthquake Research, Department of Civil Engineering, University of Nevada, Reno, Nevada, Report No. CCEER-08-01, February 2008.

CCEER 08-02 Taylor, M. and Sanders, D., "Seismic Time History Analysis and Instrumentation of the Galena Creek Bridge," Center for Civil Engineering Earthquake Research, Department of Civil Engineering, University of Nevada, Reno, Nevada, Report No. CCEER-08-02, April 2008.

CCEER 08-03 Abdel-Mohti, A. and Pekcan, G., "Seismic Response Assessment and Recommendations for the Design of Skewed Post-Tensioned Concrete Box-Girder Highway Bridges," Center for Civil Engineering Earthquake Research, Department of Civil and Environmental Engineering, University of Nevada, Reno, Nevada, Report No. CCEER-08-03, September 2008.

CCEER 08-04 Saiidi, M., Ghasemi, H. and Hook, J., "Long Term Bridge Performance Monitoring, Assessment & Management," Proceedings, FHWA/NSF Workshop on Future Directions," Center for Civil Engineering Earthquake Research, Department of Civil and Environmental Engineering, University of Nevada, Reno, Nevada, Report No. CCEER 08-04, September 2008.

CCEER 09-01 Brown, A., and Saiidi, M., "Investigation of Near-Fault Ground Motion Effects on Substandard Bridge Columns and Bents," Center for Civil Engineering Earthquake Research, Department of Civil and Environmental Engineering, University of Nevada, Reno, Nevada, Report No. CCEER-09-01, July 2009.

CCEER 09-02 Linke, C., Pekcan, G., and Itani, A., "Detailing of Seismically Resilient Special Truss Moment Frames," Center for Civil Engineering Earthquake Research, Department of Civil and Environmental Engineering, University of Nevada, Reno, Nevada, Report No. CCEER-09-02, August 2009.

CCEER 09-03 Hillis, D., and Saiidi, M., "Design, Construction, and Nonlinear Dynamic Analysis of Three Bridge Bents Used in a Bridge System Test," Center for Civil Engineering Earthquake Research, Department of Civil and Environmental Engineering, University of Nevada, Reno, Nevada, Report No. CCEER-09-03, August 2009.

CCEER 09-04 Bahrami, H., Itani, A., and Buckle, I., "Guidelines for the Seismic Design of Ductile End Cross Frames in Steel Girder Bridge Superstructures," Center for Civil Engineering Earthquake Research, Department of Civil and Environmental Engineering, University of Nevada, Reno, Nevada, Report No. CCEER-09-04, September 2009.

CCEER 10-01 Zaghi, A. E., and Saiidi, M., "Seismic Design of Pipe-Pin Connections in Concrete Bridges," Center for Civil Engineering Earthquake Research, Department of Civil and Environmental Engineering, University of Nevada, Reno, Nevada, Report No. CCEER-10-01, January 2010.

CCEER 10-02 Pooranampillai, S., Elfass, S., and Norris, G., "Laboratory Study to Assess Load Capacity Increase of Drilled Shafts through Post Grouting," Center for Civil Engineering Earthquake Research, Department of Civil and Environmental Engineering, University of Nevada, Reno, Nevada, Report No. CCEER-10-02, January 2010.

CCEER 10-03 Itani, A., Grubb, M., and Monzon, E, "Proposed Seismic Provisions and Commentary for Steel Plate Girder Superstructures," Center for Civil Engineering Earthquake Research, Department of Civil and Environmental Engineering, University of Nevada, Reno, Nevada, Report No. CCEER-10-03, June 2010.

CCEER 10-04 Cruz-Noguez, C., Saiidi, M., "Experimental and Analytical Seismic Studies of a Four-Span Bridge System with Innovative Materials," Center for Civil Engineering Earthquake Research, Department of Civil and Environmental Engineering, University of Nevada, Reno, Nevada, Report No. CCEER-10-04, September 2010.

CCEER 10-05 Vosooghi, A., Saiidi, M., "Post-Earthquake Evaluation and Emergency Repair of Damaged RC Bridge Columns Using CFRP Materials," Center for Civil Engineering Earthquake Research, Department of Civil and Environmental Engineering, University of Nevada, Reno, Nevada, Report No. CCEER-10-05, September 2010.

CCEER 10-06 Ayoub, M., Sanders, D., "Testing of Pile Extension Connections to Slab Bridges," Center for Civil Engineering Earthquake Research, Department of Civil and Environmental Engineering, University of Nevada, Reno, Nevada, Report No. CCEER-10-06, October 2010.

CCEER 10-07 Builes-Mejia, J. C. and Itani, A., "Stability of Bridge Column Rebar Cages during Construction," Center for Civil Engineering Earthquake Research, Department of Civil and Environmental Engineering, University of Nevada, Reno, Nevada, Report No. CCEER-10-07, November 2010.

CCEER 10-08 Monzon, E.V., "Seismic Performance of Steel Plate Girder Bridges with Integral Abutments," Center for Civil Engineering Earthquake Research, Department of Civil and Environmental Engineering, University of Nevada, Reno, Nevada, Report No. CCEER-10-08, November 2010.

CCEER 11-01 Motaref, S., Saiidi, M., and Sanders, D., "Seismic Response of Precast Bridge Columns with Energy Dissipating Joints," Center for Civil Engineering Earthquake Research, Department of Civil and Environmental Engineering, University of Nevada, Reno, Nevada, Report No. CCEER-11-01, May 2011.

CCEER 11-02 Harrison, N. and Sanders, D., "Preliminary Seismic Analysis and Design of Reinforced Concrete Bridge Columns for Curved Bridge Experiments," Center for Civil Engineering Earthquake Research, Department of Civil and Environmental Engineering, University of Nevada, Reno, Nevada, Report No. CCEER-11-02, May 2011.

CCEER 11-03 Vallejera, J. and Sanders, D., "Instrumentation and Monitoring the Galena Creek Bridge," Center for Civil Engineering Earthquake Research, Department of Civil and Environmental Engineering, University of Nevada, Reno, Nevada, Report No. CCEER-11-03, September 2011.

CCEER 11-04 Levi, M., Sanders, D., and Buckle, I., "Seismic Response of Columns in Horizontally Curved Bridges," Center for Civil Engineering Earthquake Research, Department of Civil and Environmental Engineering, University of Nevada, Reno, Nevada, Report No. CCEER-11-04, December 2011.

CCEER 12-01 Saiidi, M., "NSF International Workshop on Bridges of the Future – Wide Spread Implementation of Innovation," Center for Civil Engineering Earthquake Research,

Department of Civil and Environmental Engineering, University of Nevada, Reno, Nevada, Report No. CCEER-12-01, January 2012.

CCEER 12-02 Larkin, A.S., Sanders, D., and Saiidi, M., "Unbonded Prestressed Columns for Earthquake Resistance," Center for Civil Engineering Earthquake Research, Department of Civil and Environmental Engineering, University of Nevada, Reno, Nevada, Report No. CCEER-12-02, January 2012.

CCEER 12-03 Arias-Acosta, J. G., Sanders, D., "Seismic Performance of Circular and Interlocking Spirals RC Bridge Columns under Bidirectional Shake Table Loading Part 1," Center for Civil Engineering Earthquake Research, Department of Civil and Environmental Engineering, University of Nevada, Reno, Nevada, Report No. CCEER-12-03, September 2012.

CCEER 12-04 Cukrov, M.E., Sanders, D., "Seismic Performance of Prestressed Pile-To-Bent Cap Connections," Center for Civil Engineering Earthquake Research, Department of Civil and Environmental Engineering, University of Nevada, Reno, Nevada, Report No. CCEER-12-04, September 2012.

CCEER 13-01 Carr, T. and Sanders, D., "Instrumentation and Dynamic Characterization of the Galena Creek Bridge," Center for Civil Engineering Earthquake Research, Department of Civil and Environmental Engineering, University of Nevada, Reno, Nevada, Report No. CCEER-13-01, January 2013.

CCEER 13-02 Vosooghi, A. and Buckle, I., "Evaluation of the Performance of a Conventional Four-Span Bridge During Shake Table Tests," Center for Civil Engineering Earthquake Research, Department of Civil and Environmental Engineering, University of Nevada, Reno, Nevada, Report No. CCEER-13-02, January 2013.

CCEER 13-03 Amirihormozaki, E. and Pekcan, G., "Analytical Fragility Curves for Horizontally Curved Steel Girder Highway Bridges," Center for Civil Engineering Earthquake Research, Department of Civil and Environmental Engineering, University of Nevada, Reno, Nevada, Report No. CCEER-13-03, February 2013.

CCEER 13-04 Almer, K. and Sanders, D., "Longitudinal Seismic Performance of Precast Bridge Girders Integrally Connected to a Cast-in-Place Bentcap," Center for Civil Engineering Earthquake Research, Department of Civil and Environmental Engineering, University of Nevada, Reno, Nevada, Report No. CCEER-13-04, April 2013.

CCEER 13-05 Monzon, E.V., Itani, A.I., and Buckle, I.G., "Seismic Modeling and Analysis of Curved Steel Plate Girder Bridges," Center for Civil Engineering Earthquake Research, Department of Civil and Environmental Engineering, University of Nevada, Reno, Nevada, Report No. CCEER-13-05, April 2013.

CCEER 13-06 Monzon, E.V., Buckle, I.G., and Itani, A.I., "Seismic Performance of Curved Steel Plate Girder Bridges with Seismic Isolation," Center for Civil Engineering Earthquake Research, Department of Civil and Environmental Engineering, University of Nevada, Reno, Nevada, Report No. CCEER-13-06, April 2013.

CCEER 13-07 Monzon, E.V., Buckle, I.G., and Itani, A.I., "Seismic Response of Isolated Bridge Superstructure to Incoherent Ground Motions," Center for Civil

Engineering Earthquake Research, Department of Civil and Environmental Engineering, University of Nevada, Reno, Nevada, Report No. CCEER-13-07, April 2013.

CCEER 13-08 Haber, Z.B., Saiidi, M.S., and Sanders, D.H., "Precast Column-Footing Connections for Accelerated Bridge Construction in Seismic Zones," Center for Civil Engineering Earthquake Research, Department of Civil and Environmental Engineering, University of Nevada, Reno, Nevada, Report No. CCEER-13-08, April 2013.

CCEER 13-09 Ryan, K.L., Coria, C.B., and Dao, N.D., "Large Scale Earthquake Simulation of a Hybrid Lead Rubber Isolation System Designed under Nuclear Seismicity Considerations," Center for Civil Engineering Earthquake Research, Department of Civil and Environmental Engineering, University of Nevada, Reno, Nevada, Report No. CCEER-13-09, April 2013.

CCEER 13-10 Wibowo, H., Sanford, D.M., Buckle, I.G., and Sanders, D.H., "The Effect of Live Load on the Seismic Response of Bridges," Center for Civil Engineering Earthquake Research, Department of Civil and Environmental Engineering, University of Nevada, Reno, Nevada, Report No. CCEER-13-10, May 2013.

CCEER 13-11 Sanford, D.M., Wibowo, H., Buckle, I.G., and Sanders, D.H., "Preliminary Experimental Study on the Effect of Live Load on the Seismic Response of Highway Bridges," Center for Civil Engineering Earthquake Research, Department of Civil and Environmental Engineering, University of Nevada, Reno, Nevada, Report No. CCEER-13-11, May 2013.

CCEER 13-12 Saad, A.S., Sanders, D.H., and Buckle, I.G., "Assessment of Foundation Rocking Behavior in Reducing the Seismic Demand on Horizontally Curved Bridges," Center for Civil Engineering Earthquake Research, Department of Civil and Environmental Engineering, University of Nevada, Reno, Nevada, Report No. CCEER-13-12, June 2013.

CCEER 13-13 Ardakani, S.M.S. and Saiidi, M.S., "Design of Reinforced Concrete Bridge Columns for Near-Fault Earthquakes," Center for Civil Engineering Earthquake Research, Department of Civil and Environmental Engineering, University of Nevada, Reno, Nevada, Report No. CCEER-13-13, July 2013.

CCEER 13-14 Wei, C. and Buckle, I., "Seismic Analysis and Response of Highway Bridges with Hybrid Isolation," Center for Civil Engineering Earthquake Research,

Department of Civil and Environmental Engineering, University of Nevada, Reno, Nevada, Report No. CCEER-13-14, August 2013.

CCEER 13-15 Wibowo, H., Buckle, I.G., and Sanders, D.H., "Experimental and Analytical Investigations on the Effects of Live Load on the Seismic Performance of a Highway Bridge," Center for Civil Engineering Earthquake Research, Department of Civil and Environmental Engineering, University of Nevada, Reno, Nevada, Report No. CCEER-13-15, August 2013.

CCEER 13-16 Itani, A.M., Monzon, E.V., Grubb, M., and Amirihormozaki, E. "Seismic Design and Nonlinear Evaluation of Steel I-Girder Bridges with Ductile End Cross-Frames," Center for Civil Engineering Earthquake Research, Department of Civil and Environmental Engineering, University of Nevada, Reno, Nevada, Report No. CCEER-13-16, September 2013.

CCEER 13-17 Kavianipour, F. and Saiidi, M.S., "Experimental and Analytical Seismic Studies of a Four-span Bridge System with Composite Piers," Center for Civil Engineering Earthquake Research, Department of Civil and Environmental Engineering, University of Nevada, Reno, Nevada, Report No. CCEER-13-17, September 2013.

CCEER 13-18 Mohebbi, A., Ryan, K., and Sanders, D., "Seismic Response of a Highway Bridge with Structural Fuses for Seismic Protection of Piers," Center for Civil Engineering Earthquake Research, Department of Civil and Environmental Engineering, University of Nevada, Reno, Nevada, Report No. CCEER-13-18, December 2013.

CCEER 13-19 Guzman Pujols, Jean C., Ryan, K.L., "Development of Generalized Fragility Functions for Seismic Induced Content Disruption," Center for Civil Engineering Earthquake Research, Department of Civil and Environmental Engineering, University of Nevada, Reno, Nevada, Report No. CCEER-13-19, December 2013.

CCEER 14-01 Salem, M. M. A., Pekcan, G., and Itani, A., "Seismic Response Control Of Structures Using Semi-Active and Passive Variable Stiffness Devices," Center for Civil Engineering Earthquake Research, Department of Civil and Environmental Engineering, University of Nevada, Reno, Nevada, Report No. CCEER-14-01, May 2014.

CCEER 14-02 Saini, A. and Saiidi, M., "Performance-Based Probabilistic Damage Control Approach for Seismic Design of Bridge Columns," Center For Civil Engineering

Earthquake Research, Department Of Civil and Environmental Engineering, University of Nevada, Reno, Nevada, Report No. CCEER-14-02, May 2014.

CCEER 14-03 Saini, A. and Saiidi, M., "Post Earthquake Damage Repair of Various Reinforced Concrete Bridge Components," Center For Civil Engineering Earthquake Research, Department Of Civil and Environmental Engineering, University of Nevada, Reno, Nevada, Report No. CCEER-14-03, May 2014.

CCEER 14-04 Monzon, E.V., Itani, A.M., and Grubb, M.A., "Nonlinear Evaluation of the Proposed Seismic Design Procedure for Steel Bridges with Ductile End Cross Frames," Center For Civil Engineering Earthquake Research, Department Of Civil and Environmental Engineering, University of Nevada, Reno, Nevada, Report No. CCEER-14-04, July 2014.